

Open Research Online

The Open University's repository of research publications and other research outputs

Study of the Evolutionary Role of Nitric Oxide (NO) in the Cephalochordate Amphioxus, "*Branchiostoma lanceolatum*"

Thesis

How to cite:

Caccavale, Filomena (2018). Study of the Evolutionary Role of Nitric Oxide (NO) in the Cephalochordate Amphioxus, "*Branchiostoma lanceolatum*". PhD thesis The Open University.

For guidance on citations see [FAQs](#).

© 2017 The Author

Version: Version of Record

Copyright and Moral Rights for the articles on this site are retained by the individual authors and/or other copyright owners. For more information on Open Research Online's data [policy](#) on reuse of materials please consult the policies page.

oro.open.ac.uk

**Study of the Evolutionary Role of Nitric
Oxide (NO) in the Cephalochordate
Amphioxus, “*Branchiostoma lanceolatum*”**

A thesis submitted to the Open University of London for the
degree of

DOCTOR OF PHILOSOPHY

by

Filomena Caccavale

Diploma Degree in Biology

Università degli studi di Napoli Federico II

Affiliated Research Center (ARC)
STAZIONE ZOOLOGICA “ANTON DOHRN” DI
NAPOLI
Naples, Italy

November 2017

This thesis work has been carried out in the laboratory of Dr. Salvatore D’Aniello, at the Stazione Zoologica “Anton Dohrn” di Napoli, Italy.

Director of studies: Dr. Salvatore D’Aniello (BEOM, Stazione Zoologica “Anton Dohrn” di Napoli, Italy)

Internal Supervisor: Dr. Anna Palumbo (BEOM, Stazione Zoologica “Anton Dohrn” di Napoli, Italy)

External Supervisor: Prof. Ricard Albalat Rodriguez (Departament de Genètica, Microbiologia i Estadística and Institut de Recerca de la Biodiversitat (IRBio), Universitat de Barcelona, Spain)

*“Find a job you enjoy doing,
and you will never have
to work a day in your life.”*

Mark Twain

ABSTRACT

Nitric Oxide (NO) is a gaseous molecule that acts in a wide range of biological processes. NO can be produced by enzymatic and non-enzymatic pathways and, in this scenario, the enzyme Nitric Oxide Synthase (NOS) has a great importance for its exclusive role in *de novo* synthesis of NO. In the present study, the role of the NO in the embryonic development was investigated in the cephalochordate *Branchiostoma lanceolatum* (amphioxus) with the purpose of acquiring further knowledge on the ancestral role of animal *Nos* and the acquisition of new NO functions during evolution. Amphioxus has three different *Nos* genes (*NosA*, *NosB* and *NosC*) that are not orthologues of the three *Nos* of mammals (*NosI*, *NosII* and *NosIII*) deriving from an independent duplication occurred in the common ancestor of cephalochordates. The three amphioxus *Nos* genes showed a different temporal and spatial expression during development and a different susceptibility to be induced after immune stimulation. The study of the promoter regions of these genes can be very useful to identify possible diversities in regulation that can lead those peculiar expression features. In amphioxus larva, NO was mainly detected in the developing nervous system and in the pharyngeal area, before and after the mouth opening. The inhibition of NOS activity, and as consequence the enzymatic NO production, during amphioxus neurulation, resulted in the alteration of pharyngeal structures formation in the larvae, in particular opening of the mouth resulted compromised. Moreover, an alteration in larva locomotion was observed. Further studies will be necessary to reveal the exactly molecular mechanisms and the pathways in which

NO acts for establishment of the pharyngeal structures and the neuromuscular junctions early in development. For this purpose, a differential transcriptomic analysis of NOS-inhibited embryos was performed but the results are still very preliminary.

ACKNOWLEDGEMENTS

I am very thankful to my director of studies Dr. Salvatore D’Aniello (SZN) and my supervisors Prof. Ricard Albalat (Universitat de Barcelona) and Dr. Anna Palumbo (SZN) for excellent leadership, their time spent in our discussions, for their support and encouragement to pursue new ideas. Next, I thank all my labmates for friendly and stimulating atmosphere, for all their advices, nice experiences and refreshing moments we could spend together.

I would like to acknowledge Dr. Hector Escrivà (UPMC) and Dr. Stéphanie Bertrand (UPMC) for their hospitality and support during the period that I spent in their laboratory at the Oceanographic Observatory in Banyuls sur-Mer to performing experiments that are part of this work. I thank The Company of Biologists for found that travel.

I am grateful to the Molecular biology service, the MaRe unit and the AMOBIO unit of the SZN for technical assistance.

Last but not least, special thanks to my parents and family and to Luciano for their constant support and encouragement during my studies.

TABLE OF CONTENTS

ABSTRACT	I
ACKNOWLEDGEMENTS	III
TABLE OF CONTENTS.....	IV
LIST OF FIGURES.....	VII
LIST OF TABLES.....	XII
CHAPTER 1: INTRODUCTION	1
1.1 NITRIC OXIDE: SIGNALING, BIOLOGICAL FUNCTION AND BIOSYNTHESIS	1
1.2 THE EXPERIMENTAL MODEL SYSTEM: AMPHIOXUS	11
1.2.1 History of amphioxus and its anatomy.....	11
1.2.2 Phylogeny.....	17
1.2.3 Reproduction and embryology: early and late amphioxus development	20
1.3 NITRIC OXIDE AND NITRIC OXIDE SYNTHASES IN AMPHIOXUS	33
1.4 NEURONAL NOS GENE TRANSCRIPTIONAL REGULATION	39
1.5 TRANSCRIPTIONAL GENE REGULATION	42
1.5.1 Conserved non-coding regions and their gene regulatory function.....	42
1.5.2 <i>Ciona robusta</i> as model organism for transgenic experiments.....	45
CHAPTER 2: MATERIALS AND METHODS	50
2.1 ANIMALS CARE AND GAMETES COLLECTION	50

2.1.1 <i>Branchiostoma lanceolatum</i> sampling and ethics statement	50
2.1.2 <i>Branchiostoma lanceolatum</i> care	51
2.1.3 <i>Branchiostoma lanceolatum</i> spawnings.....	52
2.1.4 <i>Ciona robusta</i> sampling, care and gametes collection.....	54
2.2 <i>IN VIVO</i> EMBRYONIC MANIPULATION.....	54
2.2.1 TRIM and L-NAME treatments in amphioxus.....	54
2.2.2 LPS treatment in amphioxus	55
2.2.3 Transgenesis in <i>Ciona robusta</i>	56
2.3 AMPHIOXUS EMBRYOS COLLECTION AND FIXATION.....	57
2.4 BASIC MOLECULAR BIOLOGY PROCEDURES	57
2.4.1 RNA purification	57
2.4.2 Reverse transcription of RNA.....	58
2.4.3 DNA and RNA gel electrophoresis	58
2.4.4 Genomic DNA preparation	59
2.4.5 Molecular cloning.....	59
2.4.6 Isolation of plasmidic DNA from <i>Escherichia coli</i>	61
2.4.7 Polymerase chain reaction (PCR).....	61
2.4.8 DNA sequencing.....	62
2.4.9 Oligonucleotides.....	62
2.5 QUANTITATIVE GENE EXPRESSION	64
2.5.1 Quantitative real-time PCR (qPCR)	64
2.5.2 Digital droplet PCR (ddPCR)	65
2.6 CONSTRUCTS PREPARATION FOR TRANSGENESIS.....	66
2.6.1 Amphioxus enhancers	66
2.6.2 DNA constructs for transgenesis in <i>Ciona robusta</i>	70

2.7 NO QUANTIFICATION AND LOCALIZATION	71
2.7.1 Griess assay.....	71
2.7.2 DAF-FM diacetate assay	73
2.8 DIFFERENTIAL TRANSCRIPTOMIC ANALYSIS	73
2.9 NOS PHYLOGENETIC ANALYSIS.....	75
2.10 IMAGING.....	80
2.11 STATISTICS	80
CHAPTER 3: RESULTS.....	82
3.1 CEPHALOCHORDATES INDEPENDENT NOS DUPLICATIONS AND AMPHIOXUS NOS EXPRESSION PROFILE	82
3.2 INDUCIBLE NATURE OF AMPHIOXUS NOS GENES	85
3.3 REGULATORY MECHANISMS OF AMPHIOXUS <i>NosC</i>	87
3.4 ENDOGENOUS NO QUANTIFICATION AND LOCALIZATION.....	97
3.5 NO MODULATION DURING AMPHIOXUS DEVELOPMENT	99
3.6 DIFFERENTIAL TRANSCRIPTOMIC ANALYSIS OF NO-INHIBITED EMBRYOS.....	108
CHAPTER 4: DISCUSSION	117
CHAPTER 5: COLLABORATIVE AND RELATED PROJECTS.....	135
REFERENCES.....	140

LIST OF FIGURES

CHAPTER 1 - INTRODUCTION

Figure 1.1: Two different NO action mechanisms.

Figure 1.2: NO biosynthesis.

Figure 1.3: Schematic structure of mammalian NOS.

Figure 1.4: Human nNOS, eNOS and iNOS.

Figure 1.5: Schematic representation of animal NOS organization.

Figure 1.6: Wall chart from a Karl Georg Friedrich Rudolf Leuckart collection.

Figure 1.7: Adult amphioxus.

Figure 1.8: Difference between male and female gonads in adult amphioxus.

Figure 1.9: Phylogeny of deuterostomes.

Figure 1.10: Phylogenetic relationship within the Cephalochordata.

Figure 1.11: Amphioxus life cycle.

Figure 1.12: *Branchiostoma lanceolatum* cleavage phases.

Figure 1.13: Fate map of amphioxus gastrula stage.

Figure 1.14: Amphioxus neurulation.

Figure 1.15: Schematic representation of the three major AP subdivisions in the amphioxus central nervous system at neurula stage and the relative expression of their key markers (from Albuixech-Crespo *et al.*, 2017).

Figure 1.16: Schematic representation of the amphioxus larval nervous system.

Figure 1.17: Schematic representation and morphology of amphioxus larva with one gill-slit, seen from right side and left side.

Figure 1.18: Amphioxus mouth development hypothesis according to Kaji and collaborators (2016).

Figure 1.19: Evolutionary events regarding NOS genes in chordates.

Figure 1.20: Whole-mount immunostaining of 48 hpf *Branchiostoma floridae* larvae with a universal anti-NOS antibody.

Figure 1.21: NOS expression pattern in different tissues of adult amphioxus (from Chen *et al.*, 2008).

Figure 1.22: Amphioxus *Nos* expression pattern by *in situ* hybridization experiment in adult tissues.

Figure 1.23: *Branchiostoma lanceolatum* *NosB* and *NosC* expression during embryonic development.

Figure 1.24: Organization of the 5' end of the human NOS1 gene.

Figure 1.25: Putative cis-acting elements within neuronal nitric oxide synthase (nNOS) 1f promoter.

Figure 1.26: Schematic representation of a target gene regulatory input by CNEs.

Figure 1.27: Experimental design.

Figure 1.28: *Ciona robusta* larva.

Figure 1.29: *Ciona* larva nervous system.

CHAPTER 2 - MATERIALS AND METHODS

Figure 2.1: Adult amphioxus sampling.

Figure 2.2: Amphioxus facility at the Stazione Zoologica Anton Dohrn of Naples.

Figure 2.3: Schematic timing representation of induced spawning in *B. lanceolatum*.

Figure 2.4: Quality control of RNA samples for total RNA sequence.

Figure 2.5: Protein and coding sequences (CDS) of the *Branchiostoma lanceolatum* *NosA*, come from the draft genome sequence.

Figure 2.6: Protein and coding sequences (CDS) of the *Branchiostoma lanceolatum* *NosB*, come from the draft genome sequence.

Figure 2.7: Protein and coding sequences (CDS) of the *Branchiostoma lanceolatum* *NosC*, come from the draft genome sequence.

CHAPTER 3 – RESULTS

Figure 3.1: Phylogenetic relationship between chordate NOS proteins.

Figure 3.2: *Branchiostoma lanceolatum* *Nos* genes expression profile analysed by ddPCR.

Figure 3.3: *Branchiostoma lanceolatum* *Nos* genes expression analyses by qPCR after LPS stimulation.

Figure 3.4: *Branchiostoma lanceolatum* *NosC* genomic locus.

Figure 3.5: Amphioxus CRNs tested by transgenesis.

Figure 3.6: Cross-species regulatory activity in *Ciona robusta* of the amphioxus CNR14 and CNR15 cloned together in the construct 3.

Figure 3.7: Cross-species regulatory activity in *Ciona robusta* of the amphioxus CNR17, CNR18 and CNR19 cloned simultaneously in the construct 4.

Figure 3.8: Cross-species regulatory activity in *Ciona robusta* of the amphioxus CNR39, CNR40 and CNR41 cloned simultaneously in the construct 8.

Figure 3.9: Nitrite quantification during amphioxus embryonic development and in adult.

Figure 3.10: Nitric oxide localization by DAF-FM-DA.

Figure 3.11: Schematic representation of preliminary L-NAME and TRIM treatments performed on *Branchiostoma lanceolatum* embryos.

Figure 3.12: Amphioxus larvae after drug treatments.

Figure 3.13: SEM images of anterior part of body of amphioxus 72 hpf larvae after TRIM treatments.

Figure 3.14: Schematic representation of 100 μ M TRIM treatments performed on *Branchiostoma lanceolatum* embryos in the period 24-48 hpf.

Figure 3.15: Anterior part of the body of a TRIM-treated larva.

Figure 3.16: Schematic representation of movements in un-treated and TRIM-treated larvae.

Figure 3.17: MA-plot representation of RNA-seq results between TRIM-treated and un-treated samples.

CHAPTER 4 – DISCUSSION

Figure 4.1: Schematic representation of duplication events of *Nos* genes occurred in Chordates.

Figure 4.2: Comparison between the *Nos* expression in *Ciona robusta* and the positive regulatory activity for the amphioxus CNR 14, 15, 17, 18, 19, 39, 40, 41

Figure 4.3: Scheme of Nodal signaling pathway involved in establishment of the left/right asymmetry in amphioxus.

Figure 4.4: Gene pathways involved in left/right and mouth determination across metazoans.

CHAPTER 5 – COLLABORATIVE AND RELATED PROJEC

Figure 5.1: *Ran* expression profile and PHH3 immunostaining in amphioxus embryos and larvae.

Figure 5.2: Map of sites selected for amphioxus biogeography in Europe.

LIST OF TABLES

CHAPTER 1 – INTRODUCTION

Table 1.1: Physiological processes in which NO acts in invertebrates.

CHAPTER 2 - MATERIALS AND METHODS

Table 2.1: List of primers used for PCR experiments. For each pair of primer, the amplification product length is reported.

Table 2.2: Accession number of NOS sequences used in the phylogenetic reconstruction.

CHAPTER 3 – RESULTS

Table 3.1: Selection process schematization for the CNRs to be tested by transgenesis.

Table 3.2: Summary of results obtained from transgenesis experiments in *Ciona robusta* using amphioxus *NosC* CNRs.

Table 3.3: List of 17 down-regulated genes already annotated resulted from the differential transcriptomic analysis of TRIM-treated amphioxus embryos in the developmental interval between 24 and 30 hpf.

Table 3.4: List of 88 up-regulated genes already annotated resulted from the differential transcriptomic analysis of TRIM-treated amphioxus embryos in the developmental interval between 24 and 30 hpf.

CHAPTER 1

INTRODUCTION

1.1 NITRIC OXIDE: SIGNALING, BIOLOGICAL FUNCTION AND BIOSYNTHESIS

Nitric Oxide (NO) is a highly diffusible gas molecule and its signaling effects are determined by its chemical reactivity. NO may act in the cells where it is produced or in the adjacent cells where it rapidly diffuses through the membrane (Goretski and Hollocher, 1988; Stamler *et al.*, 1992), and so a concentration gradient occurs. Because of its free radical nature, NO is a very unstable molecule and its role as a direct signal mediator is limited to a short time window after its production (Martínez-Ruiz and Lamas, 2009). NO regulates a variety of processes ranging from the control of blood pressure and smooth muscle relaxation to immune activation and neuronal signaling (Moncada *et al.*, 1991; Esplugues, 2002; Förstermann and Sessa, 2012). NO mainly acts through the cyclic guanosine-3',5'-monophosphate (cGMP) pathway. NO binds the soluble guanylyl cyclase (Stamler *et al.*, 1992) that, as result, increases the production of cGMP, a second messenger involved in several physiological functions (Ahern *et al.*, 2002). cGMP activates several targets including cGMP-dependent protein kinase, cGMP-gated channels and phosphodiesterases (Ahern *et al.*, 2002) (Fig. 1.1A). NO interact with other molecules such as oxygen, oxygen-derived free radicals, glutathione,

and specific protein residues producing several types of post-translational modifications (Martínez-Ruiz and Lamas, 2009). In particular, NO reacts with thiol groups, mainly of cysteine residues, to produce S-nitrosylated proteins, through the intermediacy of dinitrogen trioxide, N_2O_3 , which is formed by the reaction of NO with oxygen (Martínez-Ruiz and Lamas, 2009). NO also reacts with the phenolic ring of tyrosine residues to form a 3-nitrotyrosine residue in target proteins (Martínez-Ruiz and Lamas, 2009). In this case the nitrating species is peroxynitrite, deriving by the reaction of NO with superoxide (O_2^-) to give peroxynitrite ($ONOO^-$) (Fig. 1.1B). Considering the different nature of the chemical bonds, nitrosylation is generally considered a reversible process, whereas nitration an irreversible reaction. However, the existence in the cells of mechanisms accounting for a denitrating activity has been suggested. Indeed, dynamics of protein nitration in respiring mitochondria have been reported, showing that nitration is related to oxygenation and denitration to anoxia (Aulak et al., 2004). NO may be also involved in S-glutathionylation, the incorporation of glutathione (GSH) into the protein, through the reaction between the S-nitrosothiol, S-nitrosoglutathione ($GSHNO$), and protein sulfhydryls to produce the mixed disulfide P-SSG. This can be also formed by reaction of S-nitrosylated proteins with GSH.

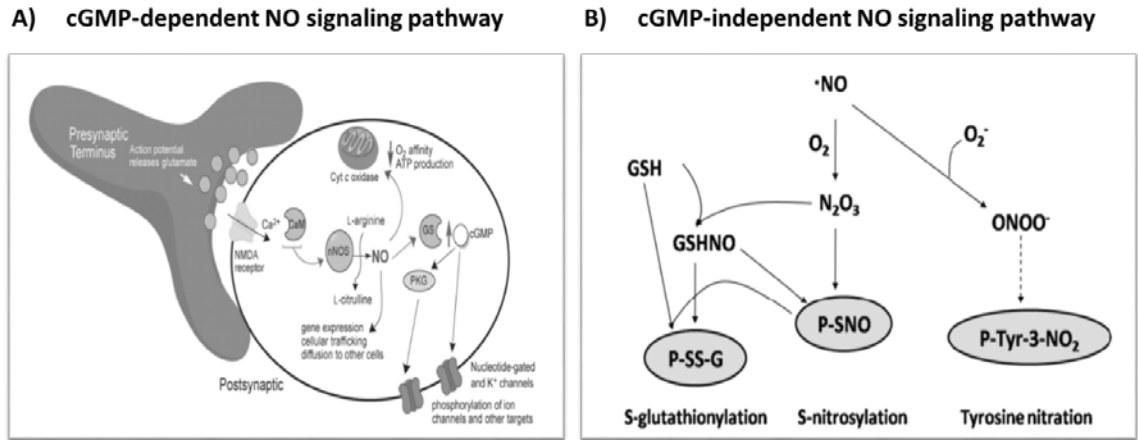


Figure 1.1: Two different NO signaling pathway. (A) cGMP-dependent pathway (Ahern *et al.*, 2002); (B) cGMP-independent pathway (adapted from Martínez-Ruiz and Lamas, 2009).

Until recently protein nitration and nitrosylation were essentially considered as a footprint of oxidative damage, but it is now becoming clear from a series of evidences reported in the literature that these processes may represent new signaling pathways. In fact, protein nitration can affect the enzymatic activity of a variety of proteins (Schopfer *et al.*, 2003) or it can mimic cell-signaling events such as adenylation (Berlett *et al.*, 1996). Thus, protein nitration has also been associated to some biological processes, such as cell maturation (Fiore *et al.*, 2009) and larval development (Ercolesi *et al.*, 2012). Protein nitration can also modulate cytoskeletal organization that represents a signaling mechanism in neuronal differentiation (Cappelletti *et al.*, 2004; Tedeschi *et al.*, 2007).

In mammals, including humans, NO is an important cellular signaling molecule involved in many physiological and pathological processes (Hou *et al.*, 1999). It is a powerful vasodilator with a short half-life of a few seconds in the blood; its vasodilatory

action plays a key role in renal control of extracellular fluid homeostasis and is essential for the regulation of blood flow and blood pressure (Yoon *et al.*, 2000). NO also serves as a neurotransmitter (Figure 1.1). Glutamate released from the presynaptic neuron binds to the NMDA receptor and causes the entrance of calcium ions. These ions bind to calmodulin which activates NOS to produce NO in the postsynaptic neuron. Unlike most other neurotransmitters that pass information only from a presynaptic to a postsynaptic neuron, NO widely and readily diffuses into cells and, so, it can act on several nearby neurons, even on those not connected by a synapse (Vizi *et al.*, 2010). It has been associated with neuronal activity and various functions such as learning and memory through the maintenance of long-term potentiation (Taqatqeh *et al.*, 2009). NO is also involved in immune response mediating macrophage cytotoxicity against microbes and tumor cells (Förstermann and Sessa, 2012).

In non-vertebrates, NO is involved in a wide spectrum of physiological processes, as feeding, blood sucking, bioluminescence, neural transmission, immune response, apoptosis (Palumbo, 2005; Di Cristo *et al.*, 2007; Krönström *et al.*, 2007; Mattiello *et al.*, 2010) and other processes listed in Table 1.1. NO is also necessary in sea urchins, in the first phases of life, as in male gametes development and in egg activation (Kuo *et al.*, 2000), as well as in the duration of the calcium transient increase, in the NAD(P)H and H₂O₂ production and in the fertilization envelope hardening (Mohri *et al.*, 2008). Moreover, NO was found to be implicated during settlement and metamorphosis in different marine organisms, such as *C. robusta*, *Ilyanassa obsolete*, *Lytechinus pictus* and *Boltenia villosa* (Table 1.1; Bishop and Brandhorst, 2001; Bishop *et al.*, 2001; Leise *et al.*, 2004; Bishop and Brandhorst, 2007; Comes *et al.*, 2007).

PHYLUM	SPECIES	BIOLOGICAL ROLE	REFERENCE
<i>Porifera</i>	<i>Axinella polypoides</i>	Environmental stress	Giovine <i>et al.</i> , 2001
	<i>Petrosia ficiformis</i>		
<i>Cnidaria</i>	<i>Aglanta digitale</i>	Swimming	Moroz <i>et al.</i> , 2004
	<i>Aiptasia diaphana</i>	Defense	Salleo <i>et al.</i> , 1996
<i>Mollusca</i>	<i>Aplysia californica</i>	Memory	Katzoff <i>et al.</i> , 2002
	<i>Ilyanassa obsoleta</i>	Metamorphosis	Leise <i>et al.</i> , 2004
	<i>Mytilus edulis</i>	Defense	Stefano and Ottaviani, 2002
	<i>Euprymna scolopes</i>	Symbiosis	Davidson <i>et al.</i> , 2004
	<i>Octopus vulgaris</i>	Learning	Robertson <i>et al.</i> , 1996
	<i>Sepia officinalis</i>	Defense	Fiore <i>et al.</i> , 2009
		Regulating blood pressure	Schipp and Gebauer, 1999
		Fertilization	Leckie <i>et al.</i> , 2003
<i>Echinodermata</i>	<i>Lytechinus pictus</i>		
	<i>Psammechinus miliaris</i>		
<i>Chordata</i>	<i>Lytechinus pictus</i>	Metamorphosis	Bishop and Brandhorst, 2001
	<i>Ciona intestinalis</i>	Fertilization	Grumetto <i>et al.</i> , 1997
		Metamorphosis	Comes <i>et al.</i> , 2007
	<i>Boltenia villosa</i>	Metamorphosis	Bishop <i>et al.</i> , 2001

Table 1.1: Physiological processes in which NO acts in invertebrates.

In cells, NO is endogenously generated by a class of heme-dependent enzymes, called Nitric Oxide Synthase (NOS), that catalyze the conversion of L-arginine to L-citrulline and NO (Fig. 1.2).

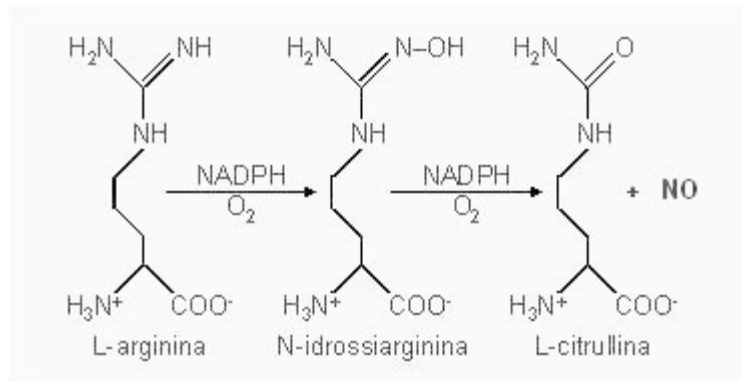


Figure 1.2: NO biosynthesis.

In mammals, there are three NOS proteins coded by three different genes: two constitutively expressed genes, the *endothelial Nos* (*eNos*, *Nos-III* or *Nos-3*) and the *neuronal Nos* (*nNos*, *Nos-I* or *Nos-1*); one *inducible Nos* (*iNos*, *Nos-II* or *Nos-2*). Neuronal and endothelial *Nos* genes are commonly associated with constitutive expression and are most commonly found in non-immunological cells e.g., neurons and endothelium (Knowles and Moncada, 1994). On the other hand, the inducible *Nos* expression has long been associated with immunological functions. Immune cells use NO, often in conjunction with reactive oxygen intermediates (ROI), to eliminate pathogens and cancer cells (MacMicking *et al.*, 1997; Xu *et al.*, 2002). NO acts non-specifically on a variety of targets and can kill targets at micromolar concentrations (Wink *et al.*, 2011). Despite their names indicate a tissue-specificity, all three *Nos* genes were indeed found in a wide variety of tissues and organs. Thus, for example, nNOS is also present in muscle, pancreatic islets, kidney, respiratory and gastrointestinal epithelia. The eNOS has been reported in cardiac myocytes, brain and kidney epithelia, whereas the iNOS in cardiac myocytes, glial cells, hepatocytes, keratinocytes (for a

review see Andreakis *et al.*, 2011). nNOS and eNOS activity is calcium-dependent, whereas iNOS is fully activated at basal intracellular calcium concentration, so its activity is calcium-independent (Calabrese *et al.*, 2007). Mammalian NOS are catalytically active when dimerized (Förstermann and Sessa, 2012); each monomer consists of a C-terminal reductase domain and an N-terminal oxygenase domain (Alderton *et al.*, 2001). These two domains are connected by a calmodulin (CaM) binding sequence (Fig. 1.3). The oxygenase domain contains a non-catalytic zinc (Zn^{2+}), heme, tetrahydrobiopterin (BH_4), and the substrate (L-arginine) binding site, where catalysis occurs. The binding mode of L-arginine in the three NOSs is identical. The reductase domain, which contains NADPH (nicotinamide adenine dinucleotide phosphate), FAD (flavin adenine dinucleotide), and FMN (flavin mononucleotide) cofactors, is divided into an NADPH-FAD binding subdomain and a FMN binding subdomain (Fig. 1.3). Because these two subdomains are connected by a flexible dodecapeptide, they can perform a hinge movement when CaM, linked with calcium, binds to its binding site (Alderton *et al.*, 2001; Andrew and Mayer, 1999). For all the three enzymes a conformational change, associated with CaM binding, is required for the electron transfer (Ghosh and Salerno, 2003). For both neuronal and endothelial NOSs, CaM binding takes place when the free intracellular calcium (Ca^{2+}) levels up to specific micromolar concentrations. Conversely, the inducible NOS, thanks to a greater affinity, carry a permanently bound CaM, which does not dissociate even at low Ca^{2+} concentrations (Cho *et al.*, 1992). Therefore, the iNOS expression is not regulated by intracellular Ca^{2+} and, in basal conditions, its activity is very low but its expression

could be regulated at the transcriptional level under certain conditions (Förstermann and Sessa, 2012).

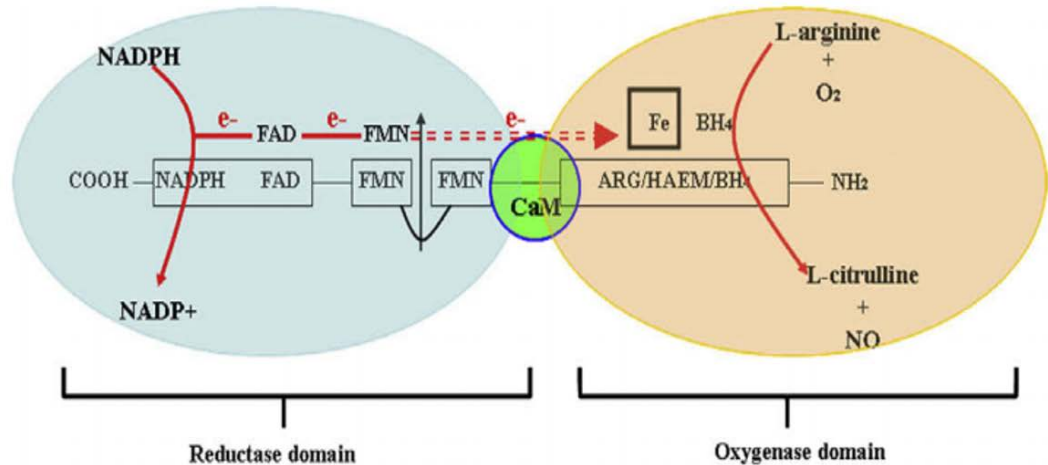


Figure 1.3: Schematic structure of mammalian constitutive NOS. It shows two domains separate by a calmodulin binding site and the flow of electrons from NADPH to heme-Fe (from Zhou and Zhu 2009).

The structural features listed above are common to all three NOSs. In addition, nNOS has a PDZ domain (Fig. 1.4) through which it can interact with other adapter proteins containing PDZ binding domains influencing the subcellular distribution and/or activity of the enzyme (Brenman *et al.*, 1996; Titheradge *et al.*, 1998; Jaffrey *et al.*, 2002). At the N-terminal part eNOS presents two post-translational modification sites: 1) glycine in positions 2 (Gly-2) is N-myristoylated after removal of the N-terminal methionine residue; 2) residues of cysteine in position 15 and 26 (Cys-15 and Cys-26) are N-palmitoylated (Fig. 1.4). Myristoylation is highly stable and generally irreversible under physiological conditions, it allows weak protein-protein and protein-lipid interactions and plays an essential role in membrane targeting (Titheradge *et al.*, 1998). In contrast,

palmitoylation is a reversible post-translational modification and, usually, it enhances the hydrophobicity of proteins, contributing to protein-membrane interactions (Robinson and Michel, 1995; Titheradge *et al.*, 1998). Both the constitutive nNOS and eNOS are characterized by the presence of the so called “autoinhibitory loop”, that is responsible of the Ca^{2+} dependence interfering with the binding of CaM. This element inhibits intradomain electron transfer but, at specific Ca^{2+} concentrations, CaM acts by displacing the autoinhibitory element allowing the enzymatic activity (Nishida and Ortiz de Montellano, 1999). The autoinhibitory loop is about 52-55 aa long and is situated within the FMN binding domain located approximately 80 aa residues at 3’ of the CaM binding sequence (Fig. 1.4b).

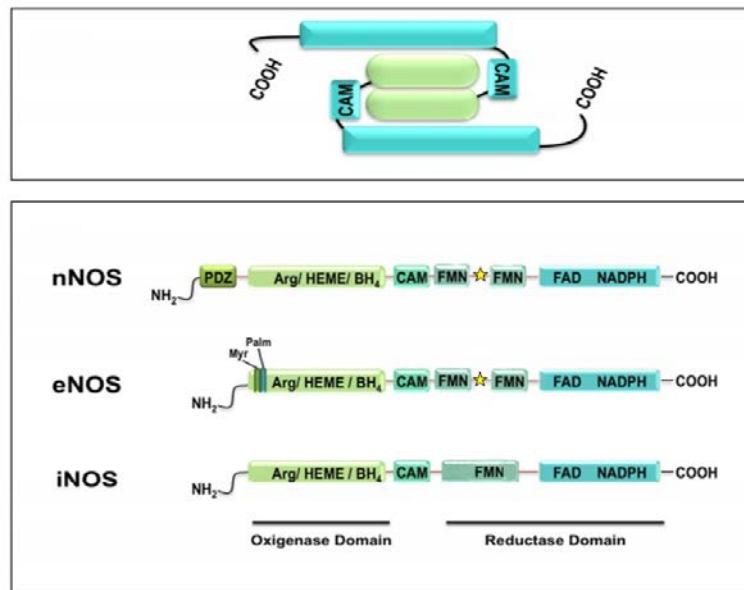


Figure 1.4: Human nNOS, eNOS and iNOS. a) Dimeric form of NOS protein. b) Human neuronal Nitric Oxide Synthase (nNOS), endothelial NOS (eNOS) and inducible NOS (iNOS) domain structure. Peculiar characteristics of neuronal and endothelia NOS are reported, respectively PDZ domain and myristoylation and palmitoylation sites, at the N-terminal of the protein. The yellow stars in the nNOS and eNOS indicate the inhibitory loop inside the FMN domain (modified from Tengan *et al.*, 2012).

Among metazoans, the NOSs amino acid sequence is highly conserved except for the N-terminal region containing the PDZ and the autoinhibitory loop. Moreover, *Nos* genes in animals show a similar genomic structure, i.e. intron positions and phases are highly conserved. At least 24 introns, in fact, are in the same position from placozoans to mammals, suggesting that these introns were already present in the ancestor *NOS* gene of metazoa (Andreakis *et al.*, 2011) (Fig. 1.5).

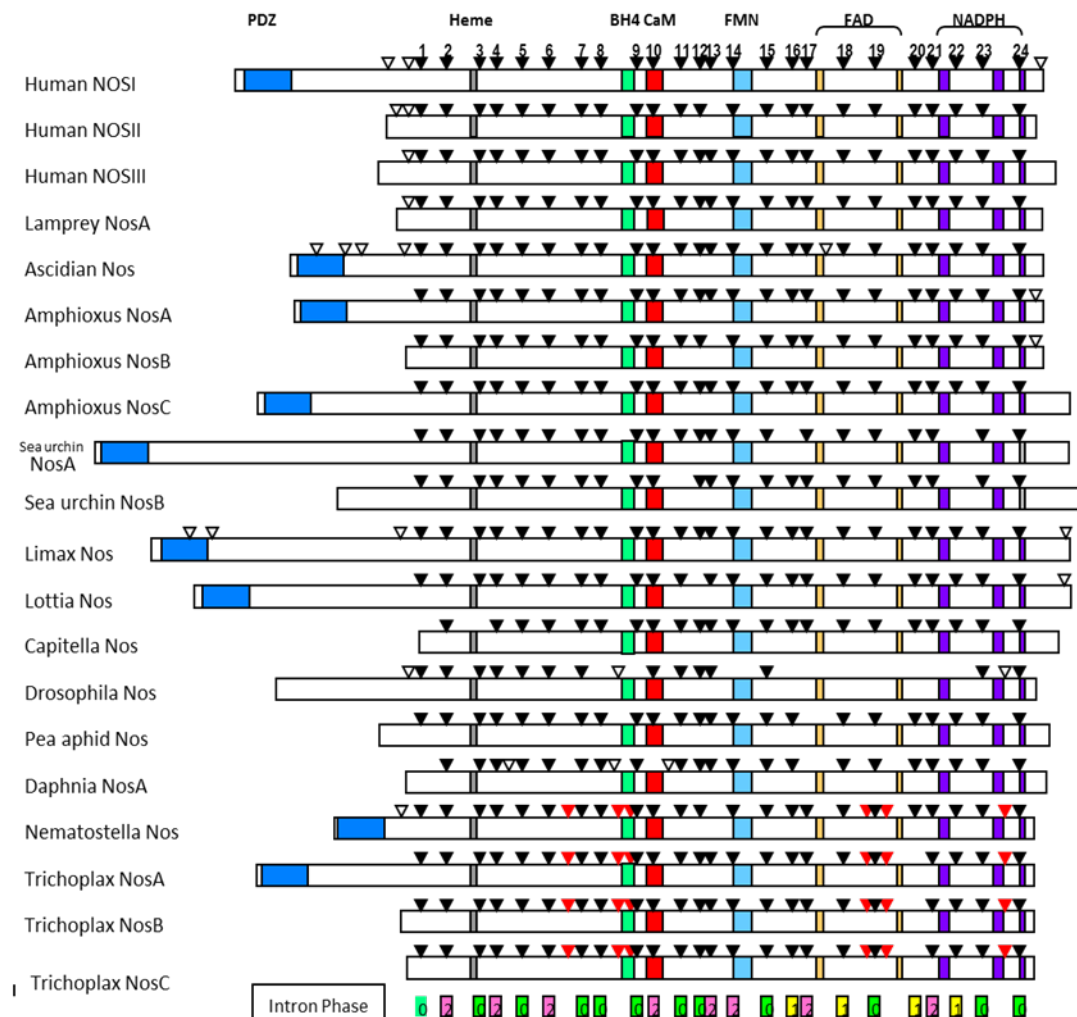


Figure 1.5: Schematic representation of animal NOS organization. Functional domains are shown as colored boxes. The positions of the introns, relative to the protein structure, are depicted by arrowheads. Black arrowheads indicate overall conserved intron positions, numbered 1–24. Red arrowheads denote intron positions conserved in no bilaterian phyla. White arrowheads denote lineage-specific introns (from Andreakis *et al.*, 2011).

1.2 THE EXPERIMENTAL MODEL SYSTEM: AMPHIOXUS

1.2.1 History of amphioxus and its anatomy

Amphioxus was firstly described by the German zoologist Peter Simon Pallas in 1767 as a mollusk of the genus *Limax* that he named “*Limax lanceolatus*”, having a streamlined body plan with both spear-shaped ends, characterized by transparent body and showing internal compartmentalized musculature (Pallas, 1767). However, Pallas’ examination was confined to the external anatomy of this animal on specimens preserved in spirit. Almost seventy years after this first description, in 1834 amphioxus was discovered for the second time in the Mediterranean sea by the Italian naturalist Gabriel Costa. A big amphioxus population was found near capo Posillipo in the north-west of the gulf of Naples (Italy) and this allowed Costa to make observations on the living animal. He recognized its affinity to fishes allied to *Cyclostomata*, a group which include lampreys and hag-fish. In his book, Costa described amphioxus as an atypical fish without eyes and nasal neither gill openings, but he mistook the structures surrounding the mouth (oral cirri) were respiratory filaments, so he suggested the name *Branchiostoma lubricum*, referring with “lubricum” to the way in which this animal slips quickly through the fingers (Costa, 1834). Two years later, William Yarrell, in his

“History of British Fishes”, was the first to describe notochord in amphioxus as a cartilaginous vertebral column and he named it *Amphioxus* (from greek “pointed on both sides”, referring to its shape) *lanceolatus* (Yarrell, 1836). Years later the scientific community adopted *Branchiostoma* (from Costa) *lanceolatum* (from Pallas) as the definitive name of the specie, while amphioxus is still used as a common name. In 1866, the embryologist Alexander Kovalevsky, looking at amphioxus and ascidian embryos, identified in both some chordates features, as the notochord, dorsal nerve cord and metameric muscle, as well as common developmental mechanisms (i.e formation of archenteron by invagination and development of nerve cord from neural folds). Therefore, he classified amphioxus and ascidians as invertebrate chordates, and this represents one of his most important contributions to chordate developmental biology.

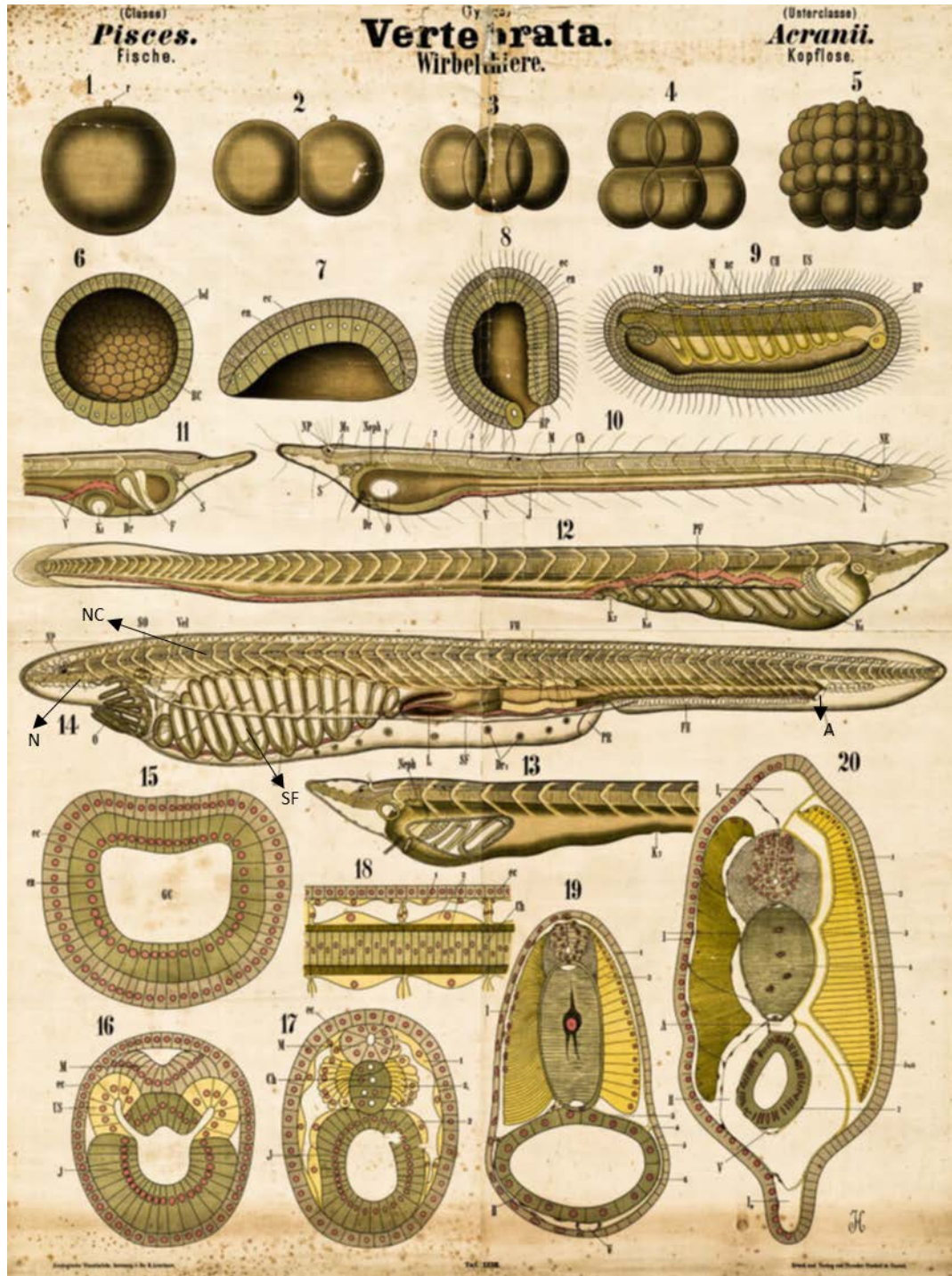


Figure 1.6: Wall chart from a Karl Georg Friedrich Rudolf Leuckart collection, the famous German zoologist and parasitologist (1822-1898). This chart shows stages through development (1–12), small adult animal (14) and their transversal sections (15-20). By the longitudinal section of the adult (14) is possible to note the four typical chordate features: pharyngeal gill slits (SF), the hollow nerve cord (NC), notochord (N) and post-anal tail [posterior to anus (A)].

Branchiostoma genus consists of about 25 species with a global distribution in shallow temperate and tropical seas close to the seashore from 0.5 to 40 m deep (Bertrand and Escriva, 2011; Desdevises *et al.*, 2011). The most well-known species for their wide use in the scientific field are: the Mediterranean species *Branchiostoma lanceolatum*, which has been mentioned earlier, also present along Atlantic coasts of Europe; the Floridian species *Branchiostoma floridae*; the Asian species *Branchiostoma belcheri* and *Branchiostoma japonicum*, present mainly in China coast at Xiamen and Qingdao.

Amphioxus is a filtered-feeding animal and its usual *modus vivendi* is to bury the whole of its body into the sand, leaving only the mouth outside with the expanded buccal cirri in order to capture food-particles through constant inflowing seawater current. Occasionally it emerges from its favorite position in the sand, especially during the reproduction period (see paragraph 1.2.3).

The anatomy of adult amphioxus is vertebrate-like. It shows all the chordate prototypic features: the dorsal cord or notochord, a dorsal hollow nerve tube, a ventral gut, a perforated pharynx with gill slits, a post-anal tail, a segmented axial muscles and gonads, a pronephric kidney and homologues of the thyroid gland and adenohipophysis (the endostyle and pre-oral pit, respectively) (Bertrand and Escriva, 2011) (Fig. 1.7). However, it lacks some typical vertebrate-specific structures, such as paired sensory organs, paired appendages, neural crest cells and placodes (Schubert *et al.*, 2006).

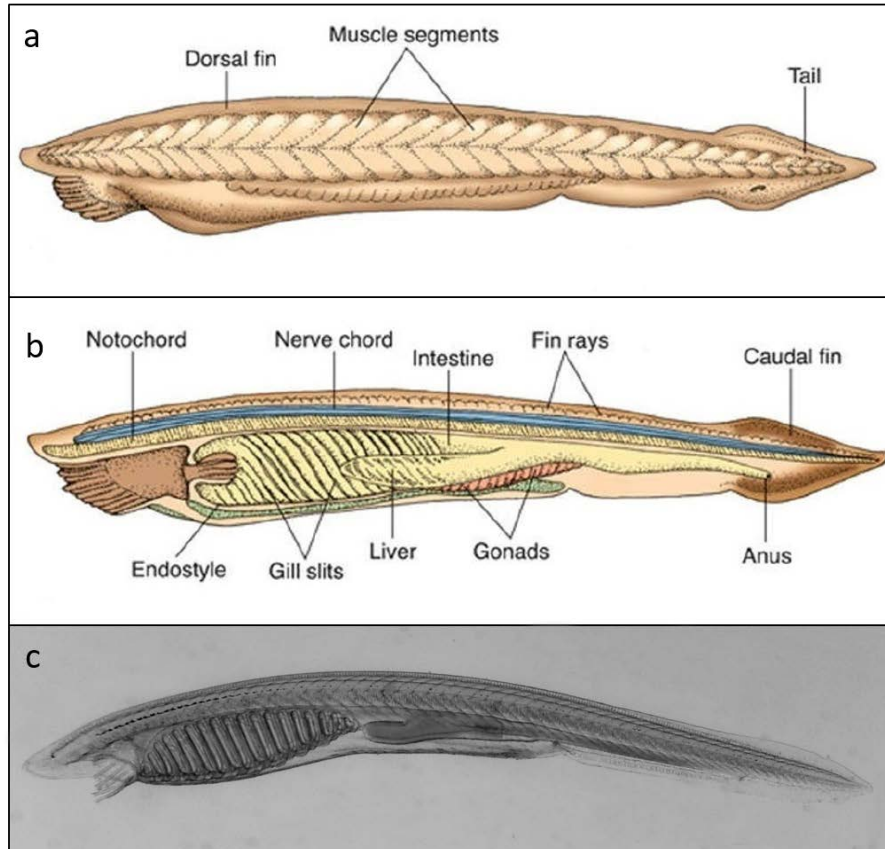


Figure 1.7: Adult amphioxus. a-b) Schematic representation of adult amphioxus anatomy; c) a picture of a small adult amphioxus.

The notochord, cylindrical muscularized rod, runs dorsally along the full length of the animal, extending anteriorly beyond the end of the nerve cord (Schubert *et al.*, 2006; Takahashi and Holland, 2004). Immediately above the notochord there is a dorsal tubular nervous system, with only a slight enlarged cerebral vesicle at its most anterior end (Lacalli, 2006). Under the notochord there is an endodermal-derived digestive tract connected anteriorly to a pharyngeal area with gill slits and ciliated gill bars. At the ventral part of the pharynx region is located the endostyle, a ciliated groove that produces mucous needed for the filter feeding mechanisms. Posteriorly to the digestive

tract there is the anal opening, beyond which occurs a short post-anal tail. The adult amphioxus possesses a laterally flattened cylindrical shape, usually not more than 6 cm in length and 0.5-1 cm in diameter. Through the transparent skin it is possible to see metameric muscle structures along the body length that enable them to swim and burrow into the sand. The sexes of amphioxus are readily distinguishable as they begin to develop their rows of testes or ovaries and it is possible to distinguish males and females by observing the gonads to the stereomicroscope (Fig. 1.8).

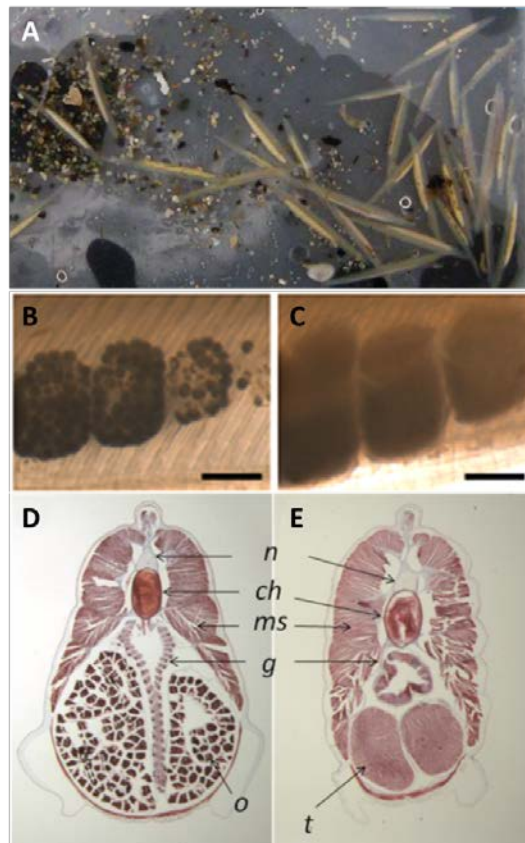


Figure 1.8: Difference between male and female gonads in adult amphioxus. A) Adult ripe amphioxus; B) Magnification of mature ovary. C) Magnification of mature testis. D) Adult *Branchiostoma lanceolatum* transversal section with mature ovary. E) Adult *B. lanceolatum* transversal section with mature testis. Abbreviations: n: neural tube, ch: notochord, ms: muscles, g: gut o: ovaris, t: testis. Scale bar of b and c is 1 mm.

1.2.2 Phylogeny

Branchiostoma is one of the genera of Cephalochordates subphylum which represents the most basal extant chordate lineage that diverged from outgroups (urochordates and vertebrates) half a billion years ago (Delsuc et al., 2006). Phylogenetic analyses based on morphological characters and rDNA 18S sequencing, placed cephalochordates as sister group of vertebrates within chordates, with tunicates basal in the phylum (Hecht *et al.*, 1987; Winchell *et al.*, 2002). But these analyses erroneously placed urochordates basal in chordates due to the fact that they are rapidly evolving, while cephalochordates and vertebrates are evolving much more slowly. However, more recent analyses of a large set of nuclear genes have established that cephalochordates represent the most basally divergent lineage of chordates (Blair *et al.*, 2005; Delsuc *et al.*, 2006, 2008) (Fig. 1.9). Therefore, cephalochordates occupy a key phylogenetic position for comparative and evolutionary studies in vertebrates (Yu and Holland, 2009).

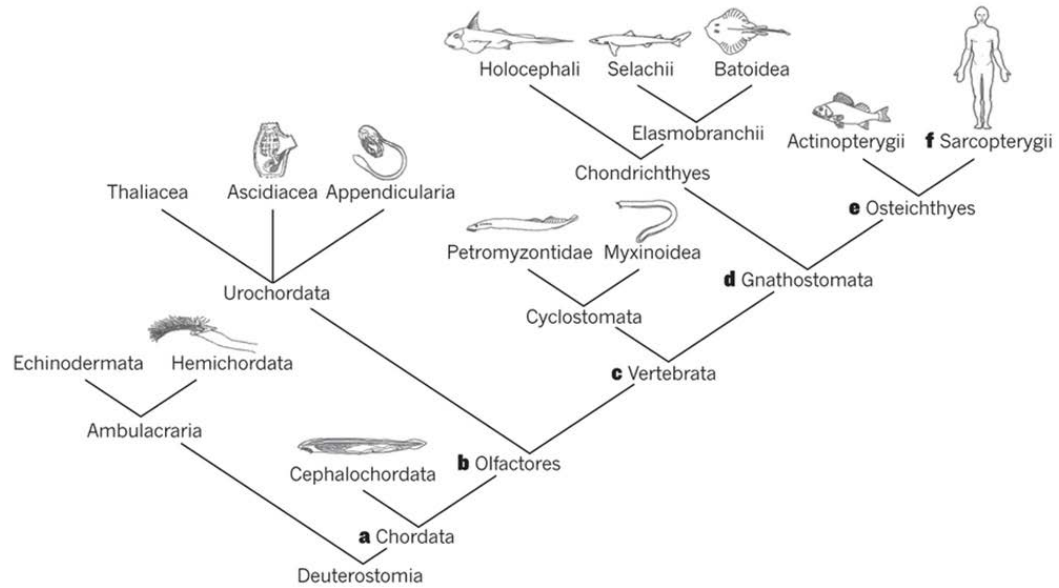


Figure 1.9: Phylogeny of deuterostomes. This phylogenetic tree shows the relationship of the major chordate and echinoderm groups (from Diogo *et al.*, 2015).

There are two other genera in Cephalochordates, *Asymmetron* and *Epigonichthys*, which are very similar to *Branchiostoma* except they have a series of gonads only on the right side of the body compared to both sides in *Branchiostoma*. A single species of *Epigonichthys* (*Epigonichthys maldivensis*) and two of *Asymmetron* (*Asymmetron lucayanum* and *Asymmetron interferum*) have been described so far; however, there may be additional cryptic species (Kon *et al.*, 2007). Nothing is known about any aspect of the *Epigonichthys* biology, while much more is known about *Asymmetron lucayanum* (Holland and Holland, 2010). A phylogenetic analysis with whole mitochondrial genome sequence revealed that *Asymmetron* diverged first, followed by *Branchiostoma* and *Epigonichthys* clades (Nohara *et al.*, 2005; Kon *et al.*, 2007; Igawa *et al.*, 2017) (Fig. 1.10). The branching order within *Branchiostoma* showed a

monophyletic relationship between *B. lanceolatum* and *B. floridae* (Igawa *et al.*, 2017; Fig. 1.10).

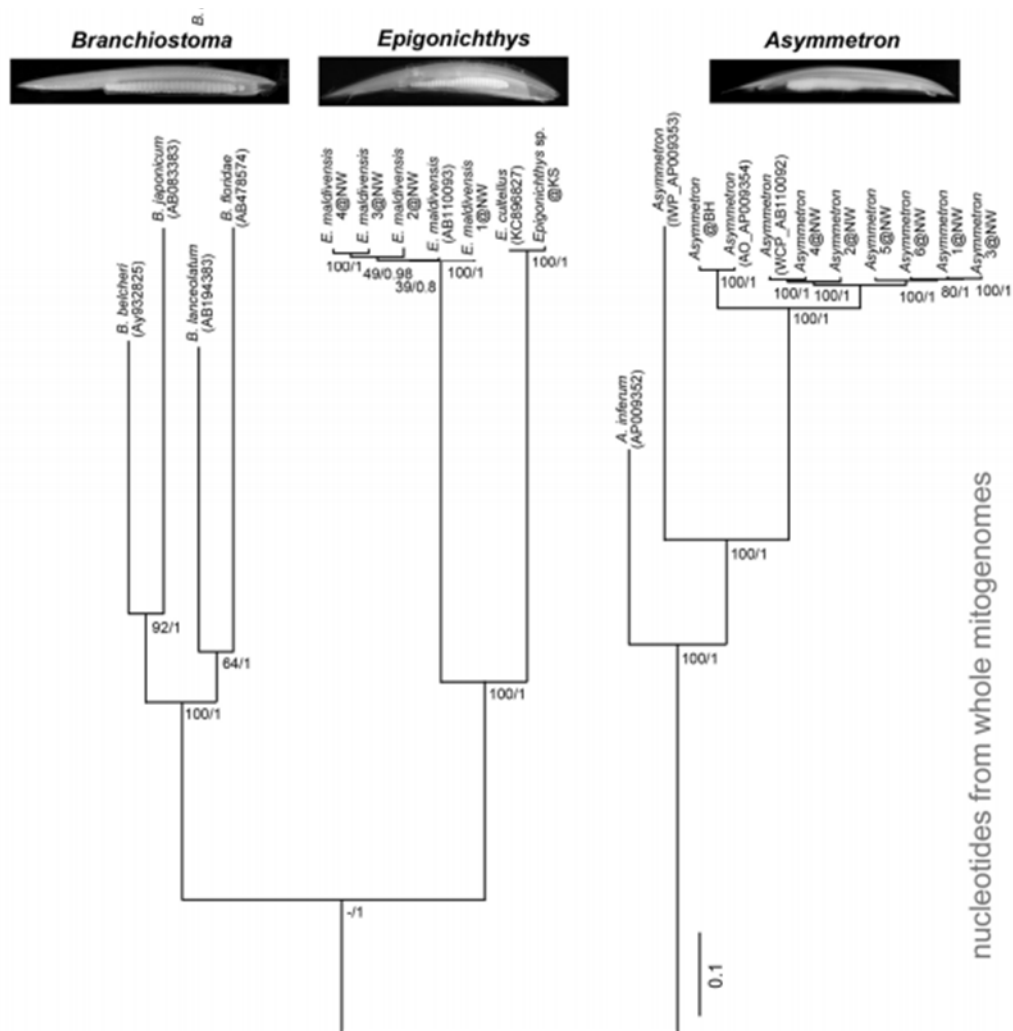


Figure 1.10: Phylogenetic relationship within the Cephalochordata. The three genera are *Asymmetron*, *Branchiostoma* and *Epigonichthys*. The phylogenetic relationship within the *Branchiostoma* genus is also reported (from Igawa *et al.*, 2017).

The genome of *B. floridae* is approximately 520 Mb in size and estimated to contain approximately 21 900 protein-coding loci (Putnam *et al.*, 2008). The amphioxus

genome exhibits considerable synteny conservation with the human genome, minimal gene losses and remarkably it has not undergone two-round whole genome duplications which occurred early in the evolution of vertebrates, known as the 2R hypothesis (Ohno, 1970; Dehal and Boore, 2005). Therefore, amphioxus generally possesses only a single paralogue (homologous genes that are derived by gene duplication from an ancestral gene) of the two to four paralogues of vertebrate genomes (Brooke *et al.*, 1998; Wada *et al.*, 1999; Cañestro *et al.*, 2007; Pascual-Anaya *et al.*, 2008; Garcia-Fernández *et al.*, 2009; Pascual-Anaya *et al.*, 2012; Pascual-Anaya *et al.*, 2013). Moreover, the “pre-duplicative” amphioxus genome possesses one representative of all the gene families that presumably existed in the ancestor of chordates, in contrast to the situation in the two other chordate subphyla, urochordates and vertebrates, which have specifically lost different members of several gene families (e.g. the homeobox-containing genes, tyrosine kinases or nuclear receptors) (D'Aniello *et al.*, 2008; Takatori *et al.*, 2008; Bertrand *et al.*, 2011). Thus, the morphological and genomic simplicity of amphioxus, together with its key phylogenetic position, make it an invaluable animal model for understanding the invertebrate to vertebrate evolutionary transition.

1.2.3 Reproduction and embryology: early and late amphioxus development

All amphioxus species have separate sexes. The reproductive period of amphioxus ranges from April to August, with slight variations depending on the species and the environmental conditions. In field, after sunset, animals move along the water column and release millions of gametes simultaneously. Zygotes develop inside their fertilization envelopes, which protect them from external aggressions during early

development. By the end of gastrulation, they begin to rotate anti-clockwise within their fertilization membrane and soon after they become neurula. At this stage, they join the planktonic community and live in it from one month to several months, depending on the species and environmental conditions (Stokes and Holland, 1995; Fuentes *et al.*, 2007). After this pelagic life period, they undergo a metamorphosis (see later in this paragraph) and slowly develop into juveniles and return to burrows in the benthic ground (Fig. 1.11). The embryology of amphioxus was first described by Kowalevsky, in 1867, who raised embryos of *B. lanceolatum* obtained in Napoli (Italy) from plankton tows. At the beginning, the major difficulty for studies of early amphioxus development was that researchers had to rely on natural spawning of the animals and rarely they obtained eggs and sperm separately in order to control the fertilization. Many misconceptions about amphioxus development arose due to the small size of amphioxus embryos and the limitations of light microscopy of that era. These errors were corrected thanks to electron microscopy studies carried out in the late 1980s. In those years, a huge amphioxus population, first described in 1980 by Wright, was rediscovered in Tampa Bay (Florida, USA) and it was found that animals could be induced to spawn in the same period that they normally spawn in field. These events have led to obtain more easily a controlled fertilization allowing the events surrounding fertilization and very early development to be studied in detail (Holland and Holland 1989, 1990, 1991, 1992, 1993).

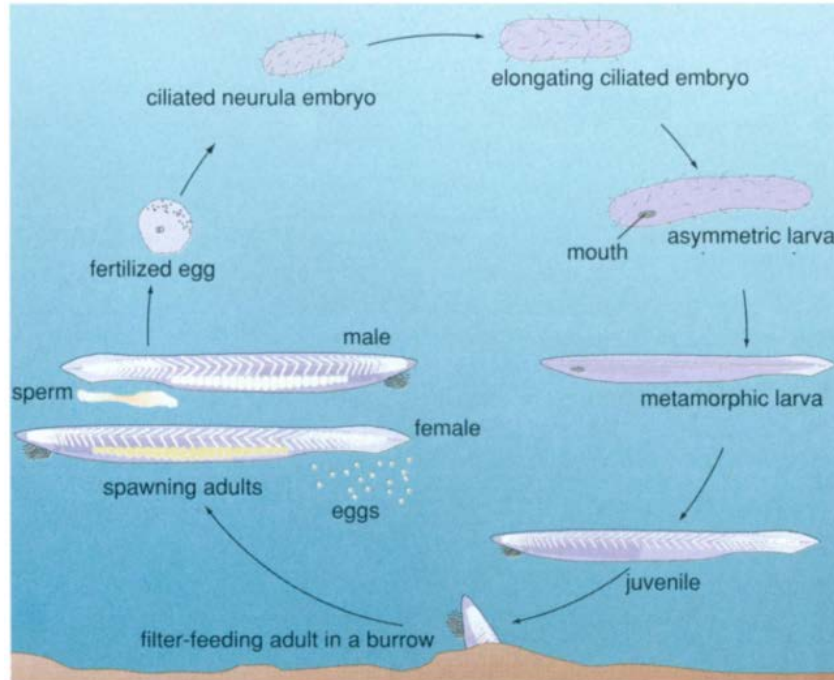


Figure 1.11: Amphioxus life cycle (Adapted from Stokes and Holland 1998)

Fertilization, cleavage and gastrulation

Amphioxus eggs are microlecithal, spherical and 100-130 μm in diameter. The spermatozoa are very small, more or less 15-20 μm in length with a rather spherical head of about 1 μm in diameter. During sperm and egg fusion, as the sperm nucleus migrates to the vegetal pole, the fertilization envelope rises (Fig. 1.12a). The egg completes the second meiotic division, the second polar body is formed and the mature egg nucleus established. In *B. floridae*, first equal cleavage starts at the animal pole more or less 60-90 minutes after fertilization, the second one occurs one hour after the first (Holland and Onai, 2012). The third cleavage divides the embryos into an animal half and a vegetal half, the animal pole of the egg becomes antero-ventral, the vegetal

pole postero-dorsal. Blastomeres are usually roughly equal in size, but sometimes vegetal blastomeres are slightly larger than animal ones (Fig. 1.12d).

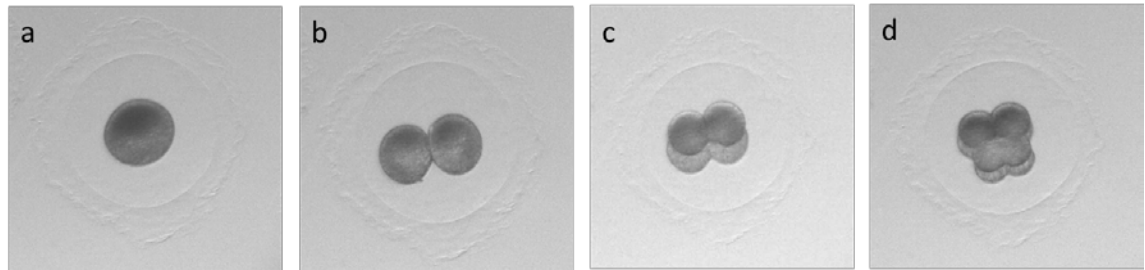


Figure 1.12: *Branchiostoma lanceolatum* cleavage phases. a) Fertilized egg with fertilization envelop; b-c-d) Zygotes at early cleavage stages, 2, 4 and 8 blastomeres respectively.

A central space among the blastomeres is formed. Virtually present in the four-cells stage, it becomes real at eight-cells stage: it is the blastocoel. The first indication of gastrulation is the flattening of the vegetal pole of the blastula. Thanks to the invagination of vegetative blastomeres, a second cavity also forms, the archenteron, which is not a true body cavity but it is considered outside and its opening is the blastopore. The blastopore constricts with the tissue at the ventral side elongating more than the dorsal side. We may now speak of the invaginating and non-invaginating layers as, respectively, endoderm (hypoblast) and ectoderm (epiblast) and of the whole structure as gastrula. After gastrulation begins, a center of very rapid division appears in the lip of the blastopore mainly on the dorsal side, this region is called germ ring. This great proliferative region contributes to add cells both to endoderm and ectoderm layers. At the late gastrula, each ectodermal cell develops a cilium and the gastrula begins to

rotate within the fertilization envelope and start to secrete hatching enzymes. At the end of gastrulation, the embryo is bilaterally symmetric, quite elongated antero-posteriorly, flattened dorsally, rounded ventrally as well as anteriorly, while at the postero-dorsal side the archenteron opens directly to the outside by a narrow blastoporal opening (it will correspond to the final anal opening in chordates). EvoDevo studies have indicated that different parts of the fertilized egg are destined to give rise to certain specific domain in adult animal in the course of a normal development (Holland and Holland, 2007; Fig. 1.13). The vegetal half of the egg and blastula is destined to become mesoderm and endoderm while the animal half ectoderm. As gastrulation progresses, the blastopore lips close bringing together the future posterior end of the embryo. During gastrulation, the animal pole shifts towards the ventral side and the future mesoderm is entirely dorsal (Holland and Holland, 2007; Holland and Onai, 2012).

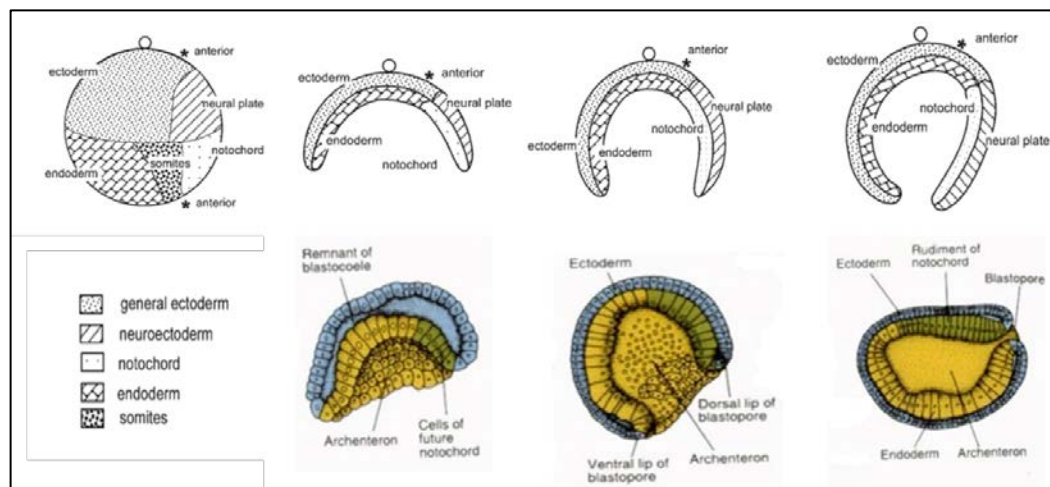


Figure 1.13: Fate map of amphioxus gastrula stage. The second polar body is at the animal pole (see circle by ectoderm). The future anterior and posterior ends of the embryo are indicated by asterisks (adapted from Holland and Holland, 2007).

Neurulation

Neurulation in amphioxus occurs in a different manner compared to those in general Vertebrates. Along the dorsal flattened surface of the late gastrula, a median strip of ectodermal cells becomes delimited from the adjacent cells that grow over it. This strip of cells is the neural plate (Fig. 1.14d-e-f). The ectoderm bounds the neural plate and it becomes elevated forming the neural folds. After ectoderm covers the neural plate, this rounds up to form a tube and the original space between the neural plate and the covering ectoderm becomes the cavity of the neural tube. At the end of neurulation, the neural plate becomes completely closed except at its anterior extremity where it remains open to the exterior in the mid-dorsal line by an opening known as neuropore (Fig. 1.14b).

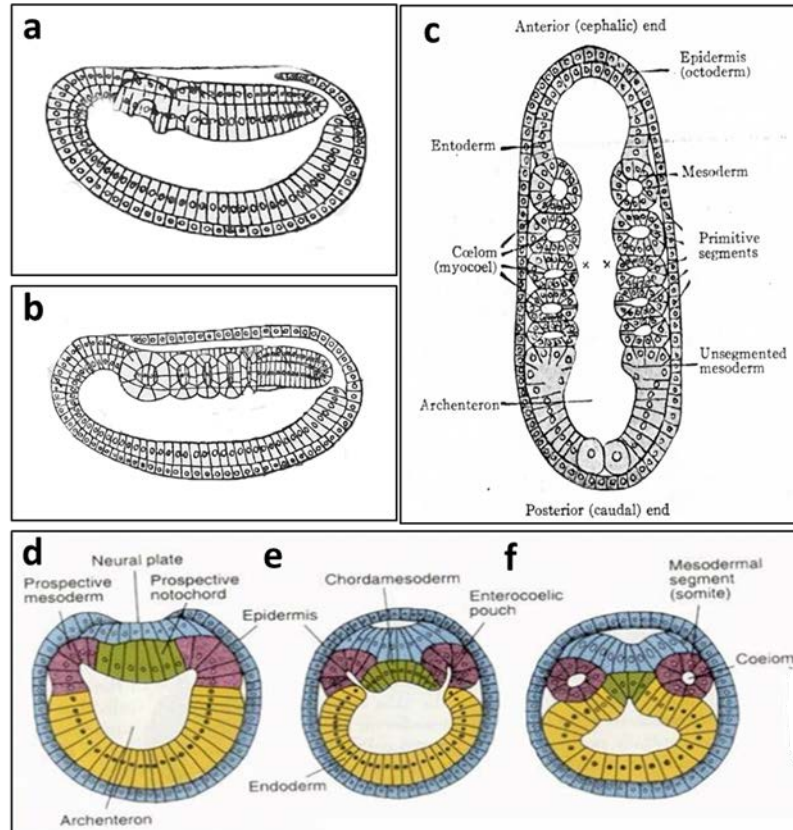


Figure 1.14: Amphioxus neurulation. a) 2 somites neurula before hatching. b) middle neurula at 5 somites stage, lateral view. c) the same neurula in b, dorsal view. d-e-f) schematic representation of neurulation process in cross-section. The territories are marked in different colors; blue: ectoderm, both neural and non-neural one; green: chorda-mesoderm; pink: somitic mesoderm; yellow: endoderm (adapted from Conklin, 1914).

Recent molecular studies performed on *B. lanceolatum* neurula stage, revealed that the amphioxus incipient neural tube is very complex with several anteroposterior (AP) and dorsoventral (DV) molecular partitions, according to axial references (Albuixech-Crespo *et al.*, 2017). Two major AP regions are observed in amphioxus neural tube: the archencephalon (ARCH) that is regionalized in a rostral hypothalamo-prethalamal primordium (HyPTh) domain (Fezf and Otx positive) and in a caudal Di-Mesencephalic primordium (DiMes) domain (Fezf negative and Otx positive); the deuteroencephalon (DEU), located posteriorly to the DiMes and containing a Rhombencephalo- Spinal primordium (RhSp) domain (Albuixech-Crespo *et al.*, 2017; Fig. 1.15).

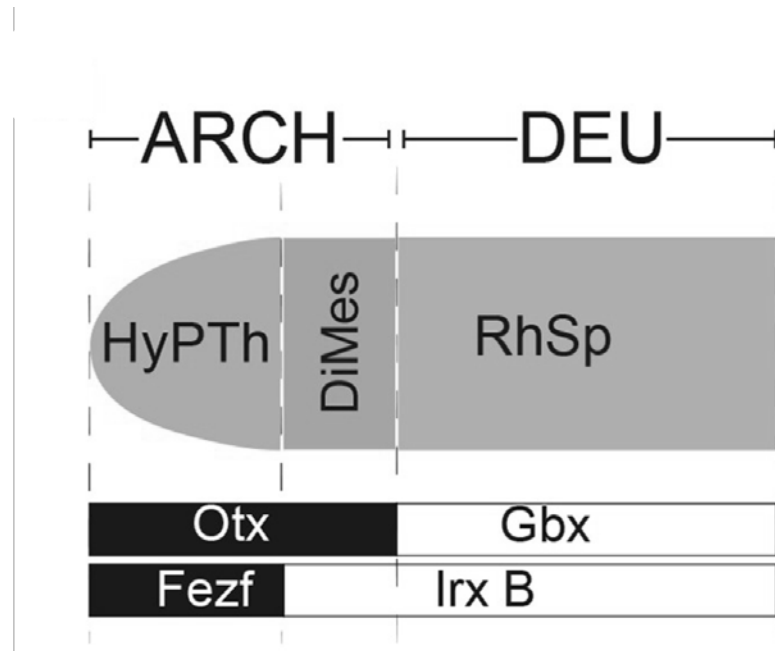


Figure 1.15: Schematic representation of the three major AP subdivisions in the amphioxus central nervous system at neurula stage and the relative expression of their key markers (Modified from Albuixech-Crespo *et al.*, 2017).

The blastopore becomes converted into the neurenteric canal, joining the lumen of the central nervous system with the lumen of the gut. This canal remains open throughout the embryonic period, until the mouth is formed. The chorda develops more slowly than the nervous system. The rudiment of this structure is a median strip of endoderm forming the roof of the archenteron, in contact with lower surface of neural plate. The chord rudiment pushes down into the archenteric cavity and appears in section concavely arched (Fig. 1.14d-e-f). At nine or ten somite formed stages, the notochord becomes completely cut off from the endoderm and close to forming a cave tube. At the neurula stage, a third intermediate layer, the mesoderm, appears. The formation of somites in amphioxus begins very early, before hatching, when mesoderm first

separates from endoderm as a pair of longitudinal band that later become divided into the first two somites in the anterior part (Fig. 1.14a). The portion of archenteric space that remains inside the forming somites it is called enterocelic cavity (Fig. 1.14c). After hatching, mesodermal somites posterior to the two formed before, continue to form successively in the elongating mesodermal folds until the formation of fourteen pairs of somites (Fig. 1.14c). Posterior to these, in the tail bud, undivided regions of mesoderm remain from which additional somites will be formed during the larval period. By the time five or six pairs of somites are formed, they begin to show alternation that is characteristic of the adult, in particular, left member comes to lie in advance of the right.

Larvae and metamorphosis

The duration of the larval period in *B. lanceolatum* is roughly about three months during which the larva is free swimming. Development is very slow and consists largely in the elaboration and modification of structures appeared before. The dorsal organs such as the neural tube, the notochord and the muscular lamella do not much change morphologically but become structurally more complex (Hirakow and Kajita, 1994). The central nervous system (CNS) of lancelets consists of a tubular nerve cord, located directly above the notochord and that extends from the anterior cerebral vesicle (CV) to the tip of the caudal fin. Comparisons of developmental gene expression together with three-dimensional reconstructions from serial TEM have shown that the amphioxus brain has homologues of most of the features of the vertebrate brain (Lacalli, 1996; Candiani *et al.*, 2012; Albuixech-Crespo *et al.*, 2017). These include a

diencephalic forebrain with a pineal homologue, a small midbrain (tectum), a hindbrain and a spinal cord (Lacalli, 1996; Candiani *et al.*, 2012; Albuixech-Crespo *et al.*, 2017) (Fig. 1.16). Forebrain and midbrain together form the CV that is extended almost to the boundary between somites 1 and 2 (Candiani *et al.*, 2012). The anterior landmark of the CV is the frontal eye, which has been proposed to be homologous to paired eyes of vertebrate. This structure consists of a pigment cup with four rows of neurons: sensory neurons, probably photoreceptor cells, that are closely related with nerve cells that communicate with the dendrites of neurons involved in the locomotory control center (Wicht and Lacalli, 2005). In the forebrain, an important structure is the lamellar body of the infundibular region. The lamellar body is generally accepted as a homolog of the vertebrate pineal organ and so, it is may responsible of the circadian rhythm. The posterior landmark of the CV is the primary motor center (PMC) that contains the anterior most motoneurons in the nerve cord and a number of large premotor interneurons.

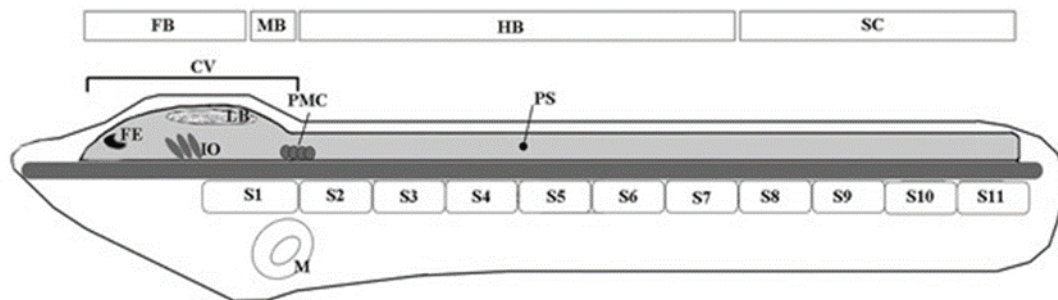


Figure 1.16: Schematic representation of the amphioxus larval nervous system. The different regions in which the amphioxus nervous system has been subdivided have been highlighted. FB: forebrain; MB: midbrain; HB: hindbrain; SC: spinal cord; PS, first pigment spot; S, somite; N, notochord; M, mouth; FE: frontal eye; IO: infundibular organ; LB: lamellar body; PMC: primary motor center; CV: cerebral vesicle (from Candiani *et al.*, 2012),

A hindbrain-like region extends from the posterior margin of the PMC to the boundary of somites 7 and 8; beyond this region there is a territory corresponding to the vertebrate spinal cord (Candiani *et al.*, 2012). The peripheral Nervous System (PNS) of amphioxus is composed of several types of neurons, and at least two types of epidermal sensory cells, widely distributed along the epithelium surface. The Type I receptors are primary sensory neurons having axons projecting to CNS, whereas the Type II receptors are axon-less secondary sensory neurons, putative chemoreceptors, with synaptic terminals arising at short distances from the cell body (Wicht and Lacalli, 2005; Candiani *et al.*, 2010).

The embryos continue to elongate and showing marked asymmetry in particular in the pharyngeal region (Fig. 1.17). The end of the larval period is marked by an extensive metamorphosis that leads to a “symmetrization” of the anterior portion of the body. The gill slits of the right and left sides develop independently, those of the left side first. The first twelve-fifteen gill slits are called “primary gill slits” and, at this stage, they are metameric and correspond with the somites. Then, the “secondary gill slits” appear also on the right side of the pharynx and dorsal to the primary series. The rudiment of the gill slits enlarges and become perforated. The dorsal margin of the gill slits moves to the ventral part and, as this migration is going on, gill slits become divided by a downward extension that forms the tongue bar of the completed structure of the adult. One of the characteristic organs of the larval stage is the club-shaped gland that is limited to this developmental stage (Goodrich, 1930). This structure arises as an evagination from the pharyngeal endoderm in late embryos and soon develops into a tube connecting the pharyngeal lumen with the external environment; the external opening is a pore in the

epidermis, near the anteroventral edge of the mouth (Hatschek, 1893). Different theories about club-shaped gland function were proposed during the years (Olsson 1983; Gilmour 1996; Holland and Yu 2002), but what seems to be the most accepted one is that this gland, together with the endostyle (see later in this paragraph), produces a thin vertical curtain of mucus to capture ingested particles and then transport them toward the most posterior gut regions (Holland *et al.*, 2009). Following the apoptotic destruction of the club-shaped gland during metamorphosis, the endostyle of juvenile and adult amphioxus presumably becomes the major (or even exclusive) source of mucus for capturing food particles in the pharyngeal lumen. The endostyle is an organ that originates as a thickening of the pharyngeal wall and it is located in front of the club-shaped gland. As well as producing mucus, it selectively binds iodine, and synthesizes and releases thyroid hormones and for this reason it was compared with vertebrate thyroid (Fredriksson *et al.*, 1984). This organ persists in adults as a major site for iodination (Ericson *et al.*, 1985), possibly because of the continued synthesis of thyroid hormones influencing tissue growth and maintenance in the juvenile and adult amphioxus. After metamorphosis, the endostyle moves from the right side of the pharynx to the ventral floor and expands longitudinally (Willcy, 1891; Paris *et al.*, 2008; Paris *et al.*, 2010; Kaji *et al.*, 2013).

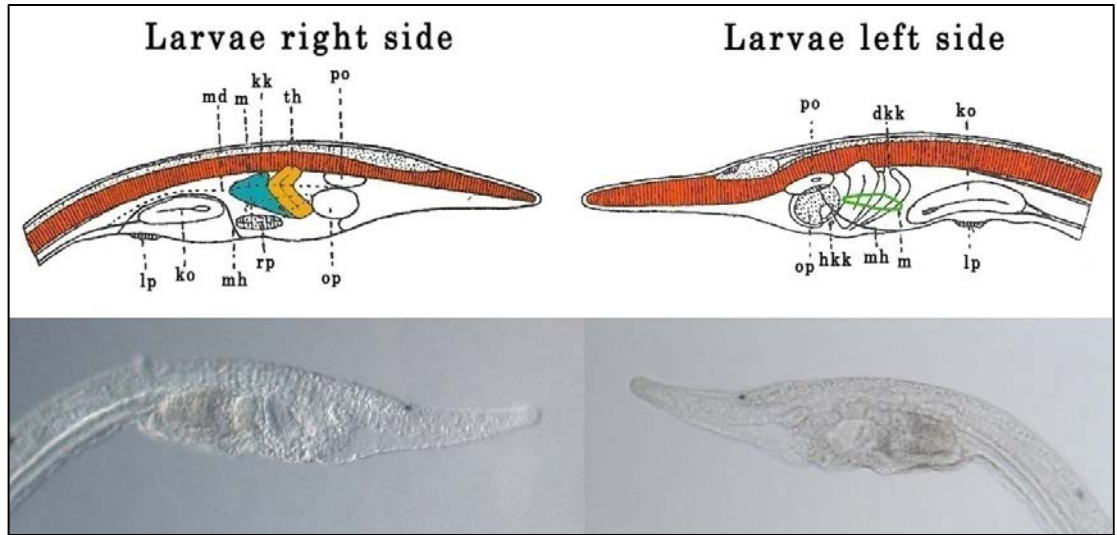


Figure 1.17: Schematic representation and morphology of amphioxus larva with one gill slit, seen from right side and left side. Abbreviations: dkk, intestinal opening of the club-shaped gland; hkk, cutaneous opening of the club-shaped gland; kk, the club-shaped gland; ko, first gill pouch; lp, left post-oral papilla; m, mouth; md, mid-ventral line of intestine; mh, ventral median line of epidermis; op, unpaired papilla; po, pre-oral pit; rp, right papilla; th, endostyle (adapted from Barrington, 1965).

Unlike in other animals, the mouth in amphioxus larva develops on the left side. Kaji and collaborators suggest that amphioxus mouth develops from the first postero-ventral outgrowth of the left somite, as a pocket, called ‘oral mesovesicle’, that opens initially into the pharynx and then into the outside environment (Kaji *et al.*, 2016) (Fig. 1.18). This process is different from what happens in other deuterostomes (Soukup *et al.*, 2013) but the involvement of mesodermal vesicles or their derivatives was found during development of other amphioxus organs such as pre-oral pit and gill slits. Moreover, the development of the oral mesovesicle is under control of the Nodal-Pitx signaling pathway, which governs asymmetric development of the whole larval body in amphioxus (Soukup *et al.*, 2015).

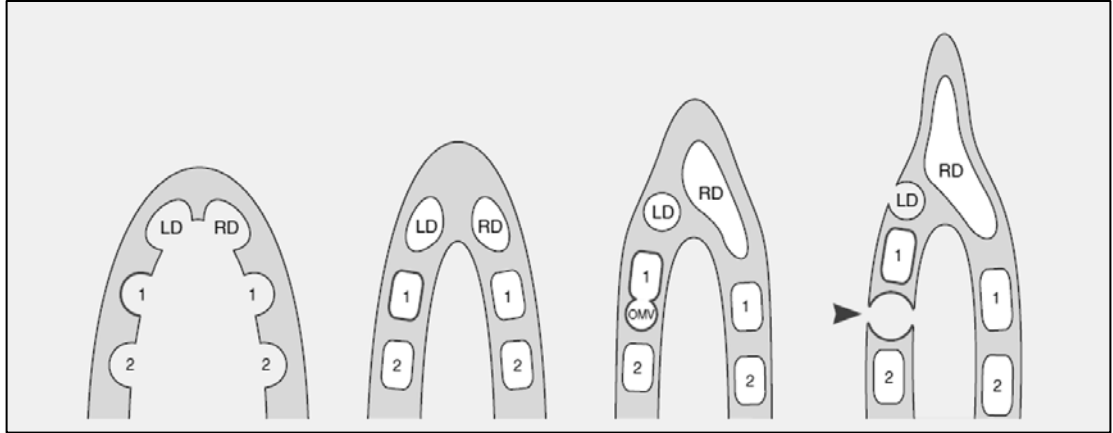


Figure 1.18: Amphioxus mouth development hypothesis according to Kaji and collaborators (2016). LD: left structures; RD: right structures; OMV: oral mesovesicle. Red arrow indicates mouth opening (adapted from Soukup and Kozmik 2016).

1.3 NITRIC OXIDE AND NITRIC OXIDE SYNTHASES IN AMPHIOXUS

Andreakis and collaborators, in 2011, have demonstrated the existence in *B. floridae* genome of three distinct amphioxus genes coding for three different NOS proteins, called *NosA*, *NosB* and *NosC* (Andreakis *et al.*, 2011) (Fig. 1.5). *NOSA* and *NOSC* contain the PDZ domain and the autoinhibitory loop (Fig. 1.5), so they were identified as neuronal NOSs. *NOSB* does not contain both elements, thus indicating its inducible feature. Evolutionary analysis showed that there is not a direct relationship between the three amphioxus NOS and the vertebrate eNOS, nNOS and iNOS but they resulted to be the product of a lineage-specific duplication event (Fig. 1.19) (Andreakis *et al.*, 2011).

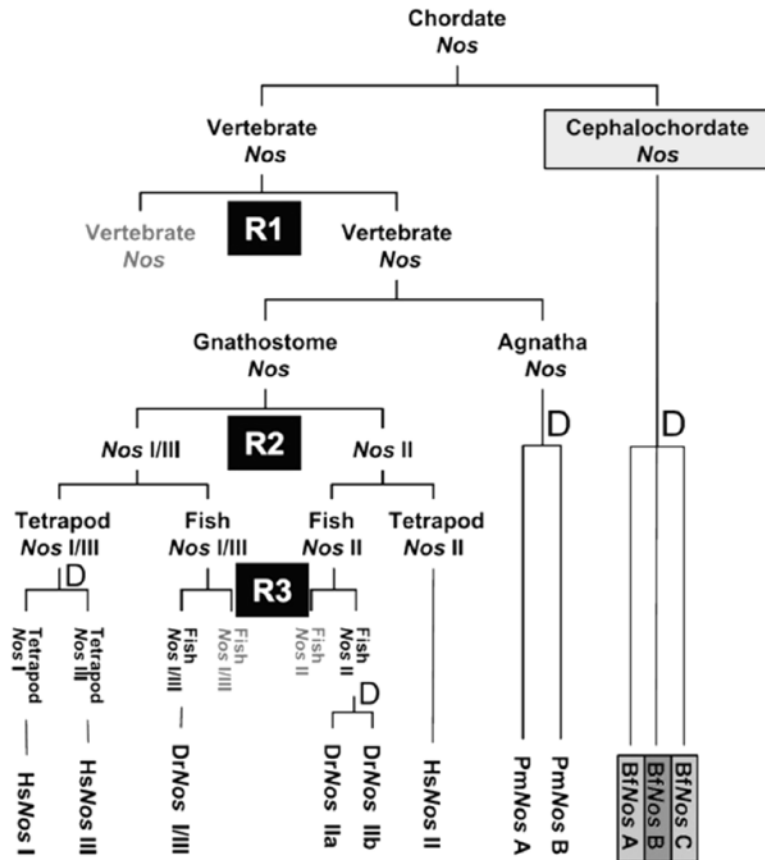


Figure 1.19: Evolutionary events regarding NOS genes in chordates. There are two different evolutionary events: whole-genome duplications (R) and lineage-specific duplications (D). Inferred gene losses during vertebrate evolution are depicted in gray (adapted from Andreakis *et al.*, 2011).

Nevertheless, before these structural evidences, some studies about NOS genes and proteins in amphioxus were performed. In 2006, Godoy and collaborators performed an immunostaining experiment on *B. floridae* larvae using a universal anti-NOS antibody directed against the C-terminal epitope DQKRYHEDIFG that is highly conserved among the different NOS proteins in vertebrates, insects and crustaceans (Pollock *et al.*, 2004). Immunostaining analyses revealed NOS presence in the larval intestine that

seems to be the major organ for NO synthesis and in the dorsal region of the club-shaped gland (csg) (Godoy *et al.*, 2006) (Fig. 1.20).

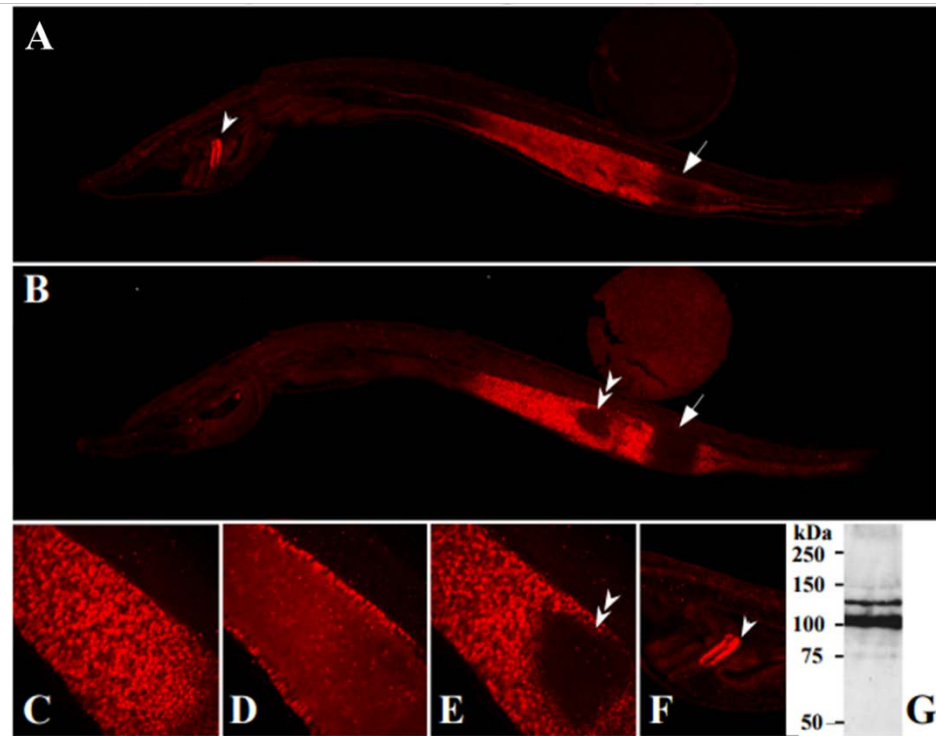


Figure 1.20: Whole-mount immunostaining of 48 hpf *Branchiostoma floridae* larvae with a universal anti-NOS antibody. (A) Right-sided view; (B) Left-sided view; (C-E) Magnified view of the right side, right and left side of the gut NOS localization; (F) Detail of the NOS staining in the dorsal region of the club-shaped gland; (G) Western blot analysis of larval protein extract with the same universal NOS antibody used for immunostaining (from Godoy *et al.*, 2006).

Other studies were performed on adult specimens. Chen and collaborators, in 2008, investigated the expression of dimethylarginine dimethylaminohydrolase (DDAH) and *Nos* genes in adult amphioxus *Branchiostoma belcheri tsingtauense* (Chen *et al.*, 2008). Both genes were detected in the neurons lining the central canal of the neural cord, in the wheel organ, in the epithelial cells of gut and midgut diverticulum, in the ciliary

epithelial cells on the inner side of branchial lamellas, in the endostyle, in the ovary and in the epidermis cells of metapleural fold and in the macrophages in the lymphoid cavities of metapleural fold (Fig. 1.21). The authors hypothesized that this co-expression may be due a conserved role of DDAH in the regulation of NO synthesis (Chen *et al.*, 2008).

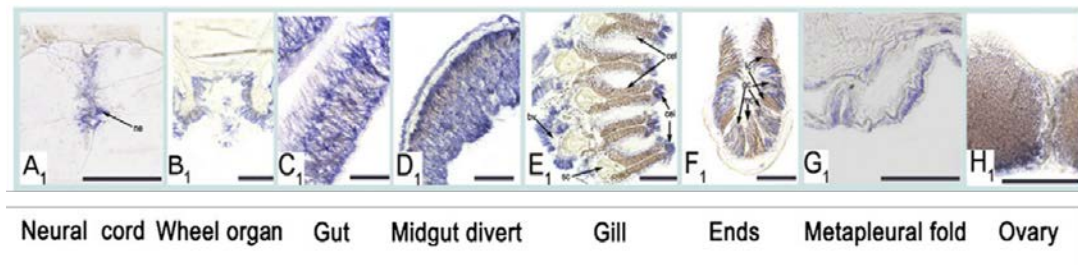


Figure 1.21: NOS expression pattern in different tissues of adult amphioxus (from Chen *et al.*, 2008).

In 2011, in a study aimed to understanding the evolution of the primordial adaptive immune system, Lin and collaborators reported the expression pattern of *Nos* in amphioxus *B. belcheri* after stimulation of the immune system by *Staphylococcus aureus* injection. *Nos* expression was detected in gill epithelium and branchial coelom macrophages, in the intestinal epithelium and perienteric coelom macrophages, in the metapleural fold epidermis and in metapleure coelom macrophages (Fig. 1.22) (Lin *et al.*, 2011).

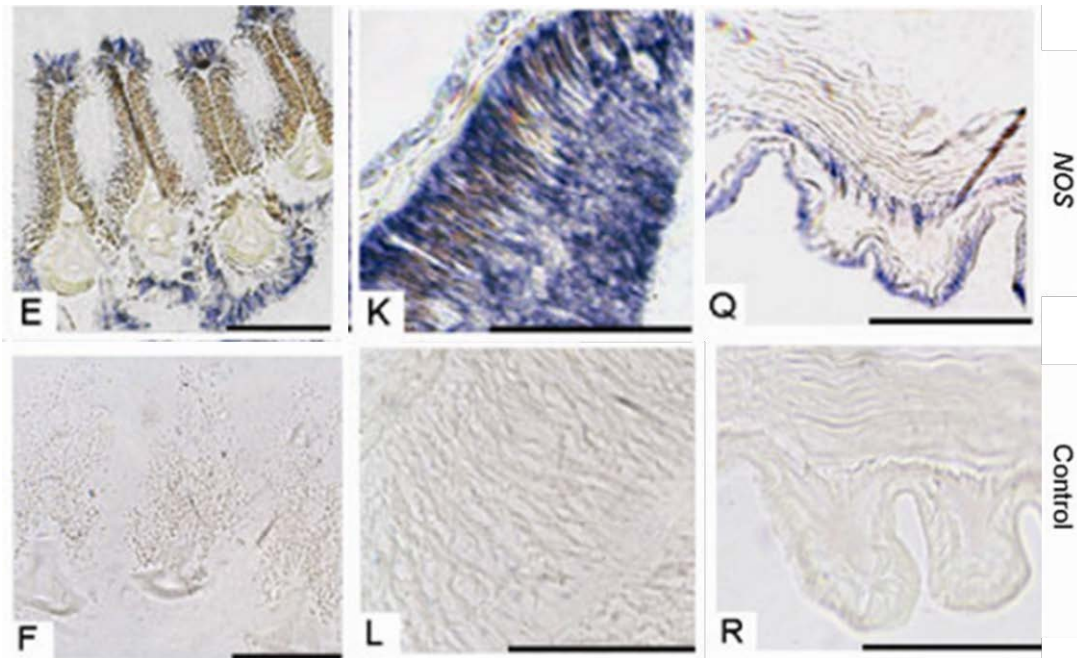


Figure 1.22: Amphioxus *Nos* expression pattern by *in situ* hybridization experiments in adult tissues. E-F) gill epithelium and branchial coelom macrophages; K-L) intestinal epithelium and perienteric coelom macrophages; Q-R) metapleural fold epidermis and metapleure coelom macrophages (adapted from Lin *et al.*, 2011).

Recently, the *B. lanceolatum* NOS genes expression pattern during embryonic and larval development were described. The whole-mount *in situ* hybridizations (WISH) presented by Annona *et al.* (2017) showed that *NosB* was expressed early in development in endoderm (Fig. 1.23b-d) while later on, and following *NosB* turning off. *NosC* expression was detected in nervous system and in the club shaped gland, from mid-neurula stage in few cells in the anterior part of the neural plate, slightly posterior to the neural pore (Fig. 1.23e); at pre-mouth larva in neural tube until the pigment spot (Fig. 1.23f); at 3 days post fertilization (dpf) larvae the *NosC* expression in the neural tube disappeared almost completely, remaining in few cells located in the most ventral

and posterior part of the cerebral vesicle and, also, expression in the club-shaped gland was found (Fig. 1.23g). *NosA* was not expressed during embryonic development (Annona *et al.*, 2017).

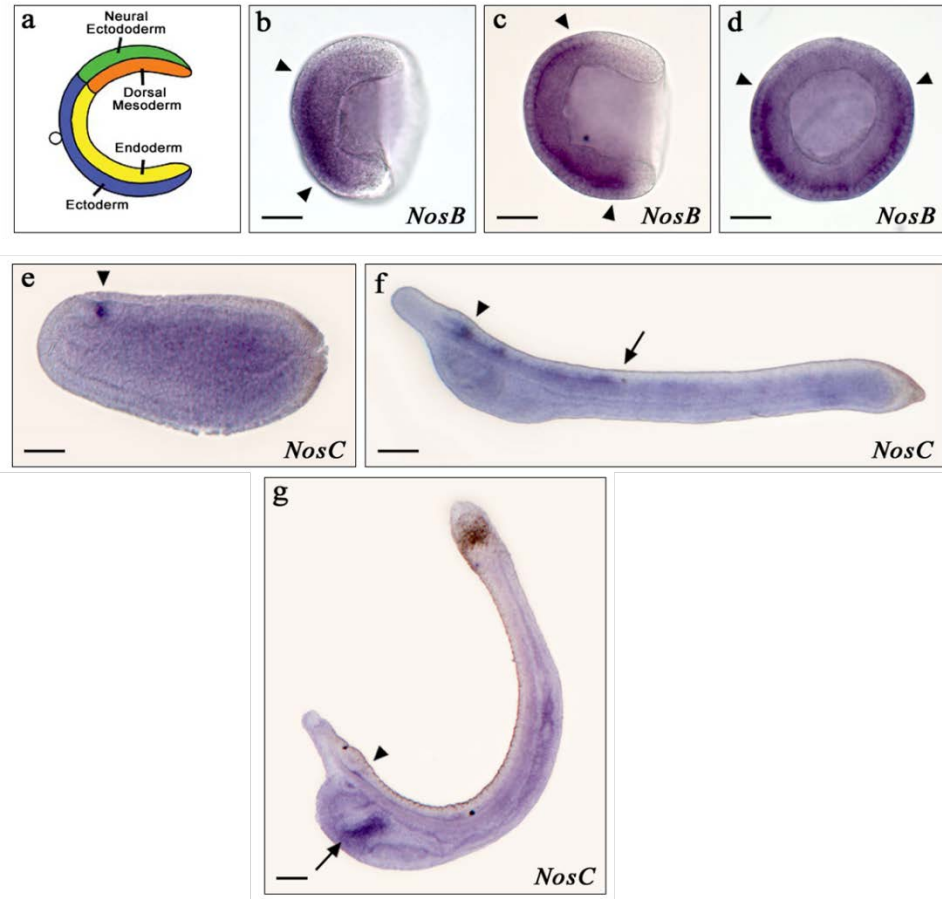


Figure 1.23: *Branchiostoma lanceolatum* *NosB* and *NosC* expression during embryonic development. a) Fate map of amphioxus gastrula stage; b) *NosB* expression at early gastrula, lateral view; c-d) *NosB* expression at mid-gastrula stage, respectively lateral and blastopore view. Arrowheads indicate the limits of the positive signal e) *NosC* expression at neurula in neuropore (arrowhead), lateral view; f) *NosC* expression at pre-mouth stage in brain vesicle (arrowhead) and in neural tube (posterior limit, arrow); g) *NosC* expression at 3 dpf larva in the brain vesicle (arrowhead) and club-shaped gland (arrow). Scale bars: 50 μ m (adapted from Annona *et al.*, 2017).

1.4 NEURONAL NOS GENE TRANSCRIPTIONAL REGULATION

The control of NOS activity is mediated by allosteric enzyme regulation, post-translational modification and subcellular targeting of the enzyme. Nevertheless, it is more important to note that NOS levels are dynamically regulated by transcriptional activity. The iNOS gene is predominantly regulated at the level of transcription by synergistic combinations of proinflammatory cytokines and bacterial wall products. Changes in eNOS mRNA levels following endothelium activation are mediated by altered rates of transcription as well as by the intriguing process of changes in mRNA stability. Instead, the nNOS mRNA is structurally diverse as a consequence of alternative promoters and alternative splicing occurring in a cell-type- and stimulus-dependent manner in various tissues (Boisesl *et al.*, 2003; Bros *et al.*, 2006). In vertebrates, several different NOS1 exon 1 variants were described (Fig. 1.24A; Oberbaumer *et al.*, 1998; Sasaki *et al.*, 2000; Bachir *et al.*, 2001; Boissel *et al.*, 2003). In human, the brain shows a predominant presence of exons 1c-d, 1f, and 1g while in brain-derived cell lines the 1a isoform show the higher activity (Saur *et al.*, 2002; Bros *et al.*, 2006). In skin, exons 1d, 1b and 1f are expressed at significant levels while in skeletal muscle and heart there is a marked expression of the exon 1d (Bros *et al.*, 2006). Computational analyses revealed the presence of several potential transcription factor's binding sites (TFBS) in the 5' flanking genomic regions of different exon 1 (Fig. 1.24B; Jeong *et al.*, 2000; Bros *et al.*, 2006).

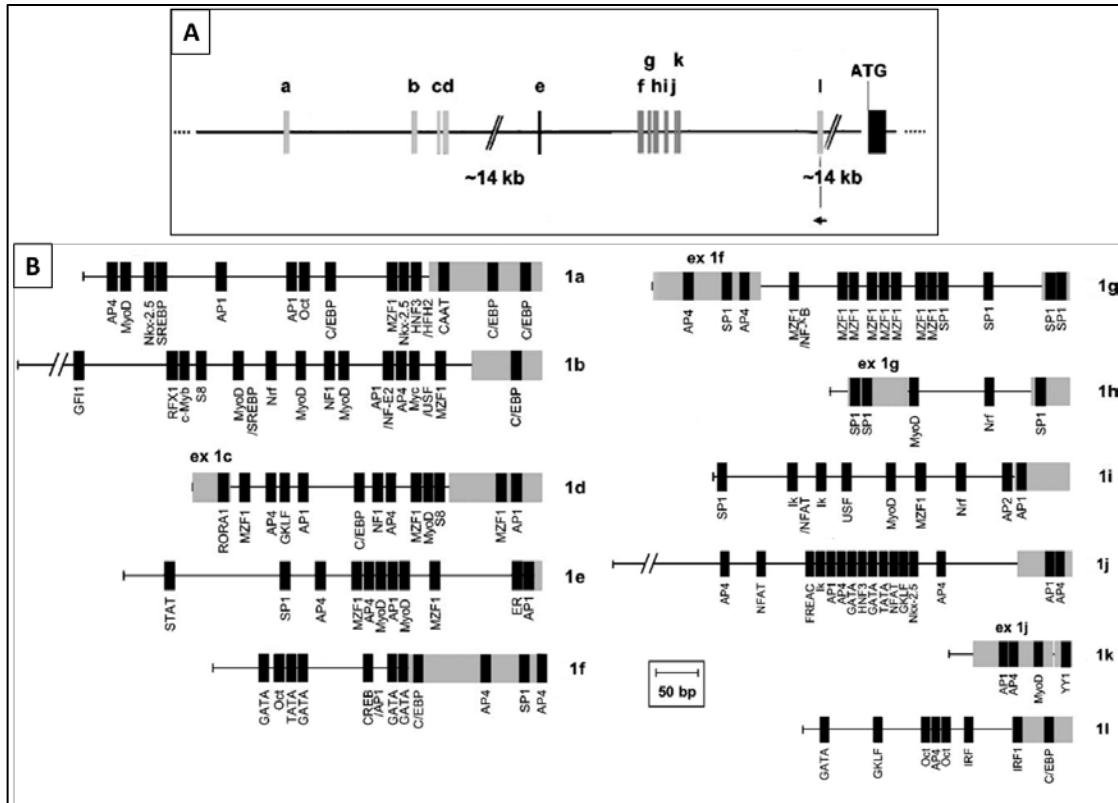


Figure 1.24: Organization of the 5' end of human NOS1 gene. A) Schematic representation of the 5' end of the human NOS1 gene showing the localization of the 12 distinct first exons (1a to 1l in grey) and of exon 2 (in black). The position of the translation start codon (ATG) on exon 2 is indicated. B) Scheme of potential transcription factor binding sites within the 5' flanking genomic regions of the various NOS1 promoters. Included exonic sequences are indicated by gray boxes. Potential transcription factor binding sites are indicated by black boxes and labeled (Adapted from Bros *et al.*, 2006).

A number of studies proved that transcription factors of stimulatory protein (Sp) and zinc finger (ZNF) families transactivate the nNOS exon 1c promoter (Saur *et al.*, 2002). It was described, in particular, the presence of a conserved cAMP response elements (CREs), within nNOS promoter, of potential functional importance. This was demonstrated thanks to experiments using dibutyl-cAMP, or others cAMP-activating agents, that increased the activity of the human NOS1 promoter related to exons 1f and

1g (Wang *et al.*, 1994; Hall *et al.*, 1994; Zhao *et al.*, 1999; Bachir *et al.*, 2001; Boissel *et al.*, 2003; Bros *et al.*, 2006). Moreover, Ca²⁺ influx also dynamically regulates nNOS expression through the binding of cAMP response element binding protein (CREB) to these CREs (Sasaki *et al.*, 2000). In brain cells, it was demonstrated that nNOS expression was induced by nerve growth factor (NGF). Deletion studies indicated that six potential ETS binding sites as well as four potential AP1 binding sites are present in the alternative promoters 1f and 1g and the activation of ETS and/or AP1 transcription factors by the RAS-RAF-MAP kinase cascade can contribute to the NGF-mediated induction (Rife *et al.*, 2000). It was also identified an active NF-κB responsive element in nNOS 1f promoter (Fig. 1.25) using chromatin immunoprecipitation assay with p65 or p50 antibody; this NF-κB responsive element was crucial for the high activity of nNOS 1f promoter in neurons (Li *et al.*, 2007).

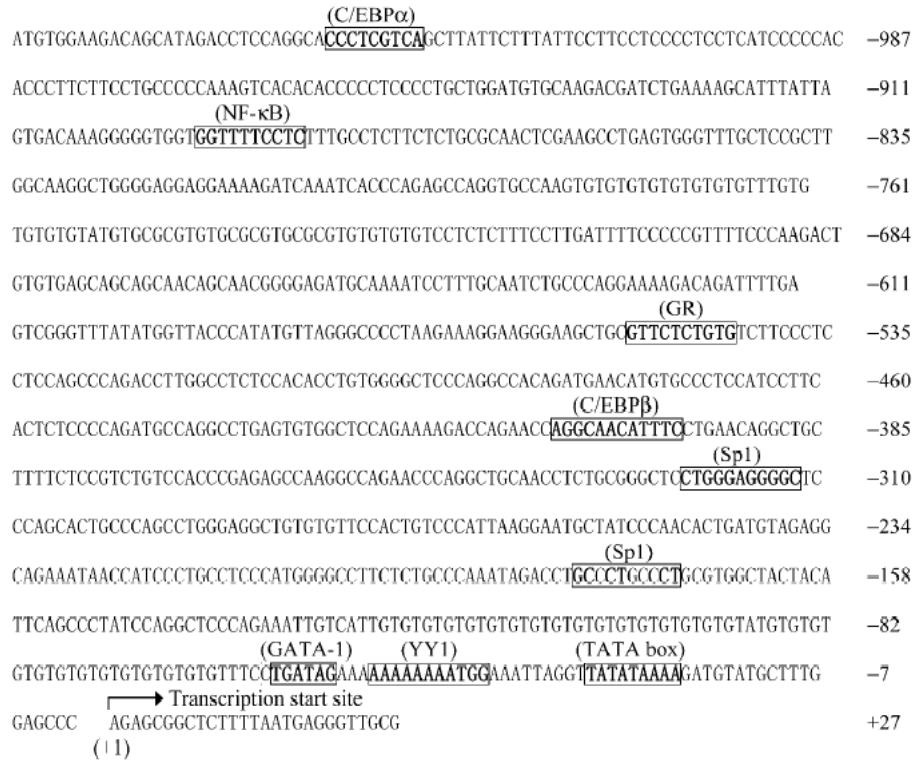


Figure 1.25: Putative *cis*-acting elements within neuronal Nitric Oxide Synthase (nNOS) 1f promoter. A typical TATA-box motif is shown to be located between -28 and -20, and several potential transcription factor-binding sites were revealed. NF- κ B: nuclear factor κ B; C/EBP: CCAAT/enhancer-binding protein; GR: glucocorticoid receptor; Sp1: stimulatory protein 1; YY1: Yin (From Li *et al.*, 2007)

1.5 TRANSCRIPTIONAL GENE REGULATION

1.5.1 Conserved non-coding regions and their gene regulatory function

Both vertebrate and invertebrate genomes contain regions that do not codify for a gene product and, nevertheless, have remained highly conserved across millions of years of evolution. Cross-species sequence comparison was shown to be an efficient approach to identify putative functional regions in non-coding DNA. Functional sequences generally stand out as more “conserved” than non-functional sequences that are subject to genetic

drift and become increasingly different between species with increasing phylogenetic distance. These regions are called conserved non-coding elements (CNEs) and are often highly associated with transcription factor binding sites (TFBSs). Several studies have also demonstrated that CNEs can function as enhancers in various developmental contexts. Both these evidences have led to the view of CNEs as *cis*-regulatory elements (CREs) driving spatial-temporal gene expression, especially during embryonic development (Nobrega *et al.*, 2003; Johnson *et al.*, 2004; Teng *et al.*, 2004; Woolfe *et al.*, 2005; Pennacchio *et al.*, 2006; Li *et al.*, 2010). Therefore, these sequences may be conserved because of a consistent gene regulatory function. These regulatory regions can lay: 1) upstream or downstream the target gene, 2) inside the introns of the target gene, 3) inside the introns of unrelated bystander genes (Fig. 1.26). CNEs driving the expression of these target genes without affecting unrelated bystander genes and they are all maintained in syntenic blocks due to the requirement for regulatory elements to remain in *cis* with their target genes.

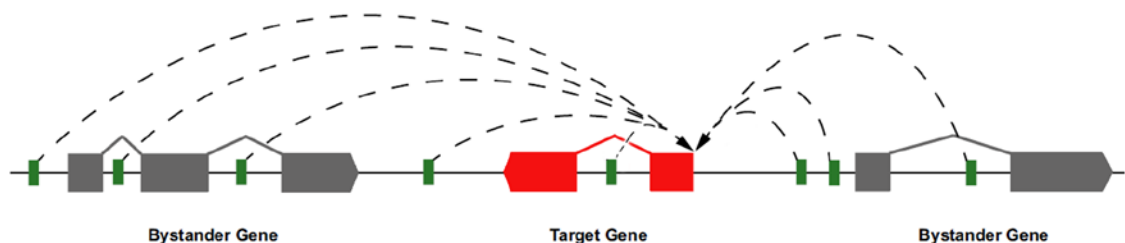


Figure 1.26: Schematic representation of a target gene regulatory input by CNEs. The dashed lines indicate the long-range interactions between CNEs (green) and the target gene (red). Bystander genes are indicated in gray and are not affected by CNEs regulatory effects (Modified from Polychronopoulos *et al.*, 2017)

A number of tools are available to identify conserved non-coding elements in genome sequences i.e PhastCons (Siepel *et al.*, 2005), Percent identity plot (PiP) (Schwartz *et al.*, 2000), and Gumbay (Prabhakar *et al.*, 2006). These tools are available on different browser and are based on a two-step process: 1) homologous regions of two or more different genomes are aligned (local or global) and the best fit for each nucleotide position is determined; 2) using a statistical method, regions where the sequence is more constrained (i.e. similar between the different organisms) than what would be expected for neutrally evolving DNA are identify. In this type of analysis, the choice of the species being compared can be used to roughly calibrate sensitivity versus specificity. The comparison of close species increases the sensitivity while that of distant species favors greater specificity.

Once identified a CNE, in order to test if it acts as enhancer, it ideally need to be fuse with a reporter gene (e.g. GFP, luciferase, LACZ) with a minimal promoter and introduce it into a living model system, essaying the reporter gene expression during development (Fig. 1.27) or in *in vitro* cell lines. In general, transgenic approaches have been very successful in identifying enhancer properties of conserved non-coding sequences, with substantial overlap between the known endogenous pattern of expression of a gene and its associated CNEs.

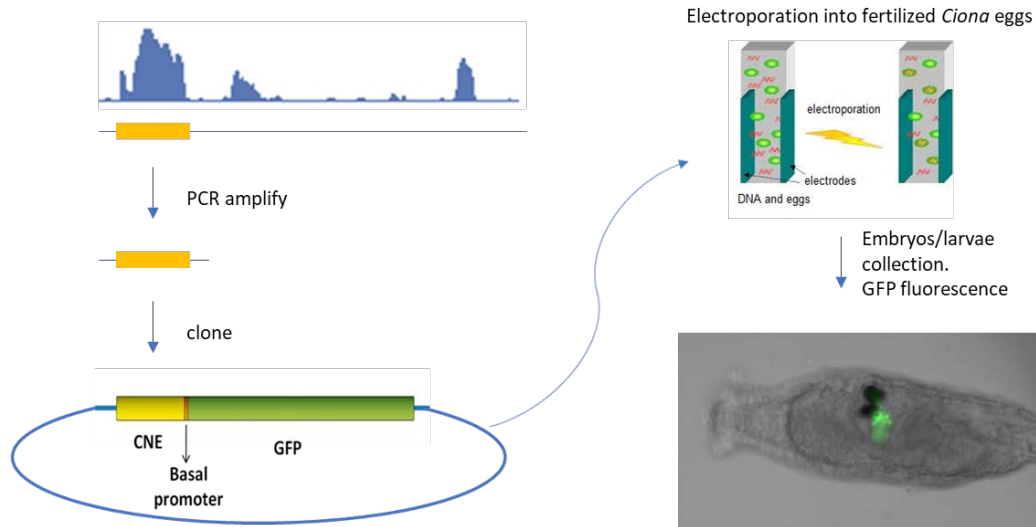


Figure 1.27: Experimental design. Identification (example alignment displayed as PhastCons diagram), cloning and transgenic testing of candidate enhancer sequence.

1.5.2 *Ciona robusta* as model organism for transgenic experiments

Ascidians, together with thaliaceans and appendicularians, are grouped as Tunicates (Lamarck, 1816) or Urochordate (Lankester, 1877) (Fig. 1.9). Only after Kowalevsky had described the tailed larval form of ascidians in 1866, containing a dorsal neural tube, the notochord and lateral muscle cells, zoologists realized that tunicates should be placed within the chordates (Fig. 1.9). Because cephalochordates shared more morphological features with vertebrates, the tunicates were initially placed at the base of *Chordata* (Hecht *et al.*, 1987; Winchell *et al.*, 2002) but, a more recent analysis established that cephalochordates, and not tunicates, are the most basally divergent lineage of chordates (Blair *et al.*, 2005; Delsuc *et al.*, 2006, 2008). The ascidian *Ciona robusta* is an important model organism for the study of developmental gene regulation, in part because transient transgenic embryos can be produced rapidly and reliably using

electroporation of fertilized eggs (for electroporation protocol in *C. robusta* see the chapter of Methods) (Davidson *et al.*, 2005, 2006; Vierra *et al.*, 2012). *C. intestinalis* transgene electroporation was first reported by Corbo *et al.* (1997). This type of transgenesis is considered to be transient and observed only in the electroporated embryos. However, it has been reported that stable transgenic lines can be produced as well (Matsuoka *et al.* 2005). The *Ciona* specimen originally described by Linnaeus (1767) was called *Ciona intestinalis* and for long time this name was used for specimens used in all the laboratories in the world. But now it is known that two closely related species were wrongly called with the same name. These two species are currently referred as *C. intestinalis* or type B (i.e. Northern Europe) and *C. robusta* or type A (i.e. Southern Europe) (Brunetti *et al.*, 2015). The animals used for the experiments described here come from the Mediterranean sea.

Many characteristics make *C. robusta* a highly tractable model: they have only 2,500 cells in the late larva; cell fates are determined very early in embryogenesis compared to those of other animals, and developmental genes have concomitantly altered functions in patterning the embryo.

Ciona robusta larval anatomy and nervous system

The tadpole larva is mostly divided into two parts, the “trunk” (or head) and the “tail” (Fig. 1.28). The head is composed by: the anterior central nervous system (CNS); the peripheral nervous system (PNS); an undifferentiated endoderm that will form the endostyle and the anterior part of the gut; an undifferentiated mesoderm from which will derive the muscles, the heart and the blood, the tunic cells. The tail is mostly composed by the caudal CNS and PNS, the notochord (axial mesoderm), the muscles

(paraxial mesoderm), a ventral endoderm that give rise to the adult intestine and a vary caudal undifferentiated endoderm.

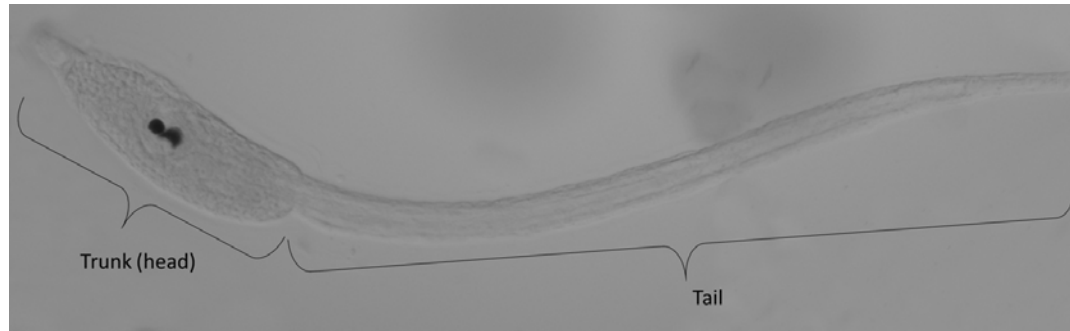


Figure 1.28: *Ciona robusta* larva. The two parts of the larva, trunk and tail, are indicated.

C. robusta larva CNS is divided, along the antero-posterior axis, in five compartments (Fig. 1.29A). Most anteriorly there is the sensory vesicle (SV), in which two pigmented cell-containing sensory structures are present: the anterior geotactic otolith and the posterior photoreceptive ocellus (Fig. 1.29B). Then there is the posterior sensory vesicle (PSV) also known as larval “brain”, containing neurons, photoreceptors and other sensory cells associated with the SV. This anterior CNS region is marked by *Otx* expression that is absent in the remainder (Ikuta and Saiga 2007). Posterior to the PSV is the neck, which is a mass of undifferentiated neuronal progenitors that express *Pax2/5/8* and *Phox2*, supporting the homology of this region with the vertebrate hindbrain (Dufour *et al.*, 2006). Caudally there is the motor ganglion (MG) composed by neurons and interneurons that drive the swimming behavior of the larva (Bone *et al.*, 1992; Horie *et al.*, 2010). The motor ganglion progenitors express specific spinal cord

motor neuron specification genes of vertebrates that support the homology of this region with the vertebrate spina cord. Most posteriorly, along the tail, there is the nerve cord (Fig. 1.29A).

The peripheral nervous system (PNS) of the *C. robusta* tadpole larva comprises a distributed population of isolated receptor neurons, most of unproved function, organized along the trunk and the tail epithelium (Fig. 1.29B; Imai *et al.*, 2007; Ryan *et al.*, 2016). In the head, these neurons are dispersed only in the anterior and dorsal regions (Imaia and Meinertzhagen, 2007). In the tail, the neurons of the PNS, called caudal epidermal sensory neurons (CESN), are regularly distributed on the dorsal (DCEN) and the ventral (VCEN) side. The dorsal neurogenetic epidermis is induced by FGF signaling while the ventral is induced by ADMP/BMP signaling (Pasini *et al.*, 2006).

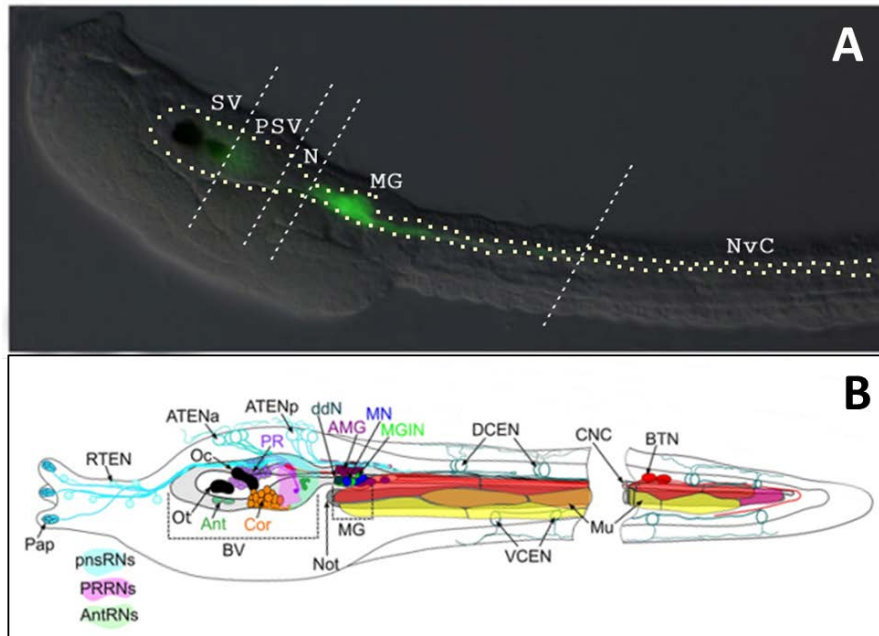


Figure 1.29: *Ciona robusta* larva nervous system. A) The five major anatomical subdivisions of the CNS are demarcated. SV: sensory vesicle; PSV: posterior sensory vesicle; N: neck; MG: motor ganglion; NvC: nerve cord. The CNS is fluorescently labeled with the vesicular acetylcholinesterase transporter (adapted from Stolfi *et al.*, 2011). B) Diagram of larva nervous system sections and cells type. Abbreviations: Pap: papilla neuron; RTEN: rostral trunk epidermal neurons; ATENa: anterior apical trunk epidermal neurons; ATENp: posterior apical trunk epidermal neurons; Oc: ocellus; Ot: otolith; Ant: antenna neuron; Cor: coronet cell; PR: photoreceptor; ddN: descending decussating neuron; AMG/Ascending MG IN: ascending motor ganglion interneuron; MGIN: motor ganglion interneuron; MN: motor neuron; DCEN: dorsal caudal epidermal neuron; VCEN: ventral caudal epidermal neuron; BTN: bipolar tail neuron; Mu: muscle; pnsRNs: PNS relay neurons; PRRNs: photoreceptor relay neurons; AntRNs: antenna relay neurons; BV: brain vesicle; MG: motor ganglion; CNC: caudal nerve cord; Not: notochord; IN: interneuron; BVINs: brain vesicle interneurons (adapted from Ryan *et al.*, 2016).

CHAPTER 2

MATERIALS AND METHODS

2.1 ANIMALS CARE AND GAMETES COLLECTION

2.1.1 *Branchiostoma lanceolatum* sampling and ethics statement

Adult amphioxus specimens (*Branchiostoma lanceolatum*) were collected from an endemic population of the Gulf of Naples (Italy) (40°48'33" N - 14°12'55" E) at a location that is not privately owned or protected in any way, according to the authorization of Marina Mercantile (DPR 1639/68, 09/19/1980 confirmed by D. Lgs. 9/01/2012 n.4). All procedures were in compliance with current available regulation for the experimental use of live animals in Italy. The animals were caught using a drudge on the soft bottom, with the support of the SZN vessel "Vetoria", and collecting 5-10 cm of sand. After the sand collection between 7 and 15 meters deep, it was sifted directly on boat using a net with a 1.25 mm mesh (Fig. 2.1).

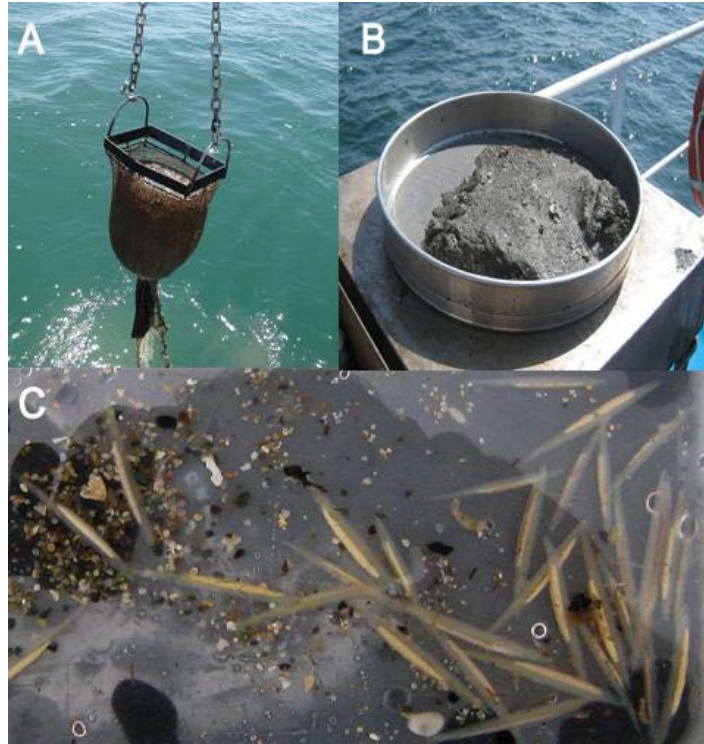


Figure 2.1: Adult amphioxus sampling. (A) Drudge used to bring sand onboard; (B) Sorting of the sand; (C) Ripe adult amphioxus specimens.

2.1.2 *Branchiostoma lanceolatum* culturing

Animal care is entrusted to the “Marine Resources for Research Unit (MaRe)” at the Stazione Zoologica Anthon Dohrn of Naples. Animals were kept in an open seawater circulating system reproducing natural thermal and light conditions with continuous aeration (Fig. 2.2). During the period of gonad maturation (April to July) the temperature was maintained at 17°C, slightly lower than the field, to avoid the natural emission of sperm and eggs in the tank. Animals were fed daily with a 1:1 mix of *Isochrysis galbana* and *Rhodomonas sp* microalgae.



Figure 2.2: Amphioxus facility at the Stazione Zoologica Anton Dohrn of Naples.

2.1.3 *Branchiostoma lanceolatum* spawnings

B. lanceolatum gonads development starts in winter and between the late spring and the beginning of the summer arrive to maturation. As mentioned above, to avoid the natural emission of sperm and eggs, the animals were kept at a low temperature (17°C). The induction of artificial spawning was performed applying a heat shock to ripe animals. Selected animals, with visible mature gonads, were placed in a water bath with a 6 degrees higher temperature than the culturing system; the day after before sunset the animals were singularly separated in glass beakers containing 100 ml of filtered sea water to avoid the uncontrolled fertilization. After approximately 30 h of exposure to the temperature stress, precisely after sunset, the animals would start to spontaneously release gametes (resembling the natural spawning) (Fig. 2.3). Upon release of gametes,

the adult animals were removed from the glass beakers, the sperm from several males was mixed to increase the fertilization percentage and kept on ice. 200-300 eggs were distributed into petri dishes with scratched bottom to avoid that they would attach to it, then they were fertilized with some drops of sperm's mix. After approximately 10 min the percentage of fertilized eggs were checked by the elevation of the fertilization membrane and if less than 65% of the eggs were fertilized, another drop of sperm would be added. Subsequently, embryos were washed twice with filtered sea water (FSW) and left to grow until desired developmental stage at 18°C.

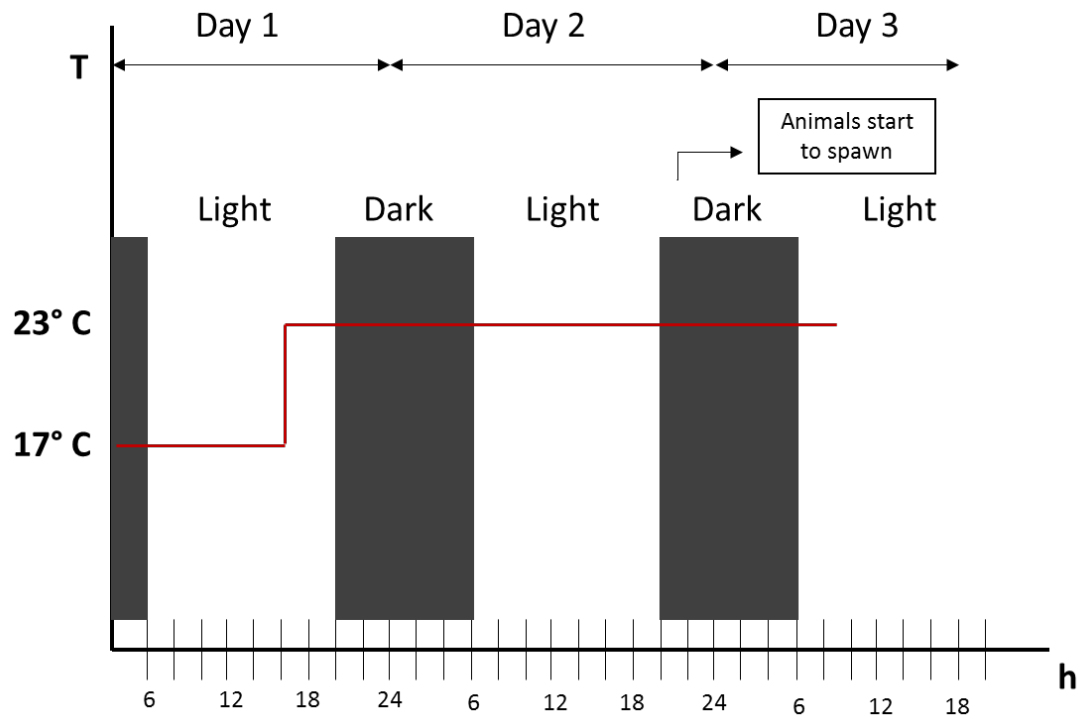


Figure 2.3: Schematic timing representation of induced spawning in *B. lanceolatum*. Dark (night) periods are represented by black area. The red line indicates the thermal shock from 17 to 23°C. Abbreviations: temperature (T), hours (h).

2.1.4 *Ciona robusta* sampling, care and gametes collection

C. robusta is a hermaphroditic broadcast spawner that is widely distributed along Mediterranean and worldwide temperate coasts. The animals used for the transgenic experiments shown in this thesis were fished by the crew of the SZN vessel “Vettoria” in the southern coastal regions of Italy, mainly in Taranto (Puglia, Italy). Once they were brought to the SZN, animals spent at least a week in an open circulating seawater tank at a temperature similar to that in the field in order to acclimate them to the new conditions. Animals care was entrusted to “Marine Resources for Research Unit (MaRe)” at Stazione Zoologica Anton Dohrn of Naples. The spawning period is restricted from early autumn to late spring. In order to obtain gametes in the laboratory it was unfortunately necessary to kill the animals, so a continuous supply of adults was necessary. Tunic and muscles were splitted by scalpel trying not to damage the gonaducts to avoid uncontrolled fertilization. Sperm and eggs were therefore separately collected until the fertilization was carried out in in petri dishes of 6cm diameter with an agarose bottoms.

2.2 *IN VIVO* EMBRYONIC MANIPULATION

2.2.1 TRIM and L-NAME treatments in amphioxus

In order to understand the role of NO during amphioxus embryonic development, we decreased the NO production using two types of soluble drugs that alter the NOS activity: an analog of L-arginine, the N ω -Nitro-L-arginine methyl ester hydrochloride (L-NAME, Sigma Aldrich, stock solution in filtered sea water, FSW) and a NOS

inhibitor, the 1-(α,α,α -trifluoro-*o*-tolyl)-Imidazole (TRIM, Cayman Chemical, stock solution in DMSO), which interfere with the binding of both L-arginine and tetrahydrobiopterin to their respective sites on NOS enzymes. Different drug concentrations and timing were tested. The L-NAME treatments were performed with 100 μ M, 1 mM and 10 mM of drug as pilot experiments. The *in vivo* experiments were performed at 50, 75 and 100 μ M TRIM. Treatments were performed in petri dishes of 3cm diameter with scratched bottoms at 18°C. Embryos developed in FSW or FSW+DMSO and in parallel embryos in the same developmental conditions but in absence of the drugs were used as control. For L-NAME treatment, we used an additional control: the inactive enantiomer N ω -Nitro-D-arginine methyl ester hydrochloride (D-NAME, Sigma Aldrich). Larvae at 72 hpf were fixed in 4% paraformaldehyde (PFA), dehydrated and stored in 70% ethanol. The larvae morphology was analyzed initially using a stereoscope and then, for image acquisition, a Zeiss EVO MA LS Scanning Electron Microscope.

2.2.2 LPS treatment in amphioxus

Lipopolysaccharides (LPS) are component of Gram negative bacterial wall and is usually used as a stimulator of the immune system. In this thesis, LPS treatment was used to investigate the possible inducible nature of at least one of the amphioxus *Nos* genes (*NosB*). 72 hpf larvae were stimulated with 10 μ g/ml of LPS from *Escherichia coli* (O26:B6, Sigma Aldrich) for 1, 2, 4, 6 and 8 hours. The LPS was dissolved in FSW. Plates in which treatment was performed, were silanized (SIGMACOTE®, Sigma Aldrich) in order to avoid LPS binding to plastic plate walls and the consequent

reduction of its concentration in solution. As control of successful stimulation of the immune system, an amphioxus Intelectin gene (*AmphiItln239631*) was used (Yan *et al.*, 2013). Intelectins are lectins (carbohydrate-binding proteins) that bind specifically soluble galactofuranose and are involved in innate immunity. In particular, *AmphiItln239631* contains a conserved fibrinogen-related domain (FReD), an intelectin domain and a putative collagen domain. The experiments were carried out in biological triplicates, each of which consisted of about 300 larvae for both control and treated. The fold change between control and LPS treated conditions were analyzed by qPCR.

2.2.3 Transgenesis in *Ciona robusta*

Before proceeding with the external introduction of DNA constructs via electroporation it was necessary to deprive the eggs from the chorion. A chemical dechoriation has been performed in a petri dish covered by a thin layer of 1% agarose in filtered sea water (FSW) containing a solution of Thioglycolic acid (1%, pH 10) and Proteinase E (0.05%) in FSW. The eggs were incubated in this solution for 5-6 minutes, shaking continuously using a glass pipette to remove the chorion and the follicular cells surrounding the eggs. In the next step, the eggs were washed several times in FSW to remove the dechoriation solution and then they were fertilized with sperm collected from two or more individuals to avoid self-sterility problems. After 10 minutes, fertilized eggs were washed 2-4 times to eliminate the exceeding sperms and then used for transgenesis experiments. The dechorionated and fertilized eggs have been transferred in a solution containing 0.77 M Mannitol containing 50-150 µg of DNA construct. The electroporation has been realized in 0.4 cm Bio-Rad Gene Pulser

cuvettes, using a Bio-Rad Gene Pulser II electroporator, at constant 50 V and 500-800 μ F, to have a time constant of 14-20 m/seconds. Afterwards, the embryos have been left to grow until desired developmental stage, at 18-20°C and then analyzed *in vivo* at the fluorescent microscope with a GFP filter and fixed for immunostaining.

2.3 AMPHIOXUS EMBRYOS COLLECTION AND FIXATION

Embryos at different developmental stages were collected and pelleted with a light centrifugation (1500-3000 rpm for 2-4 min) in order to remove much as possible sea water. For RNA extraction, they were stored at -80°C or kept in Eurozol (EuroClone) and stored at -20°C until the RNA extraction. For NO quantification (Griess assay), embryos after collection were frozen at -80°C in eppendorf tubes. For *in vivo* experiments such as NO localization or drug treatments, the embryos were kept in the petri dishes in FSW at 18°C until they reached the desired stage of development.

2.4 BASIC MOLECULAR BIOLOGY PROCEDURES

2.4.1 RNA purification

To eliminate RNAase contaminations all the procedures were carried out in sterile condition. Samples, already kept in Eurozol, were homogenized using a pestle. Then 0.1 volume of chloroform was added, mixed vigorously and centrifuged at 14.000 rpm at 4°C. The aqueous phase was collected and precipitated over night with an equal volume of isopropanol. After precipitation, the sample was then centrifuged for 30 min at

14.000 rpm at 4°C. The obtained pellet was washed with 70% Ethanol, centrifuged, air-dried and resuspended in DEPC H₂O. The sample's concentration was measured with a "NanoDrop 1000" spectrophotometer (Thermo) and RNA integrity was checked on a 1% agarose gel. The total RNA was kept at -80°C until use. For differential transcriptomic analyses, RNA was purified with the RNeasy Mini Kit from QIAGEN following the protocol supplied by producer.

2.4.2 Reverse transcription of RNA

cDNA was obtained by *in vitro* reverse transcription using 0.5-1 µg of total RNA. This enzymatic reaction leads the synthesis of the DNA strand complementary to the RNA template using an RNA polymerase. The reaction was carried out with the SuperScript VILO cDNA Synthesis kit (Invitrogen). Reaction was performed, in a final volume of 20 µl, in a thermocycling according to the following setting program: 25°C for 10 min, 42°C for 60 min, 85°C for 5 min. The cDNA obtained was kept at -20°C until use.

2.4.3 DNA and RNA gel electrophoresis

In order to evaluate the RNA integrity or to separate DNA fragments on the base of their length, a horizontal agarose gel electrophoresis was performed. The concentration of the agarose was chosen according to the length of the expected DNA fragment. The gel was prepared with 1X TBE buffer (1.1 M Tris; 900 mM Borate; 25 mM EDTA; pH 8.3) and 0.5 µg/ml Ethidium Bromide. DNA samples were mixed with Loading Buffer 1X (0.25% Bromphenol Blue; 15% Ficoll 400, 120 mM EDTA, 0.25% Xylene Cyanol)

and the appropriate molecular marker. Electrophoresis was normally settled at the voltage of 90-100 V. For RNA, the procedure was similar to that used for DNA with slight modifications to avoid RNA degradation, but it was not prepared in denaturation conditions: the electrophoresis camera was RNase-free, the running buffer was fresh prepared. The samples were boiled before the electrophoretic run in order to remove secondary structures.

2.4.4 Genomic DNA preparation

Genomic DNA was isolated from whole adult animals or from their caudal fin, in 20 μ l of 50 mM NaOH. The samples were heated for 5 minutes at 95°C in a thermos-block, followed by cooling to 4°C. 100 mM Tris-HCl pH 8.0 was added in a 1:10 ratio. The samples were briefly centrifuged to collect the lysate in the bottom and 2 μ l of the supernatant, containing the DNA, used for PCR reaction.

2.4.5 Molecular cloning

Molecular cloning is a technique used to insert recombinant DNA into a vector that will be replicate in host organisms. It consists of three phases: DNA ligation, transformation and hosting bacterial growth.

DNA ligation: T4 DNA Ligase catalyzes the formation of a phosphodiester bond between juxtaposed 5'-phosphoryl and 3'-hydroxyl termini in duplex DNA. The PCR fragments were ligated with the commercial plasmids p-GEM-T Easy vector (Promega).

Each ligation reaction was carried out in a final volume of 20 μ l in distilled H₂O and containing 50-100 ng of vector DNA linearized. The moles of insert DNA were added in 3-5 fold vector moles and 2 μ l of ligation buffer (10X T4 DNA Ligase buffer: 500 mM Tris-HCl pH 7.5, 100 mM MgCl₂, 100 mM dithiothreitol, 10 mM ATP, 250 μ g/ml bovine serum albumin) and 1 μ l of T4 DNA Ligase (1 unit/ μ l) (Promega). The reaction mix was incubated at 4°C overnight or two hours at room temperature, and used to transform competent bacteria.

Bacterial transformation and growth: The transformation of vectors containing DNA of interest was performed by electroporation in bacterial cells *Escherichia coli* DH5 α provided by the Molecular Biology Service of SZN and stored at -80°C. When needed the cells were gently defrosted on ice for 10 min, and the 40 μ l were mixed with 4 μ l of dialyzed vector (more or less 40 ng), then the mix was transferred quickly into electro-cuvette. The electric shock was performed in a “Bio-Rad Gene Pulser” applying a constant voltage of 1.7 V. The cells transformed were placed in 800 ml of Luria Bertani (LB) medium shaking at 270 rpm at 37 °C for 1 hour, then the bacterial cells were plated on LB solid medium (NaCl 10g/l, tryptone 10 g/l, yeast extract 5 g/l, agar 15 g/l) in the presence of ampicillin (50 μ g/ml) to which the plasmids were resistant. IPTG and X-gal (40 μ l + 40 μ l, respectively) were added for the blue-white screening technique and grown overnight at 37°C.

2.4.6 Isolation of plasmidic DNA from *Escherichia coli*

Escherichia coli positive colonies were picked from the plates and grown overnight at 37°C by shaking in 3 ml of LB medium containing 0,1 mg/ml of ampicillin. In order to reduce the number of colonies to purify, PCR colony screening was used to detect positive colonies. The colonies were individually picked using a sterile plastic tip and dissolved into 12,5 µl of PCR reaction mix. M13 forward and M13 reverse primers, that are more or less 60 bp up- and downstream the insert on the vector, were used for the amplification (primers sequences are listed in Table reported in section 2.16). Mini or Maxi plasmid DNA isolations (Mini-prep or Maxi-prep) were carried out according to the protocol supplied of GenElute™ Plasmid Miniprep Kit (Sigma) and GenElute™ Plasmid Maxiprep Kit (Sigma). The elute DNA was quantified with the “NanoDrop 1000” spectrophotometer (Thermo) as absorbance at 260 nm.

2.4.7 Polymerase chain reaction (PCR)

Polymerase chain reaction (PCR) is a method that allows exponential amplification of short DNA sequences within a longer double stranded DNA molecule. Each amplification reaction was conducted in a volume of 12,5 to 100 µl of reaction mix depending on the purpose of the experiment and it was composed by sterile H₂O, 1X reaction buffer, 1.75 mM MgCl₂, 0.2 mM dNTP, 50 pM of each primer, 1 U/µl of GoTaq DNA polymerase (Promega) and 1 ng of DNA template for each µl of final reaction. The amplification cycles were conducted by means of Thermal Cycler Perkin-Elmer-Cetus. After denaturation at 95°C for five min, 30 amplification cycles were

performed as follows: denaturation at 94 °C for 30 sec, annealing at 55-65°C for 30 sec (depending on the primers), extension at 72°C for 0.5-1.5 min (considering 1 min to synthesize 1 kb). An extra extension cycle of 10 min was carried out at 72 °C to complete all DNA strands. To purify the amplified DNA from the excess of buffer and dNTPs, the PCR Purification kit (Invitrogen) was used according to the protocol's instructions. The concentration of the obtained DNA was measured using a "NanoDrop 1000" spectrophotometer (Thermo) and checked on a 1-1.5% agarose gel with the appropriate molecular marker.

2.4.8 DNA sequencing of individual plasmids

The DNA sequencing was carried out at the Molecular Biology Service of SZN using Automated Capillary Electrophoresis Sequencer 3730 DNA Analyzer (Applied Biosystems) using a BigDye® Terminator v3.1 Cycle Sequencing Kit (Life Technologies).

2.4.9 Oligonucleotides

The following table (Table 2.1) shows all the primers used for the experiments reported in the present thesis.

Primer name	Sequence (5' → 3')	Product length
Digital Droplet PCR and qPCR		
Bl_NosA_Fw	AGTACAGTCATCTCCAGAAC	221 bp
Bl_NosA_Rv	TCTTGCAAGCGCTTCTATCTG	
Bl_NosB_Fw	AGTTTACTCCCGGCGATCA	191 bp
Bl_NosB_Rv	AGAACATGGCGGCAAACGC	
Bl_NosC_Fw	CAGGATTCTGCGCGTTTGC	197 bp
Bl_NosC_Rv	GGAGCTAGCCTCGTCATG	
Bl_L32_Fw	GGCTTCAAGAAATTCCTCGTC	117 bp
Bl_L32_Rv	GATGAGTTTCCTCTTGCGCA	
Bl_ITLN_Fw	CTTCTGGAGCGTGTGGCAG	183 bp
Bl_ITLN_Rv	CCTCTTTGGCCTCATTCTGGG	
Sequencing		
T3	ATTAACCCTCACTAAAGGG	
T7	AATACGACTCACTATAGGG	
SP6	GATTTAGGTGACACTATAG	
M13Fw	CGTTGTAAAACGACGGCCAGT	
M13Rv	TTTCACACAGGAAACAGCTATGAC	
Amphioxus CNRs amplification and cloning - NosC, Intron 1 -		
CNRs 2-3 Fw	CTACCCATACCTCTAGGTATGG	1571 bp
CNRs 2-3 Rv	CTAATATTGCTTGGCCGGTTTC	
CNRs 6-9 Fw	CCTTGCCGGTTGTAGAGTG	1617 bp
CNRs 6-9 Rv	GTCATGGGTCTATGGCGATG	
CNRs 14-15 Fw	CATGTGAGGGCTAGCTAGGCAC	1301 bp
CNRs 14-15 Rv	GTTGTGTCCCTATTGTCCTTG	
CNRs 17-18-19 Fw	GGAATAGCAACTCCTCGCTG	1741 bp
CNRs 17-18-19 Rv	GAAAGACAGGTGCAGCCCTAAC	
Amphioxus CNRs amplification and cloning - NosC, Intron 2 -		
CNR 30 Fw	CCAATGTACCCGAGCACTAAC	509 bp
CNR 30 Rv	CGGGTTCGTCCTTAGTAATAGC	
CNR 33 Fw	CCTCACCGACAAAGACCAAG	453 bp
CNR 33 Rv	GTGACTTGTGAGTGCAGGTGG	
CNR 34 Fw	GAGAGGAATAGTTGTGGCCG	613 bp
CNR 34 Rv	GTCGTATGACGGATGTGATCAG	
CNRs 39-40-41 Fw	CATTGCCTGTGATGTACATTG	1364 bp
CNRs 39-40-41 Rv	GACAAACTCTCTGGTCGATAGG	

CNR 45 Fw	GACTTACCAACCTGAGGAAGC	742 bp
CNR 45 Rv	CATACTGTCAATGAGTCACTGTAG	

Table 2.1: List of primers used for PCR experiments. For each pair of primer, the amplification product length is reported.

2.5 QUANTITATIVE GENE EXPRESSION

2.5.1 Quantitative real-time PCR (qPCR)

mRNAs expression profile was monitored using quantitative real time PCR (qPCR). Optimal cDNA concentration to use was established empirically, through serial dilutions. The qPCR was carried out in triplicate with a ViiATM 7 Real-Time PCR System (Applied Biosystems) in a 384-multi-well plate. Each reaction was performed in a final volume of 10 μ l containing 0.7 pmol/ μ l of each primer, 5 μ l of SYBR Green mix with ROX (Applied Biosystems) and 1 μ l of diluted cDNA. Thermal cycling parameters were: 95°C for 15 sec, 40 cycles at 60°C for 1 min followed by a denaturation step from 60°C to 95°C with a continuous detection at 0.015°C/sec increment for 15 min to verify the presence of a single product. The results were analysed using the ViiA™ 7 Software and exported into Microsoft Excel for further analysis. Quantification results were expressed in terms of cycle threshold (Ct). The Ct values were averaged for each triplicate. Amphioxus ribosomal protein L32 gene was used as endogenous control for the experiments (Kozmikova *et al.*, 2013). Differences between the mean Ct values of the tested genes and those of the reference gene were calculated as $\Delta Ct_{gene} = Ct_{gene} - Ct_{reference}$. Relative expression was analyzed as $2^{-\Delta Ct}$. Relative fold changes in expression levels were determined as $2^{-\Delta\Delta Ct}$.

2.5.2 Digital droplet PCR (ddPCR)

ddPCR is a method for performing digital PCR that utilizes a water-oil emulsion droplet system using a combination of microfluidics and proprietary surfactant chemistries. Droplets are formed in a water-oil emulsion that partitions the nucleic acid samples into 20,000 nanoliter sized droplets, with background and target DNA randomly distributed among the droplets. Sample partitioning is key to ddPCR. Following PCR, each droplet is analyzed or read to determine the fraction of PCR-positive droplets in the original sample. These data are then analyzed using Poisson statistics to determine the target DNA template concentration in the original sample. The benefits of ddPCR technology are different, in particular it allows to accurately evaluate very low gene expression, like that of *Nos* genes. *Nos* genes expression were evaluated at gastrula (10hpf), middle neurula (24 hpf), pre-mouth larva (48 hpf), open-mouth larva (72 hpf) and small adult (1,2 cm length). Amphioxus ribosomal protein L32 was used as the reference gene (Kozmikova *et al.*, 2013). Experiment was performed in biological triplicates. For my experiments, approximately 550 ng of total RNA, from each developmental stage analyzed, were reverse transcribed. For each sample, 3 ng of cDNA was mixed with 10 μ l of 2X ddPCR Evagreen Supermix, 0.5 pM of each primer and nuclease-free water to a total reaction volume of 20 μ l. The entire reaction mix of 20 μ l was then loaded into a sample well of a DG8 Cartridge for the QX200/QX100 droplet generator. This was then followed by adding 70 μ l of droplet generation oil for probes into the oil wells of the cartridge, according to the QX200/QX100 Droplet Generator Instruction Manual. The cartridge was then inserted into the Automated Droplet Generator. After droplet generation, the droplets were transferred to a 96-well plate and then sealed with foil

using the PX1 PCR plate sealer. Thermal cycling was performed according to the following protocol: enzyme activation at 95°C for 10 min (1 cycle), denaturation at 94°C for 30 sec followed by annealing/extension at 60°C for 30 sec (40 cycles), enzyme deactivation at 98°C for 10 min (1 cycle) followed by hold at 4°C. After thermal cycling, the sealed plate was placed in a QX200 droplet reader and the absolute gene expression level per well for the probes and reference genes were quantitated using QuantaSoft software. The gene expression values for each sample were normalized to the housekeeping gene. The values for the absolute level of gene expression as obtained by ddPCR were then subjected to the t-test for each gene under the triplicate conditions, with a resulting P-value. A P-value of less than 0.05 was considered significant.

2.6 CONSTRUCTS PREPARATION FOR TRANSGENESIS

2.6.1 Amphioxus enhancers

Amphioxus putative enhancer fragments, included in the non-coding region of the 1st and 2nd intron of *NosC* gene, were cloned from *B. lanceolatum* genomic DNA. Conserved sequences were retrieved from an alignment between three different *Branchiostoma* species (*B. lanceolatum*, *B. floridae* and *B. belcheri*; see Results). 17 Kb upstream the translation start codon ATG (intron 1) and the entire intron 2, downstream to the ATG, were considered for analysis. Sequences were taken from genome draft version B171nemr, kindly provided by the “*Branchiostoma lanceolatum* genome consortium”. The primers used to amplify these regions, are reported in the Table 2.1 in section 2.4.9. These regions were tested *in vivo* in *C. robusta* to verify the possible

presence of enhancers. The sequences of genomic DNA fragments cloned and tested *in vivo* are listed below and the localization of each fragment on *B. lanceolatum* scaffold Sc0000060 is indicated by numbers. The sequences in red correspond to conserved non-coding regions (CNR).

Sc0000060:252628-253878 (CNRs 2-3, intron 1)

GACGTTTGAGTTGGGCCAGGCTGGTACCTTTTTGGTTTTAGGTTTCTGTATGCGTTTTGTCTTGGTGTGTGTGAGTAGTATTATCTCCATGGAAAAATGGAGATATTGTTTTGGGTGTCTGTGTCTGTCTGTCTGTTTGTCTGTCTGTTTGTCTGTTTCCGGACTACTGTAGTCAGCATAACTCAAGAGCCCTTGATGGATTACAATGATATTTGGTATGTGGGCGGGTGTGTGAAGCCGAAATCAAGGTCGATTTTGGGCCCTGGTATGTGACCTTGGTACTGAGTAGAACCTCAATTTTTGTATCTTTGACCTGGACGTGCTGTGGTCTTGATATTTGGGTGGCAGATAGCTTGTGATGTAATAAAGAAAGTGGAGTAGGTTAGGGCCCCATAGCAGCTTCTCTGGAACTGCAGGGGCGTTTTTAAATATTGTTGAGTGACAATATGGGAGCGGAAAAATGGTGTAAACGGAAGATTGCTTGGCCCGCGCCGGTCCAGAGTTGGTCCCGCTGACTGGCAGGAAGGGAAGATTTTTGGCCTGGGTCCAAAGTTGGTCGCTGGCTGACAGGAAAAATGCATAAACAGAAATAGAGAGAAAACTACAATAATGAATAAAAAAGAAATTCACAAAACTCTCAATAGAGAAAAGTATCATTGAGATGTGAGATTTTGAATTTCTGTATACTAATGCGTACGCTTATCGCTGCATCTTCGACAACATCCGTACCCTAACAGCCGAAAGAGTCAAAGAACAATTAACCAACTTTTGAAGGGTAAAGTCAAACGTAGTGACTTTATCATGTTGCACGTTTCATGTTGCGTGACAGAACGTGGCATTCTGCACGTATCCGGAGTCATTTGTTTTCAGTTTTTATTACCGATACGAGCAGGGAGACAGAACTAGGTTATTATGAGATTAATAACTCATTTTTGAGATTAATAACTCTGACAAAACGCAAAATTCCTCATACTCTAGACATGATACAATCGAAACAGCGTATTCAACAGGTTAAATTTCTAACCCAAACTTTTGATATCCATAAAATTTGACATCGTTTTACATCAAAATGCTAATGCCATTTTCAATAATCATCAGAGGTCATCAAAAACAAATATGTTTCGGTTAAAAAGATTCTGCCTGTTTCGTATAGTGCAGACATAGATTGTTACGATCCAATTATCATTCCAGAGATACCGGGGTAATTTTTCTCAAGGTGACTCCGCTCATTGCAAGTGTGCCGTTTTCAGATCTANGACTCCGTCCTATTGCAAGTGTGCCGTTTTCATGTCTACATGTCCTTAGTTAGTTTTACCTTCGGGAGGGAGGGTCCGCTCCGACGGGAGTATTGTTTTGGTGGTGTGTTGTGCCGACCCATAACTCAATATCCATTGGATGGACTGTTATGTTTTGGTATGCGGGTAGGTAATAAAGAAACCGGCCAAGCAATATTAG

Sc0000060:254561-255958 (CNRs 6-9, intron 1)

CCTTGCCGGTTGTAGAGTGGTATATACGTGTCAAACCTTTTTCGCTGGCTTCGTTTTCGAGATATTCACCTCCCTAGTATTGGCGTAAAGCCTGAGGTCTATACCAC TAAGGCCAATTATAAGATCTTGGCGACTGTATCACATAGTATTTCTGTAGAACATGTTATCAAAGTATCATACTGGTTTTGCCATTCTTGGAGTGAAAAAAGAA GAAAATTTCTTTTACATGGAGTAGCTTGATACCACTGTTAAGATTGGACCAAGGAGTTTTAAACCTCCTTGATTGGACAGACCTGTGAATATCAACTGGGACCC TAACAGAGCCCTCTATCAGGTACTGTTGGTACTGCAACATCCTCACTGGACCCCTTATTTTGCAGCAAGATTAGAGAGGACTATTAATAAACTTTCTCCTCGCTTAT GGCAGCGCCGAACCACCGTGCACCTTGACCTTTGCTCCTACCGCACTCACAAGGGCAAAAATGTGACGGGCTCTCCAAGTTCAAAGGCTATATCTCACTTCTCT GCGTCTTTGTGAAACTTGTCTCAGCTATCCTAATTAATCTTCCCTGTGTCGAGTCTGAGTGATATTCCTCCCTTTGACCAAGGCCTATTGAACACGCTGTGT AGATGAATAAATGCCCTTACGAGTGCCTTTGGGTCAGACCTGCGTCTATTGGCCCTGACTTAACACAATCAACAATCACAAGAGCGACTTTGACTCTATA CACTAATAACCTTGTCTGACTTCTGTGACTAGGTTATCATGATTATAGGTTCTCGATGGAAGTTTTCTTAATAATGTATGACGCTCCTTTGAGTCTAGTTAA GTGCTGTGGCAAGGTAGGATGTTGAAGAATCAACAATAACTCAAAGGCGTTGATCAATTAAGTATGACGAGGACTTTGGTACTAGGTTACCATAA CAGTAGCTCTTTCAAAGGCTCTTTCTACCTAAAGTAATAACCTAAGCTTCTCTCGGAGTAGTAGCTGGTAAAAATGGTGGAGGTTTTAAGGAGGCAACAAC TAAAAGACACAGCCTTCTGTTGAATAGTCGTACCATCGTCGTACCATCGTCGTACCATCGTCGTACCATCGTCGTACCATCGTCGTACCATCGTCGTACCAACTTCGT ACCAAGTGGTACGATCGCAACTGTGGACGCTTTGGGAGAGTAGTTTCATCTTTTATAAAAATCAGCTGCTTGTACGAAAAGGGCTGTAATAAATCCTTG TCGGTGGTTGGTTCTGTACAGCCTGCTGAAAATCGTACGACATTAACAAAATCGCACGACACCCGACTACGAATGTGACCGCACCAGAATTTGAGGTGTTCTA ACATGAAAACAAGGCAGAGAAAGGAATGAAAACCTTTGCCCTAACAAAATATAGTAATTTCAACTATAGCTAGCATCAACACTCCTTATTGTTTGACTCTTTT TTAGAAGCTGTACCGTAGTAAGAAACGACTTTAATTGACTTCAGTGATAACTTACACATAGAATGGGTATCAAAAAAGACTTTATCAGGTTGCTACTTAACTCTTA GACTACAGGGATCCCATCGCCATAGACCCATGAC

Sc0000060:259006-260100 (CNRs 14-15, intron 1)

CATGTGAGGGCTAGCTAGGCACGCCATACCTACCAATCTTACAGTGAGTACTTTTCAATATGATACAGTCATATCTTTGATGCAGATATTTTATGATATA
AAACCGCCCTCGAGGGAAGGTTTCATAAGTGGGGTAATGTCGTTAATAGACGATACCGGATTGAATCAAAGGCTTACGTGGTTTAAAGTTATTACCAAT
TTCTGAATTTAGTCAAGTGAGAAAAGTAAACTTTTGGCAGCGGTAGGGAGATGTATATGAGGTAACGTAACGTACAGGCAGAAATCAGATGGCGTCTT
TTCCATTAGTGTAGGGAATGAAAATGTCATCAAAAAGTATTAATGTAATAAACTGGTGAACCGGTGATTTTGTATAGATAATATCAACAGCTTATTAGG
TCAAGTACACATACATGTTAAATGCTTCGCTACGTTTTTGTGGGGGGGGGCGTGGGCTATGTTTTATGGCATTAAATACAGATTAGTTTCTCACATTTAA
CATCTATATCAAACTTTTACTCCTAGAATATATAGTTTTCTTCCACCTCTAGCTTTGTCCTCTACCCATTGCAATGTGTTTTATCATTTTAAATCAAAATCAATGA
ATCCACAGGGTGCCAGAAATAGTAACTCGAGCCGTTTTCTGTAGATACGTGTTATCCCCCTTGCCAGCAGGGCTTAGTTTTGAGAACGTGCAGATACGGAATG
CCCAATTAATAATGAGACTCATTGCGAGCTCCATATTTGTTTCTAACCCCTAACACATCACAATAGATAGCGCGCCGAGAATTATACATAATTGATTACGCAAGG
CCGGCGTTTTTACAAGACGACATGGCAGAATCGATAAAACCACCATACTCTACATTGCATGTCTATTGATCCAACTGGAAGTCAATGTGGGGCCTTCCGGT
TGGGACGGAATTTATTTCCCGCGGGTGTCTTACTAGTCCCGCTTAACGCTACGATAACGGCCGCTGATAAAAAGAAATGATGGCGAGAAGGGCGAGAG
AGAGAGTATATCTGTTTTAGGGCTACAATTTACGGGAAGTAAGCCGATTTCCCTGCCGATTTCCCTGCAGGAATTCTGACACCTGGAGTAATTTCTGAAAAAG
ACTTTTATGAGGTACAGCAACACGCTGTACTTGAGCGACATGAACGATAAGTAACGACGGATTGGCAAAGAGAAGCATCGCTCATTTTATGATGGGTACTTAC
ATCTTGAGGACACTTACAAGGACAATAGGGACACAAC

Sc0000060:261310-262816 (CNRs 17-18-19, intron 1)

GGAATAGCAACTCCTCGTGAAAAATATACCTACTACTACTGAAACAGCGAGGAAACTTGCTGCTCTATGTGCCACTAGGCGCAACAAGGGTCTGAACGAACG
AATTACTTCACTTTGTTTATGTTCCACACGGCAAGGGTCTAGATTACTTAAATACTTGACAGTCGTGTTCTTTCGAGATAAAGAATAAGACGAGGAAAGAGGCTT
CCATGCTTAAAGAAATGTTATCAGCTTCATATCATGGCATGTTCTTTACCGTATTTTATTCTCTACTGTGCATCGAGTGTTATTCAATGAAACCGCCGCGCC
TTCAAAGGCACAGCTTGAAGTGAACAGTACGATCAGTGATCAACCGTTTTGTAAGGCAATGACTTTAAATCTTTGCTCTCTTTTACAAGATTATGTATGCCCA
TACGTATAGTAGACCGTTTTCTTGAAGGAGCCTACAATAAAGTATCTTTGACTTTCAATTTCTTTTACTCTTTAACTTGGTTGACAGTGATCCTTTGAGATGCC
AATCAGTCTTCCCGTGGGTTATTTGTAGGCTTTTCTTCCAGACCTTTCCGGCTTTGAAAAATTTTCAAAACACGACCCGGAAGCGTCTTCAGCATCCCTCAATT
AGTTGCTTTTACTCCATGACAGAAGACTCCATCTGAAATTTAGATCTCAGTCAGTAGGAATGCGGTTGCTAGGTTCTTGATTAATGTGCTGTTTGAAGAT
TATGTGTTTTGTGGACTCCGAGTCTGTTTGTATGTTGTTGAGCGTGGCAGGAAGAACAAAAAGAACTACAAAATGATTGTCATTAATCGTACATCAGACATG
ACAGGTAGTCCGGTCAATGGAAGAGGCTACTACTTCCAGGGGAGGTTGTTTTGGTCGATCTGTTGTCTGTGTTTTCGCAGATCTTATTCTC
CATATGCTAGCCACATTCACCGTACAGCGGTAAGGGAGTGATAAATTGACATATAAAATGTTAATCAAGCCTTTATTTGCATAAATAATGAACTACAATTAAG
AGGACATACGGGAAACTTTTAGAATTTACGAAAGCGAATGGAGGCGAACCTTATTCTAACTATGAGAACTTTATCATTTTGTGACAGTGTGAAATATGGTTA
ACCATTCCAGGTTGTTGATACGATTACGAGGCAATCCGTAGTTATGTATCATTACATGAAATGTCAGGTGTAAGGTAGCATTATGGTCAAATATCACATCTCA
AATCCTCAATGACATTCGCTAGCGAGTCCGCTGTTGTTGCTAATGATGTGAAATCTTACCGGCAAGTATACAGTTAGCTTGTGGCACGAGATTGATTTT
CTTGGTCTTTTAGCAGTGTCTTCAAGAACATCAAAAAGGCGAAGTCAAGTACTCTAGCTGTGACTGGAGTCCGTCGCTGGAATTAAGCACATAATTACGCT
ATAGCCTACGACATTCAGCCTGCTTGCAAAAGTTCAGTATTTTGTTCATAACGACACCCTAGGTGTGAAGATGGGTAGAGATTGTTCAAAGAAATGGTCATGG
ACATGAAATAGCTTTATAGTATGCTACTATAGGCTTGTCCCTGTAGCTCAACTGGTAGCAGCCTCACAGTTAGCTCCTGGTTCCAAATAATTGCTAGCTGGGAG
ACCCTAGTTCAATCCTGGGTCATAGAAATTTGTTAGGGCTGCACCTGTCTTTC

Sc0000060:267947-268277 (CNR 30, intron 2)

CCAAATGACCCGAGCACTAACTATAAAGTTGTCGTATCGTACTTGAAGTTAGCCTGCCAGGCTTTAAGTGTGTGCACACTCTGGGTGTTGTTCTGTAGCTGAG
TGACAACATGCTGTGTAATGCCGATCCTCTTCGTCGCACAAAAGGGGGTCAATGGATGGACAAATGGATCAATACTTAAACCCACATTACCTTGAGAACCTGT
CAAGAACACTTAAACCAATTTGAAATCATAACGCGCCCAAGTACTTAAATGATTTATACCAAAACACTGTGCGCCTGCAGTTATTTCTATCAAGCACCGGTATG
TCTTTTTTCTTCAAGTAAAAGAAGGTTGATTCGACTTGTATCCATCAACCTACGTTTTAAATGATGCTAATGTTGAGGACAGCTATTTTCTGTGAGGACCA
TTCATTTT ATTTATTTATTGTTTTCAGCATGTACATGCCAGGTTGCCCTGTTAG CCGGAGGCTATTACTAAGGACGAACCCG

Sc0000060:269813-270132 (CNR 33, intron 2)

CCTCACCGACAAAGACCAAGGTAAGACGTTTTCTCAGAGAAAACGTCGTTCAAGAAAAAAATAGATTAAACAGAACATTTTCTTCTGTGGCTCAAAGGCGTT
GGAGACGATACCTAATAGTTCTGCCCTTAAAGTAGCAAGTTATTACTCTAGCGTGTAAAGAAAGTGGTGGTTTACACGATACGGCTTCCGACGGAATCTAAT
TGCAGCTCGATATGTTTATCAGTCTGGAACAGAGCAATATAAATGGTGTGAGATTAGTGTGCGCTTCTTTTGTATGCGTTTTTACAGAAAGGAGATTGACTGGA
GAGCTTTTTTAAAGAAAAGAAAGCGTTTTTGGAGGAAAAGGAGAACTTTGAAGTATGGGTGCGCAATCATCCGTCAGAGATGTACAGTCAAACGGGCAAC
GGCCTGGAGAAGGCAACCACTGCACTACAA GTCAC

Sc0000060:270836-271288 (CNR 34, intron 2)

GAGAGGAATAGTTGTGGCCGGGATTTTTACTCTCTCTCCCGGACTCTACCCACTCGACCGAAAACCTAGATCTGCTTGCAGAATACTTTAGACAT
CTCCACGCCTGTCTGAATAGTTCTTTAGCGATGTCGTTGTGCATAAGTTTTCTTTCAAAGTTTTCGGCTTTGTTGGAAGAAAACATAAATCCCACTACATAGGG
TGTCCGATGACGCAAATGACCAACTTAACATAACATATTGCCAATAACACTGATGAATGTTTTCCGTTTCCTTTGAAACTGCGGTAGGCAAGTGAATCG
TTAGATGTGCGAGAGAAATCTTTTTGAAAATTGACATGTGCAGCAGAGTGAAACAATCTTTCTAACACAATCGGCTAGCCCCAGGGGGGATCACCATTAT
GACGTTGTTTTGGCAATAAAGCCACACTGATCTATTAGGGTTTTGACATTTGCACGCGCAGACTCGTTAATGACGAAAATGCACATCCACACATGTCCATCT
TAAGAAGGCATCAAAAAGCCAACAATACTTCGTATGCATTACAGACATGTGCATTTAA GGGCCTGATCACATCCGTCATACGAC

Sc0000060:273236-274482 (CNRs 39-40-41, intron 2)

CATTGCCTGTGATGTACATTGATGATTACATATCCTTGAAGCAGGTTCTTATTGCTTCATTGAGCATGAGCCGGGTAGCAAATTTGATGCACGACAGCCG
GAAGATCTTACAGGCTCAACAGACTCAGTTATTTTATTGAATGCCATTATTTTTGTGGATGCTATCTTATAAGTCACTTGTCTTAGTCGCTTAAAGGCCACAG
AAGTAAATTTATAGATGACATCTCCACAGACTCCAAAATAATGAGATAGGGCGAAAAAACAAGCGGGCAACAACAAAATAAGATTCTATATTTTCA
AATTTAGAGATCATAAATCTTTTTAAACAAAATTGAGGCGAAAAATATGATATCATGACCAACATGTCTTTATAACTGATTCAACCAATGAGGCTTCATGCAT
GTATATAATATAAAACATCTTGAATCAACAGAGGACATGTCGTTGTAGATGTGTATACATCTCAATAGACTAACTACAACAATGAGAAAACGGCTTGTATA
CCATCATGATCAGGAAATCTGGTATTATGCAATGAAACACCTTAGACTGTCAACATGACACTGTCTTGAAGATGTGTATACAGCTCAGTTAAGTAGAAG
AAATGCAGAAAACAGCTTGCATACCATCATGGGCATTTCGATTTTTGTTTACGACATATTTGCCAATTTTTGGCATATTGACCACCGTCGGAGGGCAATGAAAT
TCTTGTTTTTGTTTTTAAATCAGGCGAAAATCAATGAGCGCGCTGATGTATCCACAAAATACTTGTGTGACCTAAAGGTAACAAACACAGTCCACCAGAA
GGATCTGCTCTTATGTCTCAACACAAAGGTTGCGAAGGTTCTCAACCGACTTACATGTGTCAAAACCCCTTGTATCCACGGCAATCCACATCTAAAGTTTCAA
GACATCACACGAACATCAAAGCGCACAGAGCCCGCTAAACATACCTTCTCATGCCACCGAGAAATGAAATCTTCTAGAACGGTGTCTGTTATTTTCTATCACACC
TTTGCCTATAGTTTCTCAACGCGGTGATTTGAAACATTAGATTGAGAACAACCTTGGTTTTATGCACTCGCTGTCGTTGCCGAACGAACGGGCGACAACCCCGTGT
CACGCAAGTCAATTAACCTTAGTAGCAGCAGCCGCTTATTACTGCGTCTTACAACTGATACCCTCTGATAAAGTATTGATCATTGGCCAAAGTAA
GGTTGGCAAAATCAAGTGGTAATAGAAGCGGAGGACGTGGGTGGTATTGGCAAAATACCTATG ATTCAAAACCTTCTATCGACCGAGAGTTTGTCT

Sc0000060:277769-278327 (CNR 45, intron 2)

GACTTACCAACCTGAGGAAGCTATTACAGAGAACAGATCTAGAAGTTACTAACTTGGGTGGTTTTCTAATCCGACCACGCCCTGTAGTTCATAGTTGCTGTGT
CTCCATCTCGAAGTGGATGATACGACTAATCGTGAGATAGCGGAAACATGCGTTATTGATGCCCGTTACCACGTACGCCCTCGCTCAGAGATGCCTANCTCG
CTACGAGCGTGTCTCCAGCCGTTTCCCCCATATCCTTTCATCGGCAAGCACACCGCCGTTTAAATCCCTAAATGAGTGCCTTACATGCCATCCGTCAGAGTCAA
TCAGGTAGTAATCTTTCAATGATAAGGCAGCTTGCGCCAATTGATGCGTTGCCATTTAGCGGGCAGCAGCAAGCCCTTAGGCACGTAGACACAGATGTCG
CTATTACATTTTATCCCTCTAAACGGTAGACAATTGCTGCTAACGTTCCGGAGGGGAATACTCATAAGTGAAGTGAATGATGTTAAGCATAGAGGTCGGAGAC
AGATTACTCGGCCGGAACCTAAGCAAGACACTCGTCAACATGCAAGTCTGACCAATAGGAAATAAAGTGGCTTTGACAGCTCTGAAGGCAAAATACATTG
CTGCATAAGCTGATCAAAATTTGGAAAATAGTAAATGGTCGTGCCACAGTATTTGTAAGATCTTATCCGCCACGTGTTGTGTAATCTACAGTGACTCATTG
ACAGTATG

The selection criteria used to decide which CNRs will be tested for *in vivo* transgenesis were:

1) The presence of putative transcription factor binding sites (TFBSs). In order to detect potential TFBSs, I used JASPAR database that is an open-access database of annotated, high-quality, matrix-based transcription factor binding site profiles for multicellular eukaryotes. The profiles were derived exclusively from sets of nucleotide sequences experimentally demonstrated to bind transcription factors (Sandelin *et al.*, 2004). In the perspective of a comparative analysis of neuronal *Nos* regulation among chordates, to

identify the potential TFBSs in the genomic regions of interest I used vertebrates JASPAR matrix models with a very high profile score threshold of 99%.

2) The presence of putative TFBSs already described in human neuronal NOS promoters. The CNRs selection based on this criterion can promote the discovery of evolutionarily conserved active regulatory regions.

3) The presence of putative TFBSs for transcription factors (TFs) that co-express with *NosC* in amphioxus embryos.

2.6.2 DNA constructs for transgenesis in *Ciona robusta*

DNA digestion with restriction enzymes: analytic and preparative plasmid DNA digestions have been performed with the appropriate restriction endonucleases in total volumes of 50 μ l. The digestion reaction has been prepared as follows: 2,5 μ g of DNA (GFP-SV40 vector and pGEMT easy vector in which CNR were cloned), suitable restriction enzyme buffer 1/10 (Roche), SphI and SalI restriction enzymes (5 unites enzyme per 1 μ g of DNA) and BSA (1/100, if required). Specific reaction temperatures have been used as suggested by manufacturer's instructions. In order to prevent self-ligation, a convenient amount of double strand linearized DNA has been incubated with 1 U of Calf Intestinalis Alkaline Phosphatase enzyme (CIAP; Roche) per 1 pmol 5' ends of linearized DNA, in 1x CIP dephosphorylation buffer (Roche), at 37°C for 30 min.

DNA ligation: each ligation reaction has been carried out in a final volume of 20 μ l with a mixture containing 1X T4 Ligase buffer (50 mM Tris-HCl pH 7.5, 10 mM MgCl₂, 10 mM dithiothreitol, 1 mM ATP, pH 7.5) and 1 U of T4 DNA Ligase (New England

Biolabs). The proportion of plasmid vector and insert DNA was usually kept 1:3, and the total amount of DNA was kept within 50-100 ng. The reaction mix has been incubated at 16°C overnight or 3 h at R.T. and used to transform competent bacteria.

2.7 NO QUANTIFICATION AND LOCALIZATION

2.7.1 Griess assay

NO quantification has been hampered by the physiological short half-life of this gaseous free radical, so alternatively integrated nitric oxide production can be estimated from determining the concentrations of nitrite and nitrate final products. The measurement of nitrate and nitrite concentration or of total nitrate and nitrite (together) concentration is routinely used as an index of NO production (Moshage *et al.*, 1995).

Samples preparation: several samples for each developmental stage were collected and homogenized in 500 µl of 1X PBS, subsequently several cycles of sonication were performed to obtain the membrane fractionation. The sonication was performed on ice with 3 cycles of 1 min, with amplitude of 30%. After the homogenization, a centrifugation of 10 min at 13.000 rpm allowed to separate the liquid fraction, in which there are proteins.

Bradford protein assay: Bradford protein assay is a simple and accurate procedure to determinate the concentration of solubilized protein. It involves the addition of an acidic dye to the protein solution, and subsequent measurement at 595 nm with a spectrophotometer or microplate reader. Comparison using a standard curve provides a relative measurement of the protein concentration of the sample. To obtain a calibration

curve, and subsequently to quantify the protein concentration in the samples bovine serum albumin (BSA) was used as standard at three different concentrations: 3, 6 and 9 μg in PBS 1X. For each sample 200 μl of Biorad solution was added, μl of BSA for several concentrations of solutions and up to 1 ml with PBS 1X. After ten minutes of incubation the samples were read at the spectrophotometer and the value were used to construct the calibration curve; in particular the angular coefficient of the fit line was used to calculate the protein concentration of the samples.

Griess reaction: the reaction described below was first reported by Johann Peter Griess in 1879 as a method of the analysis of nitrite (Green *et al.*, 1982). Before measuring the concentration of nitrites, all the nitrates were converted to nitrites using the nitrate reductase (NaR). To obtain a standard curve useful to quantify nitrite concentration in our samples, the Griess reaction was performed on sodium nitrite solutions at different molarity: 0 μM (blank); 2,5 μM ; 5 μM ; and 10 μM in PBS 1X. For this assay, nitrite is first treated with a diazotizing reagent, e.g., sulfanilamide (SA), in acidic media to form a transient diazonium salt. This intermediate is then allowed to react with a coupling reagent, N-naphthylethylenediamine (NED), to form a stable azo-compound. The intense purple color of the product allows nitrite assay with high sensitivity. The absorbance of this adduct at 540 nm is linearly proportional to the nitrite concentration accordingly NO concentration in the sample (Sun *et al.*, 2003). Aliquots (50 μg of total protein in 150 μl) were incubated for ten minutes in the dark with equal volume of 1% (wt/v) SA in 5% H_3PO_4 and then for ten minutes with equal volume of 0,1% (wt/v) N-(1-naphthyl)- ethylenediaminedihydrochloride. The samples were measured at the spectrophotometer and results were expressed as nmol of NO per mg of protein. For the

conversion of nitrates to nitrites, 50 µg of total protein were incubated for 2 h at 25°C with NaR (0.24 U/ml) and the co-factors FAD and NADPH (final concentration 5 µM and 0.2 mM, respectively) in a final volume of 150 µl. Then, samples were incubated with SA and N-(1-naphthyl)- ethylenediaminedihydrochloride, as reported above. The efficacy of nitrate reduction by NaR was tested on known concentrations of nitrate with a recovery of nitrite of 90–100%.

2.7.2 DAF-FM diacetate assay

NO localization was performed using 4-amino-5-methylamino-2',7'-difluorofluorescein diacetate (DAF-FM-DA), which is the most sensitive cell permeable and non-fluorescent reagent that combines with the NO forming benzotriazole, a fluorescent compound (Kojima *et al.*, 1999). Embryos at different developmental stages and conditions were incubated for 20 min in the dark with 5 µM DAF-FM-DA in FSW. After treatment, the animals were washed in FSW for 30 min and quickly fixed in 4% PFA. The fluorescence was visualized with ZEISS Axio Imager Z1 fluorescence microscope equipped with a filter $\lambda_{\text{EXC}} = 470 \pm 40$, $\lambda_{\text{EM}} = 525 \pm 50$.

2.8 DIFFERENTIAL TRANSCRIPTOMIC ANALYSIS

Samples preparation: total RNA for transcriptomic analysis was isolated from TRIM-treated embryos as described above. The RNA integrity number (RIN) was measured at the Genomics and Bioinformatics Services of Genomix4Life (Italy) (See Results chapter). For the sequencing, the embryos chosen started to be treated at 24 hpf and

collected at 30 hpf. The experiment was performed in triplicate, for each replicate an untreated (control) and a treated sample were sequenced.

RNA sequencing: Next generation sequencing (NGS) experiments, comprising samples quality control, were performed by Genomix4life S.r.l. Indexed libraries were prepared from 1 ug/ea purified RNA with Indexed libraries were prepared from 1 ug/ea purified RNA with TruSeq Stranded Total RNA Library Prep Kit according to the manufacturer's instructions. Libraries were quantified using the Agilent 2100 Bioanalyzer (Agilent Technologies) and pooled such that each index-tagged sample was present in equimolar amounts, with final concentration of the pooled samples of 2 nM. The pooled samples were subject to cluster generation and sequencing using an Illumina NextSeq500 System in a 1x75 single read format (30 million of reads) at a final concentration of 10 pmol. The raw sequence files generated (.fastq files) underwent quality control analysis using FastQC.

(<http://www.bioinformatics.babraham.ac.uk/projects/fastqc/>).

RNA-seq data analysis: the analysis of sequencing data was performed by the research group of Doctor Héctor Escrivà from the Observatoire Océanologique in Banyuls-sur-mer (France). It has been used Bowtie2 to map reads against the transcriptome and idxstats to do the counting. The package DESeq2 on R has been used to do the differential expression analysis (Love, *et al.*, 2014). The package DESeq2 provides methods to test for differential expression by use of negative binomial generalized linear models; the estimates of dispersion and logarithmic fold changes incorporate data-driven prior distributions. The final output was provided as an .xls files containing gene-level and transcript-level differential expressions. Gene Ontology and Pathway

Enrichment Analysis are performed with an adjusted p-value <0.1 (treated vs untreated).

2.9 NOS PHYLOGENETIC ANALYSIS

B. lanceolatum Nos genes were annotated in the genome draft version B171nembr, kindly provided by the “*Branchiostoma lanceolatum* genome consortium”. *B. lanceolatum* Nos genes’ sequences are shown in figures 2.5, 2.6 and 2.7. *B. belcheri* Nos genes were identified from the automated predictions of NCBI. To find *A. lucayanum* Nos genes, we screened a previously published transcriptome assembly (Yue *et al.*, 2014). *A. lucayanum* NosC gene coding sequence which was very fragmented in short contigs. Two of these, GESY01098362 and GETC01143078, overlapped and we reconstructed a longer sequence, which was used for the phylogenetic analysis. Briefly, we did TBLASTN searches using the amino acid sequences of the three NOSA, NOSB and NOSC proteins from *B. floridae*, and the candidate scaffolds, contigs or transcripts were further analyzed by means of GeneWise2 as implemented in the EBI website (Birney *et al.*, 2000; Li *et al.*, 2015) and manual curation. Other NOS proteins included in the phylogenetic analysis were collected from public databases such as Ensembl and NCBI. The accession numbers for all the sequences used for phylogenetic analyses are reported in Table 2.2.

>Bl_NosA_protein

MEGQQNIIVVGLV**KREVDGLGLSAKRREVPGHSAVVIEEIVIRGGPADHTGMVQPGDTIVAVNGODIEGLSYQEATK**VIRDIEFGPKPVELVLRGPKWF
HTYLETVRLSTGETKTIVRVTRPNGPIGALTLIIQRMRGNTFDKRAIRKLENRGEIPLNNRNVANGDVIKSI³⁰PSGTIANGCPVTHGHRAAATVGPSTRRR
PVRLKNLWLNERRINDNLHSAKNDLNP⁶⁰CNDGRCLGPLMRPRPFTAPGYFRPKEEVL⁹⁰EQA¹²⁰KKFIF¹⁵⁰EYASLKSSDAGERDRRWRD¹⁸⁰VQVVEEKGVYHLT
YDELLYGAKMSWRNAPRCIGRIQW²¹⁰SKLQLFDARDVTTARGMFEAICRHIKWCTNGNIRSAITVFP²⁴⁰PRTDGRHDYKVVNGQFLKYAAYQLPDGSILG
DPINLEFTEVQALGWKGEGRFDLLPMVLSANGEDPEWFDLPKDIVMEVNIITHPKYDWFEE²⁷⁰LGIKWYCVAVSNMLFDCGGLEFSAAPFSGWYMG
EVRDRLCENRNLNITEAVGKRMGLDVARSSSLWKDAVFVEVNI³⁰⁰AVLH³³⁰SFQRNNTT³⁶⁰IMD³⁹⁰HHTASETFMKHLENEQRL⁴²⁰GGPSEI⁴⁵⁰VV⁴⁸⁰VE⁵¹⁰SS⁵⁴⁰TE⁵⁷⁰TF
PDZ **heme** **BH4** **CaM** **FMN** **inhibitory loop** **FAD** **NAPDH**
RPSFEYQEDAWLLHLWRKKPEHPVLLKYAYDENPK**KYVRLKEVALVAFVAVLMMKALNKRVT**TTILYAT**ETGKSESFASSTLGIF**
KHAFDAKMMCMDEYDITNLEKEELVIVVSTSTFGNGDPPDNGEAFQALLHMRHPG**SDKKRSGSVRRVSSI**SRASYRR**QOKLLRQLRDGGALGKRVY**
GVFALGSRAYPHFCAFGHADITLFESLGAERIHPVGEDEL⁶⁰⁰CGQEE⁶³⁰SFR⁶⁶⁰AWAK⁶⁹⁰GA⁷²⁰FK⁷⁵⁰SAC⁷⁸⁰ERY⁸¹⁰DV⁸⁴⁰GH⁸⁷⁰DN⁹⁰⁰MEEANASL⁹³⁰GS⁹⁶⁰DF⁹⁹⁰SW¹⁰²⁰AP¹⁰⁵⁰GK¹⁰⁸⁰FR¹¹¹⁰VL¹¹⁴⁰Q¹¹⁷⁰TK¹²⁰⁰G
LPETDILEGLSKLHRRTVVSSTVISR¹²³⁰TQLQ¹²⁶⁰AP¹²⁹⁰ESSR¹³²⁰QT¹³⁵⁰CL¹³⁸⁰VAC¹⁴¹⁰TE¹⁴⁴⁰FG¹⁴⁷⁰QG¹⁵⁰⁰QELR¹⁵³⁰YV¹⁵⁶⁰PD¹⁵⁹⁰HV¹⁶²⁰AV¹⁶⁵⁰FPANEDRLVQAILDRVEKGTNPDAVIQIEALQEKKI
GAGLVKSWTPHRLPTCSLR¹⁶⁸⁰TALS¹⁷¹⁰RYLD¹⁷⁴⁰VTP¹⁷⁷⁰SP¹⁸⁰⁰QL¹⁸³⁰LL¹⁸⁶⁰YLAM¹⁸⁹⁰HAT¹⁹²⁰SSR¹⁹⁵⁰ERAE¹⁹⁸⁰LEAL²⁰¹⁰GK²⁰⁴⁰G²⁰⁷⁰LY²¹⁰⁰ED²¹³⁰WK²¹⁶⁰FE²¹⁹⁰AA²²²⁰PT²²⁵⁰PE²²⁸⁰VL²³¹⁰QHY²³⁴⁰PS²³⁷⁰LQ²⁴⁰⁰VPP²⁴³⁰ALL²⁴⁶⁰LS²⁴⁹⁰QL²⁵²⁰P
VL**QORYYSIS**SPHMY²⁵⁵⁰PQ²⁵⁸⁰I²⁶¹⁰HAT²⁶⁴⁰VAV²⁶⁷⁰KY²⁷⁰⁰TR²⁷³⁰GG²⁷⁶⁰QG²⁷⁹⁰PE²⁸²⁰SX²⁸⁵⁰NL²⁸⁸⁰NT²⁹¹⁰IK²⁹⁴⁰SNE²⁹⁷⁰SVP³⁰⁰⁰CF³⁰³⁰IR³⁰⁶⁰TAK³⁰⁹⁰NF³¹²⁰HL³¹⁵⁰PENS³¹⁸⁰SL³²¹⁰PL³²⁴⁰V**VGPGGTGIAPLRSFWQQR**QVDI
KAGTASGHPPGDMTLVFGCRQSRVDHIYKEETAQARRD**GA**LDLTYAL**SRE**PGT**TKTY**VDII**IR**QQIPKKVLDLVLK**DGGHIYVCGDVTMATDV**GET
VQRILVHKGMSVARAEDFINMKDN**NRVHEDIFG**VTLKT**HEVE**DAARKRSPSFI**LS**SENTSL

>Bl_NosA_CDS

ATGGAGGGACAACAGAACATCATCGTCGTCGGACTGGTCAAGAGGGAGGTTGATGGACTGGGATTATCGGCGAAGCGACGGGAAGTACCCGGTCA
CTGCGGTGGTTCATCGAGGAGGTGATCCGAGGCGGGCTGCTGACCACACCCGGGATGGTGCAGCCAGGGGACACCATCGTCGCTGTAACCGGGCAGGA
CATCGAGGGGTTGTCGTACCAGGAGGCGACCAAGGTATCAGGGACATCGAGCCAGGGAGCCGGTGCAGCTCGTCTCCGCGGACCGAAGTGGTTT
CACACCTACCTGGAGACCGTCCGCTGAGCACCAGGGGAGACAAAACCTGTGCGAGTCCACAGGCCTAACGGGCCATCGCGCCCTGACCCCTCTCA
TACAGCCGATGAGAGGCAACACTTTTGACAAGAGAGCCATCCGTAACCTTGAGAATCGCGGCAGAAATCCCGCTCAACACCGTGGTGTGGCGAACGG
TCAGCTGATCAAGAGCATCCCCAGCGGCACCATAGCGAACCGGCTGTCCGGTCACTGGGCACAGGGCAGCCAGGTGGGACCGTCCAGGACAGGAGG
CGAGTGGACTGAAGAAGCTGGCTGAACGAAGGAAATCAATGACCCCTCACTCGAAGGCAAAACGACTTGAACCGGCAACAGCAGCCGATGATGTC
TCGGTCCGCTGATGCGACCAGCCGTTACAGCACCAGGCTACTTCCGACCGAAGGAAGAAGTCTCGAACAAGCAAAGAAGTTCATCTTCGAGTA
CTACGCCTTTTGAAGAGTTCGGATGCTGGTGAAGGAGTGCACCAAGATGCATCGGACGTATCCAGTGGTCCAACTGCAGCTGTTTGACGCC
GTGAGCTCAACAGGCCAGAGGAATGTTGAGGCTATCTGCCGACACATCAAATGGTGCACACTAACGGCGGGAATATCAGGCTGCCATTACCGTCTT
CCCGCCACGACGGGCGGTCGCCATGACTACAAGGTGTGGAACGGCCAGTCTCCTGAAATATGCCGCCTACCAGCTGCCGTGACGGGTCCATCCTCGGC
GATCCCATCAACCTAGAATTACAGAGGTATGCCAGGCTCTGGCTGGAAGGGAGAGGGCACACGGTTCGACCTGCTGCCATGGTCTGTCTGCTA
ACGGGGAGGACCCGGAGTGGTTCGACCTCCCGAAGGACATCGTATGGAGGTCAACATCACACATCCCAAGTACGACTGGTTCGAGAGTTGGGCAT
CAAGTGCATCAAGAGATGGCGAATGTTGAGGCTGTCACACATGTTGTTGACTGCGCGGCTGGAGTTCAGCGGCTCCCTCAGCGGCTCCCTCAGCGGACG
GAGGTGGGACGGACCTGTGTGACGAGAACAGGCTCAACATCACAGAAGCAGTAGGAAAGAGAAATGGGTCTGGACGTCGAAAGACTCCTCCCTCT
GGAAAGACGCGCTTTTCGTGGAGGTCAACATCGCCGCTTTCGACAGCTTCCAGCGCAACACACGACGATATGGATACCCACAGGCTTCGGAGAC
GTTTTCATCAAGAGATGGCGAATACCATGTGAGGCCCTCTTCGAAATATCAGGAGGACGCAATGGTGCCTTCACTCGTGGAGGAAGAGATCCGGCAGT
ACCCAGTCTTCTGAAGTACGCCTACGATGAAAACCCCAAAGGAAGTATCGTCTGAAGGAGTGGCTCTGGCGGTAAAGTTCGCTGCCGTGCTGAT
GAAGAAAGCTCTCAACAAGCAGTGAAGACCACCATCCTGTACGCCACGGAAACGGCAAGTGGAAATCATTCGCATCTTACACTCGGGATATTC
AAACAGCTTTCGACGCAAGATGATGTGTATGGATGAGTACGACATAACAAACCTGGAGAAGGAGGAACCTCGTCATCGTCGTCACCAGTACCTTCG
GGAACGGAGACCCCGGACAAACGGAGAGGCTTTTGGTCAGGCTTTGCTCCACATGAGGCACCCACCTGGAAGTATAAAAAGAGATCCGGCAGTGT
ACGGAGGGTGAAGGGGACGAGCTGTGTGGACAGGAGGAGTCTTCCGGGCTGGGCCAAGGGCGCTTTAAGTCCGCATGTGAGAGGTACGACGT
GGCCATGAGCTGAACATGGAGGAGGCGAACCGCTCCTTCCGCAAGTACTCAGCTGGGCGCTGGGAAGTTCGGTCTCACAGCAACAGGAGGA
CTGCCGAGACAGACATCCTGGAGGTTGTCCAAGTGCATCGCAGAACAGTGTGTCCAGTACAGTATCTCCAGAAGTACAGCTACAAGCTCCGG
AGTCCAGCCGACAGACTGCTGGTGAACCTGAAACTCACGGGGCCAGGAGCTGAGTATGTTCCCGGGGATCACGTGGCGCTCTCCAGCCAA
TGAGGACCGACTAGTGCAGGCGATTTGACAGAGTGGAGAAGGAACAAACCCGACGCGCTCATTAGATGAAGCGCTGCAAGAGAAAAAAT
GGAGCTGGTGGTTCGAGCAGGCGCCGACTCTGCCGAGGTCGACGACTACCCGCTCCCTGCAGGTCGCGCCGCTGCTGCTCAGTACAGCTGCCG
GTCTGCAGCAGCGCTACTACTCCATCAGCTCCTCCACACATGTACCCGGGCGAGATCCACGCTACTGTAGCCGTGGTCAAGTACAGGACGCGT
GTGGCCAGGGTCTGAGCAGCAGCGGTGTGTGTTCTAACTGGCTCAACACCATCAAGNTTCTAACTGGCTCAACACTATCAAGAGCAACAGTCTGGT
CCTTGCCTATTTCGACGCGCAAGAATTTCCACCTTCTGAGAATCCTCCTCCTGTCTGATGGTAGGTCCCGGACTGGCATCGCCCTCTCA
GGAGCTTCTGGCAGCAGAGACAGGTGGACATCAAGGCTGGTACCGCGTCCGGACATCCTCCAGGTGACATGACCTGGTGTTCGGCTGTAGACAGT
CAGGCTGGACCATCTACAAGGAGGAGACGGCGCAGGCAAGGAGAGACGGAGCCCTGACAGACCTTACTACTGCACTGTCCAGGGAACACGGGACA
ACTAAGACCTAGTCCAAAGACATCATACGTCAGCAAAATCCCAAGAAGGTGCTGGACCTGGTTCTAAAAGATGGCGACACATCTACGTGTGGT
ACGTCACCATGGCCACTGACCTCGCGGAGACCGTTCAGCGAATCCTGGTGAAGCACGGAGGGATGTCTGTGCCAGGGCAGAGGACTTCATCAATAA
CATGAAGGACAACACCGTTACCATGAGGACATCTTCCGTGTGACACTGAAGACACACGAGGTAGAGGATGCAGCTCGCAAGAGAAGTCCGCTTTT
ATCAGTCTTTCCGAAGAGAACACGCTCTTTGTGA

Figure 2.5: Protein and coding sequence (CDS) of the *Branchiostoma lanceolatum* NosA, come from the draft genome sequence. In the protein sequence, the functional domains are highlighted: blue=PDZ; grey=heme; green=BH4; red=CaM; light blue=FMN; pink=inhibitory loop; yellow=FAD; purple=NAPDH.

```

>Bl_NosB_protein
MPPVQSRENTDINSVNPNGCPFTGSTSTAPRAQILTDHLRNKHLTDTLHLKATNVAPCSSGKCMGSVVRQREPFPPGYKRPKEEVLQAKEFIDD
YYASMKKENSAAEHERRWIDIQAQVEEKGLYDLEYDELLYGAKMAWRNASRCIGRYQWNNLQVIDYRNVKTAQEMFDAACDHIRYATKDGQMKTAISI
FPMRTDGKHDYKFWNKYLFQYAGYQPDGSGVIGDPANVELTEVCQSLGWKKGKTPYDFLPAIVSANGEDPVI FEWPEDEVPLELELRHPKHDWFELA
IKVNCVPLQGDMLFDVGGMQFPACPITGWFOSTEPVRDLDENRYNMAEII AKKLYDTSRYNSLWKDAAFLEVHIAVIHSFQMKGMVTDQPYTLTE
SFMKHMEREHRVR RCSPDWVWVPEPSSSLVDFHDFMLNYHL PALEYQEAGWKIHTWKTPPTAPIFTQYIRTKKRCSEFKAAAMAVMPASGLMRK
FLNKRVRSTILFASQTGKAETFSNSLCDLHKHAFDAKVVCMDEYDMAQLDKQLVVIIVTSTFGNGDPPDNGETTFARALMQMKNKNGQASPRDPLSS
VRFAVFAFGSRAYPHFCAGHSVDTLLEQLGARRVHAVGEGDELCOQEESEFRWAESAFAKSACLSYDVGHGVDMEATANLLGSDLSWAPDKFRLVQ
AKTKTDTDILQGLSTVHRKNVVPCTFISRITQLQAPDSSRQITILVRLDTKDNEELEFTPGDHLGVFPANEDHLVQAILLDRIEGTTKPPDVLVIEALHK
KLTAAVVTKWMPFERLPPCSRLRTALSQYLDITPPSPQLLGSLSMHTSAPSERAELEELAKGGTKYENWKFERAPTLPEVLQDYPQLVPPALLLS
QLPVLQORYYISSSPHMYPGEIHATLAVVSYRSQGGKGPVHNGVCSWFNRLEEGETVPCFVRAAKNFHLPADPSMPVLMVGPGTGIAPLRSFWQC
RQMDIKSGNGQGNHGDMLVFGCRQSQIDHIYKDETAQAKTDGALTDIYTAYSREPDPKTYVQHVLNQLSERVKELLKNGHIYVCGDVAMADP
VCTTVQKILEEKSAMTSTESALIRMLKDSNRVHEDIFGVTLNTEKVEARAASVESAESNAKRHTIIGNQQSGDQLSMH

```

```

>Bl_NosB_CDS
ATGCCACCGGTACAATCCAGAGAAACGAACGACACCAATCCAATGTCACCCCGAACGGGTGTCCCTTTACGGGTCTACCAGCACAGCTCCGCGGA
GAGCCCAGATTCTGACAGACCCTGCGGAACAAGCACTTGACCGATACCTTACACCTGAAGGCAACCAATGTAGCCCCCTGTAGTTCAGGGAAATG
CATGGGCTCGGTCCTTCCGACAGAGAGACCGCTTCCCCCGGGTTACAAGAGGCGAAGGAAGAAGTTCGGAACAGCGAAGGAAATTTATCGACGAC
TACTACGCTTCGATGAAAAAGAAACAGTGCAGAACATGAGAGCGGTGGATCGACATACAAGCCAGGTCGAAGAGAAGGTTTGTACGACCTGG
AGTACGATGAGCTTCTGTATGGCGCAAATAATGGCCTGGCGGAACGCATCCAGATGTATCGGACGGTACCAATGGAAACAACCTTACAAGTATTGACTA
TCGCAACGCTCAAGACGGCCAAAGAAATGTTGACGCCGCTGCGATCATATTAGGTACGCCACCAAGGATGGGCAGATGAAGACTGCCATCAGCATT
TTCCCAATGCGCACAGATGAAAAACAGCACTACAAGTTCTGGAACAAGTACCTGTTTTCAGTACGCTGGGTACCAGACGCGACAGCGTTCAGTCATTG
GAGATCCCGCAAATGTGGAACTTACCAGGTTGTGCCAAAGCCTCGGCTGGAAGGGCAAAGAACTCCATATGATTTCTACCCGCCATTTGCTTCG
TAACGGAGAGACCCGGTTCATCTTGAATGGCCAGAACGCTACCCTGGAACCTGGAACCTCGGCATCCAAAGCAGCACTGGTTCGAAAGAGCTGGCC
ATAAAGTGAACTCGTACCCTGCAAGGGGACATGCTATTGACGTTGGCGGGATGCAGTTTCGCGCATGTCCAAATCAGAGCTGGTTTCAGAGCA
CGGAGCCCGTGGCGATCTGTGGACGAAAACAGATACAACATGGCAGAGATCATCGCCAAGAAGTTGGGATATGACACTTCCCGGTACAACCTCGCT
GTGGAAGGATGCTGCCTTCTGGAGGTTACATTCAGATTATACACTCTTTTCAGATGAAGGGAGTGATGACCCAGGATCAAGTACACCCCTGACCCGAG
AGCTTCATGAAGCATATGAGAGGGAAACACCGTGTCCGCGCGGGTGTCCGTCGGACTGGGTCTGGATCGTTCCCTCCCTGCTCCTCTCACTC
CCGTCCTCCACCAGGAGATGTGAACCTCAGGCCGCTCTGGAGTACCAGAGGGGGATGGAAAGATACATACATGGAAGACTCCTCCGAC
TGCCCCCATCTTACACAGTACATCCGCACAAAGAAGCGCTGCAGTTTCAAAGCGGCAGCGATGGCTGTGATGTTTGTCTCAGGGCTGATGAGAAAAG
ACTCTGAACAAGAGAGTGAAAGTCCACGATCCTCTTCGCTCTCAGACCCGAAAGGCAGAGACATCTCCAACCTCACTGTGCGACCTCCATAAGCATG
CATTTCGATGCAAAGTGGTGTGTATGGATGAGTATGACATGGCGCAACTCGACAAAGAGCAACTGGTCTCATAGTGACAAGTACTTTTGGAAACGG
GGATCCCGGACCAATGGCGAGACCTTCGCTCGTCTTAAATGCAATGAAGAACAAGAATGGTCAAGCAAGTCCAAGAGACAGCCCGCTGAGCTCT
GTGAGGTTTGGCGTGTTCGCCCTGGATCCCGGGCCTACCCGCACTTCTGTGCTTTCGGCCACAGCGTGGACACCTCCTGGAACAGCTGGGGCTC
GGCGGTCCACCGCTGGGCGAAGGGGACGAACTGTGCGGCCAGGAGGATCATTTCCGCGCATGGGCAGAGAGTGACATCAAGTCTGCCTGTTTGGAG
TTACGATGTTGGGCACGGTGTGACATGAACGAAGCCACTGCCAATCTGCTGGGCAGCGATCTGAGTTGGGCGCCGACAAGTTCGACTTGTACAG
GCCAAGACTAAGACGGCACTGACATTTACAAAGTTTTGTCCACTGTGCATCGTAAGAATGTTGTGCCTTGTACCTTTATTTACGGACCCAACTGC
AGGCACCTGACTCAAGTCGACAAACCATCTTAGTTCCGCTGGACACGAAGGACAACAAGAGTTGGAGTTTACTCCCGGCGATCACCTCGGGCTTT
CCCGCCAAATGAAGACCACCTTGTTCAGGCGATCTTAGATAGAATCGAGGGTGGAAACCAAACCGGATGATGTGCTGGAGATAGAAGCGCTGCACAAG
AAGCTGACGGCAGCTGTGGTACGAAAACGTGGATGCCTTTCGAGCGTTTTCGCCCATGTTCTTTTGGCACGGCACTCTCCAGTACCTGGACATCA
CAACCCACCATCGCCGAGCTGTTGGGTAGTCTGTCCATGCACACAGCGCTCCATCAGAGCGAGCAGAGCTGGAGGAACTCGTAAGGGTGGTAC
AAGTACGAGAAGTTCGAGCGCGCCCTACCCTACCGGAGGTGCTGCAGGACTACCCGTCCTACAGGTTCCCCCGCCCTGCTGCTGAGT
CAGCTGCCTGTCTGACGACGCGCTACTACTCCATCAGCTCCTCCCAACACATGTACCCGGGAGAGATCCACGCTACTTTAGCTGTGGTCAGCTACC
GTTCTCAGGGCGAAAGGGTCCGGTACACAACGGCGTTTGTCTCCTCGTGGTTTAAACAGGCTTGAGGAGGGTAAACGGTCCCTGCTTCTGTCAGAGC
GGCGAAGAAATTTCCACCTCCCTGCCGACCCCTTCAATGCCTGTGCTGATGGTCCGCCCGGTACGGGCATCGCCCGCTGCGCAGCTTCTGGCAGCAA
CGCCAGATGACATCAAGTCCGGCAACGGTCAGGGAGGTAACCATGGTGACATGACGCTGGTGTTCGGATGTCGACAGTCCAGATAGACACATCT
ACAAGGACGAGACGGCCAGGCCAAGACAGACGGAGCGTGCAGGACATTTATACAGCCTACTCCAGAGAACCGGACACACCAAAGACCTACGTCGA
GCATGTTTGTACAACTCTCCGAGAGAGTGAAGAACTCCTGAAGAAATAATGGACATATCTATGTCTGTGTTGAGCTAGCCATGGTGTATGAC
GTATGCACCACCGTGCAGAAAATACTGGAAGAAAAGTCCGCGATGACGTCGACGGAGAGCGAAGCATTAAATCAGAATGTTGAAGGACTCCAATCGCT
ATCAGAGGACATCTTTGGGGTACTCTCAACACAAGGAGGTTTCGAGAGCGCTCGAAGCGTTCGAGTTCAGCCGAGAGCAATGCAAAACGACACAC
CATCGGAAATGGCCAGCAAAGCGGAGACCAGCTATCTATGCACTAG

```

Figure 2.6: Protein and coding sequence (CDS) of the *Branchiostoma lanceolatum* *NosB*, come from the draft genome sequence. In the protein sequence, the functional domains are highlighted: blue=PDZ; grey=heme; green=BH4; red=CaM; light blue=FMN; yellow=FAD; purple=NAPDH.

>Bl_NosC_protein

MEIRPNVIAVLLMKREGDGLGFLVKQRSCNPPVIVSDVVRGGAADQSLIQVGDLLSVDGTSLETVPYSDALQVIRAVEVGPKEIILRGPGEFATKLETTFTGTGIPKTVRITTAESPLRSLALSAPARRLIKRIITGNSHVKSIDHINAEALKEKETVSNGLPGLDHSGRMETPKTCCSSIAVQTSPEEPTTKEVNGQCNGNATVAQLDKTKLTLDTISIALKRESVNGNELGRPIESGPPSSRRNSATLSPSAKPRFARMKNLWLDKQMTDTHLHKATPINPCSGTKCLGSLMRPNAAAQAQSARPAVEARPKDEVLEHAKFLDEFFASIKRANTQAHKQRWAEAKVQIEEKWYELTQEMELTYGAKLAWRNAPRCVGRITQWSLQVFDARYVTTARGMYEAI CNHIKYATNKGNLRSAITFPARTDGKHDFFKVVNSQFVRYAGYKQPDGSVVGDPASVEFTEICQSLGWKGNKGNPFVLPMLVLSANGQDPELFELSRDLVLEVLKHPKYAWFKELGMKMYALPAPANMLFDVGVGVEFPAAFPFGWYMCTEIGRDLCDINRYNYTEQIAKRMGLDTGRASSLWRDLAMIEANVALILHSFQTGNVTITDHHITACE SPMKHMENEQRLLRPSYEQEDAWKTHVWKKKEDTKRIMP GKAKRKFPGKEVAKAVKFSAKLMGKALAKRVKATILYA TETGKSERYAKTGTGKSERYAKTVCEIFKHAFDAKVMCMDDYDIMHLEHETLVIVVTSTFGNGDPPDNGESFGQALLEMRHPPMNDNDRPPIRRVSESSSDGGHTKRLSSISSATERRRKFHQMKERDMSMDLDGGPLSNVRFSAFGLGSRAYPGFCFAFAHAVDTLFGELGGERIYKMGGEDELCEQESFRKWKAGVFKACADTFVCGDDLNMSEASSTLLNSDATWSPDKFRLIPAEVKEFEIWEGLSKVHHRNVVPCRLISRENLAQPSDREGRETLVRLDSQGSDDLNVVPGDHLAVFPANEDHLVQAVLDRDLNAPDPSIVNMEVLQEQPTPLGAIRTWMTSERLPPCSLRLTALSRYFDITTPSPQLLOHLATQATDEEEKLEVLGKGDARYEDWKFERTPNLVLEVEDYPSLKVAPTLTLLSPLFPQQRYYSISSQRMYPGEIHAIVAVVRFATQGGVPTHNGVCSWLNRIEKDDIVPCFVRGAQNFHLPEDPTVPLMNVGPGGLIAPFRSEWQHRQMEVTSGDPHHRPKYQMTLVFGCRQKMDDIYKHETAQAKEDGALTEVYLTALSREPVPKSVQNVILDLIPEKVCIDL LMKLNGHFFVYCGDVSMAADV CNTLEKAMEKQQGMTPNKAQDFVDKLDKCNRHEDIDFVTLRTQEVTDTRVSAARKNWRVVKRLRPSTVVPTRGLSPVRESSLSLSTPMSTPSATPANSPYSSPLHRPDPTVCANGDPLSLHIEE

>Bl_NosC_CDS

ATGGAGATTGGCCTAACCTGATTGCCGTC AAGTGTGAAGAGGGAGGGGATGGACTAGGCTTCTGGTGAAGCAGCGCTCTCGCAACCTCCAGTCATCGTCTGACGTGGTGGAGGGCGGCGCAGACC AAAGCGGGTGTGATCAAGTCGGCGACTTATCCTCTCCGTCGACGGCAGGATTTGGAGACCGTGCCTACAGCGACGTCTACAGGTTCTCAGGGCGGTGGAGGTGGGAAAACCGACGGAGATCATCTCCGCGGGCCGAAGTTTTCGCGACGAAGCTCGAGACCACTTCAGGGGACTGGCATCCCGAAAACCGTCCGAATAACCACTCGCGAAAGCCCTCTCGCTCTCTGCGCTCTCGCGGCTCGCAGGCTCATCAAGAGGATAACCGCAACTCTCACGTCAAATCAATCGACCACATCAACGCAGAAAGCGCTCAAAGAGAAAGAACTGTTTCTAATGGACCGCTAGGCACTGACCAAGCGCGAAC AATGGAGAGCGCCAAAGAGCTGTCGTCTATCGCTGTACAGACATCACAGAGAAGAACCCACCAAAAGAACTCAACGGACAGTCAACAGGCAATGCCAGCGTTGCACAGCTAGACAAGAAAAGTACTAGACACGATTTCTATCGCTGTAAAGAGGGAGAGCGTCAACGGGAATGAGCTGGGAAGGCCCATCGAGTCGGGGC CGCTTTCGGGGAACTCGGCCACGCTGAGCCCGTCCGCAAAACCGAGGTTTCGCCGATGAAGAACTGGCTGAAGCAAGCAGATGACACAGACACCTGCA CAACAAGCTACACCGATAAACCCATGTTCCGGTACAAAGTGTCTGGCTCGTTGATGCGTCTAACGCCGTGCCAACGCAAGCGCCGCGCTGGG GAGGCGAGACCGAAGATGAAGTCTTAGAGCACGCCAAAGAGTTCCTGGACGAAATTTTCGGCTCAATCAAACCGCTAACACACAGGCACAAAGCAGAGAT GGGCGGAAGCGAAGGTGCAGATCGAGGAGAAGGTTGGTACGAGCTGACGCAGATGGAGCTGACCTACGGAGCAAGCTCGCTGGAGGAACCGCCAGATG TGTCGGCAGAATACAGTGGTCTAAGCTACAGGTGTCGACGCTCGGTACGTAACAGCACGAGGCATGTAAGAACCATTGCAACCATATCAAGTATGCA ACCAACAGGGAAACCTCAGTTCGGCCATCACTATCTCCCGCTCGACCGATGGCAAAACCGACTCAAGGTGGGAACCTCGCAGTTTTCGGGTATGCCG GATACAAGCAGCGGAACTTCGGTCTGGTGAACCGCAAGCTGACTGATGATCTGCCAGAGCTGGGATGGAAGGGAAGAACCGGCTTGA TGCTCTGCCCATGGTGTCTGTCTGTAACCGTCAGGACCCGAGCTGTGAGCTGTCAAGGACCTAGTGTGGAGGTGGAGCTCAACATCCCAAGTATGCG TGGTTCAAAGAGCTTGAATGAAGTGTACGCCCTGCGCGCGTGGCTAACATGCTGTTTCGACGTGGCGGAGTGCAGTTCCGGCAGCGCCCTCAGCGGCT GTACATGTGCACGGAGATCGGCAGAGACCTGTGCGACATCAACAGATAACACAGCAAAATGGCAAAGGATGGGCTTGATACAGGACGAGCGCTC GTCACTTTCGGAGAGACCTGGCTATGATCGAGGCAAAATGTCCCACTTCTCAAGTCTTTCAGACAGCAATGTGACCATCACCGGCTCCCGGCTGGAG GTCCTTCAAGACCATGGAGAAGCAAGCAGCGCTGCGCGGTGGTGTCCGGCGGACTGGGTCTGGATCGTCCCGCTGTCTCTGCTTCTCACTCCGCTT TCCACCAGGAGATGATCAGTACTATCTGAGACCGTCTGACGAATATCAGGAGATGCGTGGAAAGACCCAGTGTGGAAGAAGAAGGAGGACACCAAGAGGAT CATGCCCTGGGAAGCGAAAAGAAAGTTCCGGCTTCAAGGAAGTGGCCAAAGCTGTGAAGTTCTCTCAAAGCTGATGGGAAGCGCTGGCCAAAGCGGTGAAG GCAACCATTTCTGTACGCTACAGAGACCGCAAGTCCGAGCGATACGCTAAGACGGNACCGGCAAGTCCGAGCGGTACGCCAAAACCGGTCTGTGAAATCTTCA AGCAGCGGTTGATGCCAAGGTGATGTTATGGATGATTATGACATCATGCACCTGGAAATGAGACACTGGTTCATCGTGTGACACGACTTTCGGCAACGG TGACCCACCGCAATGGGAGTCTGTTGGCCAAAGCCTTCTGGAGATGCGACATCCACCAATGGACAACAACGACACAGACCCCTATACGGCGGGTTCT GAATCAAGCAGCGACGGTGGGCACAGAACGGCTGAGCAGCATTTCCAGCAGCGCCACCGAGCGGCCCGGAAGTTCTCGCACCAGATGAAGGAGCGGGACA TGGACAGTATGACCTGGACCGCGGGCCCTCAGTAATGTCAGGTTTCGGCTTTCGGCTTGGTTCGCGGCTACCCAGGATTTTCGGCGTTTCGGCATCG GTTTGAACCCCTGTTCCGTTGAGCTGGGAGGAGAACCGATCTACAAGATGGGGAGGGGACGAGCTGTCCGGACAGGAGGATCAITTCGAAAGTGGGCTAAA GCGGTGTTCAAGCGCGCTGTGATCTTTCTGTGTCGGTGAACCTAAACATGAGCGAGGCTAGCTCCACCCTGTGAATTCGGACGCAACCTGGTCAACGG ACAAGTTCGACTCATTCGGCAGAGGCGTTAAGGATTTGAAATCTGGGAAGGACTATCGAAGGTGCACCATAGAAAAGTGGTACCCTGCAGACTCATCTC CAGAGAAAACCTGCAAGCACCCGACTCTGGCCGGAGACCATCTGGTGAAGTACTAGACTCCAGGGCTGGACGATCTGAATATGTGCCCGGCGACCATCTC GCCGCTTTCGGGCAATGAGGACCACTTGTGCAAGCCGTGCTGACCGACTGGACAACGCTCCGACCCGACAGTATCGTCAATATGGAGGTTTCCAAAG AGAAGCAGACGGCTAGGAGCCATACGAACATGGATGACGAGCGAGAGACTTCCCGCTGTCTCCCTCGGACCGCCCTGTCTCGTACTTTGACATCACGAC GCCTCCATCGCTCAGTACTGCAGCATCTGGCTACACAAGCTACAGATGAGGAGGAGAAGAAAGAACTGGAGGTTTTGGGAAGGGTGACCGGAGGTATGAA GACTGGAAGTTTGAAGCTACCCGAACCTCGTAGAGTCTCTGAGACTACCCGTCCTGAAAGTGGCTCCGACCTCTGCTGAGTCACTACCCCTCAGTCC AGCAGCGTACTACTCCATCAGCTCATCACAGGATGTACCCGGGAGAAAATCCACGCTACCGTCCAGTGGTTCAGGTTTGGCACTCAGGTTGGCGTGGGTC TACCCACAACGGAGTCTGCTCATCTGGTTGAAACCGAATCGAAGAGATGATATCGTACTTTGTTTCGTGCGGGGGGACAAAACCTTCCATCTACCCGAGGAC CCCACGGTTCCGCTGATGATGGTAGGTCGGGGACTGGCATCGCGCGTTCCGAGCTTCTGGCAGCACAGGACAGTGGAGGTCACCTTGTGTTGAGCCACATC ATCGGCCAAAGTACGGCCAGATGACGTTAGTATTCGGCTGTCCGACGCTAAAATGGACGACATCTACAAGCACGAGACAGCACAGGCAAGGAGGACGGCGC CTGACTGAGGTTCAACCGCTCTGTCCAGGAGCCGGCGTACCAAGTCTGATGTGTCAGAACGTCATCTGGACTGATTCGGAGAAAGGTTGCGGACCTC CTGATGAAGCATAACGCGCAATTTCTAGTCTGCGGGGACTTCCATGGCAGAGCTCTGCAACACGCTGGAGAAAGGTCATGGAAAACAGCAGGCGATGA CCCCCAACAGGCCAAGGACTTCTGTCGACAAGCTGAAGGACTGCAACCGATACCATGAGGACATCTTTGGGGTAACTTGAAGGACCCAGGAGGTGACTGACCG GTGTGCGCTCGGCCAGCTAAGAACTGGGTGCGGGTGAAGAGACTGCGGCCAGCACGGTGGTCCCGCCACAGAGGTTCTCACCAGTACGTGAGAGTTCG TCCTTGTCTACTACGCCATGTCACCGCTCCGCCACTCCCGCAACTCCCCCTACTCTCACCCTGACCGGCCGATCCGACTGTGTGTGCCAACGGCG ATCTACCCAGTCAACATTGAGGAATAA

Figure 2.7: Protein and coding sequence (CDS) of the *Brachiostoma lanceolatum* *NosC*, come from the draft genome sequence. In the protein sequence, the functional domains are highlighted: blue=PDZ; grey=heme; green=BH4; red=CaM; light blue=FMN; pink=inhibitory loop; yellow=FAD; purple=NAPDH.

Species	NOSI	NOSII	NOSIII	NOSA	NOSB	NOSC
<i>Homo sapiens</i>	AAB49040	AAB60366	AAA36365	-	-	-
<i>Asymmetron lucayanum</i>	-	-	-	GESY01069733 GESY01069734 GESY01069736 GESY01069735 GESY01069737 GESY01069738	GETC01128572 GETC01128573	GETC01013682 GETC01013681 GESY01015049 GESY01007340 GESY01007341 GETC01000005 GESY01098362 GETC01143078
<i>Branchiostoma lanceolatum</i>	-	-	-	Figure 2.7	Figure 2.8	Figure 2.9
<i>Branchiostoma floridae</i>	-	-	-	XP_002608547	XP_019636970	XP_002605826
<i>Branchiostoma belcheri</i>	-	-	-	XP_019623080	XP_019636970	XP_019631555
<i>Ciona robusta</i>	XP_009861972					
<i>Ciona savignyi</i>	ENSCSAVG00000009725					
<i>Strongylocentrotus purpuratus</i>	XP_003729305					

Table 2.2: Accession number of NOS sequences used in the phylogenetic reconstruction.

For the phylogenetic analysis, NOS amino acid sequences were aligned using the MUSCLE algorithm (Edgar, 2004) as implemented in MEGA v7, release 7161111-i38651 with default parameters, and saved in fasta format. The alignment was trimmed by trimAl version 1.2rev59, using the '-automated1' parameter. The trimmed alignment was then formatted into a nexus file using readAl (Capella-Gutiérrez *et al.*, 2009) (bundled with the trimAl package). A Bayesian inference tree was inferred using MrBayes 3.2.6 (Ronquist *et al.*, 2012), under the assumption of an LG+I+G evolutionary model. Two independent MrBayes runs of 1.000.000 generations, with 4 chains each, were performed. The tree was considered to have reached convergence

when the standard deviation was stabilized under a value <0.01 . A burn-in of the 25% of the trees was performed to generate the consensus tree (750,000 post-burn trees).

2.10 IMAGING

Scanning Electron Microscopy (SEM): biological specimen was chemically fixed, dehydrated through an ethanol series and then dried at the critical point, a method used to minimize specimen distortion due to drying tensions. The samples were mounted on a stub of metal with adhesive, coated with 40 - 60 nm of metal such as Gold/Palladium and then observed in the microscope. For images acquisition, a Zeiss EVO MA LS Scanning Electron Microscope was used.

Optical microscopy: the embryos were kept in 80% glycerol or they were observed *in vivo*. Then, the samples were placed on the microscope slides with glass spacers on the left and the right sides in order to avoid that the cover slip crushed them. For bright field and Differential Interference Contrast (DIC) images acquisition, a Zeiss Axio Imager.Z2 equipped with a digital camera was used. For fluorescence images, the ad-in APOTOME was connected to the microscope.

2.11 STATISTICS

The statistical analyses of molecular tests were performed with Two-way Student's t-test using the Microsoft Office 2010 Excel analysis tool "T-Test: Two-Sample

Assuming Equal Variance” where tails = 2 (two-tailed) was applied. Statistical significance cut off criteria was set at $p < 0.05$.

CHAPTER 3

RESULTS

3.1 CEPHALOCHORDATES INDEPENDENT NOS DUPLICATIONS AND AMPHIOXUS NOS EXPRESSION PROFILE

I have identified the *Nos* repertoire of different cephalochordate species and analysed their evolutionary history in comparison with other chordates. Previous studies have showed the presence of three different *Nos* genes in *B. floridae* genome derived from independent gene duplications (Andreakis *et al.*, 2011). A phylogenetic analysis was performed using NOS protein sequences collected from genomic and transcriptomic databases in different cephalochordate species, from two different genera: *Branchiostoma* and *Asymmetron*, which represent the most distantly-related lineages within cephalochordates. I found in each of the species analysed three paralogues NOS, that resulted to be one to one in orthology with *B. floridae* NOSA, NOSB and NOSC (Fig. 3.1). These results suggested that duplication events that originated the three cephalochordate *Nos* genes occurred in the last common ancestor of extant amphioxus, and from our phylogenetic analysis they were not orthologues to vertebrate NOS. This implies that they have independently duplicated in the lancelet lineage.

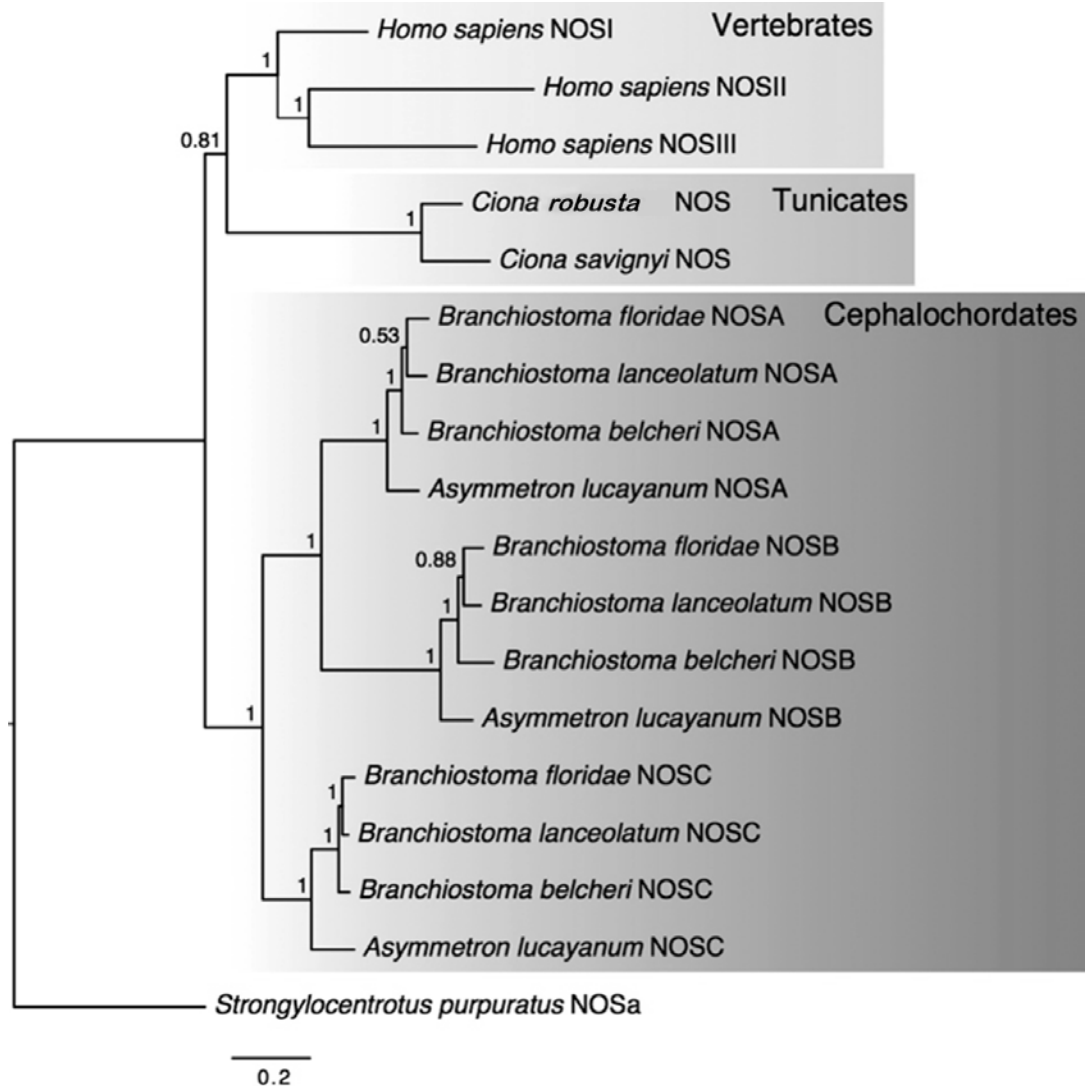


Figure 3.1: Phylogenetic relationship among chordate NOS proteins. Sea urchin *Strongylocentrotus purpuratus* was used as outgroup (from Annona *et al.*, 2017; experiment performed by the author).

In addition to identifying the evolutionary scenario of the three amphioxus NOS, I have also analysed *B. lanceolatum* *NosA*, *NosB* and *NosC* expression profile during embryonic development and in the adult stage, using the ddPCR methodology, in order to better characterize them. This study can help shed light on the diverse range of NO physiological roles during amphioxus development, which is the main goal of this PhD

thesis project. *NosB* is significantly expressed at 10 hpf while, later in development, it seemed completely turned off (Fig. 3.2a). This result is in agreement with the one obtained by the *in situ* hybridization experiments. *NosB* mRNA was detected in the endoderm at early and middle gastrula stages that correspond to 10 and 12 hpf (Fig 1.23 b-d) (Annona *et al.*, 2017). Both *NosA* and *NosC* were classified as *neuronal Nos* thanks to the presence of the PDZ domain (Andreakis *et al.*, 2011). *NosC* is expressed during embryonic and larval development while *NosA* is expressed only during the adult stage (Fig. 3.2b-c). For *B. lanceolatum*, *NosC* transcripts localization pattern was described in embryonic and larval stages: it is expressed in neural tube from neurula (24 hpf) to pre-mouth larva (48 hpf) while at open-mouth larva (72 hpf) the gene is detected in a restricted region of the cerebral vesicle and in the club-shaped gland (Fig 1.23g) (Annona *et al.*, 2017). No embryonic or larval expression of *NosA* was described by Annona *et al.* (2017). Overall, my ddPCR results are in agreement with these *in situ* hybridization data. Such a clear distinction in the temporal expression could be due to a different transcriptional regulation of these duplicated *neuronal Nos* genes (*NosA* and *NosC*) allowed by the progressive accumulation of changes in their respective promoters. To verify this hypothesis, I planned to perform a regulatory mechanisms analysis for the amphioxus *Nos* genes (see later in this chapter) that could shed light on the existence of different enhancers in *NosA* and *NosC* promoters.

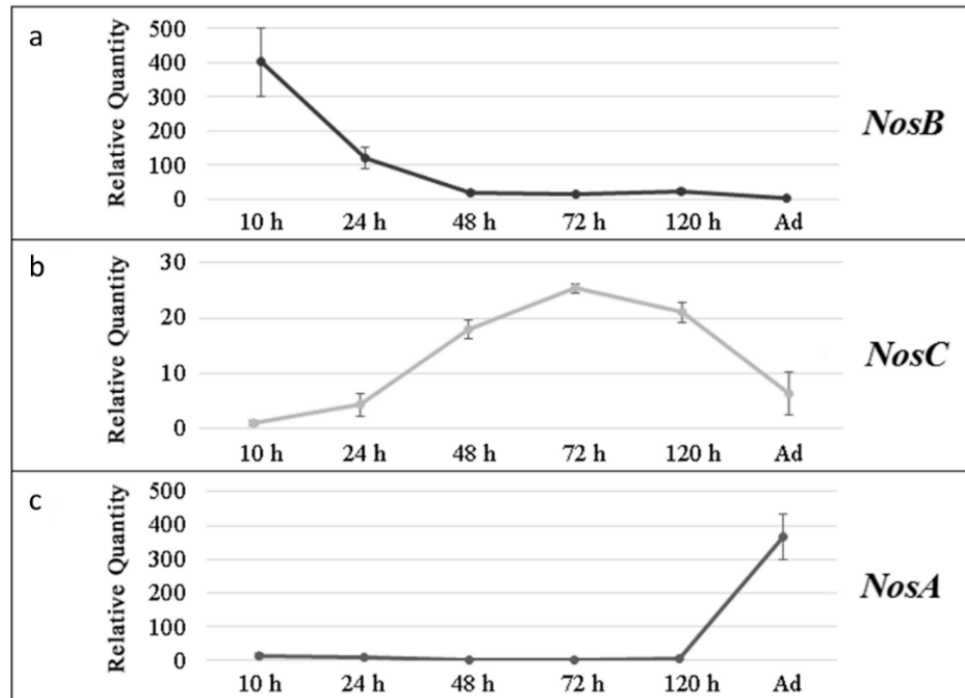


Figure 3.2: *Branchiostoma lanceolatum* *Nos* genes expression profile analysed by ddPCR. a) *NosB*; b) *NosC*; c) *NosA*. For each gene, expression is reported as relative fold change to the stage where the gene is less expressed. P-value <0,05 (from Annona *et al.*, 2017; experiment performed by the author).

3.2 INDUCIBLE NATURE OF AMPHIOXUS NOS GENES

Despite the different *Nos* genes that have been associated with particular cell types and concept of constitutive vs inducible used to classify them, several questions remain about whether these associations have been applied too strictly. This issue is still controversial but there are some evidences that neuronal and endothelial *Nos* could be inducible under some circumstances, and conversely, inducible *Nos* can be constitutively expressed (Amin *et al.*, 1995; Vaz *et al.*, 2011; Jiang *et al.*, 2013; Mattila and Thomas 2014). In amphioxus, NOSA and NOSC have been identified as neuronal NOS due to the presence of the PDZ domain and the inhibitory loop sequences, while

NOSB has been identified as inducible because it lacks the distinctive feature of a constitutive NOS, i.e, the inhibitory loop between the two FMN-binding domains (Andreakis *et al.*, 2011) and the PDZ domain. In order to shed light on the possible inducible nature of the three amphioxus *Nos* genes, I performed a stimulation of the immune system by means of lipopolysaccharides (LPS) treatments on 72 hpf larvae for 1, 2, 4, 6, 8 hours and then I analysed the expression levels of the three *Nos* genes. Indeed, LPS is commonly used as an activator of the immune response, and it is known that NO production is induced under these conditions. First of all, I conducted toxicity tests to choose the right concentration of the drug that would allow me to stimulate the immune system of larvae without causing their premature death. After these preliminary tests, I selected 10 µg/ml as the LPS concentration to use for my experiments. Then, as control, I analysed the *AmphiItln239631* expression levels after 1, 2, 4, 6, 8 hours of LPS treatment as evidence of the immune system stimulation (Fig. 3.3a), in fact it is known that they increase under LPS stimulation in amphioxus (Yan *et al.*, 2013). *AmphiItln239631* was upregulated after 2 and 8 hours of treatment (Fig. 3.3a), in comparison with untreated conditions, demonstrating the immune system stimulation. In the same experimental conditions, *NosA* expression was induced after 8 hours of treatment, with a fold change of 14 in comparison with untreated larvae (Fig. 3.3b). The *NosB* expression also increased after 8 hours of LPS stimulation but there was a fold change of only 2 times in comparison with untreated conditions (Fig. 3.4c). There was no significant variation in *NosC* expression after LPS stimulation in the time and concentration conditions used for this experiment (Fig. 3.3d).

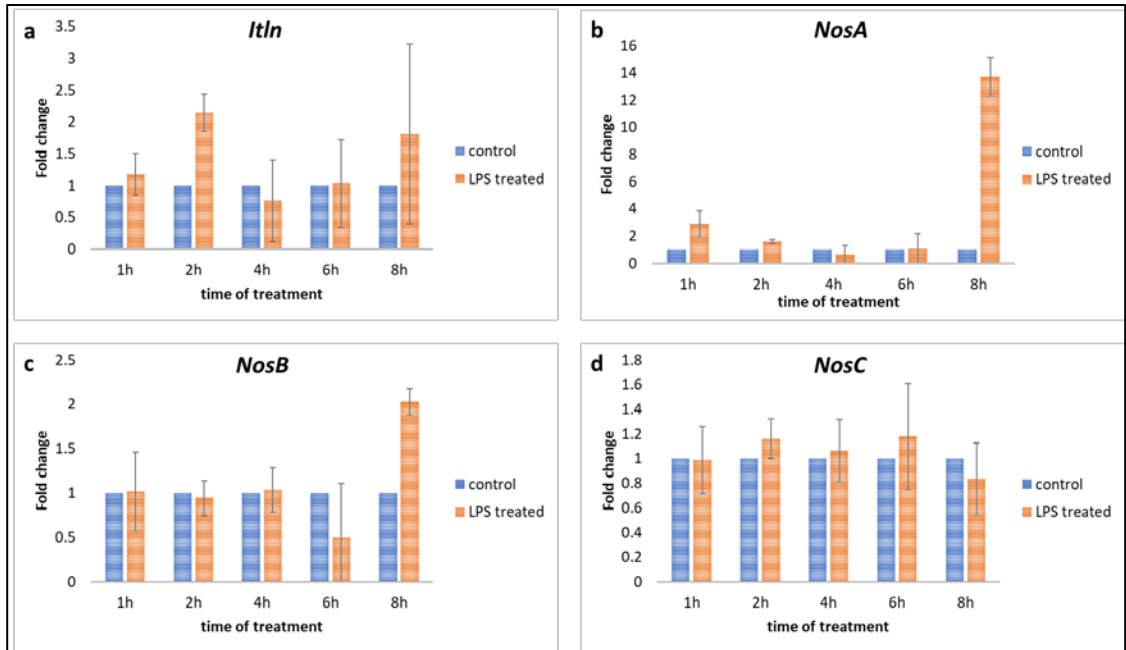


Figure 3.3: *Branchiostoma lanceolatum* *Nos* genes expression analyses by qPCR after LPS stimulation. a) *AmphiItln239631* expression in 72 hpf amphioxus larvae after 1, 2, 4, 6 and 8 hours of LPS treatment in comparison with un-treated animals. b) *NosA*, c) *NosB*, and d) *NosC* expression levels in 72 hpf larvae after 1, 2, 4, 6 and 8 hours of LPS treatment in comparison with un-treated animals.

3.3 REGULATORY MECHANISMS OF AMPHIOXUS *NosC*

One of the purposes of this PhD thesis project was to reveal key features of amphioxus *Nos* genes regulation. First of all, I focused my attention on the promoter of *NosC*, the amphioxus neuronal *Nos* that is expressed during embryonic and larval development (Fig. 3.2) (Annona *et al.*, 2017). In order to study the regulation of *NosC*, I have identified putative enhancer sequences in its promoter testing their transcriptional activity by transgenesis experiments in *C. robusta* (invertebrate chordate).

To find *cis*-regulatory elements of *NosC*, I decided to consider the first and second intronic regions in which often enhancers are present (Fig. 3.4). I focused on 17 kb

upstream (intron 1) and 15 kb downstream (intron 2) genomic regions relative to the ATG (respectively Sc0000060:250211-267133 and Sc0000060:267743-282638 in *B. lanceolatum* genome draft (version BI71nemr) (Fig. 3.4).

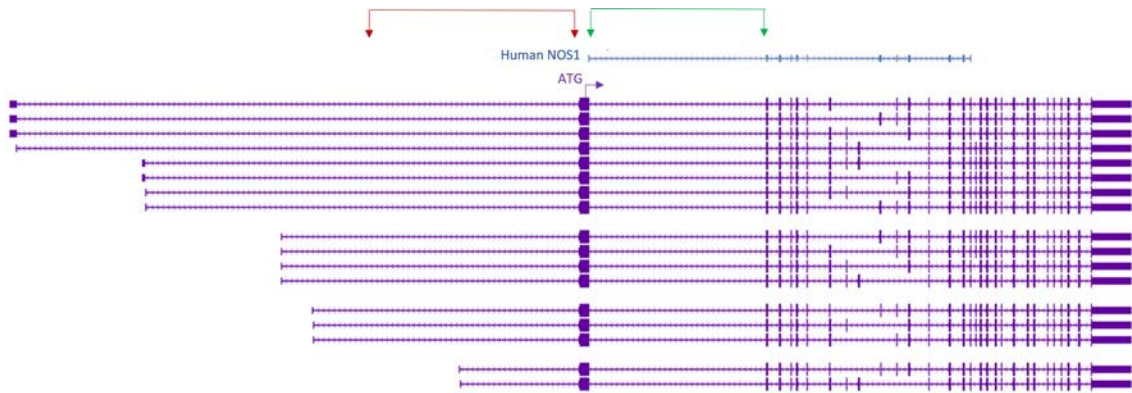


Figure 3.4: *Branchiostoma lanceolatum* *NosC* genomic locus. In blue is reported the aligned Human NOS1 protein. The position of the translation start codon (ATG) on exon 2 is indicated. On the left are indicated the alternative first introns. In purple are indicate several predicted *NosC* isoforms, the boxes are the predicted exons spaced by introns. Red arrows indicate the analysed genomic region upstream the ATG; green arrows indicate the analysed genomic region downstream the ATG.

The comparative alignment of these genomic regions between three closely related amphioxus species - *B. floridae*, *B. belcheri* and *B. lanceolatum* - revealed the presence of several conserved non-coding regions (CNR) using PhastCons program (Fig. 3.5, blue peaks). In order to identify putative transcription factor (TF) binding motives I used JASPAR database. I surveyed exclusively the CNRs highlighted by comparative *in silico* analyses. An early preliminary selection of possible active enhancers was performed on the base of the information already present in literature about *neuronal Nos* enhancers. Moreover, I paid more attention to those TFs that from expression patterns known in literature could co-localize with amphioxus *NosC*. The selection

process is schematized in the table 3.1. Thank to this sorting, some CNRs were selected to be tested in transgenesis experiments and they were cloned in 9 distinct constructs, as shown in figure 3.5 (see Methods for constructs preparation).

CNRs highlighted by comparative <i>in silico</i> analyses	Putative TFBSs are present (JASPAR prediction)	These putative TFBSs are already described in human neuronal NOS promoter	The TFs binding these TFBSs co-express in amphioxus with <i>NosC</i>	CNRs highlighted by comparative <i>in silico</i> analyses	Putative TFBSs are present (JASPAR prediction)	These putative TFBSs are already described in human neuronal NOS promoter	The TFs binding these TFBSs co-express in amphioxus with <i>NosC</i>
CNR1	✓			CNR 24			
CNR 2	✓	✓	✓	CNR 25			
CNR 3	✓	✓	✓	CNR 26			
CNR 4	✓			CNR 27	✓		
CNR 5	✓			CNR 28	✓		
CNR 6	✓		✓	CNR 29	✓		
CNR 7				CNR 30	✓		✓
CNR 8				CNR 31			
CNR 9	✓		✓	CNR 32			
CNR 10	✓	✓	✓	CNR 33	✓		✓
CNR 11				CNR 34	✓	✓	✓
CNR 12	✓		✓	CNR 35			
CNR 13	✓		✓	CNR 36			
CNR 14	✓	✓		CNR 37			
CNR 15	✓		✓	CNR 38			
CNR 16				CNR 39	✓		✓
CNR 17	✓	✓	✓	CNR 40	✓	✓	✓
CNR 18	✓		✓	CNR 41	✓	✓	
CNR 19	✓	✓	✓	CNR 42			
CNR 20				CNR 43			
CNR 21				CNR 44			
CNR 22	✓			CNR 45	✓		✓
CNR 23				CNR 46			

(see page 92 for the legend)

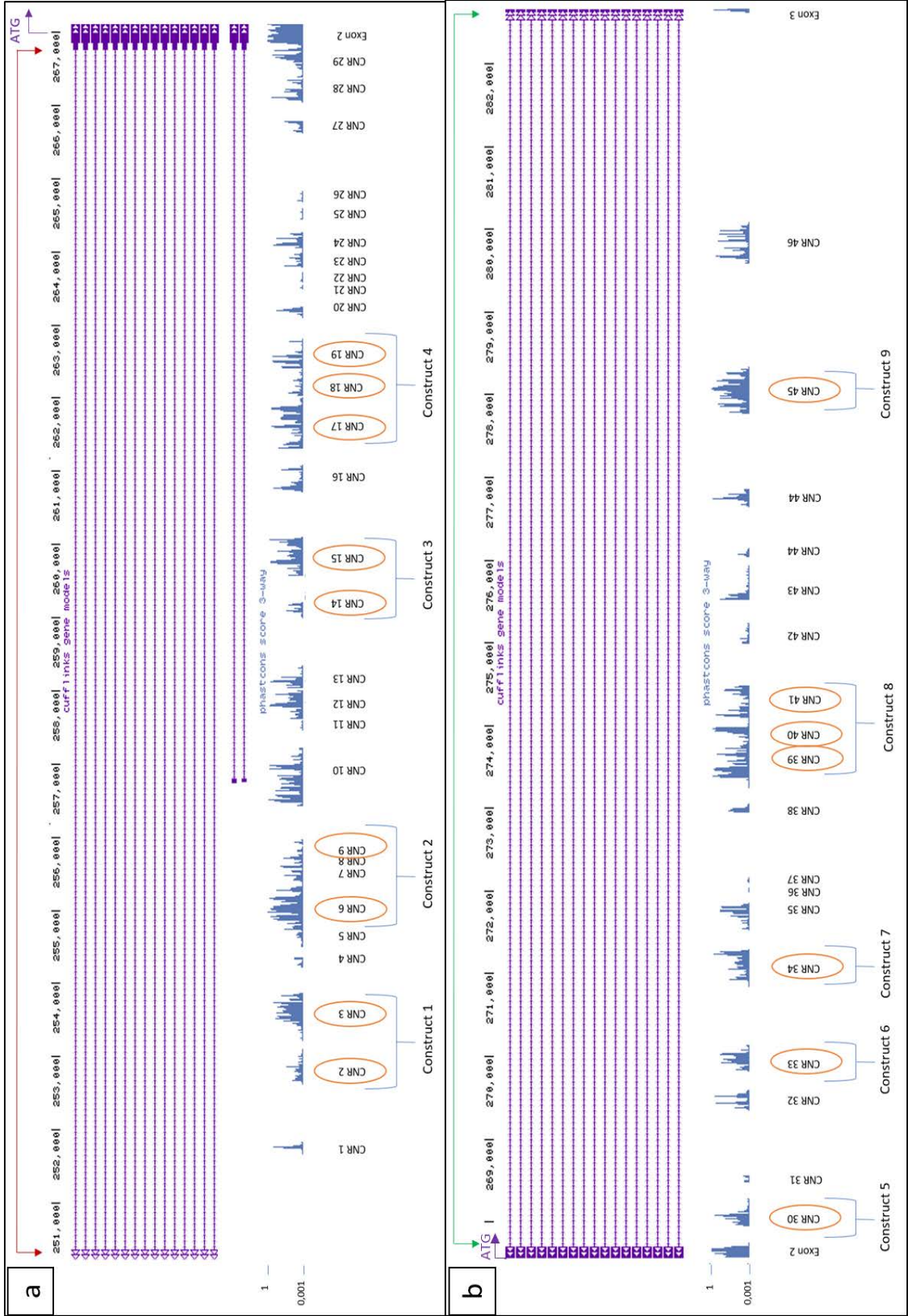


Table 3.1: Selection process schematization for the CNRs to be tested by transgenesis. The ticks indicate that the CNRs respect the selection criteria. If at least two of the three criteria were met, the CNR was tested by transgenesis.

Figure 3.5: Amphioxus CRNs tested by transgenesis. a) Magnification of 17 kb upstream the ATG of *B. lanceolatum* *NosC* showed in figure 3.4. b) Magnification of 15 kb downstream ATG of *B. lanceolatum* *NosC* showed in figure 3.4. In blue are shown the conservation tracks between *B. lanceolatum*, *B. floridae* and *B. belcheri*. Red ovals indicate selected CNRs that were tested in transgenesis analyses.

Preliminary results were obtained in *C. robusta* using 16 amphioxus *NosC* CNRs in 9 constructs (Table 3.2). Embryos were let to grow and larvae were observed *in vivo* under the fluorescent microscope. Constructs 3, 4 and 8 directed expression of GFP in *C. robusta* nervous system. The specificity of the signal, for each experiment, was demonstrated using the pSP72 vector containing the TATA box and the GFP reporter gene as negative control. This negative control vector was inserted by electroporation in *C. robusta* fertilized eggs simultaneously with other constructs.

Construct name	Total number of larvae observed*	Positive GFP expression*	Percentage of positive
Construct 1	190	0	0%
Construct 2	210	0	0%
Construct 3	205	58	30%
Construct 4	200	81	40%
Construct 5	200	0	0%
Construct 6	201	0	0%
Construct 7	196	0	0%
Construct 8	208	42	20%
* they were calculated as averages of three distinct experiments			

Table 3.2: Summary of results obtained from transgenesis experiments in *Ciona robusta* using amphioxus *NosC* CNRs.

The electroporation of construct 3 allowed me to detect GFP expression in approximately 30% of transgenic *C. robusta* larvae in the motor ganglion (MG) and in the dorsal caudal epidermal neurons (DCENs) (Fig. 3.6b-e-f). The motor ganglion is a compartment of *C. robusta* CNS that consists of motor neurons and interneurons. The negative control resulted in the absent GFP expression in embryos (Fig. 3.6f). No specific GFP expression was detected in earlier developmental stages.

In the genomic region included in construct 3, different putative TFs binding sites were predicted with a relative profile score threshold of 99% using vertebrate matrix models from JASPAR database. I carefully studied the literature regarding *neuronal Nos* enhancers, mostly in vertebrates, and I crossed the information found with JASPAR prediction and the expression pattern of these predicted TFs in amphioxus. In this way, I made a list of the putative enhancers, present in this region, that could regulate amphioxus *NosC* transcription (Fig. 3.6a). The transcription factors able to bind those putative enhancers are: Nuclear Factor I (NfI) and Nk2-related homeobox gene (Nkx2.1).

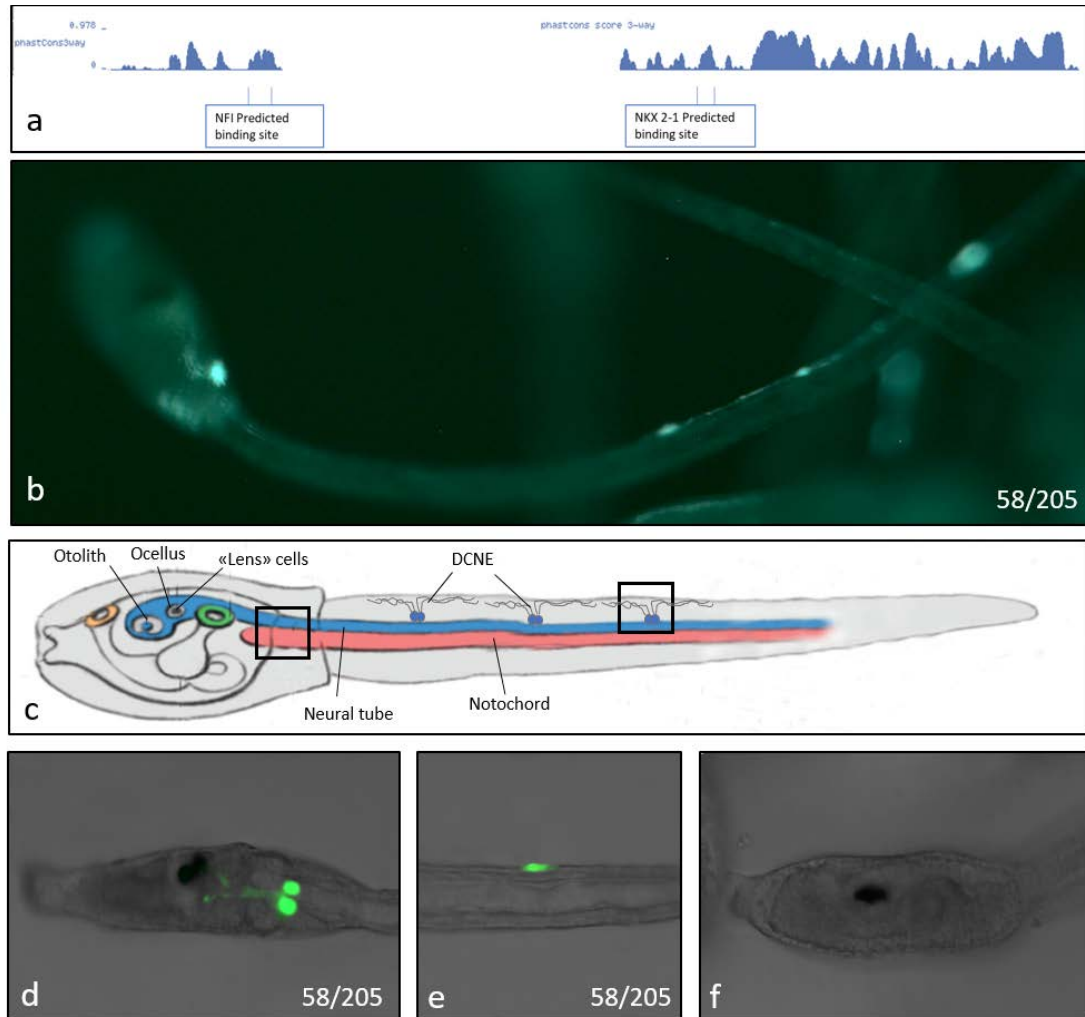


Figure 3.6: Cross-species regulatory activity in *Ciona robusta* of the amphioxus CNR14 and CNR15 cloned together in the construct 3. a) Results of PhastCons analysis of genomic regions called CNR14 and CNR15. In the blue boxes are reported the transcription factors binding sites predicted by JASPAR. b) Transgenic *C. robusta* larva using construct 3 (amphioxus CNR14 and CNR15 together). c) Schematic representation of *C. robusta* larva; DCNE: dorsal caudal epidermal neurons. d) GFP expression directed by construct 3 in *C. robusta* motor ganglion. e) GFP expression directed by construct 3 in *C. robusta* DCNE. f) Negative control *C. robusta* larva electroporated with empty pSP72 vector.

In the experiment with the construct 4 containing amphioxus CNR17, CNR18 and CNR19, 40% of larvae showed a clear GFP fluorescent signal in the CNS. Few photoreceptor cells of the ocellus were positive (Fig. 3.7c). Negative control larvae did

not show any specific GFP fluorescent signal (Fig. 3.7d). No specific GFP expression was detected in earlier developmental stages. Following all the steps described above for construct 3, I also identified in this region some putative enhancers that can regulate amphioxus *NosC* transcription (Fig. 3.7a): Nuclear Factor I (NfI), Tcf11 and Gata3.

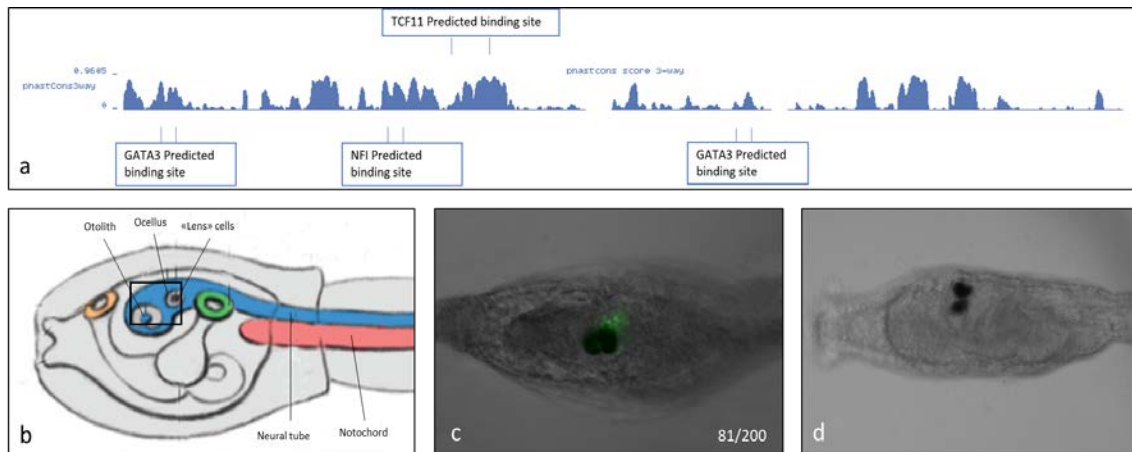


Figure 3.7: Cross-species regulatory activity in *Ciona robusta* of the amphioxus CNR17, CNR18 and CNR19 cloned simultaneously in the construct 4. a) Result of PhastCons analysis of genomic regions called as CNR 17, CNR 18 and CNR 19. In the blue boxes are reported the transcription factors binding sites predicted by JASPAR. b) Schematic representation of *C. robusta* larva, head. c) GFP expression directed by construct 4 in photoreceptor cells of the *C. robusta* ocellus. d) Negative control *C. robusta* larva electroporated with empty pSP72 vector.

Also the construct 8 directed the expression of GFP in the *C. robusta* CNS. GFP fluorescent signal was detected in both pigmented sensory organs, the otolith and the ocellus, in 20% of transgenic larvae (Fig. 3.8c). The negative control did not show any specific GFP fluorescent signal (Fig. 3.8d). No specific GFP expression was detected in earlier developmental stages. As described for previous promoter regions already tested, also for this one the JASPAR TFs binding sites prediction was carried out. The putative

enhancers here contained putative binding sites for: Nuclear Factor I (NfI), Tcf11, Meis, and Retinal Homeobox Protein (Rx) (Fig. 3.8a).

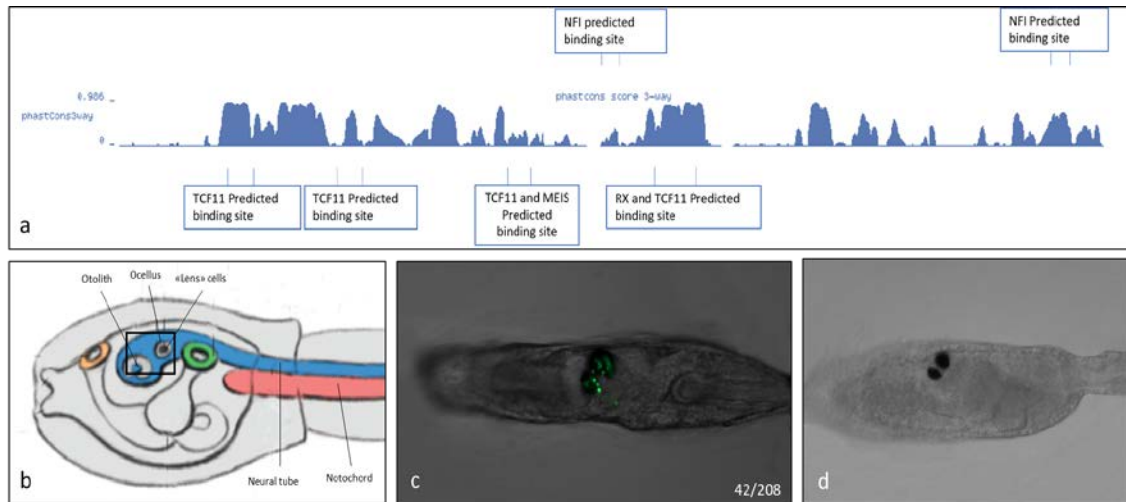


Figure 3.8: Cross-species regulatory activity in *Ciona robusta* of the amphioxus CNR39, CNR40 and CNR41 cloned simultaneously in the construct 8. a) Result of PhastCons analysis of genomic regions called CNR39, CNR40 and CNR41. In the blue boxes are reported the transcription factors binding sites predicted by JASPAR. b) Schematic representation of *C. robusta* larva, head. c) GFP expression directed by construct 8 in the ocellus and the otolith. d) Negative control *C. robusta* larva electroporated with empty pSP72 vector.

The results obtained in *C. robusta* demonstrated that its gene regulatory machinery was able to recognize exogenous conserved non-coding elements from amphioxus *NosC* promoter. This allowed me to formulate preliminary hypotheses about the amphioxus *NosC* regulation and the evolutionary conservation of neuronal *Nos* regulation in basal chordates.

3.4 ENDOGENOUS NO QUANTIFICATION AND LOCALIZATION

The major pathway for NO metabolism is the stepwise oxidation to nitrite (NO^{2-}) and nitrate (NO^{3-}) (Moncada *et al.*, 1991). In the plasma or other physiological fluids, NO is quickly oxidized to nitrite, where it remains stable for several hours (Kelm, 1999). NO^{2-} derived from NO autoxidation is rapidly converted to NO^{3-} via its oxidation by oxyhemoproteins. During low intake of nitrite/nitrate conditions, enzymatic NO formation from NOS accounts for the majority of nitrite (Moncada *et al.*, 1991). Therefore, the quantification of total nitrite, also the one coming from the reduction of nitrate, is a good index to evaluate the NO amount in embryos or tissues, which indirectly measures NOS activity. I quantified the total nitrite during amphioxus development and in adult animals by Griess assay and I found approximately 5 ng of nitrite per mg of proteins in almost every analysed stage (Fig. 3.9). The only exception was the 3 days-old larvae in which I detected higher amounts of nitrite corresponding to 23,5 ng of nitrite per mg of proteins (Fig. 3.9). This peak of NO production, and presumably in NOS activity, could be linked with the mouth morphogenesis.

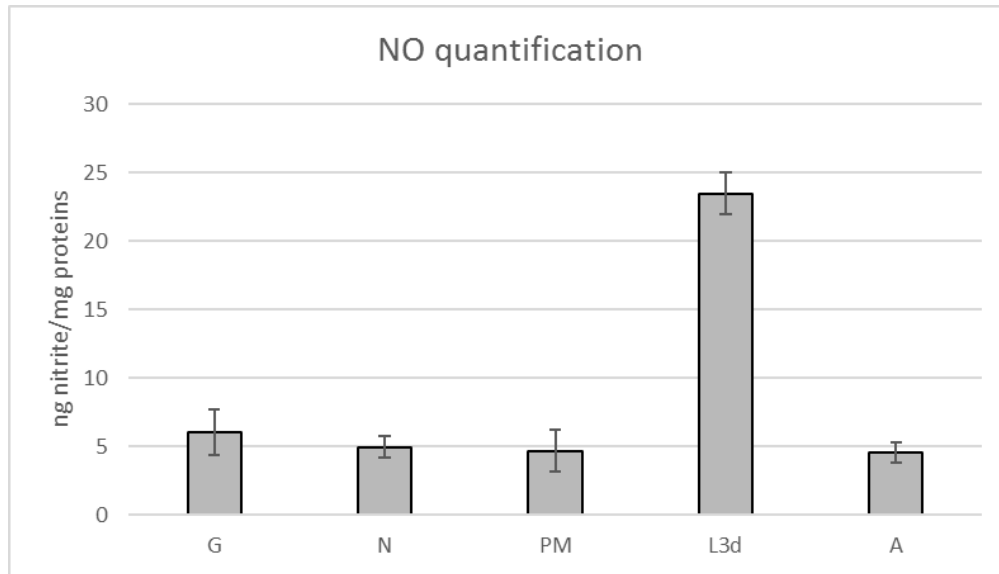


Figure 3.9: Nitrite quantification during amphioxus embryonic development and in adult. The results are expressed as ng of nitrite/mg of proteins. G: gastrula (10 hpf); N: neurula (24 hpf); PM: pre-mouth larva (48 hpf); L3d: larva 3 dpf; A: adult.

The NO localization using DAF-FM-DA revealed that in 48 hpf larvae, NO positive cells were abundant along all the neural tube (arrows in Fig. 3.10a) and in the most caudal extremity of the larvae, probably the future anal region (tandem arrows in Fig. 3.10a). Additionally, a strong NO fluorescent signal was observed in the area corresponding to the future mouth and gill slits (arrowhead in Fig. 3.10a). At 72 hpf, I observed a higher density of NO positive cells around the mouth, in the ventral part of the first gill slit and in the club shaped gland (arrowheads in Fig. 3.10b). Afterwards a punctuate signal is still present in the rostral area as well as caudally in both the hindgut and anus (Fig. 3.10, arrow and tandem arrows, respectively).

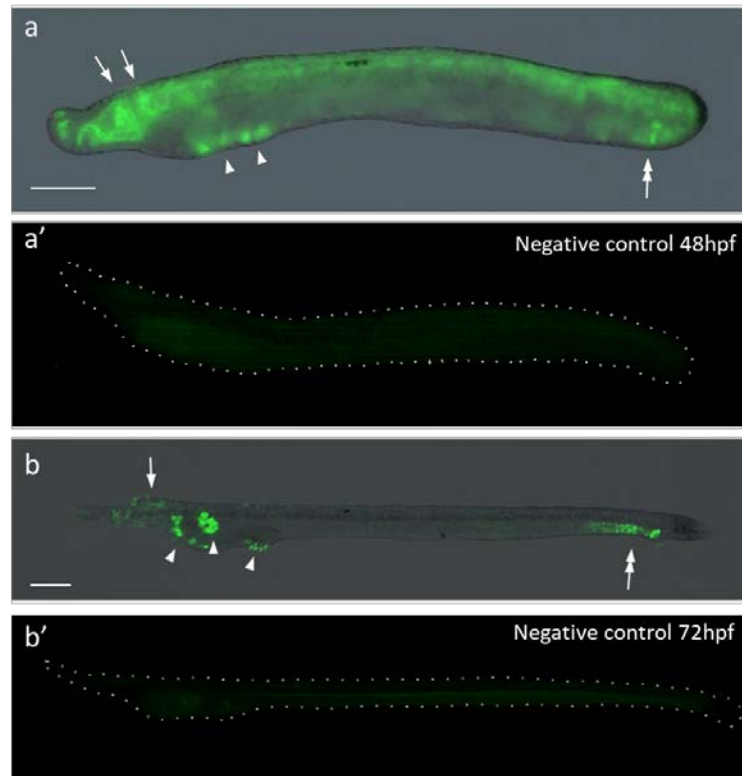


Figure 3.10: Nitric oxide localization by DAF-FM-DA. (a) 48 hpf and (b) 72 hpf developmental stages were analysed. Arrows indicate the nervous system; arrowheads show the pharyngeal area, mouth and gill slits; tandem arrows indicate hindgut. a' and b' are the negative control embryos that were not treated with DAF-FM-DA, exposed at the same laser intensity of the embryos in a and b. Orientation: up = dorsal; down = ventral; left: anterior; right: posterior. Scale bars: 50 μ m. (from Annona *et al.*, 2017; experiment performed by the author).

3.5 NO MODULATION DURING AMPHIOXUS DEVELOPMENT

The NO system provides opportunities for experimentally enhancing or blocking the production of NO and observe specific phenotypes. One of the possible mechanisms for NO manipulation is the inhibition of NOS activity through the addition of an inert analogous of L-arginine, such as L-NAME or L-nitro arginine (L-NA), or of a molecule that avoid the link with important co-factors, such as TRIM. The use of these inhibitors

is very useful for *in vivo* studies to define the physiological role of NO. In my experiments, I used both L-NAME and TRIM to decrease NO production during amphioxus embryonic development. The drugs were tested at several concentrations and added at different developmental stages (Fig. 3.11). L-NAME was used at 100 μ M, 1 and 10 mM while TRIM was used at 25, 50, 75 and 100 μ M. L-NAME 100 μ M and TRIM 25 μ M did not affect embryonic development. L-NAME 1 mM, TRIM 50, 75 and 100 μ M affected the development of embryos as described below (Fig. 3.12). L-NAME 10 mM instead resulted toxic. As a control for L-NAME treatments I used D-NAME, the inactive D- form enantiomer, at the same experimental conditions. D-NAME did not affect amphioxus development (Fig. 3.12b).

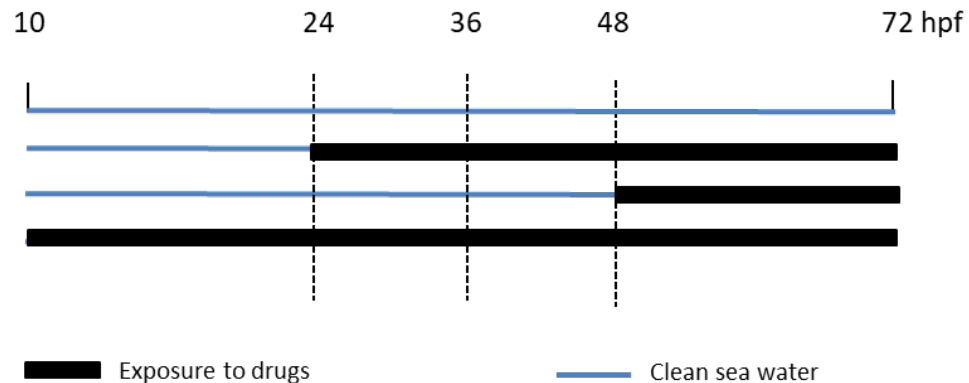


Figure 3.11: Schematic representation of preliminary L-NAME and TRIM treatments performed on *Branchiostoma lanceolatum* embryos. Black bars indicate the period in which embryos were exposed to drug; blue lines indicate the period in which embryos were kept in FSW without drug.

The inhibition of NOS activity, that reflects in lower amounts of endogenous NO, caused defects from the early development throughout the whole developmental process (complex morphogenetic defects, data not shown), but I did not thoroughly analyse this

phenotype. Further studies will be needed to understand if this development defection is a specific effect of NO depletion and if NO, in amphioxus, has a role in coordination of morphogenetic movements and cell cycle during early development as already described for other organisms (Kuzin *et al.*, 1996; Peunova *et al.*, 2007).

When the treatments were performed later in development at 24 hpf, corresponding to 5-6 somites neurula, and maintained until 72 hpf, the larvae showed an interesting phenotype. The presence of the consistently similar phenotype using both drugs (L-NAME and TRIM) reassured me that it is a specific effect and not due to the possible toxicity of the drug itself. The observed phenotype relates to an alteration of the morphology of the mouth and the pharyngeal region (Fig. 3.12 a and c).

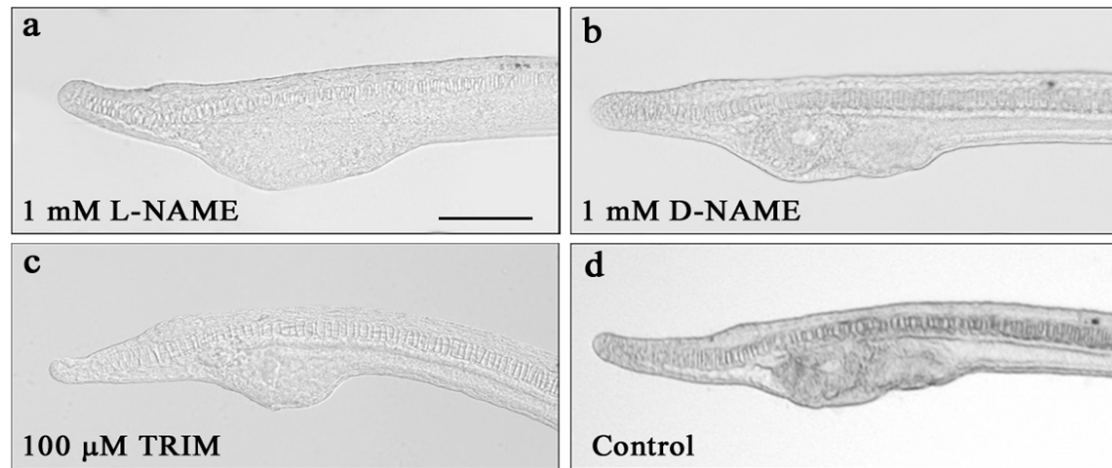


Figure 3.12: Amphioxus larvae after drug treatments. a) 72 hpf larva without mouth comes from 1 mM L-NAME treatment started at neurula stage. b) 72 hpf larva after 1 mM D-NAME treatment started at neurula stage. c) 72 hpf larva without mouth comes from 100 μM TRIM treatment started at neurula stage. d) Untreated 72 hpf larva used as control. Orientation: up = dorsal; down = ventral; left: anterior; right: posterior. (from Annona *et al.*, 2017; experiment performed by the author).

Phenotypes were divided into three categories: “wild type” (normal pharyngeal and mouth morphology), “mild” (malformed mouth and altered pharyngeal morphology) and “severe” (complete absence of the mouth and gill slits, altered pharyngeal morphology) (Fig. 3.13). Phenotypes with increasing degree of malformation could be due to the natural different sensitivity between individuals. The effect of the inhibitors was concentration-dependent. In fact, using TRIM 50 μ M the proportions of the mild and severe phenotypes are almost the same while at 75 and 100 μ M TRIM the proportions of larvae without mouth increased to 68% and 72%, respectively (Fig. 3.13).

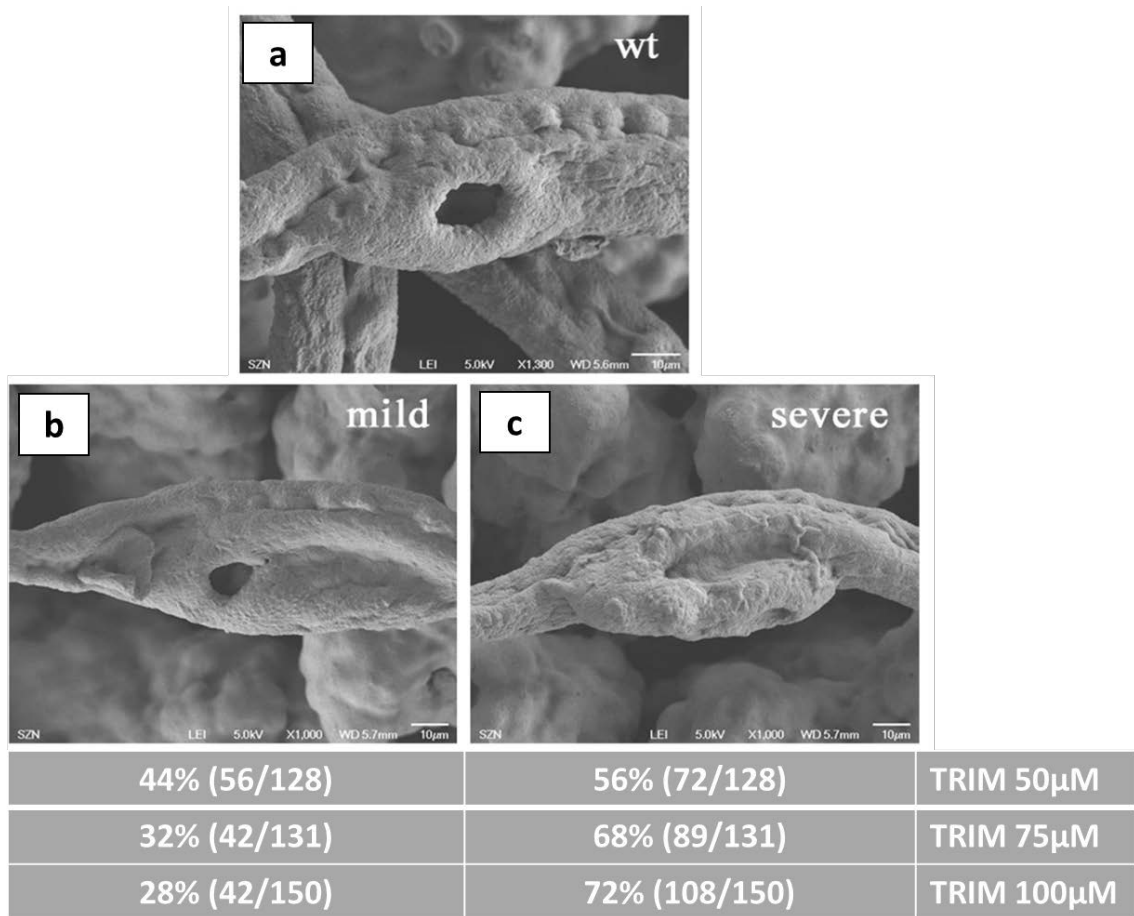


Figure 3.13: SEM images of anterior part of body of amphioxus 72 hpf larvae after TRIM treatments. a) untreated larva with a normal phenotype. b) 100 μ M TRIM treated larva that shows a mild altered phenotype. c) 100 μ M TRIM treated larva that shows a severe altered phenotype. Orientation: up = dorsal; down = ventral; left: anterior; right: posterior. In correspondence of b and c the proportions of the mild and severe altered phenotypes depending on drug concentration are reported. (Adapted from Annona *et al.*, 2017; experiment performed by the author).

These results allowed me to hypothesize the involvement of NO in the process of mouth formation and of the entire pharyngeal region morphogenesis in amphioxus. Moreover, the incubation at 48 hpf in the presence of the inhibitor resulted in larvae with a wild-type phenotype (data not shown). All together these data suggest that in pharynx and mouth morphogenesis NO play a key role in the interval from 24 to 48 hpf. In order to understand when exactly NO acts in this process, I performed a series of short-term treatment experiments in which TRIM (100 μ M) was applied to *B. lanceolatum* embryos for different time periods during development from 24 to 48 hpf, and the resulting phenotypes were subsequently observed at the 72 hpf stage. The results of treatments that started at 24 hpf and stopped at 30, 36, 42 or 48 hpf were 100% of larvae with an altered phenotype (Fig. 3.14), in the proportions between mild and severe phenotypes as previously described (Fig. 3.13). The addition of TRIM at 30 or 36 hpf caused alterations in the phenotype in approximately 70% of larvae (Fig. 3.14). From 42 hpf, NOS inhibition did not affect larvae morphology, in fact 100% of animals showed a normal phenotype (Fig. 3.14).

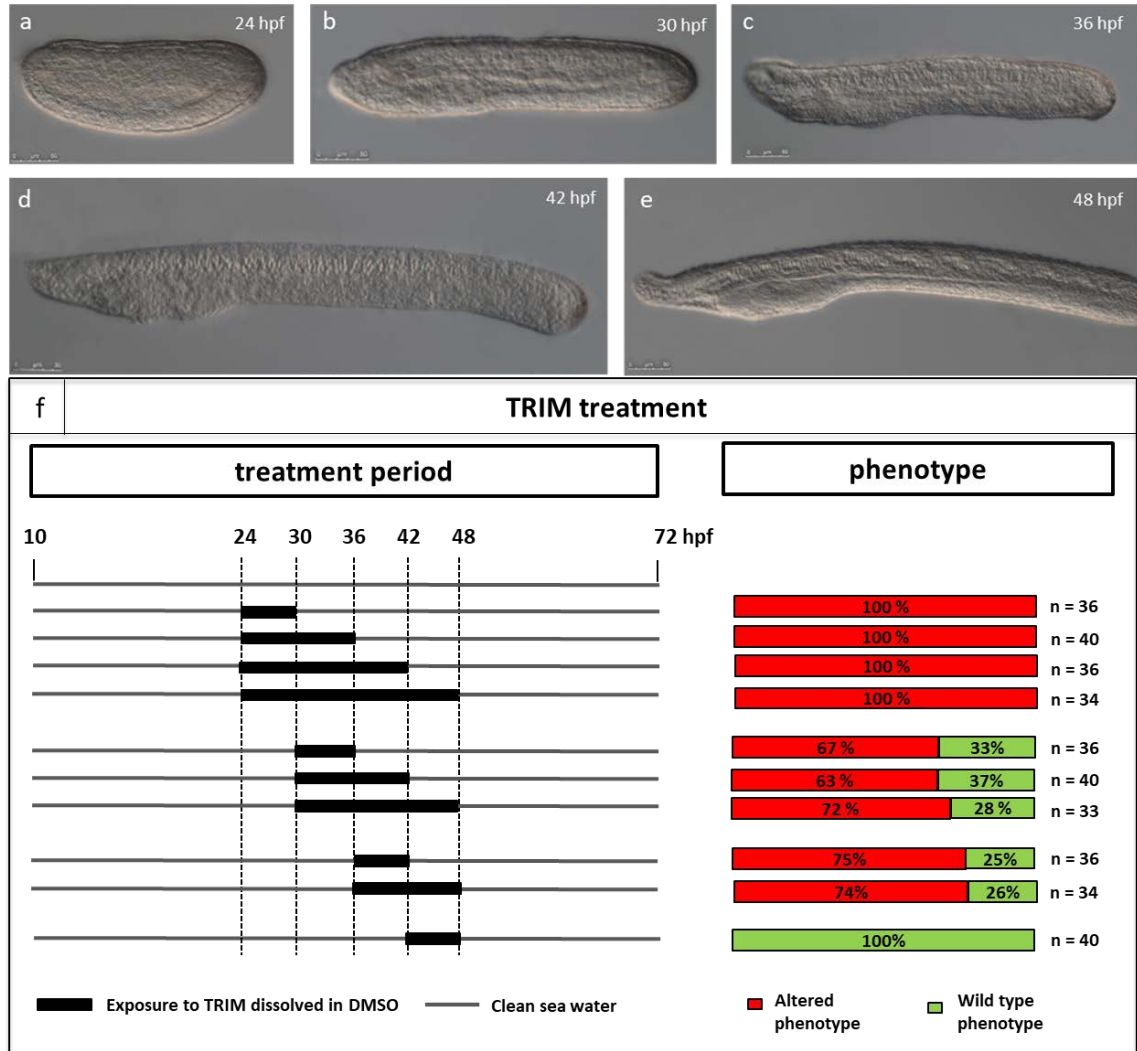


Figure 3.14: Schematic representation of 100 μ M TRIM treatments performed on *Branchiostoma lanceolatum* embryos in the period 24-48 hpf. On the top, there are reported the developmental stages used for the treatments a: 24 hpf; b) 30 hpf; c) 36 hpf; d) 42 hpf; e) 48 hpf. Orientation: up = dorsal; down = ventral; left: anterior; right: posterior. In f), there is the scheme of treatment period performed. On the left, there are the percentage of altered (red) and wild type (green) phenotype observed for each treatment period; n: total number of larvae observed.

These results demonstrated that larval morphology is most susceptible to NO depletion during neurulation and probably the pathway downstream NO signal acts in the interval from 24 to 42 hpf. In fact, the inhibition of NO production at the beginning of this

period brings to the maximum effect on larvae phenotype (100% alteration) while the addition of drugs at 30 and 36 hpf allows a small percentage of larvae with a normal phenotype (Fig. 3.14). The absence of altered phenotype by adding TRIM to 42 hpf means that, at this time, the putative pathway downstream NO is no longer active and for this reason NO depletion does not affect it. Moreover, the TRIM-treated larvae showed an incomplete formation of the club-shaped gland and the endostyle. The only pharyngeal structure that was not affected from the inhibition of NO was the pre-oral pit (Fig. 3.15a and b).

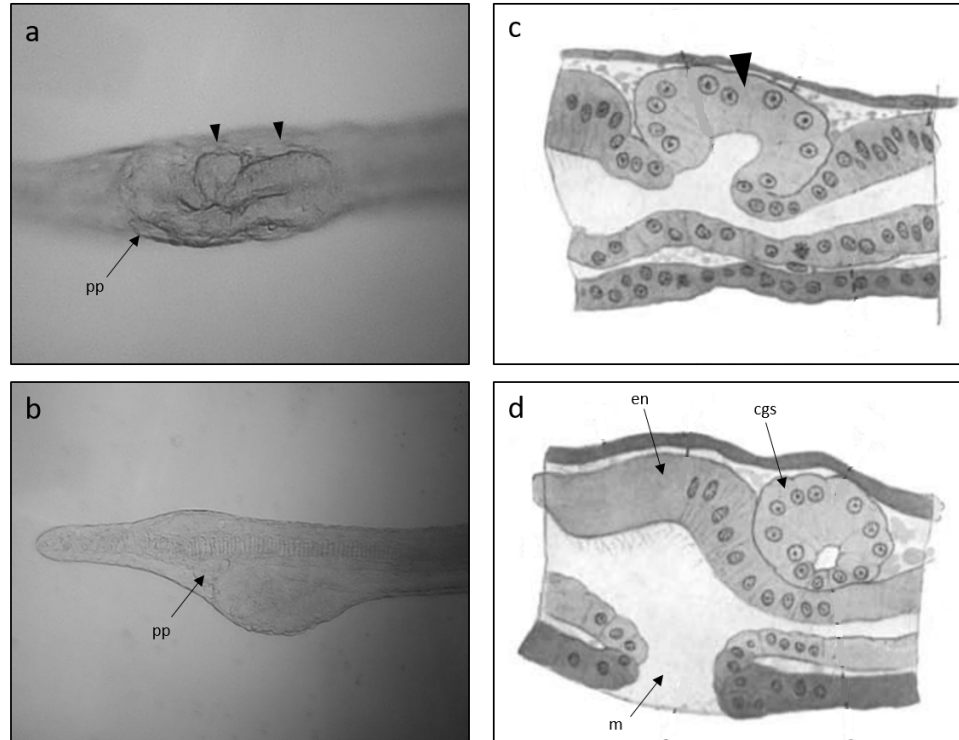


Figure 3.15: Anterior part of the body of a TRIM-treated larva. a) the pharyngeal area of a larva after TRIM treatment. Orientation: up = right side; down = left side; left: anterior; right: posterior. On the left side, there is only the pre-oral pit indicated by the arrow, on the right side there are incomplete formed club-shaped gland and endostyle that are indicated by arrowheads. b) lateral view of the anterior part of the body of a larva after TRIM treatment, left side. The pre-oral pit is indicated by an arrow. Orientation: up = dorsal; down = ventral; left: anterior; right: posterior. c-d) schematic representation of the normal amphioxus pharyngeal region development, frontal section (Adapted from Goodrich, 1930). Orientation: up = right side; down = left side; left: anterior; right: posterior. pp: pre-oral pit; en: endostyle; cgs: club-shaped gland; m: mouth.

Another effect that I noticed after inhibition of NOS activity was an alteration in larval movement, when TRIM treatment was maintained until larval stage. The first muscular movements appear at the stage of pre-mouth larvae and consist in simple body flexions that increase in complexity until they become a complete undulatory (approximately sinusoidal) wave in 72 hpf larvae. These movements are similar to adult amphioxus

ones (Stoke, 1997). In general, larvae grown in presence of TRIM were less active than un-treated ones and, some of them showed jerky movements as shown in Figure 3.16. I hypothesized that NO acts in the formation or functioning of the neuromuscular junctions and for this reason the absence or decrease of NO can cause alteration in locomotion. I did not analyse in detail this phenotype but in the future, further studies aimed to clarify the role of NO in this process are necessary.

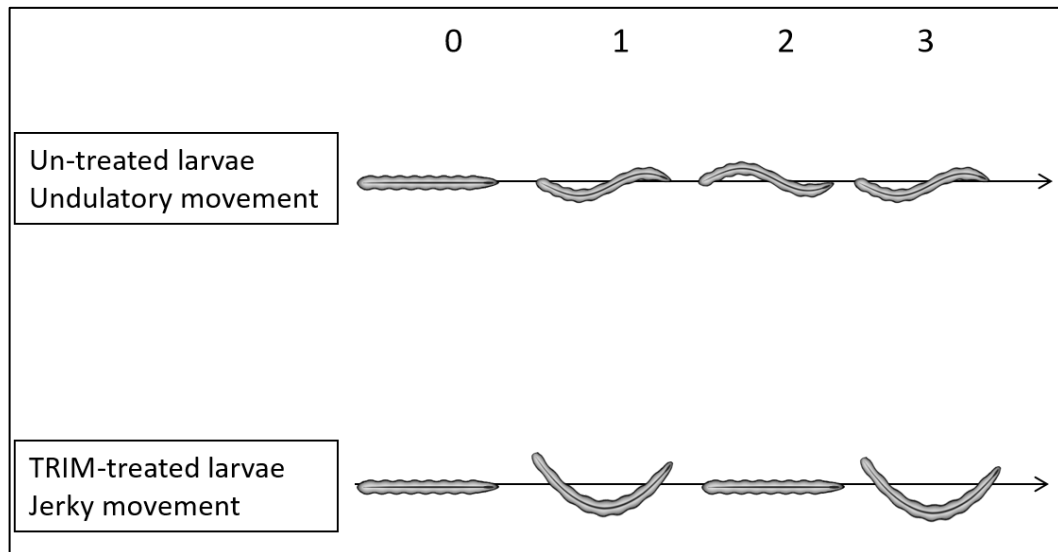
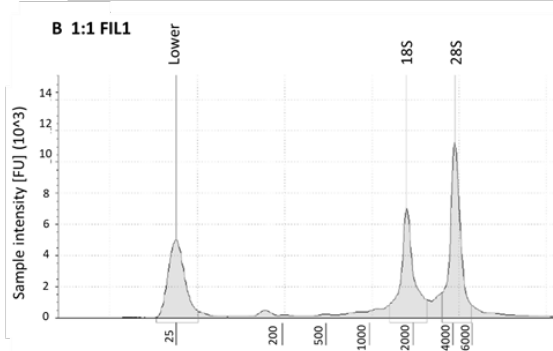


Figure 3.16: Schematic representation of movements in un-treated and TRIM-treated larvae. On the top, the undulatory movement of un-treated larva is showed. Down is represented the jerky movement of a TRIM- treated larva. The number (0-1-2-3) indicate the steps, the arrows indicate the direction of movement.

3.6 DIFFERENTIAL TRANSCRIPTOMIC ANALYSIS OF NO-INHIBITED EMBRYOS

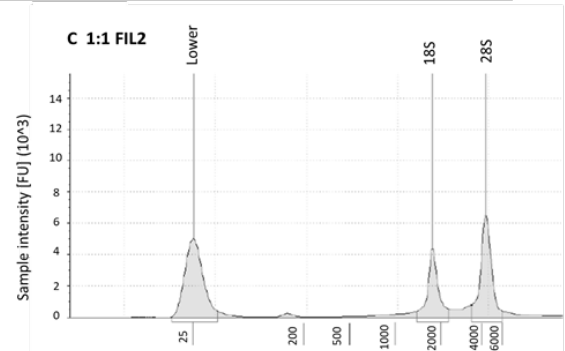
To have insights at molecular level of the consequences of the induces NO inhibition during embryonic development I performed an RNAseq experiment with three biological replicates in each of two conditions, un-treated and TRIM-treated. Embryos were treated for 6 hours (from 24 to 30 hpf) before being collected for the assay. Samples were assessed after dilution by using Nanodrop spectrophotometer (Fig.3.17A) to evaluate purity and TapeStation4200 (Fig. 3.17B-G) to evaluate integrity.

A	Sample ID	Nucleic Acid Conc.	Unit	A260	A280	260/280	260/230	Sample Type
	1:1 FIL 1	64,8	ng/μl	1,619	0,766	2,11	1,38	RNA
	1:1 FIL 2	34,7	ng/μl	0,868	0,397	2,18	0,28	RNA
	1:1 FIL 4	45,2	ng/μl	1,13	0,524	2,16	1,39	RNA
	1:1 FIL 5	43,2	ng/μl	1,08	0,482	2,24	0,28	RNA
	1:1 FIL 7	68,5	ng/μl	1,713	0,799	2,14	1,7	RNA
	1:1 FIL 8	101,2	ng/μl	2,531	1,189	2,13	0,6	RNA



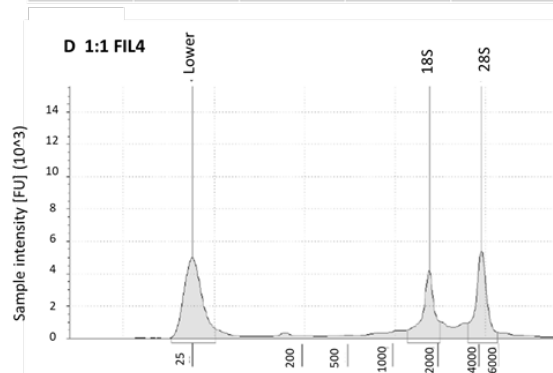
Sample table

Well	RINe	28S/18S (Area)	Conc. [ng/μl]	Sample description
B1	9.6	1.3	69.4	1:1FIL1



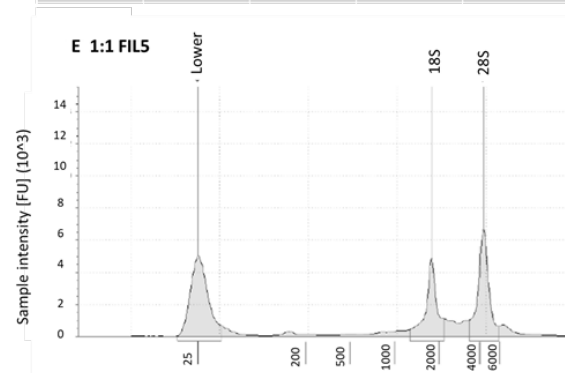
Sample table

Well	RINe	28S/18S (Area)	Conc. [ng/μl]	Sample description
C1	10	1.6	34.3	1:1FIL2



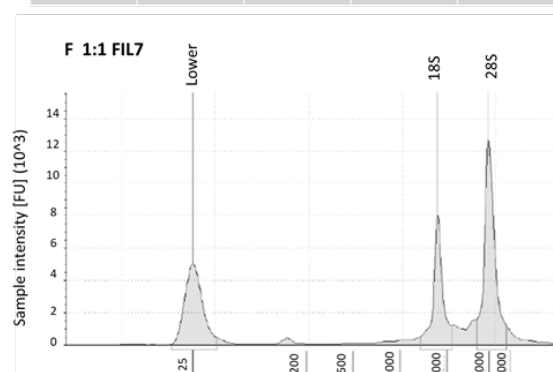
Sample table

Well	RINe	28S/18S (Area)	Conc. [ng/μl]	Sample description
D1	9.1	1.2	38.6	1:1FIL4



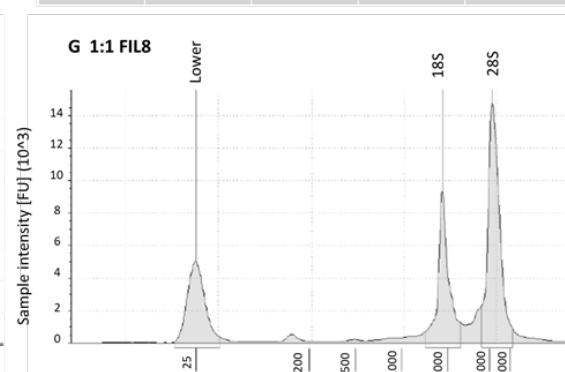
Sample table

Well	RINe	28S/18S (Area)	Conc. [ng/μl]	Sample description
E1	9.6	1.3	41.5	1:1FIL5



Sample table

Well	RINe	28S/18S (Area)	Conc. [ng/μl]	Sample description
F1	10	1.8	62.8	1:1FIL7



Sample table

Well	RINe	28S/18S (Area)	Conc. [ng/μl]	Sample description
G1	10	1.7	79.4	1:1FIL8

Figure 3.17: Quality control of total RNA samples evaluated by using A) a Nanodrop spectrophotometer, and B-G) TapeStation4200. FIL1: control female 1; FIL2: treated female 1; FIL4: control female 2; FIL5: treated female 2; FIL7: control female 3; FIL8: treated female 3.

Next generation sequencing (NGS) was carried out by Genomix4life (Italy) while the analysis of sequencing data was performed in collaboration with the research group of Dr Héctor Escrivà from the Observatoire Océanologique in Banyuls-sur-mer (France) (for details see Materials and Methods). This analysis showed that, with a P value < 0,01, 283 genes were up-regulated and 49 genes were down-regulated after TRIM treatment in the developmental period 24-30 hpf (Fig. 3.18).

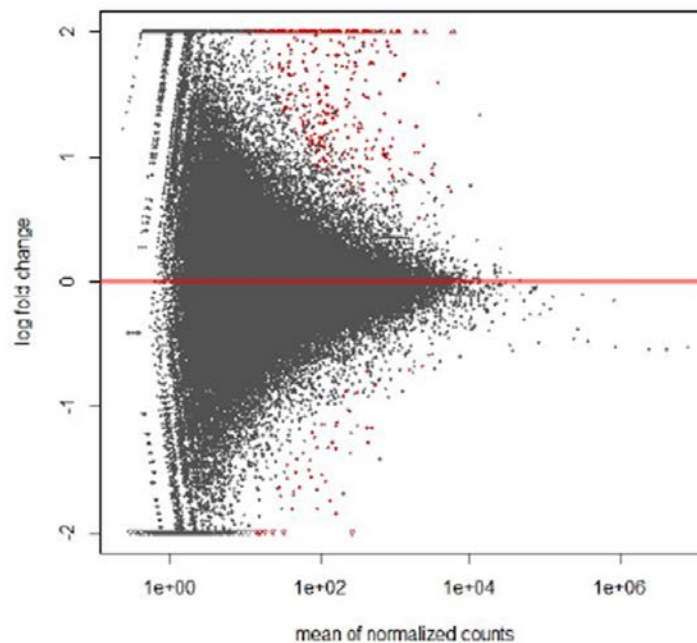


Figure 3.18: MA-plot representation of RNA-seq results between TRIM-treated and un-treated samples. Red plots are the affected genes with an adjusted P value <0,01. The genes with a logFold-change <0 are downregulated. The genes with a logFold-change >0 are upregulated.

17 genes among those down-regulated (Table 3.3) and 88 genes among those up-regulated have already been annotated (Table 3.4). Up- and down-regulated genes were subjected to gene ontology (GO) enrichment analysis in order to identify if differentially expressed genes were involved in same specific biological processes (BP), molecular function (MF) or cellular component (CC).

The results of GO analysis are summarized in Figure 3.18 for down-regulated genes and in Figure 3.19 for up-regulated ones.

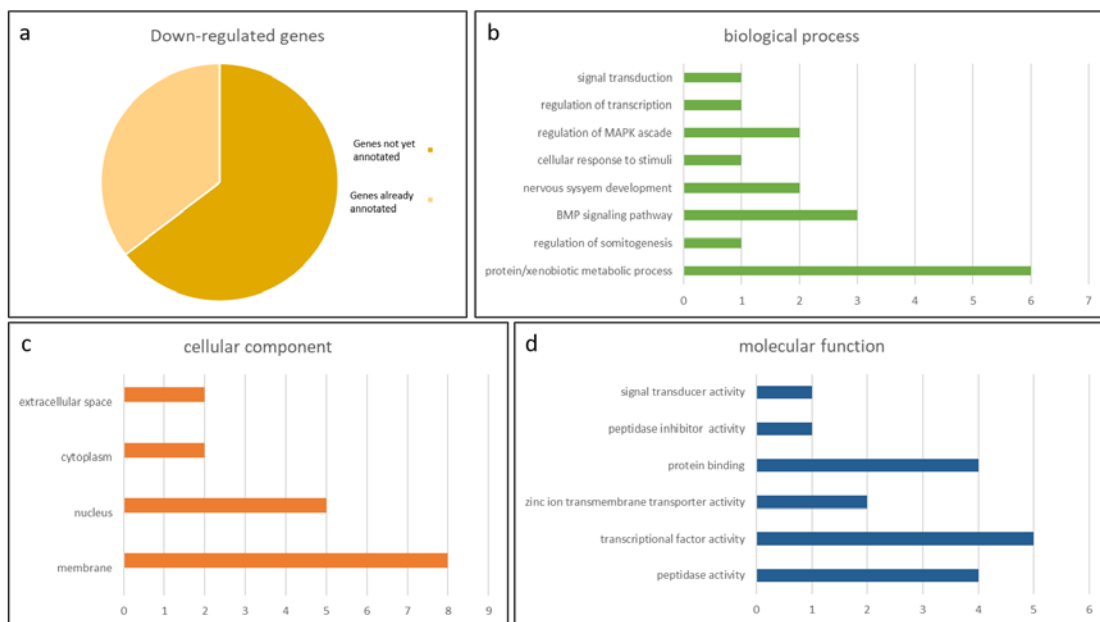


Figure 3.18: Summary of gene ontology (GO) enriched analysis of down-regulated genes in TRIM-treated amphioxus embryos in comparison with un-treated ones. a) Proportion between genes not yet annotated and genes already annotated. b) Results for the ontology category of biological process; c) Results for the ontology category of cellular component; d) Results for the ontology category of molecular function. The length of the bars is proportional to the number of genes in the term. Vertical axis represents gene ontology while horizontal axis indicates the number of genes in each ontology category.

Down-regulated genes			
Gene name	Abbreviation	Gene name	Abbreviation
matrix metallo ase-24 precursor	MMP24	NK1 transcription factor-related 1	NKX1-1
doublesex- and mab-3-related transcription factor 2 isoform X1	DMRT2	angiopoietin-related 7	ANGPTL7
zinc transporter ZIP10 isoform X2	SLC39A10	matrix metallo ase-14 precursor	MMP14
72 kDa type IV collagenase precursor	MMP2	metallo ase inhibitor 4 precursor	TIMP4
runt-related transcription factor 1	RUNX1	sprouty- EVH1 domain-containing 3 isoform X3	SPRED3
POU class transcription factor 2	POU2	matrix metallo ase-9 precursor	MMP9
opsin-5-like	OPN5L1	histidine N-acetyltransferase-like	NAT
winged helix transcription factor AmphiFoxE4	FoxE4	platelet derived and vascular endothelial growth factor receptor	PDGFR
zinc transporter ZIP6-like	SLC39A6		

Table 3.3: List of 17 down-regulated genes already annotated resulted from the differentia transcriptomic analysis of TRIM-treated amphioxus embryos in the developmental interval between 24 and 30 hpf. Gene nomenclature is based on best BLAST hit and does not imply that the amphioxus gene is a one-to-one orthologue of the gene named.

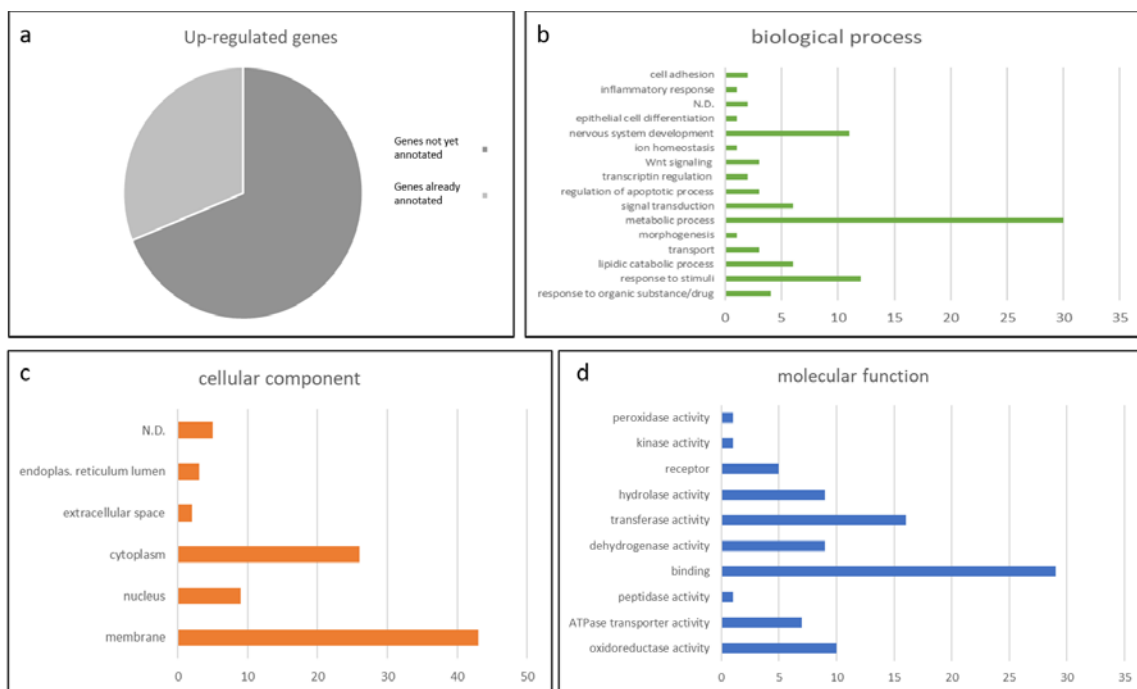


Figure 3.19: Summary of gene ontology (GO) enriched analysis of up-regulated genes in TRIM-treated amphioxus embryos in comparison with un-treated ones. a) Proportion between genes not yet annotated and genes already annotated. b) Results for the ontology category of biological process; c) Results for the ontology category of cellular component; d) Results for the ontology category of molecular function. The length of the bars is proportional to the number of genes in the term. Vertical axis represents gene ontology while horizontal axis indicates the number of genes in each ontology category.

UP-REGULATED GENES			
GENE NAME	ABB.	GENE NAME	ABB.
cytochrome P450	CYP450	aldehyde dehydrogenase family 3 member B1 isoform X2	ALDH3B1
multidrug resistance-associated 5 isoform X4	MRP5	alcohol dehydrogenase 6 isoform X3	ADH6
ATP-binding cassette sub-family A member 3	ABCA3	arrestin domain-containing 3	ARRDC3
fatty acid-binding 12 isoform X3	FABP12	acylcarnitine hydrolase-like isoform X1	Ces2c
unconventional myosin-XV isoform X2	MYO15A	aldo-keto reductase family member C1	AKR1C1

1,5-anhydro-D-fructose reductase	AKR1E2	E3 ubiquitin- ligase TRIM56	TRIM56
sulfotransferase family cytosolic 2B member 1 isoform X4	SULT2B1	homeobox Meis2 isoform X1	Meis2
retinol-binding 2 isoform X1	RBP2	very low-density lipo receptor isoform X1	VLDLR
prostaglandin G H synthase 2 precursor	PTGS2	frizzled-6 isoform X1	FZD6
DBH-like monooxygenase 1	MOXD1	ammonium transporter Rh type A precursor	RHAG
3 beta-hydroxysteroid dehydrogenase Delta 5	HSD3B1	betaine--homocysteine S-methyltransferase 1	BHMT
UDP-glucuronosyltransferase 2B31-like isoform X1	UGT2B31	epoxide hydrolase 4 isoform X1	EPHX2
phosphatidylcholine translocator ABCB4 isoform X4	ABCB4	choline ethanolaminephosphotransferase 1 isoform X1	CEPT1
retinal dehydrogenase 2	ALDH1A2	phosphotriesterase-related isoform X2	Pter
alpha-2,8-sialyltransferase 8B precursor	ST8SIA2	dehydrogenase reductase SDR family member on chromosome X isoform X4	DHRXSX
steryl-sulfatase isoform X1	STS	N-acetylated-alpha-linked acidic dipeptidase 2 isoform X3	NAALAD2
hexokinase-2 isoform X1	HK2	D-aspartate oxidase	DDO
pre-B-cell leukemia transcription factor 4 isoform X1	PBX1	solute carrier organic anion transporter family member 5A1 isoform X1	SLCO5A1
arylsulfatase E isoform X1	ARSE	sterol 26- hydroxylase mitochondrial	CYP27A1
retinoic acid receptor alpha isoform X1	RARA	NHL-repeat-containing 4	NHLRC4
myeloperoxidase isoform X1	MPO	homeobox Hox-A3	HOXA3
retinol dehydrogenase 13 precursor	RDH13	hydroxyacylglutathione mitochondrial isoform X1	HAGH
acetyl- cytosolic-like	ACAT2	carboxylesterase-like precursor	CES1
estradiol 17-beta-dehydrogenase 11 isoform X1	HSD17B11	CMP-N-acetylneuraminate-beta-galactosamide-alpha-2,3-sialyltransferase 1	ST3GAL1
oxidative stress-induced growth inhibitor 2 isoform X3	OSGIN1	vitamin D 25-hydroxylase	CYP2R1
homeobox Hox-A1 isoform X1	HOXA1	pyrethroid hydrolase Ces2e-like	CES2
sulfide:quinone mitochondrial	SQOR	butyrophilin subfamily 1 member A1 isoform X1	BTN1A1
frizzled-2 precursor	FZD2	glycine N-methyltransferase	GNMT
frizzled-4 precursor	FZD4	peroxisomal acyl-coenzyme A oxidase 2 isoform X2	ACOX2
spermatogenesis-associated 31A6-like isoform X1	SPATA31A6	erythrocyte band 7 integral membrane	STOM
prostaglandin reductase 2 isoform X1	PTGR2	glutathione S-transferase theta-2-like	GSTT2
neuroigin-1 isoform X1	NLGN1	acyl- dehydrogenase family member 11	ACAD11
1-aminocyclopropane-1-carboxylate synthase 1 isoform X1	ACCSL	hypoxanthine-guanine phosphoribosyltransferase	HPRT1

phospholipase ABHD3	ABHD3	homeobox Nkx-	NKX-
leucine-zipper-like transcriptional regulator 1	LZTR1	oxysterols receptor LXR-alpha isoform X1	NR1H3
copper-transporting ATPase 1 isoform X1	ATP7A	FAD-dependent oxidoreductase domain-containing 2 isoform X1	FOXRED2
kelch 18 isoform X4	KLHL18	patched domain-containing 3	PTCHD3
mitochondrial dicarboxylate carrier isoform X1	SLC25A10	haloacid dehalogenase-like hydrolase domain-containing 2 isoform X1	HDHD2
leucine-rich repeat and IQ domain-containing 1 isoform X1	LRR1Q1	ependymin-related protein	EPDR
cellular Retinoic Acid Binding Protein	CRABP	cell adhesion molecule 2-like	CADM2
ankyrin repeat domain-containing protein 1-like	ANKRD1	amiloride-sensitive sodium channel	SCNN1
serine O-acetyltransferase-like	SAT	sulfatase-modifying factor 1-like	SUMF1
fibrillin-1-like	FBN1	erythrocyte band 7 integral membrane	STOM
plasminogen receptor (KT)-like	PLGRKT	ADP-dependent glucokinase-like	ADPGK

Table 3.4: List of 88 up-regulated genes already annotated resulted from the differential transcriptomic analysis of TRIM-treated amphioxus embryos in the developmental interval between 24 and 30 hpf. Gene nomenclature is based on best BLAST hit and does not imply that the amphioxus gene is a one-to-one orthologue of the gene named.

The majority of genes resulted up- or down-regulated in our differential transcriptomic analysis are involved in metabolic processes, probably implemented as a response to the presence of the drug (ie cytoplasmic enzymes). A substantial portion of genes differentially expressed between treated and control samples are involved in nervous system development. This is coherent with the well-known role of the NO in neurogenesis and the *NosC* expression pattern in amphioxus but these genes are not of interest for the phenotype that I described in previous paragraph (3.5, pharyngeal-altered phenotype). Only few genes can directly or indirectly be involved in the development of pharyngeal structures: Runx and MMPs are belong to BMP signaling pathway; DMRT regulate the Nodal pathway action; FoxE and PDGFR (VEGFR in

amphioxus) are involved in club shaped gland and endostyle development; Raldh, RAR, Hox1 and Hox3 are belong to the retinoic acid pathway, known to be involved in the correct pharyngeal region development in amphioxus. These genes will be the focus of future analyses.

CHAPTER 4

DISCUSSION

NO is a small signaling molecule that was identified and described for the first time in 1989, and in 1992 it was entitled as the “Molecule of the Year” by the journal *Science* (Koshland, 1992). Over the years, a huge number of papers have been published regarding several aspects of NO biology with different aims and model organisms, from bacteria to mammals (Bryan *et al.*, 2009). It has been shown the involvement of NO in several biological processes (both physiological and pathological), like the neurotransmission, regulation of blood pressure and immune response. Most of the studies were carried out in mammals but the interest of the role that NO plays in non-mammalian organisms have steadily increased. In this way, the spectrum of known processes of NO’s involvement has expanded enormously including, for example, response to stress conditions (*P. lividus*, Migliaccio *et al.*, 2014), apoptosis, epidermis development (*X. laevis*, Tomankova *et al.*, 2017), metamorphosis (*C. intestinalis*, Comes *et al.*, 2007; *Lytechinus pictus*, Bishop and Brandhorst, 2001) and craniofacial development (*Xenopus laevis* and *Danio rerio*, Jacox *et al.*, 2014). NOS enzymes are the most crucial factor in NO production for their exclusive role in the *de novo* synthesis of NO, and thus decisive in the physiological functions of NO system. Therefore, investigating the ancestral role of animal *Nos* genes and their novel acquired

functions during evolution is an issue of broad interest to understand the importance of NO system in the evolution of animals.

The main goal of this PhD project was the investigation of physiological roles of amphioxus NO during embryonic and larval development. For this purpose, different aspects of the NO system have been considered: 1- the general evolutionary scenario and the specific position that amphioxus NOS proteins occupy; 2- a better characterization of the three amphioxus *Nos* genes; 3- the analysis of the phenotype deriving by inhibition of NO production during amphioxus embryonic development and the differential transcriptomic analysis generated under specific conditions.

Andreakis and colleagues (2011) highlighted the extraordinary high degree of conservation of *Nos* genes among Metazoan, in particular the domain organization as well as intron positions and phases. In *B. floridae*, three different *Nos* were identified, *NosA*, *NosB* and *NosC* (Andreakis *et al.*, 2011), but the topology of the deuterostome NOS phylogeny indicated that the multiple amphioxus *Nos* genes derived from independent duplication events with respect to vertebrates. A deeper comparative analysis in the cephalochordate subphylum revealed that not only *B. floridae* but also the other two sister species, *B. lanceolatum* and *B. belcheri*, have three paralogues *Nos* genes, that resulted orthologues of *B. floridae* *NosA*, *NosB* and *NosC*. The same scenario was also found for *Asymmetron*, which was the first to diverge within cephalochordate's group, followed by *Epigonichthys* and *Branchiostoma* clades. The comparison between *Branchiostoma* and *Asymmetron* lineages is highly informative for postulating the ancestral condition of all cephalochordates (Kon *et al.*, 2007). This analysis suggested that the duplication events that originated the three cephalochordate *Nos* genes occurred

in the last common ancestor of extant amphioxus (Fig. 4.1; Annona *et al.*, 2017). Moreover, we demonstrated that it is an independent cephalochordate duplication since *NosA*, *NosB* and *NosC* are not orthologues to vertebrates *NosI*, *NosII* and *NosIII*. In the case of vertebrate, the fact that *Nos* duplicates are linked to *Hox* clusters demonstrated that they derive from the two round of genome duplication occurred at the stem of vertebrates (Andreakis *et al.*, 2011).

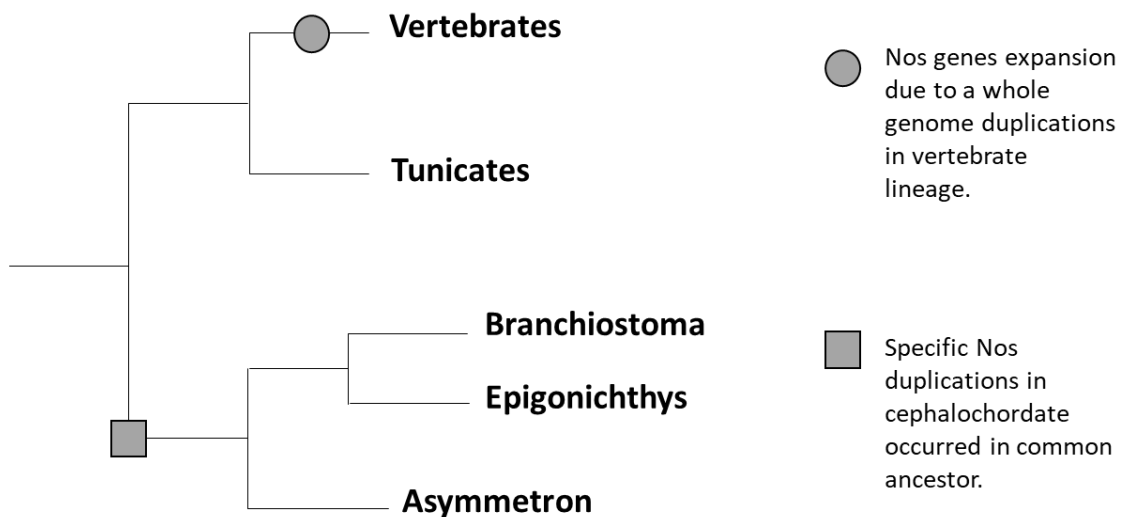


Figure 4.1: Schematic representation of duplication events of *Nos* genes occurred in Chordates. Gene duplications in the last common ancestor of cephalochordates gave rise to three distinct amphioxus *Nos* genes. In the vertebrate lineage, instead, *Nos* genes have a different evolutionary origin because they come from two whole genome duplications.

For mammals, NOS are classified in neuronal, endothelial and inducible on the base of the presence or absence of following characteristics in the protein sequence: neuronal NOS proteins have the PDZ domain which targets the enzyme to synapses, endothelial NOS is myristolated and/or palmitoylated on specific aminoacidic residues at the N-

terminal of the protein which is required for its localization in endothelial cells, while inducible NOS lacks any specific localization features. Another classic distinction is between constitutive and inducible expressed *Nos* genes. The constitutive *Nos* (neuronal and endothelial) are always basal expressed, while inducible *Nos* expression can be stimulated, at transcriptional level, by cytokines, LPS and other agents (Förstermann and Sessa, 2012). At the protein level, the difference between constitutive and inducible NOS is based on the affinity with CaM and so on the possibility to perceive intracellular Ca^{2+} concentration variations. The constitutive NOS activity is regulated by Ca^{2+} and CaM: it has low affinity to CaM and binds it when the free intracellular Ca^{2+} levels increase to specific micromolar concentrations. Conversely, the inducible *Nos* has greater affinity with CaM and binds it permanently, also at low Ca^{2+} concentrations (Cho *et al.*, 1992).

Indeed, *Nos* cannot be clearly classified in terms of these mammalian/vertebrate subtypes and the distinction between constitutive and inducible expression is not so strict. Metazoan showed multiple events of *Nos* gene loss and gain in various lineages, for example many basal metazoans such as *Trichoplax* have 3 different *Nos* while insects or tunicates have only one *Nos* (Andreakis *et al.*, 2011). There are several cases in which features observed in distinct genes in vertebrates have been found in a unique *Nos* in invertebrates. For example, the only *Nos* found in *Nematostella* share sequence features comparable to the *iNos*-like organization (i.e. without the insertion in the reductase domain) while the single *Nos* found in tunicates presents the PDZ domain as a neuronal-like *Nos*. Further, the presence of any localization feature does not correlate with the phylogenetic positions, also suggesting an independent incorporation of those

motifs in the basic Nos structure. The possibility to be induced in certain inflammatory conditions is not an exclusive feature of the iNos. For example, the scallop *Chlamys farreri* possess only one Nos with both PDZ domain and autoinhibitory loop suggesting that it is a typical neuronal Nos (Jiang *et al.*, 2013). Nevertheless, the transcriptional activation of *C. farreri* Nos has been observed after stimulation with PAMPs and TNF- α causing a range of immune responses, including the responses of NO (Beutler and Rietschel, 2003), and therefore it has also inducible features. Interestingly, some evidences indicate in vertebrates the inducible character of *nNos*, in certain inflammatory conditions (Amin *et al.*, 1995; Vaz *et al.*, 2011). Amphioxus *NosA* and *NosC* were identified as *neuronal Nos* because they have both the PDZ and the inhibitory loop, while *NosB* as inducible (Andreakis *et al.*, 2011). In amphioxus, that for many aspects represents a connection between invertebrates and vertebrates, the stimulation of the immune system by LPS treatment, performed for this project, caused the induction of the *NosA* and *NosB* expression (Fig 3.3). Therefore, *NosB* was found to be inducible as expected from its structural features but we demonstrated here that at least one of the two amphioxus neuronal Nos (*NosA*) seems to have characteristics typical of inducible genes. These evidences, together with structural ones described before, led us to conclude that inducibility is an ancestral feature of *Nos* genes. The possible evolutionary scenario is that the inducible-like Nos is the ancestral prototype of the enzyme and the multiple constitutive-like Nos lineage specific could be independently derived from iNos-like proteins. The process that led this transition might include independent events of insertion of the autoinhibitory loop in the Nos reductase domain and of the localizations domain at the N-terminal.

In addition to the fact that the two amphioxus neuronal genes, *NosA* and *NosC*, behave differently upon a stress stimulus, they resulted different also from a temporal expression point of view. *NosA* in our experiments was expressed exclusively in adulthood (Fig. 3.2c). Indeed, only *NosB* and *NosC* were expressed during embryonic and larval development, showing a complementary trend (Fig. 3.2a-b). *NosB* was highly expressed during gastrulation and it is interesting to mention that in vertebrates the involvement of NO is reported in morphogenetic cell movements that allow convergent axial extension. In particular, NO seems to suppress cell division and facilitate cell movements during early development (Kuzin *et al.*, 1996; Peunova *et al.*, 2007). These evidences, together with the result that I obtained, allowed me to hypothesize that, during amphioxus gastrulation, NO produced by *NosB* could perform a similar function in the determination of axial elongation, as previously described for vertebrate. This speculation is also supported by the evidence that, inhibition experiments of the Nos activity early in development caused complex morphogenetic defects (see later in this chapter for more details about Nos activity inhibition experiments). Nevertheless, this hypothesis must be confirmed by further in-depth studies. Regarding *NosA* and *NosC*, it was interesting to understand: 1) what has caused their temporal expression separation and different inducible nature, and 2) what this temporal separation means in terms of *NosA* and *NosC* functions during amphioxus development and physiology.

The clear distinction in temporal expression and in stress susceptibility of *NosA* and *NosC* could be due to a different transcriptional regulation probably enhanced by the progressive accumulation of changes in their respective promoters. To start clarify this, I used *C. robusta* as experimental tool to study the regulatory activity of amphioxus

NosC promoter. Among many putative CNRs identified *in silico*, only few of them have shown a positive activity in directing the expression of the reporter gene. In particular, I have detected positive regulatory activity for the CNR 14, 15, 17, 18, 19 upstream the *NosC* transcription start codon and the CNR 39, 40, 41 downstream the *NosC* transcription start codon. These positive amphioxus CNRs driven GFP expression in *C. robusta* nervous system: in the posterior part of the pigmented sensory organs, in the otholite and in the ocellus (CNR 17, 18, 19 and CNR 39, 40, 41; Fig. 4.2b and c respectively), in the motor ganglion (MG) and in the dorsal caudal epidermal neurons (DCENs) (CNR 14, 15; Fig. 4.2a and f). It was already reported that, in *C. robusta* middle larva (previously indicated as *Ciona intestinalis*), *Nos* mRNA was visible in the posterior part of the sensory vesicle in a series of cells arranged in a circle and in the fibres that originate from the sensory vesicle and arrive to the visceral ganglion passing through the neck (Fig. 4.2d; Comes *et al.*, 2007). At late larva in *C. robusta*, *Nos* was also detected in the central portion of the tail exclusively present in the epidermis (Fig. 4.2e; Comes *et al.*, 2007).

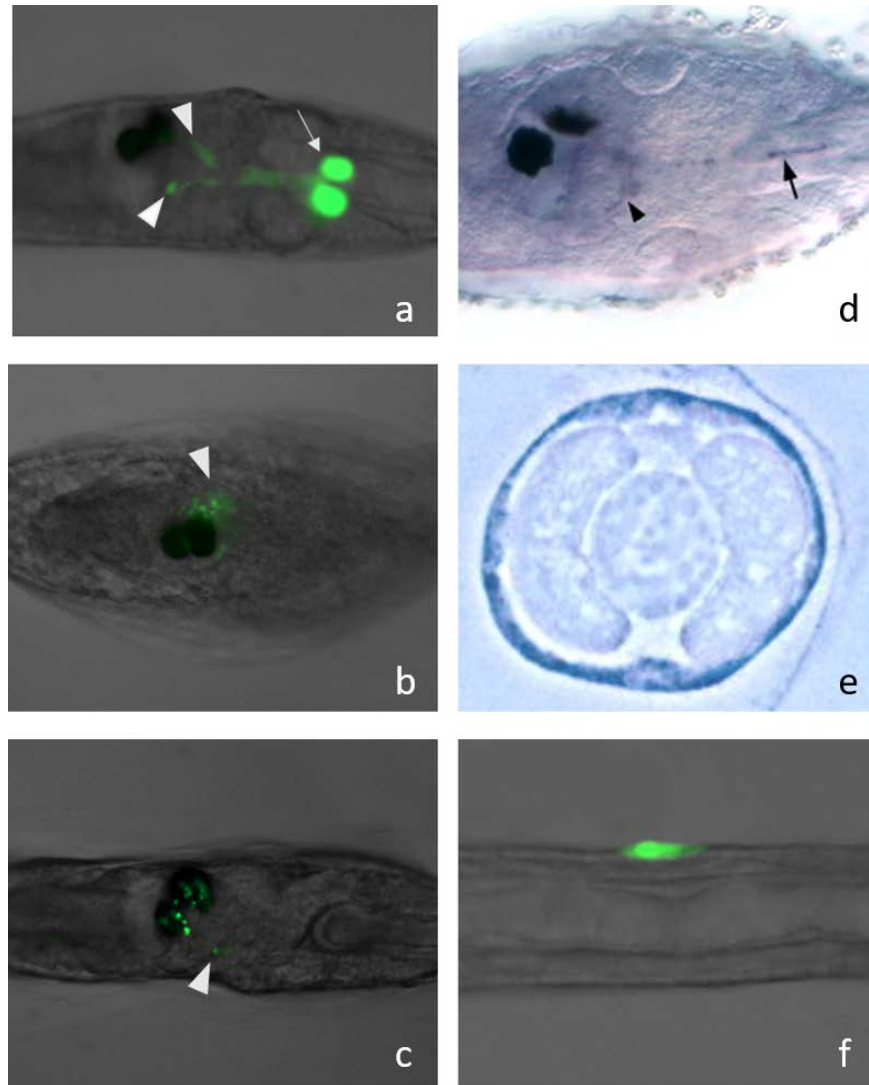


Figure 4.2: Comparison between the *Nos* expression in *Ciona robusta*, previously described by Comes and colleague in 2007, and the positive enhancer activity for the amphioxus CNRs showed in this thesis in the chapter 3. a-b-c-f) Results from the present project (see Chapter 3). d-e) *Nos* expression in *C. robusta* from Comes *et al.*, 2007.

The results that I obtained testing amphioxus CNRs were mostly comparable with *C. robusta* *Nos* expression pattern at middle larva stage suggesting not only that these genomic regions close to amphioxus *NosC* transcription start codon (Fig. 3.5b-c) contain regulatory elements but also that these elements are evolutionary conserved

among basal chordates. Further studies will be necessary to clarify the reasons for the slight discrepancies found between my results and the *C. robusta Nos* expression reported in literature (i.e the signal in the DCENs, in the otholite and in the ocellus resulted from my transgenetic experiments but that were not detected by Comes and colleagues for *C. robusta Nos* expression).

During larval development, I observed a peak of NO production at 3 dpf larval stage that was mainly localized in the pharyngeal area before and after mouth opening (Fig. 3.10a-b). The biological function of this high amount of NO in the pharyngeal area, when mouth has been already opened, could be linked with the primary antimicrobial defense reactions, associated to the feeding and the gut functions, and with the process of metamorphosis. In fact, the expression of *NosC* at 3 dpf larval stage was detected in the club-shaped gland (Annona *et al.*, 2017), a transient structure that produce mucous secretions that aid in the food capture and processing (Gilmour, 1996). The club-shaped gland was also proposed to be source of antimicrobial secretion (Godoy *et al.*, 2006) as well as to produce hormones of metamorphosis (Wickstead, 1967). The involvement of NO in metamorphosis was already described for other invertebrates such as *C. robusta*, *I. obsoleta*, *L. pictus* and *B. villosa* (Bishop and Brandhorst, 2001; Bishop *et al.*, 2001; Leise *et al.*, 2004; Comes *et al.*, 2007). In particular, in *C. robusta* NO acts in metamorphosis down-regulating ERK specific phosphatases (MKP1 and MKP3), in this way ERK is phosphorylated and active. ERK activation precedes the wave of apoptosis necessary for tail regression and metamorphosis (Ercolesi *et al.*, 2012). Interestingly, it has been demonstrated the presence of a highly innervated portion of the pharynx in pre- and post-metamorphic larvae, indicating that the club-shaped gland, together with

the other pharyngeal structures (the pre-oral pit and the endostyle) probably is involved in important morphological processes in amphioxus mouth opening and rostral metamorphosis (Kaji *et al.*, 2009).

In order to clarify the role of NO during amphioxus development, its enzymatic production was inhibited by TRIM and the resulting phenotype was described. In my experiments, I specifically inhibited the NO production presumably deriving from *NosC*, according to *in situ* hybridization results in which it is clearly showed that *NosC* is the only *Nos* gene expressed from neurula to larva stage (Annona *et al.*, 2017). The most evident phenotype observed was the alteration of the pharyngeal region formation, in particular there was the absence of mouth and gill slits and the not complete formation of club-shaped gland and endostyle. Any other body features were apparently not affected from the TRIM treatment. A temporal and combinatorial treatment approach allowed us to predict that probably the crucial time window for NO action during amphioxus development could reasonable be from 24 to 42 hpf. TRIM treatments in this window, in fact, resulted active on mouth and gill slits determination, while after this time interval the treatment resulted 100% inefficient giving an unaltered phenotype.

The involvement of NO in mouth formation was already suggested in vertebrates. It was demonstrated that NO depletion during *Xenopus* and zebrafish embryonic development, in particular during neurulation, causes no mouth opening, with a small stomodeal invagination, while the other structures of the extreme anterior domain (EAD) were correctly specified (Jacox *et al.*, 2014). Jacox and colleagues also showed that nNOS and NO acted as members of the Kinin-Kallikrein pathway in determination of that

specific process. In order to understand the pathway in which NO acts in amphioxus for the regulation of pharyngeal region formation, I performed a differential transcriptomic analysis of amphioxus embryos that were treated with TRIM from 24 to 30 hpf.

Preliminary results showed a down-regulation of *FoxE* that, in wild-type amphioxus embryos, is expressed towards the right pharyngeal wall and, in larvae, marks the club-shaped gland (Yu *et al.*, 2002; Soukup *et al.*, 2015). This expression pattern suggests the involvement of FoxE in the formation and in the function of the club-shaped gland and the absence of this structure in the amphioxus TRIM-treated larvae could be due precisely to the down-regulation of this gene. Other interesting results, shown by the preliminary analysis of the differential transcriptome, are the down-regulation of some genes belonging to BMP signaling pathway (*Slc39A10*, *Slc39A6*, *Runx*, *MMPs*) and of a gene involved in regulation and action of Nodal pathway (*Dmrt*). (Tables 3.1 and 3.2). Moreover, genes coding for Frizzled receptors (*Frz2*, *Frz4*, *Frz6*) were upregulated indicating an activation of the WNT pathway. It was reported that this pathway must be downregulated to allow the mouth opening (Fig. 4.3, Soukup *et al.*, 2015). In amphioxus, it has been demonstrated that Nodal signaling patterns the left-right axis of the embryo and in particular it is necessary for the left-side expression of downstream genes as well as for left-side morphogenesis (Fig. 4.3; Soukup *et al.*, 2015).

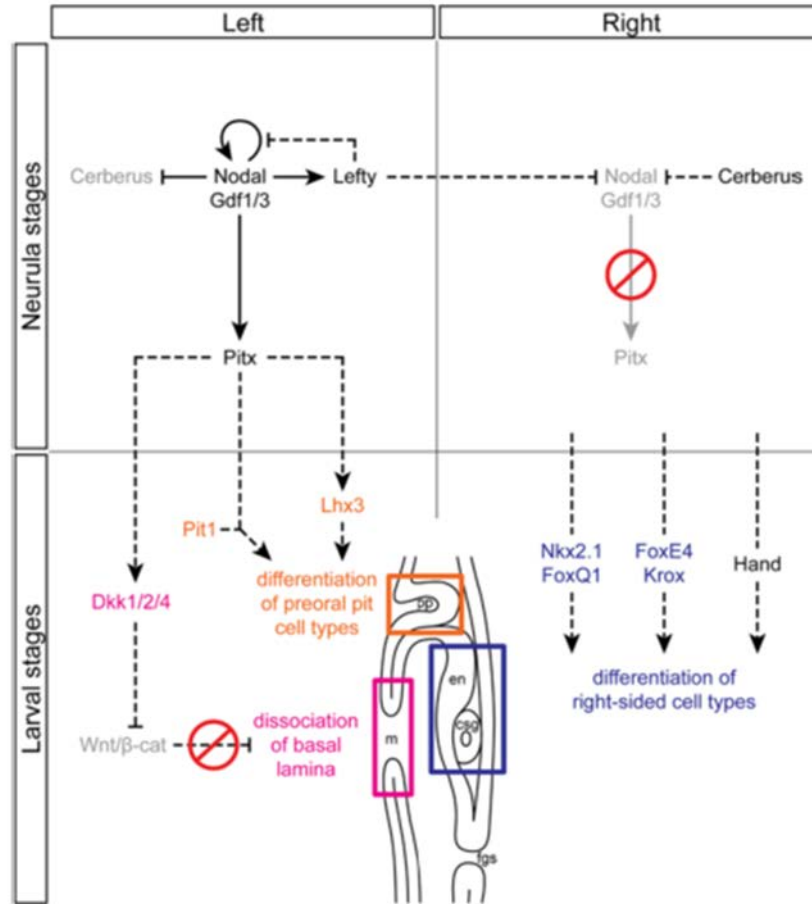


Figure 4.3: Scheme of Nodal signaling pathway involved in establishment of the left/right asymmetry in amphioxus. Dotted lines indicate proposed interactions based on the data from other chordates. Abbreviations: csg, club-shaped gland; en, endostyle; fgs, first gill slit; m, mouth; pp, pre-oral pit (from Soukup *et al.*, 2015).

Soukup and colleagues (2015) observed that the inhibition of Nodal signaling with specific drugs caused the loss of left-sided structures, as the mouth and the pre-oral pit. Indeed, when I treated amphioxus neurulas with TRIM, I observed developing larvae without the mouth but with the pre-oral pit normally formed, indicating that NO may be affects only the branch of the Nodal signal pathway which concerns the opening of the mouth (pink in Fig. 4.3). Nevertheless, a more recent study has revealed more details

about amphioxus mouth formation (Kaji *et al.*, 2016). Kaji and colleagues suggested that during neurulation a mesodermal vesicle, called oral mesovesicle (OMV), forms from the left side of the first somite, at the boundary between the first and the second somite. Afterwards, the OMV get fused with the epithelium on the left side of the pharynx, and through the perforation of the epithelium it gave birth to the mouth (Fig. 1.18). In agreement with the results reported by Soukup *et al.* 2015, they showed that the formation of the OMV (and of the mouth) was under the control of the Nodal-Pitx signal pathway. Moreover, this OMV expressed *Dkk1/2/4* (a gene downstream Pitx; Fig. 4.3), *Frzb1* and *Pax2/5/8*, that have been suggested to have a role in the dissolution of basal lamina and so in epithelial perforations (Edelman and Jones, 1995; Kozmik *et al.*, 1999; Dickinson *et al.*, 2009). In fact, it was proposed that mouth formation arise through perforation of ectoderm-mesoderm and endoderm-mesoderm bi-layered membranes (Goodrich, 1934). The same process was proposed for gills opening, and for this reason gills and mouth formations are comparable. This is also supported by the evidence that both mouth and gills formations were affected by perturbation of BMP signaling pathway, in fact Dorsomorphin caused no opening of mouth and gills in larvae (Kaji *et al.*, 2016). It is very interesting that, decreasing NO production with TRIM, I obtained a very similar phenotype and that the differential transcriptomic analysis of TRIM-treated embryos revealed the down-regulation of genes belonging to BMP signaling (*Slc39A10*, *Slc39A6*, *Runx1*). Therefore, it is plausible to hypothesize that both mouth and gill slits formation processes are under the control of the BMP pathway and that NO plays a crucial regulatory role in it.

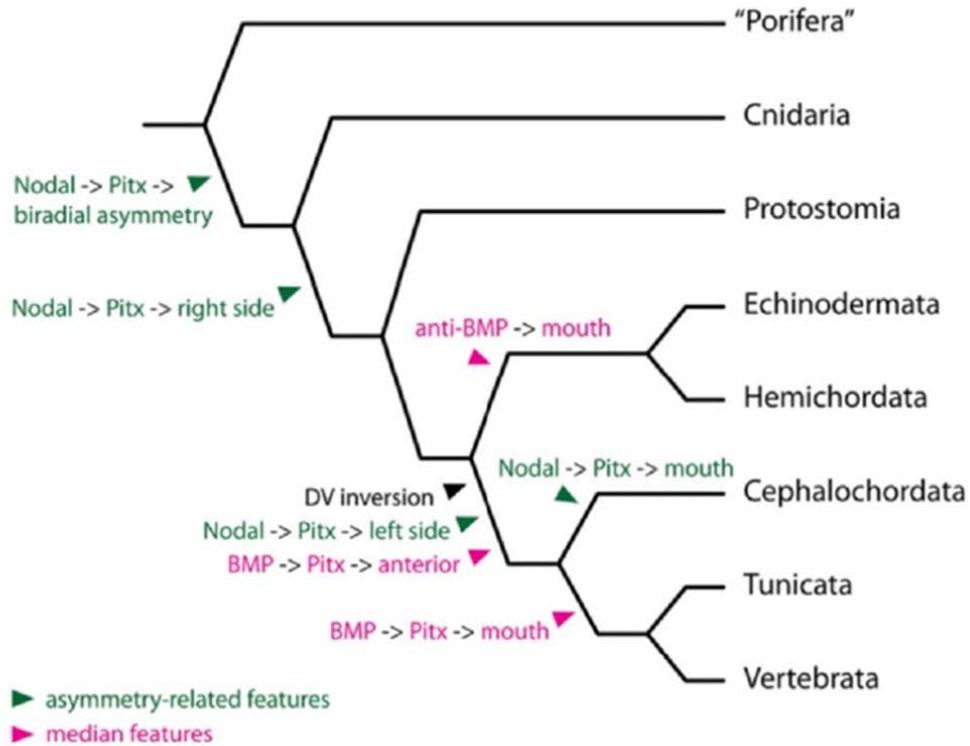


Figure 4.4: Gene pathways involved in left/right and mouth determination across metazoans. Green text marks left/right asymmetric expression; magenta text marks median expression. In protostomes, echinoderms and hemichordates, the Nodal-Pitx pathway regulates determination of the right side. In chordates, after dorso/ventral inversion, it determines the left side. BMP signaling occurred at the anterior neural boundary. BMP signaling suppresses oral development in echinoderms and hemichordates, while it promotes oral development, through Pitx, in tunicates and vertebrates. It does not seem to have the same role it has in other chordates (from Soukup *et al.*, 2015).

After the dorso/ventral inversion occurred at the base of the chordate phylum, it has been demonstrated that Nodal-Pitx signaling controls the development of the left-side structures while BMP-Pitx pathway is involved in determination of anterior organs. Furthermore, inside this scenario, the position of the mouth changed from an anti-BMP and non-Pitx territory (echinoderms and hemichordates) to a pro-BMP and Pitx-expressing territory (tunicates and vertebrates). Indeed, in olfactores, the mouth

develops at the anterior neural boundary (Dickinson *et al.*, 2007; Christiaen *et al.*, 2007; Soukup *et al.*, 2013) that is marked by the expression of Pitx factors downstream BMP signaling and *Otx2* at its most-anterior domain. Cephalochordates have a key position in this evolutionary scenario. It was already described the involvement of Nodal-Pitx signaling in mouth determination in amphioxus (Soukup *et al.*, 2015), and I also found this evidence in my preliminary differential transcriptomic results. On the other hand, it is currently unclear if the BMP signaling plays any role in amphioxus mouth development, as in other chordates (Fig. 4.4). The peculiar left-sided mouth in amphioxus has long been a matter of debate about it is homologous or not to the median mouth of vertebrates. The studies carried out for my PhD thesis project could add new details about the role of both Nodal and BMP pathways in the amphioxus mouth formation, their possible crosstalk and, most of all, the possible role of NO in regulating both signaling pathway in such important developmental process.

Another pathway affected by NOS inhibition resulted that of retinoic acid (RA) (*Raldh*, *RAR*, and the direct targets *Hox1* and *Hox3*) indicating that NO directly or indirectly controls it during amphioxus embryonic development. The RA signaling pathway regulates anter-posterior patterning of pharynx in chordates. For many years, in vertebrates, the role of the neural crests in organizing pharyngeal development was emphasized but it has now been defined the key role of pharyngeal endoderm in the patterning of the pharynx (Graham and Richardson, 2012). Evidently, the role of pharyngeal endoderm in this process predates the evolution of neural crest. In amphioxus RA signaling must be suppressed in the anterior portion of the gastrula for the proper specification of the pharynx and it must also be finely regulated during the

neurula stage for its correct partitioning (Koop *et al.*, 2014). Normally RAR is not expressed in anterior part of amphioxus body while RA-treated embryos show an ectopic *RAR* expression in the pharyngeal area (Escriva *et al.*, 2002) that can affect expression of genes involved in its development. It will be necessary to verify whether this ectopic expression occurs in the NOS-inhibited embryos and if it can regulate the expression of other genes that affected in the differential transcriptomic analysis.

The inhibition of NO production by TRIM treatment in amphioxus at neurula up to larval stage, resulted also in an alteration in locomotion of 3 dpf larvae. It is known that NO is a bioactive signaling molecule that is known to affect a wide range of neurodevelopmental processes. The treated larvae showed a general inactivity with sporadic jerking movements as reported in Figure 3.16. Amphioxus myotomes consist of separate sets of superficial and deep muscle fibers that are thought to be responsible for slow swimming and escape behavior, respectively (Ruppert, 1997). Therefore, the altered behavior observed in TRIM-treated larvae could be due to a disorder in neuromuscular junctions (NMJs) formation. However, NO functional relevance to NMJs development is not fully understood. In *X. laevis* NOS activity was localized in postsynaptic portions of embryo muscle cells and it was demonstrated that NO stimulates agrin-induced aggregation of a complex of proteins, including acetylcholine receptors (AChRs) (Schwarte and Godfrey, 2004). In fact, when *Xenopus* embryos were exposed to NOS inhibitors from stage 24, in which the innervation of the myotomes had not yet begun, to the stage 31, when rows of functional synapses had formed, the postsynaptic differentiation was blocked (Schwarte and Godfrey, 2004). The formation of NMJ involves the differentiation of both the presynaptic nerve terminal and the

postsynaptic apparatus of the muscle cell, resulting in a functional synapse. NO acts also as a retrograde signaling molecule that could play a role into regulating differentiation of presynaptic nerve terminals at developing NMJs (Thomas and Robataille, 2001). In order to understand if NO in amphioxus is involved in NMJs differentiation through the same mechanisms described for vertebrates, a deeper study will be necessary in future. Moreover, short-term TRIM treatments could be useful to identify the precise interval in which NO acts to define the NMJs, just as I did for the pharyngeal structures formation.

FUTURE PERSPECTIVES

The results obtained during my PhD have opened interesting future research prospects and several points need to be deepened and completed:

- Keeping in mind the results obtained about the inducible nature of the amphioxus *Nos* genes, it would be very interesting to analyze also their expression by whole-mount in situ hybridization (WISH) and to study the endogenous NO production and localization by Griess assay and DAF-FM-DA after LPS treatment. All these analyses should be consistent and they should provide comprehensive data not only about the inducible nature of the different amphioxus *Nos*, but also about where (in what tissue or structure) each *Nos* is induced. Unfortunately, to complete such experiments I will have to wait for the next amphioxus spawning season.

- As regard the amphioxus *NosC* promoter analysis, the positive regulatory activity of the CNRs already tested will be confirmed by immunostaining using anti-GFP antibody. In this way, I can be sure that the observed fluorescent signal is due to the presence of the GFP construct and activity of the amphioxus CNR. The positive CNRs will be divided in smaller fragments that will be tested up to identify the regulative elements, which have only been hypothesized so far on the basis of the JASPAR analysis (see chapter 3). Finally, these promising CNR could be tested in zebrafish to assay the evolutionary conservation of the neuronal *Nos* regulation mechanism in chordates. The same analysis will be also performed on the genomic region up- and downstream the *NosA* TSS in order to clarify the possible regulatory differences between the two amphioxus neuronal *Nos* genes that can justify their different inducible nature and temporal expression.
- Starting from the preliminary results obtained from the differential transcriptomic analysis after TRIM treatment, the goal is to improve the analysis already done and to have a complete view of the NOS inhibition effects. The most interesting genes will be analyzed by WISH experiments. The characterization of the NO action and the establishment of its molecular interactions with other networks, that have been altered after NOS inhibition, will be important to clarify the role that NO plays in the process of pharyngeal structures formation.

CHAPTER 5

COLLABORATIVE AND RELATED PROJECTS

Collaborative project: Eukaryote-specific Ran GTPase controls mitosis in Mediterranean amphioxus.

During the course of my Ph.D., I had the possibility to collaborate with Dr. Filomena Ristoratore's research group at the Stazione Zoologica Anton Dohrn Napoli. The project in which I was involved concerns the study of the Ran evolution in metazoans.

My contribution in this collaborative project was to perform WISH experiments to reveal the *Ran* expression during amphioxus development (Fig. 5.1a-d). Moreover, I carried out whole-mount immunostaining using the mitotic marker Phospho anti-Histone H3 (S10) (PHH3) (Fig. 5.1e-h).

The aim of these experiments was to correlate the *Ran* expression pattern with the mitotic process. I also participated in figures preparation and in the critical discussion of the results, moreover I contributed in writing the manuscript that is in preparation at the moment of my Ph.D. thesis submission.

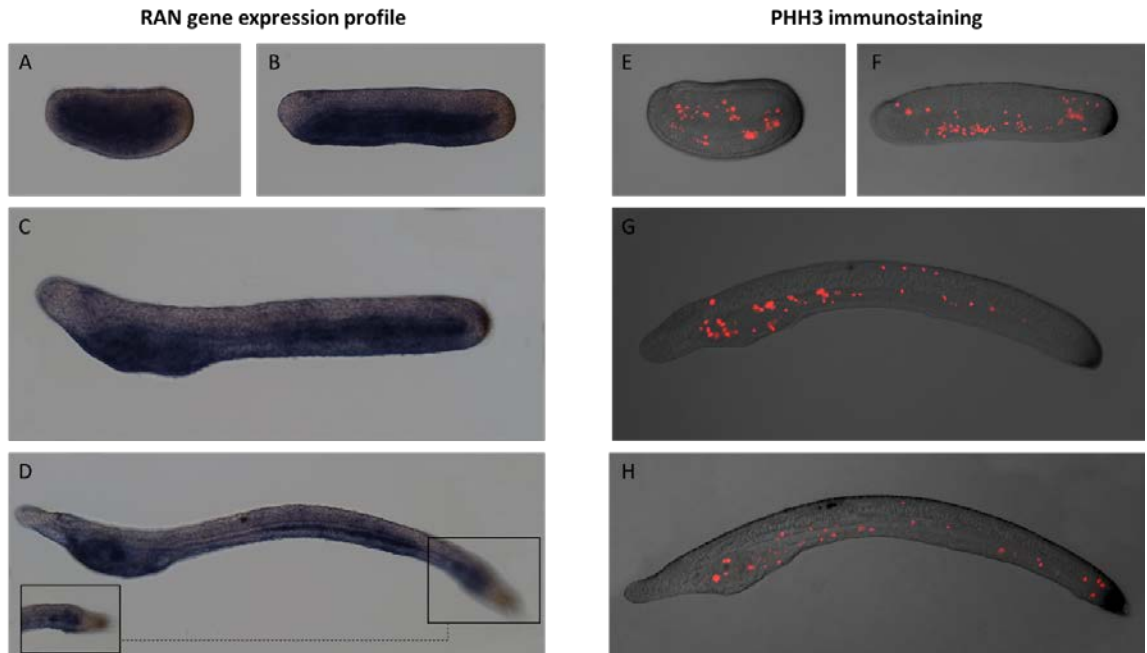


Figure 5.1: *Ran* expression profile and mitotic cells (PHH3 immunostaining) in amphioxus embryos and larvae. A-D) WISH of *Ran* during amphioxus development. A) middle neurula; B) late neurula; C) pre-mouth larva; D) open-mouth larva, in the square on the left there is a focus on the anus. E-H) Whole-mount immunostaining using PHH3 during amphioxus development. E) middle neurula; F) late neurula; G) pre-mouth larva; H) open-mouth larva.

Materials and Methods

Amphioxus embryo collection

I used embryos obtained from the local amphioxus species, *Branchiostoma lanceolatum*, from the Gulf of Naples (Italy) that were fixed and stored at -20°C in 70% ethanol for *in situ* hybridization and immunostaining experiments.

Whole-mount *in situ* hybridization

For this experiment, I followed the WISH protocol reported by Annona *et al.* (2017).

Whole-mount immunostaining

Embryos were rehydrated in PBT and blocked for 1h at RT in 2 mg/mL BSA, 10% goat serum in PBT 1X (Blocking solution). The embryos were incubated over night at 4°C in rat Phospho anti-Histone H3 (S10) antibody, diluted 1:250 in blocking solution. After rinsed 7x20 min in PBT, the secondary antibody, Alexa Fluor® 555 - Goat Anti-Rat IgG H&L, was added (dilution 1:500 in blocking solution) for 2 h at 4°C, and embryos were rinsed again 7x20 min in PBT. Embryos were mounted in 80% glycerol in PBS, and observed by Axio Imager used in connection with ApoTome (Zeiss).

Related project: Amphioxus biogeography in Europe.

During my PhD project, I had the opportunity work in a parallel project on the amphioxus *Branchiostoma lanceolatum* biogeography in Europe. We selected key collection locations in Europe and specially in Italy for this analysis (Fig. 5.2). My contribution in this project was the selection of discriminative genes to use for the analyses, the amplification and sequencing of selected genes for all the samples. In addition to the classic markers that are usually used for this type of study, I also used an intronic region of the *B. lanceolatum* *NosC* since this gene is highly conserved among metazoans (Andreakis *et al.*, 2011).

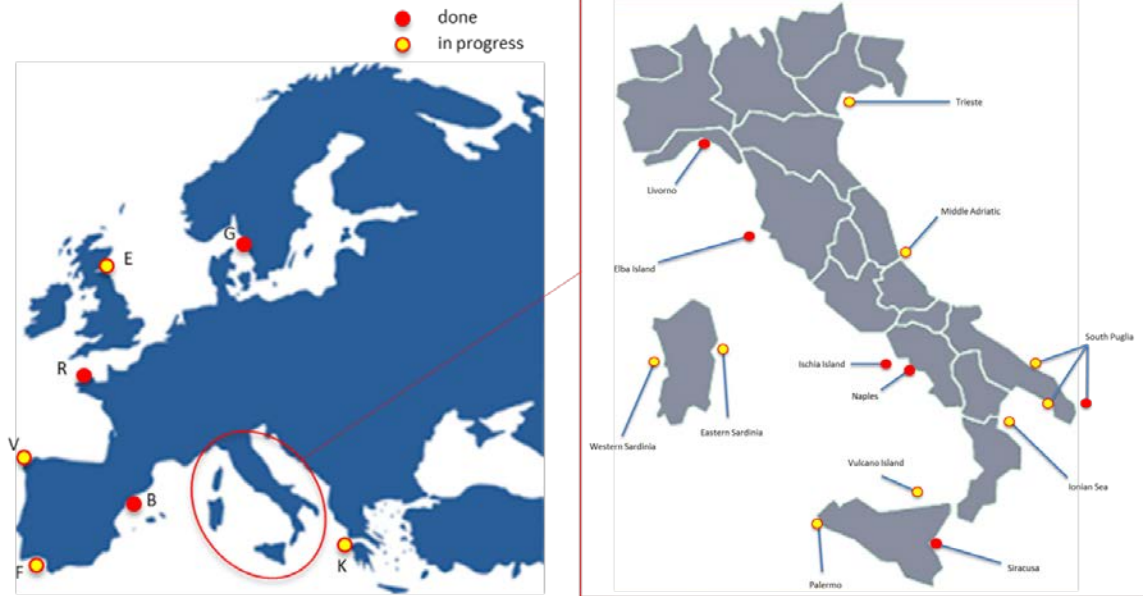


Figure 5.2: Map of locations selected for amphioxus biogeography in Europe. In the red square, there is a zoom on the Italian peninsula. The red dots indicate the sites already analyzed, the yellow dots indicate the sites not yet analyzed. G: Göteborg (SE); E: Edinburgh (UK); R: Roscoff (FR); V: Vigo (ES); F: Faro (PT); B: Banyuls-sur-Mer (FR); K: Kefalonia (GR).

Materials and Methods

Genomic DNA extraction

Genomic DNA was extracted, from a piece of adult amphioxus tail, in 20 μ l of 50 mM NaOH. The samples were heated for 5 min at 95°C in a thermo-block, followed by cooling to 4°C. 100 mM Tris-HCl pH 8.0 was added 1:10. The samples were briefly centrifuged to collect the lysate in the bottom of the tube and 2 μ l of the supernatant containing genomic DNA, used for PCR reactions.

Markers

Different genes were used as marker to analyze the conservation between the samples.

The list of genes is as follows:

- **Ribosomal genes markers:** Cyclooxygenase 1 (Co1 or Cox1)
Ribosomal ribonucleic acid 12S (rRNA12S)
Ribosomal ribonucleic acid 16S (rRNA16S).
- **Nuclear genes markers:** Internal Transcribed Spacer 2 (ITS2)
Pyruvate dehydrogenase (PDH)
Neuronal Nitric Oxide Synthase C (NOS-C, intron).
- **Microsatellites** (in progress): Branb-4 (GTTT)₁₁ accession number EF583886,
Branb-3 (TGTGT)₈ accession number FJ960511 (Li *et al.*, 2013).

Sequences and alignments

DNA sequencing was performed as described in Chapter 2. The alignment was carried out using the Multiple Sequence Alignment tool “Clustal Omega” of EMBL.

REFERENCES

- ADOLF, B., CHAPOUTON, P., LAM, C. S., TOPP, S., TANNHÄUSER, B., STRÄHLE, U., GÖTZ, M. & BALLY-CUIF, L. 2006. Conserved and acquired features of adult neurogenesis in the zebrafish telencephalon. *Dev Biol*, 295, 278-93.
- AHERN, G. P., KLYACHKO, V. A. & JACKSON, M. B. 2002. cGMP and S-nitrosylation: two routes for modulation of neuronal excitability by NO. *Trends Neurosci*, 25, 510-7.
- ALBUIXECH-CRESPO, B., LÓPEZ-BLANCH, L., BURGUERA, D., MAESO, I., SÁNCHEZ-ARRONES, L., MORENO-BRAVO, J. A., SOMORJAI, I., PASCUAL-ANAYA, J., PUELLES, E., BOVOLENTA, P., GARCIA-FERNÁNDEZ, J., PUELLES, L., IRIMIA, M. & FERRAN, J. L. 2017. Molecular regionalization of the developing amphioxus neural tube challenges major partitions of the vertebrate brain. *PLoS Biol*, 15, e2001573.
- ALDERTON, W. K., COOPER, C. E. & KNOWLES, R. G. 2001. Nitric oxide synthases: structure, function and inhibition. *Biochem J*, 357, 593-615.
- AMIN, A. R., DICESARE, P. E., VYAS, P., ATTUR, M., TZENG, E., BILLIAR, T. R., STUCHIN, S. A. & ABRAMSON, S. B. 1995. The expression and regulation of nitric oxide synthase in human osteoarthritis-affected chondrocytes: evidence for up-regulated neuronal nitric oxide synthase. *J Exp Med*, 182, 2097-102.
- ANDREAKIS, N., D'ANIELLO, S., ALBALAT, R., PATTI, F. P., GARCIA-FERNÁNDEZ, J., PROCACCINI, G., SORDINO, P. & PALUMBO, A. 2011. Evolution of the nitric oxide synthase family in metazoans. *Mol Biol Evol*, 28, 163-79.
- ANDREW, P. J. & MAYER, B. 1999. Enzymatic function of nitric oxide synthases. *Cardiovasc Res*, 43, 521-31.
- ANNOVA, G., CACCAVALE, F., PASCUAL-ANAYA, J., KURATANI, S., DE LUCA, P., PALUMBO, A. & D'ANIELLO, S. 2017. Nitric Oxide regulates mouth development in amphioxus. *Sci Rep*, 7, 8432.

- AULAK, K. S., KOECK, T., CRABB, J. W. & STUEHR, D. J. 2004. Dynamics of protein nitration in cells and mitochondria. *Am J Physiol Heart Circ Physiol*, 286, H30-8.
- BACHIR, L. K., LAVERRIÈRE, J. N. & COUNIS, R. 2001. Isolation and characterization of a rat nitric oxide synthase type I gene promoter that confers expression and regulation in pituitary gonadotrope cells. *Endocrinology* **142**, 4631-4642
- BARRINGTON, E. J. W., 1965. Biology of Hemichordata and Protochordata. *Science*, 149, 49-50.
- BERLETT, B. S., FRIGUET, B., YIM, M. B., CHOCK, P. B. & STADTMAN, E. R. 1996. Peroxynitrite-mediated nitration of tyrosine residues in Escherichia coli glutamine synthetase mimics adenylation: relevance to signal transduction. *Proc Natl Acad Sci U S A*, 93, 1776-80.
- BERTRAND, S., BELGACEM, M. R. & ESCRIVA, H. 2011. Nuclear hormone receptors in chordates. *Mol Cell Endocrinol*, 334, 67-75.
- BERTRAND, S. & ESCRIVA, H. 2011. Evolutionary crossroads in developmental biology: amphioxus. *Development*, 138, 4819-30.
- BEUTLER, B. & RIETSCHER, E. T. 2003. Innate immune sensing and its roots: the story of endotoxin. *Nat Rev Immunol*, 3, 169-76.
- BIRNEY, E. & DURBIN, R. 2000. Using GeneWise in the Drosophila annotation experiment. *Genome Res*, 10, 547-8.
- BISHOP, C. D., BATES, W. R. & BRANDHORST, B. P. 2001. Regulation of metamorphosis in ascidians involves NO/cGMP signaling and HSP90. *J Exp Zool*, 289, 374-84.
- BISHOP, C. D. & BRANDHORST, B. P. 2001. NO/cGMP signaling and HSP90 activity represses metamorphosis in the sea urchin *Lytechinus pictus*. *Biol Bull*, 201, 394-404.
- BISHOP, C. D. & BRANDHORST, B. P. 2007. Development of nitric oxide synthase-defined neurons in the sea urchin larval ciliary band and evidence for a chemosensory function during metamorphosis. *Dev Dyn*, 236, 1535-46.
- BLAIR, J. E. & HEDGES, S. B. 2005. Molecular phylogeny and divergence times of deuterostome animals. *Mol Biol Evol*, 22, 2275-84.

- BOISSEL, J. P., ZELENKA, M., GÖDTEL-ARMBRUST, U., FEUERSTEIN, T. J., FÖRSTERMANN, U. 2003. Transcription of different exons 1 of the human neuronal nitric oxide synthase gene is dynamically regulated in a cell- and stimulus-specific manner. *Biol Chem* **384**, 351-362.
- BONE, Q. 1992. On the locomotion of ascidian tadpole larvae. *J. Mar Biol Assoc UK*, **83**, 907-919.
- BRENNAN, J. E., CHAO, D. S., GEE, S. H., MCGEE, A. W., CRAVEN, S. E., SANTILLANO, D. R., WU, Z., HUANG, F., XIA, H., PETERS, M. F., FROEHNER, S. C. & BRETT, D. S. 1996. Interaction of nitric oxide synthase with the postsynaptic density protein PSD-95 and alpha1-syntrophin mediated by PDZ domains. *Cell*, **84**, 757-67.
- BROOKE, N. M., GARCIA-FERNÁNDEZ, J. & HOLLAND, P. W. 1998. The ParaHox gene cluster is an evolutionary sister of the Hox gene cluster. *Nature*, **392**, 920-2.
- BROS, M., BOISSEL, J. P., GÖDTEL-ARMBRUST, U. & FÖRSTERMANN, U. 2006. Transcription of human neuronal nitric oxide synthase mRNAs derived from different first exons is partly controlled by exon 1-specific promoter sequences. *Genomics* **87**, 463-473.
- BRUNETTI, R., GISSI, C., PENNATI, R., CAICCI, F., GASPARINI, F., MANNI, L. 2015. Morphological evidence that the molecularly determined *Ciona intestinalis* type A and type B are different species: *Ciona robusta* and *Ciona intestinalis*. *J Zoolog Syst Evol Res*, **53**, 186-193.
- BRYAN, N. S., BIAN, K., MURAD, F., 2009. Discovery of the nitric oxide signaling pathway and targets for drug development. *Front Biosci*, **14**, 1-18.
- CALABRESE, V., MANCUSO, C., CALVANI, M., RIZZARELLI, E., BUTTERFIELD, D. A. & STELLA, A. M. 2007. Nitric oxide in the central nervous system: neuroprotection versus neurotoxicity. *Nat Rev Neurosci*, **8**, 766-75.
- CANDIANI, S., MORONTI, L., PENNATI, R., DE BERNARDI, F., BENFENATI, F. & PESTARINO, M. 2010. The synapsin gene family in basal chordates: evolutionary perspectives in metazoans. *BMC Evol Biol*, **10**, 32.
- CANDIANI, S., MORONTI, L., RAMOINO, P., SCHUBERT, M. & PESTARINO, M. 2012. A neurochemical map of the developing amphioxus nervous system. *BMC Neurosci*, **13**, 59.

- CAPELLA-GUTIÉRREZ, S., SILLA-MARTÍNEZ, J. M. & GABALDÓN, T. 2009. trimAl: a tool for automated alignment trimming in large-scale phylogenetic analyses. *Bioinformatics*, 25, 1972-3.
- CAPPELLETTI, G., TEDESCHI, G., MAGGIONI, M. G., NEGRI, A., NONNIS, S. & MACI, R. 2004. The nitration of tau protein in neurone-like PC12 cells. *FEBS Lett*, 562, 35-9.
- CAÑESTRO, C., YOKOI, H. & POSTLETHWAIT, J. H. 2007. Evolutionary developmental biology and genomics. *Nat Rev Genet*, 8, 932-42.
- CHEN, D., LIN, Y. & ZHANG, H. 2008. Characterization and expression of two amphioxus DDAH genes originating from an amphioxus-specific gene duplication. *Gene*, 410, 75-81.
- CHO, H. J., XIE, Q. W., CALAYCAY, J., MUMFORD, R. A., SWIDEREK, K. M., LEE, T. D. & NATHAN, C. 1992. Calmodulin is a subunit of nitric oxide synthase from macrophages. *J Exp Med*, 176, 599-604.
- CHRISTIAEN, L., JASZCZYSZYN, Y., KERFANT, M., KANO, S., THERMES, V. & JOLY, J. S. 2007. Evolutionary modification of mouth position in deuterostomes. *Semin Cell Dev Biol*, 18, 502-11.
- COMES, S., LOCASCIO, A., SILVESTRE, F., D'ISCHIA, M., RUSSO, G. L., TOSTI, E., BRANNO, M. & PALUMBO, A. 2007. Regulatory roles of nitric oxide during larval development and metamorphosis in *Ciona intestinalis*. *Dev Biol*, 306, 772-84.
- CONKLIN E.G. 1914. Facts and factors of development. New York: *Popular Science Pub. Co*, 84, 531.
- CORBO, J. C., LEVINE, M. & ZELLER, R. W. 1997. Characterization of a notochord-specific enhancer from the Brachyury promoter region of the ascidian, *Ciona intestinalis*. *Development* **124**, 589-602.
- COSTA, O. G. 1834. Cenni zoologici ossia descrizione sommaria delle specie nuove di animali scoperti in diverse contrade del regno nell' anno 1834. Naples: *Azzolino & Comp.*
- D'ANIELLO, S., IRIMIA, M., MAESO, I., PASCUAL-ANAYA, J., JIMÉNEZ-DELGADO, S., BERTRAND, S. & GARCIA-FERNÁNDEZ, J. 2008. Gene expansion and retention leads to a diverse tyrosine kinase superfamily in amphioxus. *Mol Biol Evol*, 25, 1841-54.
- DAVIDSON, B., SHI, W., BEH, J., CHRISTIAEN, L. & LEVINE, M. 2006. FGF signaling delineates the

- cardiac progenitor field in the simple chordate, *Ciona intestinalis*. *Genes Dev* **20**, 2728-2738.
- DAVIDSON, B., SHI, W. & LEVINE, M. 2005. Uncoupling heart cell specification and migration in the simple chordate *Ciona intestinalis*. *Development* **132**, 4811-4818.
- DAVIDSON, S. K., KOROPATNICK, T. A., KOSSMEHL, R., SYCURO, L. & MCFALL-NGAI, M. J. 2004. NO means 'yes' in the squid-vibrio symbiosis: nitric oxide (NO) during the initial stages of a beneficial association. *Cell Microbiol*, **6**, 1139-51.
- DEHAL, P. & BOORE, J. L. 2005. Two rounds of whole genome duplication in the ancestral vertebrate. *PLoS Biol*, **3**, e314.
- DELSUC, F., BRINKMANN, H., CHOURROUT, D. & PHILIPPE, H. 2006. Tunicates and not cephalochordates are the closest living relatives of vertebrates. *Nature*, **439**, 965-8.
- DELSUC, F., TSAGKOGEOGA, G., LARTILLOT, N. & PHILIPPE, H. 2008. Additional molecular support for the new chordate phylogeny. *Genesis*, **46**, 592-604.
- DESDEVISES, Y., MAILLET, V., FUENTES, M. & ESCRIVA, H. 2011. A snapshot of the population structure of *Branchiostoma lanceolatum* in the Racou beach, France, during its spawning season. *PLoS One*, **6**, e18520.
- DI CRISTO, C., FIORE, G., SCHEINKER, V., ENIKOLOPOV, G., D'ISCHIA, M., PALUMBO, A. & DI COSMO, A. 2007. Nitric oxide synthase expression in the central nervous system of *Sepia officinalis*: an in situ hybridization study. *Eur J Neurosci*, **26**, 1599-610.
- DICKINSON, A. & SIVE, H. 2007. Positioning the extreme anterior in *Xenopus*: cement gland, primary mouth and anterior pituitary. *Semin Cell Dev Biol*, **18**, 525-33.
- DICKINSON, A. J. & SIVE, H. L. 2009. The Wnt antagonists Frzb-1 and Crescent locally regulate basement membrane dissolution in the developing primary mouth. *Development*, **136**, 1071-81.
- DIOGO, R., KELLY, R. G., CHRISTIAEN, L., LEVINE, M., ZIERMANN, J. M., MOLNAR, J. L., NODEN, D. M., TZAHOR, E. 2015. A new heart for a new head in vertebrate cardiopharyngeal evolution. *Nature*, **520**, 466-73.
- DUFOUR, H. D., CHETTOUH Z, DEYTS C, DE ROSA R, GORIDIS C, JOLY JS, BRUNET JF. 2006. Precranial origin of cranial motoneurons. *Proc Natl Acad Sci U S A* **103**, 8727-8732.

- EDELMAN, G. M. & JONES, F. S. 1995. Developmental control of N-CAM expression by Hox and Pax gene products. *Philos Trans R Soc Lond B Biol Sci*, 349, 305-12.
- EDGAR, R. C. 2004. MUSCLE: multiple sequence alignment with high accuracy and high throughput. *Nucleic Acids Res*, 32, 1792-7.
- ERCOLESI, E., TEDESCHI, G., FIORE, G., NEGRI, A., MAFFIOLI, E., D'ISCHIA, M. & PALUMBO, A. 2012. Protein nitration as footprint of oxidative stress-related nitric oxide signaling pathways in developing *Ciona intestinalis*. *Nitric Oxide*, 27, 18-24.
- ERICSON, L., FREDRIKSSON, G., OFVERHOLM, T., 1985. Ultrastructural localization of the iodination centre in the endostyle of the adult amphioxus (*Branchiostoma lanceolatum*). *Cell Tissue Res*. 241, 267-273.
- ESCRIVA, H., HOLLAND, N. D., GRONEMEYER, H., LAUDET, V. & HOLLAND, L. Z. 2002. The retinoic acid signaling pathway regulates anterior/posterior patterning in the nerve cord and pharynx of amphioxus, a chordate lacking neural crest. *Development* **129**, 2905-2916.
- ESPLUGUES, J. V. 2002. NO as a signalling molecule in the nervous system. *Br J Pharmacol*, 135, 1079-95.
- FIORE, G., MATTIELLO, T., TEDESCHI, G., NONNIS, S., D'ISCHIA, M. & PALUMBO, A. 2009. Protein nitration is specifically associated with melanin production and reveals redox imbalance as a new correlate of cell maturation in the ink gland of *Sepia officinalis*. *Pigment Cell Melanoma Res*, 22, 857-9.
- FUENTES, M., BENITO, E., BERTRAND, S., PARIS, M., MIGNARDOT, A., GODOY, L., JIMENEZ-DELGADO, S., OLIVERI, D., CANDIANI, S., HIRSINGER, E., D'ANIELLO, S., PASCUAL-ANAYA, J., MAESO, I., PESTARINO, M., VERNIER, P., NICOLAS, J. F., SCHUBERT, M., LAUDET, V., GENEVIERE, A. M., ALBALAT, R., GARCIA FERNANDEZ, J., HOLLAND, N. D. & ESCRIVA, H. 2007. Insights into spawning behavior and development of the European amphioxus (*Branchiostoma lanceolatum*). *J Exp Zool B Mol Dev Evol*, 308, 484-93.
- FÖRSTERMANN, U. & SESSA, W. C. 2012. Nitric oxide synthases: regulation and function. *Eur Heart J*, 33, 829-37, 837a-837d.

- FREDRIKSSON, G., ERICSON, L. E., OLSSON, R., 1984. Iodine binding in the endostyle of larval *Branchiostoma lanceolatum* (Cephalochordata). *Gen. Comp. Endocrinol.* 56, 177-184.
- GARCIA-FERNÁNDEZ, J. & BENITO-GUTIÉRREZ, E. 2009. It's a long way from amphioxus: descendants of the earliest chordate. *Bioessays*, 31, 665-75.
- GHOSH, D. K. & SALERNO, J. C. 2003. Nitric oxide synthases: domain structure and alignment in enzyme function and control. *Front Biosci*, 8, d193-209.
- GILMOUR, T. H. J. 1996. Feeding methods of cephalochordate larvae. *Israel J. Zool.* 42 (Suppl), 87-95.
- GIOVINE, M., POZZOLINI, M., FAVRE, A., BAVESTRELLO, G., CERRANO, C., OTTAVIANI, F., CHIARANTINI, L., CERASI, A., CANGIOTTI, M., ZOCCHI, E., SCARFÌ, S., SARÀ, M. & BENATTI, U. 2001. Heat stress-activated, calcium-dependent nitric oxide synthase in sponges. *Nitric Oxide*, 5, 427-31.
- GODOY, L., GONZÁLEZ-DUARTE, R., ALBALAT, R., 2006. S-nitrosogluthathione reductase activity of amphioxus ADH3: insights into the nitric oxide metabolism. *Int J Biol Sci.*, 2, 117.
- GOODRICH E.S. 1930. The development of the Club-shaped Gland in Amphioxus. 155-164.
- GOODRICH E.S. 1934. The early development of the nephridia in amphioxus: Part II, the paired nephridia. *Q J Micr Sci*, 76, 655-74.
- GORETSKI, J. & HOLLOCHER, T. C. 1988. Trapping of nitric oxide produced during denitrification by extracellular hemoglobin. *J Biol Chem*, 263, 2316-23.
- GRAHAM, A., RICHARDSON, J. 2012. Developmental and evolutionary origins of the pharyngeal apparatus. *Evodevo*, 3, 24.
- GREEN, L. C., WAGNER, D. A., GLOGOWSKI, J., SKIPPER, P. L., WISHNOK, J. S., TANNENBAUM, S. R. 1982. Analysis of nitrate, nitrite, and [15N] nitrate in biological fluids. *Anal Biochem*, 126, 131-8.
- GRUMETTO, L., WILDING, M., DE SIMONE, M. L., TOSTI, E., GALIONE, A. & DALE, B. 1997. Nitric oxide gates fertilization channels in ascidian oocytes through nicotinamide nucleotide metabolism. *Biochem Biophys Res Commun*, 239, 723-8.

- HALL A. V., ANTONIOU H., WANG Y., CHEUNG A. H., ARBUS A. M., OLSON S. L., LU W. C., KAU C. L. AND MARSDEN P. A. 1994. Structural organization of the human neuronal nitric oxide synthase gene (NOS1). *J. Biol. Chem.* 269, 33 082–33 090.
- HATSCHEK, B., 1893. The amphioxus and its development. Swan, Sonnenschein & Company.
- HECHT, M., WALLACE, B., PRANCE, G., SCHAEFFER, B. 1987. Deuterostome Monophyly and Phylogeny. *Evol. Biol.* Springer US. 179-235.
- HIRAKOW, R., KAJITA, N. 1994. Electron microscopic study of the development of amphioxus, *Branchiostoma belcheri tsingtauense*: the neurula and larva. *Kaibogaku Zasshi*, 69, 1-13.
- HOLLAND, L. Z. & ONAI, T. 2012. Early development of cephalochordates (amphioxus). *Wiley Interdiscip Rev Dev Biol*, 1, 167-83.
- HOLLAND, N. D. & HOLLAND, L. Z. 1989. Fine Structural Study of the Cortical Reaction and Formation of the Egg Coats in a Lancelet (= Amphioxus), *Branchiostoma floridae* (Phylum Chordata: Subphylum Cephalochordata = Acrania). *Bio Bull*, 176, 111-122.
- HOLLAND, N. D. & HOLLAND, L. Z. 1990. Fine Structure of the Mesothelia and Extracellular Materials in the Coelomic Fluid of the Fin Boxes, Myocoels and Sclerozoels of a Lancelet, *Branchiostoma floridae* (Cephalochordata = Acrania). *Acta Zool.*, 71, 225–234.
- HOLLAND, N. D. & HOLLAND, L. Z. 1991. The fine structure of the growth stage oocytes of a lancelet (= amphioxus), *Branchiostoma lanceolatum*. *Invertebr. Reprod. Dev.*, 19, 107-122.
- HOLLAND, N. D. & HOLLAND, L. Z. 1992. Early Development in the Lancelet (=Amphioxus) *Branchiostoma floridae* from Sperm Entry through Pronuclear Fusion: Presence of Vegetal Pole Plasm and Lack of Conspicuous Ooplasmic Segregation. *Bio Bull*, 182, 77-96.
- HOLLAND, N. D. & HOLLAND, L. Z. 1993. Embryos and larvae of invertebrate deuterostomes. Essential developmental biology: a practical approach. (Stern CD, Holland PWH, Eds.), Oxford; New York: IRL Press at Oxford University Press, 21-32.
- HOLLAND, L. Z., HOLLAND, N. D. 2007. A revised fate map for amphioxus and the evolution of axial patterning in chordates. *Integr Comp Biol*, 47, 360-72.

- HOLLAND, N. D., PARIS, M., KOOP, D., 2009. The club-shaped gland of amphioxus: export of secretion to the pharynx in pre-metamorphic larvae and apoptosis during metamorphosis. *Acta Zool.*, 90, 372-379.
- HOLLAND, N. D. & HOLLAND, L. Z. 2010. Laboratory spawning and development of the Bahama lancelet, *Asymmetron lucayanum* (cephalochordata): fertilization through feeding larvae. *Biol Bull*, 219, 132-41.
- HORIE, T., NAKAGAWA, M., SASAKURA, Y., KUSAKABE, T.G., TSUDA, M. 2010. Simple motor system of the ascidian larva: neuronal complex comprising putative cholinergic and GABAergic/glycinergic neurons. *Zool Sci*, 27, 181-190.
- HOU, Y. C., JANCZUK, A. & WANG, P. G. 1999. Current trends in the development of nitric oxide donors. *Curr Pharm Des*, 5, 417-41.
- IGAWA, T., NOZAWA, M., SUZUKI, D. G., REIMER, J. D., MOROV, A. R., WANG, Y., HENMI, Y. & YASUI, K. 2017. Evolutionary history of the extant amphioxus lineage with shallow-branching diversification. *Sci Rep*, 7, 1157.
- IKUTA, T. & SAIGA, H. 2007. Dynamic change in the expression of developmental genes in the ascidian central nervous system: revisit to the tripartite model and the origin of the midbrain-hindbrain boundary region. *Dev Biol* 312, 631-643.
- IMAI, J. H. & MEINERTZHAGEN, I. A. 2007. Neurons of the ascidian larval nervous system in *Ciona intestinalis*: II. Peripheral nervous system. *J Comp Neurol* 501, 335-352.
- JACOX, L., SINDELKA, R., CHEN, J., ROTHMAN, A., DICKINSON, A., SIVE, H. 2014. The extreme anterior domain is an essential craniofacial organizer acting through Kinin-Kallikrein signaling. *Cell Rep*, 8, 596-609.
- JAFFREY, S. R., BENFENATI, F., SNOWMAN, A. M., CZERNIK, A. J. & SNYDER, S. H. 2002. Neuronal nitric-oxide synthase localization mediated by a ternary complex with synapsin and CAPON. *Proc Natl Acad Sci U S A*, 99, 3199-204.
- JEONG, Y., WON, J., KIM, C. & YIM, J. 2000. 5'-Flanking sequence and promoter activity of the rabbit neuronal nitric oxide synthase (nNOS) gene. *Mol Cells* 10, 566-574.

- JIANG, Q., ZHOU, Z., WANG, L., YUE, F., WANG, J. & SONG, L. 2013. A scallop nitric oxide synthase (NOS) with structure similar to neuronal NOS and its involvement in the immune defense. *PLoS One*, 8, e69158.
- JOHNSON, D. S., DAVIDSON, B., BROWN, C. D., SMITH, W. C. & SIDOW, A. 2004. Noncoding regulatory sequences of *Ciona* exhibit strong correspondence between evolutionary constraint and functional importance. *Genome Res* **14**, 2448-2456.
- KAJI, T., HOSHINO, Y., HENMI, Y., YASUI, K., 2013. Longitudinal Observation of Japanese Lancelet, *Branchiostoma japonicum*, Metamorphosis. *Dataset Pap Biol.* 2013, 6.
- KAJI, T., REIMER, J. D., MOROV, A. R., KURATANI, S. & YASUI, K. 2016. Amphioxus mouth after dorso-ventral inversion. *Zoological Lett*, 2, 2.
- KAJI, T., SHIMIZU, K., ARTINGER, K. B. & YASUI, K. 2009. Dynamic modification of oral innervation during metamorphosis in *Branchiostoma belcheri*, the oriental lancelet. *Biol Bull*, 217, 151-60.
- KATZOFF, A., BEN-GEDALYA, T. & SUSSWEIN, A. J. 2002. Nitric oxide is necessary for multiple memory processes after learning that a food is inedible in aplysia. *J Neurosci*, 22, 9581-94.
- KELM, M. 1999. Nitric oxide metabolism and breakdown. *Biochim Biophys Acta*, 1411(2-3), 273-89.
- KNOWLES, R. G. & MONCADA, S. 1994. Nitric oxide synthases in mammals. *Biochem J*, 298 (Pt 2), 249-58.
- KOJIMA, H., URANO, Y., KIKUCHI, K., HIGUCHI, T., HIRATA, Y. & NAGANO, T. 1999. Fluorescent Indicators for Imaging Nitric Oxide Production. *Angew Chem Int Ed Engl*, 38, 3209-3212.
- KON, T., NOHARA, M., YAMANOUE, Y., FUJIWARA, Y., NISHIDA, M. & NISHIKAWA, T. 2007. Phylogenetic position of a whale-fall lancelet (Cephalochordata) inferred from whole mitochondrial genome sequences. *BMC Evol Biol*, 7, 127.
- KOOP, D., CHEN, J., THEODOSIOU, M., CARVALHO, J. E., ALVAREZ, S., DE LERA, A. R., HOLLAND, L.Z., SCHUBERT, M. 2014. Roles of retinoic acid and *Tbx1/10* in pharyngeal segmentation: amphioxus and the ancestral chordate condition. *Evodevo* **5**, 36.
- KOSHLAND, D. E., JR., 1992. Editorial: The Molecule of the Year. *Science*. 258, 1861.

- KOZMIK, Z., HOLLAND, N. D., KALOUSOVA, A., PACES, J., SCHUBERT, M. & HOLLAND, L. Z. 1999. Characterization of an amphioxus paired box gene, *AmphiPax2/5/8*: developmental expression patterns in optic support cells, nephridium, thyroid-like structures and pharyngeal gill slits, but not in the midbrain-hindbrain boundary region. *Development*, 126, 1295-304.
- KOZMIKOVA, I., CANDIANI, S., FABIAN, P., GURSKA, D. & KOZMIK, Z. 2013. Essential role of Bmp signaling and its positive feedback loop in the early cell fate evolution of chordates. *Dev Biol*, 382, 538-54.
- KRÖNSTRÖM, J., DUPONT, S., MALLEFET, J., THORNDYKE, M. & HOLMGREN, S. 2007. Serotonin and nitric oxide interaction in the control of bioluminescence in northern krill, *Meganyctiphanes norvegica* (M. Sars). *J Exp Biol*, 210, 3179-87.
- KUO, R. C., BAXTER, G. T., THOMPSON, S. H., STRICKER, S. A., PATTON, C., BONAVENTURA, J. & EPEL, D. 2000. NO is necessary and sufficient for egg activation at fertilization. *Nature*, 406, 633-6.
- KUZIN, B., ROBERTS, I., PEUNOVA, N. & ENIKOLOPOV, G. 1996. Nitric oxide regulates cell proliferation during *Drosophila* development. *Cell*, 87, 639-49.
- LACALLI, T. C. 1996. Frontal eye circuitry, rostral sensory pathways and brain organization in amphioxus larvae: evidence from 3D reconstructions. *Philos. Trans. R. Soc. Lond., B, Biol. Sci.* 351, 243-263.
- LACALLI, T. C. 2006. Prospective protochordate homologs of vertebrate midbrain and MHB, with some thoughts on MHB origins. *Int J Biol Sci*, 2, 104-9.
- LAMARCK, J.B. 1816. *Histoire Naturelle Des Animaux Sans Vertèbres*. Verdière, Paris.
- LANKESTER, E.R. Memoirs: notes on the embryology and classification of the animal kingdom: comprising a revision of speculations relative to the origin and significance of the germ-layers. *Q J Microsc Sci*, 2, 399-454.
- LECKIE, C., EMPSON, R., BECCHETTI, A., THOMAS, J., GALIONE, A. & WHITAKER, M. 2003. The NO pathway acts late during the fertilization response in sea urchin eggs. *J Biol Chem*, 278, 12247-54.

- LEISE, E. M., KEMPF, S. C., DURHAM, N. R. & GIFONDORWA, D. J. 2004. Induction of metamorphosis in the marine gastropod *Ilyanassa obsoleta*: 5HT, NO and programmed cell death. *Acta Biol Hung*, 55, 293-300.
- LI, W., COWLEY, A., ULUDAG, M., GUR, T., MCWILLIAM, H., SQUIZZATO, S., PARK, Y. M., BUSO, N. & LOPEZ, R. 2015. The EMBL-EBI bioinformatics web and programmatic tools framework. *Nucleic Acids Res*, 43, W580-4.
- LI, W., ZHONG, J. & WANG, Y. 2013. Genetic diversity and population structure of two lancelets along the coast of China. *Zoolog Sci*, 30, 83-91.
- LI, Q., RITTER D, YANG N, DONG Z, LI H, CHUANG JH, GUO S. 2010. A systematic approach to identify functional motifs within vertebrate developmental enhancers. *Dev Biol* **337**, 484-495.
- LI, Y. ZHAO, Y., LI, G., WANG, J., LI, T., LI, W., LU, J. 2007. Regulation of neuronal nitric oxide synthase exon 1f gene expression by nuclear factor-kappaB acetylation in human neuroblastoma cells. *J Neurochem* **101**, 1194-1204.
- LIN, Y., CHEN, D., ZHANG, W., CAI, Z., CHEN, Z., ZHANG, N., MAO, B. & ZHANG, H. 2011. Characterization of the immune defense related tissues, cells, and genes in amphioxus. *Sci China Life Sci*, 54, 999-1004.
- LOVE, M. I., HUBER, W. & ANDERS, S. 2014. Moderated estimation of fold change and dispersion for RNA-seq data with DESeq2. *Genome Biol*, 15, 550.
- MACMICKING, J., XIE, Q. W. & NATHAN, C. 1997. Nitric oxide and macrophage function. *Annu Rev Immunol*, 15, 323-50.
- MARTÍNEZ-RUIZ, A. & LAMAS, S. 2009. Two decades of new concepts in nitric oxide signaling: from the discovery of a gas messenger to the mediation of nonenzymatic posttranslational modifications. *IUBMB Life*, 61, 91-8.
- MATTIELLO, T., FIORE, G., BROWN, E. R., D'ISCHIA, M. & PALUMBO, A. 2010. Nitric oxide mediates the glutamate-dependent pathway for neurotransmission in *Sepia officinalis* chromatophore organs. *J Biol Chem*, 285, 24154-63.
- MATTILA, J. T. & THOMAS, A. C. 2014. Nitric oxide synthase: non-canonical expression patterns. *Front*

Immunol, 5, 478.

- MATSUOKA, T., AWAZU, S., SHOGUCHI, E., SATOH, N. & SASAKURA, Y. 2005. Germline transgenesis of the ascidian *Ciona intestinalis* by electroporation. *Genesis* **41**, 67-72.
- MIGLIACCIO, O., CASTELLANO, I., ROMANO, G. & PALUMBO, A. 2014. Stress response to cadmium and manganese in *Paracentrotus lividus* developing embryos is mediated by nitric oxide. *Aquat. Toxicol.* 156, 125-134.
- MOHRI, T., SOKABE, M. & KYOZUKA, K. 2008. Nitric oxide (NO) increase at fertilization in sea urchin eggs upregulates fertilization envelope hardening. *Dev Biol*, 322, 251-62.
- MONCADA, S., PALMER, R. M. & HIGGS, E. A. 1991. Nitric oxide: physiology, pathophysiology, and pharmacology. *Pharmacol Rev*, 43, 109-42.
- MOROZ, L. L., MEECH, R. W., SWEEDLER, J. V. & MACKIE, G. O. 2004. Nitric oxide regulates swimming in the jellyfish *Aequorea victoria*. *J Comp Neurol*, 471, 26-36.
- MOSHAGE, H., KOK, B., HUIZENGA, J. R. & JANSEN, P. L. 1995. Nitrite and nitrate determinations in plasma: a critical evaluation. *Clin Chem*, 41, 892-6.
- NISHIDA, C. R. & ORTIZ DE MONTELLANO, P. R. 1999. Autoinhibition of endothelial nitric-oxide synthase. Identification of an electron transfer control element. *J Biol Chem*, 274, 14692-8.
- NOBREGA, M. A., OVCHARENKO, I., AFZAL, V. & RUBIN, E. M. 2003. Scanning human gene deserts for long-range enhancers. *Science* **302**, 413.
- NOHARA, M., NISHIDA, M., MIYA, M. & NISHIKAWA, T. 2005. Evolution of the mitochondrial genome in cephalochordata as inferred from complete nucleotide sequences from two epigonichthys species. *J Mol Evol*, 60, 526-37.
- OBERBÄUMER, I., MOSER, D. & BACHMANN, S. 1998. Nitric oxide synthase 1 mRNA: tissue-specific variants from rat with alternative first exons. *Biol Chem* **379**, 913-919.
- OHNO, S. 1970. Evolution by gene duplication. London: *George Allen & Unwin Ltd*. Berlin, *Heidelberg* and New York: *Springer-Verlag*.

- OLSSON, R. 1983. Club-shaped gland and endostyle in larval *Branchiostoma lanceolatum* (Cephalochordata). *Zoomorphology*, 103, 1-13.
- PALLAS, P. S. 1767. *Limax lanceolatus*: descriptio *Limacis lanceolaris*. *Spicilegia Zoologica*, quibus novae imprimis et obscurae animalium species iconibus, descriptionibus. 9-14.
- PALUMBO, A. 2005. Nitric oxide in marine invertebrates: a comparative perspective. *Comp Biochem Physiol A Mol Integr Physiol*, 142, 241-8.
- PARIS, M., ESCRIVA, H., SCHUBERT, M., BRUNET, F. D. R., BRTKO, J., CIESIELSKI, F., ROECKLIN, D., VIVAT-HANNAH, V. R., JAMIN, E. L., CRAVEDI, J.-P., 2008. Amphioxus postembryonic development reveals the homology of chordate metamorphosis. *Curr Biol.*, 18, 825-830.
- PARIS, M., HILLENWECK, A., BERTRAND, S. P., DELOUS, G., ESCRIVA, H., ZALKO, D., CRAVEDI, J.-P., LAUDET, V., 2010. Active metabolism of thyroid hormone during metamorphosis of amphioxus. *Integr Comp Biol.*, 50, 63-74.
- PASCUAL-ANAYA, J., ADACHI, N., ALVAREZ, S., KURATANI, S., D'ANIELLO, S. & GARCIA-FERNÁNDEZ, J. 2012. Broken colinearity of the amphioxus Hox cluster. *Evodevo*, 3, 28.
- PASCUAL-ANAYA, J., D'ANIELLO, S. & GARCIA-FERNÁNDEZ, J. 2008. Unexpectedly large number of conserved noncoding regions within the ancestral chordate Hox cluster. *Dev Genes Evol*, 218, 591-7.
- PASCUAL-ANAYA, J., D'ANIELLO, S., KURATANI, S. & GARCIA-FERNÁNDEZ, J. 2013. Evolution of Hox gene clusters in deuterostomes. *BMC Dev Biol*, 13, 26.
- PASINI, A., AMIEL, A., ROTHBÄCHER, U., ROURE, A., LEMAIRE, P., DARRAS, S. 2006. Formation of the ascidian epidermal sensory neurons: insights into the origin of the chordate peripheral nervous system. *PLoS Biol* 4, e225.
- PENNACCHIO, L. A., AHITUV N., MOSES A.M., PRABHAKAR S., NOBREGA M.A., SHOUKRY M., MINOVITSKY S., DUBCHAK I., HOLT A., LEWIS K.D., PLAJSER-FRICK I., AKIYAMA J., DE VAL S., AFZAL V., BLACK B.L., COURONNE O., EISEN M.B., VISEL A., RUBIN E.M. 2006. In vivo enhancer analysis of human conserved non-coding sequences. *Nature* 444, 499-502.

- PEUNOVA, N., SCHEINKER, V., RAVI, K. & ENIKOLOPOV, G. 2007. Nitric oxide coordinates cell proliferation and cell movements during early development of *Xenopus*. *Cell Cycle*, 6, 3132-44.
- POLYCHRONOPOULOS, D., KING, J. W. D., NASH, A. J., TAN, G. & LENHARD, B. 2017. Conserved non-coding elements: developmental gene regulation meets genome organization. *Nucleic Acids Res* **45**, 12611-12624.
- POLLOCK, V. P., MCGETTIGAN, J., CABRERO, P., MAUDLIN, I. M., DOW, J. A., DAVIES, S. A., 2004. Conservation of capa peptide-induced nitric oxide signalling in Diptera. *J Exp Biol.* 207, 4135-45.
- PRABHAKAR, S., POULIN, F., SHOUKRY, M., AFZAL, V., RUBIN, E.M., COURONNE, O., PENNACCHIO, L. A. 2006. Close sequence comparisons are sufficient to identify human cis-regulatory elements. *Genome Res* **16**, 855-863.
- PUTNAM, N. H., BUTTS, T., FERRIER, D. E., FURLONG, R. F., HELLSTEN, U., KAWASHIMA, T., ROBINSON-RECHAVI, M., SHOGUCHI, E., TERRY, A., YU, J. K., BENITO-GUTIÉRREZ, E. L., DUBCHAK, I., GARCIA-FERNÁNDEZ, J., GIBSON-BROWN, J. J., GRIGORIEV, I. V., HORTON, A. C., DE JONG, P. J., JURKA, J., KAPITONOV, V. V., KOHARA, Y., KUROKI, Y., LINDQUIST, E., LUCAS, S., OSOEGAWA, K., PENNACCHIO, L. A., SALAMOV, A. A., SATOU, Y., SAUKA-SPENGLER, T., SCHMUTZ, J., SHIN-I, T., TOYODA, A., BRONNER-FRASER, M., FUJIYAMA, A., HOLLAND, L. Z., HOLLAND, P. W., SATOH, N. & ROKHSAR, D. S. 2008. The amphioxus genome and the evolution of the chordate karyotype. *Nature*, 453, 1064-71.
- RIFE, T. K., XIE, J., REDMAN, C. & YOUNG, A. P. 2000. The 5'2 promoter of the neuronal nitric oxide synthase dual promoter complex mediates inducibility by nerve growth factor. *Brain Res Mol Brain Res* **75**, 225-236.
- ROBERTSON, J. D., BONAVENTURA, J., KOHM, A. & HISCAT, M. 1996. Nitric oxide is necessary for visual learning in *Octopus vulgaris*. *Proc Biol Sci*, 263, 1739-43.
- ROBINSON, L. J. & MICHEL, T. 1995. Mutagenesis of palmitoylation sites in endothelial nitric oxide synthase identifies a novel motif for dual acylation and subcellular targeting. *Proc Natl Acad Sci U S A*, 92, 11776-80.

- RONQUIST, F., TESLENKO, M., VAN DER MARK, P., AYRES, D. L., DARLING, A., HÖHNA, S., LARGET, B., LIU, L., SUCHARD, M. A. & HUELSENBECK, J. P. 2012. MrBayes 3.2: efficient Bayesian phylogenetic inference and model choice across a large model space. *Syst Biol*, 61, 539-42.
- RUPPERT E.E. 1997. Cephalochordata (Acrania). In: Harrison FW, Ruppert E.E., editors. *Microscopic anatomy of invertebrates*, 15. New York: *Wiley-Liss*, 349–504.
- RYAN, K., LU, Z. & MEINERTZHAGEN, I. A. 2016. The CNS connectome of a tadpole larva of. *Elife* 5.
- SALLEO, A., MUSCI, G., BARRA, P. & CALABRESE, L. 1996. The discharge mechanism of acontial nematocytes involves the release of nitric oxide. *J Exp Biol*, 199, 1261-7.
- SANDELIN, A., ALKEMA, W., ENGSTRÖM, P., WASSERMAN, W. W. & LENHARD, B. 2004. JASPAR: an open-access database for eukaryotic transcription factor binding profiles. *Nucleic Acids Res* 32, D91-94.
- SASAKI, M., GONZALEZ-ZULUETA M, HUANG H, HERRING WJ, AHN S, GINTY DD, DAWSON VL, DAWSON TM. 2000. Dynamic regulation of neuronal NO synthase transcription by calcium influx through a CREB family transcription factor-dependent mechanism. *Proc Natl Acad Sci U S A* 97, 8617-8622.
- SAUR, D., SEIDLER, B., PAEHGE, H., SCHUSDZIARRA, V. & ALLESCHER, H. D. 2002. Complex regulation of human neuronal nitric-oxide synthase exon 1c gene transcription. Essential role of Sp and ZNF family members of transcription factors. *J Biol Chem* 277, 25798-25814.
- SCHIPP, R. & GEBAUER, M. 1999. Nitric oxide: a vasodilatory mediator in the cephalic aorta of *Sepia officinalis* (L.) (Cephalopoda). *Invert Neurosci*, 4, 9-15
- SCHOPFER, F. J., BAKER, P. R. & FREEMAN, B. A. 2003. NO-dependent protein nitration: a cell signaling event or an oxidative inflammatory response? *Trends Biochem Sci*, 28, 646-54.
- SCHUBERT, M., ESCRIVA, H., XAVIER-NETO, J. & LAUDET, V. 2006. Amphioxus and tunicates as evolutionary model systems. *Trends Ecol Evol*, 21, 269-77.
- SCHWARTE, R. C. & GODFREY, E. W. 2004. Nitric oxide synthase activity is required for postsynaptic

differentiation of the embryonic neuromuscular junction. *Dev Biol*, 273, 276-84.

SCHWARTZ, S., ZHANG Z, FRAZER KA, SMIT A, RIEMER C, BOUCK J, GIBBS R, HARDISON R, MILLER W. 2000. PipMaker--a web server for aligning two genomic DNA sequences. *Genome Res* **10**, 577-586.

SHIMELD, S. M., PURKISS, A. G., DIRKS, R. P., BATEMAN, O. A., SLINGSBY, C. & LUBSEN, N. H. 2005. Urochordate betagamma-crystallin and the evolutionary origin of the vertebrate eye lens. *Curr Biol*, 15, 1684-9.

SIEPEL, A., BEJERANO G, PEDERSEN JS, HINRICHS AS, HOU M, ROSENBLOOM K, CLAWSON H, SPIETH J, HILLIER LW, RICHARDS S, WEINSTOCK GM, WILSON RK, GIBBS RA, KENT WJ, MILLER W, HAUSSLER D. 2005. Evolutionarily conserved elements in vertebrate, insect, worm, and yeast genomes. *Genome Res* **15**, 1034-1050.

SOUKUP, V., HORÁČEK, I. & CERNY, R. 2013. Development and evolution of the vertebrate primary mouth. *J Anat*, 222, 79-99.

SOUKUP, V., KOZMIK, Z. 2016. Zoology: A New Mouth for Amphioxus. *Curr Biol*, 26, R367-8.

SOUKUP, V., YONG, L. W., LU, T. M., HUANG, S. W., KOZMIK, Z. & YU, J. K. 2015. The Nodal signaling pathway controls left-right asymmetric development in amphioxus. *Evodevo*, 6, 5.

STAMLER, J. S., SINGEL, D. J. & LOSCALZO, J. 1992. Biochemistry of nitric oxide and its redox-activated forms. *Science*, 258, 1898-902.

STEFANO, G. B. & OTTAVIANI, E. 2002. The biochemical substrate of nitric oxide signaling is present in primitive non-cognitive organisms. *Brain Res*, 924, 82-9.

STEINERT, J. R., CHERNOVA, T. & FORSYTHE, I. D. 2010. Nitric oxide signaling in brain function, dysfunction, and dementia. *Neuroscientist*, 16, 435-52.

STOKES, M. D., HOLLAND, N. D. 1995. Embryos and larvae of a lancelet, *Branchiostoma floridae*, from hatching through metamorphosis: growth in the laboratory and external morphology. *Acta Zool.* 76, 105-120.

SUN, J., ZHANG, X., BRODERICK, M., FEIN, H. 2003. Measurement of nitric oxide production in


biological systems by using Griess reaction assay. *Sensors*, 3, 276-284.

- TAKAHASHI, T. & HOLLAND, P. W. 2004. Amphioxus and ascidian Dmbx homeobox genes give clues to the vertebrate origins of midbrain development. *Development*, 131, 3285-94.
- TAKATORI, N., BUTTS, T., CANDIANI, S., PESTARINO, M., FERRIER, D. E., SAIGA, H. & HOLLAND, P. W. 2008. Comprehensive survey and classification of homeobox genes in the genome of amphioxus, *Branchiostoma floridae*. *Dev Genes Evol*, 218, 579-90.
- TAQATQEH, F., MERGIA, E., NEITZ, A., EYSEL, U. T., KOESLING, D. & MITTMANN, T. 2009. More than a retrograde messenger: nitric oxide needs two cGMP pathways to induce hippocampal long-term potentiation. *J Neurosci*, 29, 9344-50.
- TEDESCHI, G., CAPPELLETTI, G., NONNIS, S., TAVERNA, F., NEGRI, A., RONCHI, C. & RONCHI, S. 2007. Tyrosine nitration is a novel post-translational modification occurring on the neural intermediate filament protein peripherin. *Neurochem Res*, 32, 433-41.
- TENG, Y., GIRARD, L., FERREIRA, H. B., STERNBERG, P. W. & EMMONS, S. W. 2004. Dissection of cis-regulatory elements in the *C. elegans* Hox gene *egl-5* promoter. *Dev Biol* **276**, 476-492.
- TENGAN, C. H., RODRIGUES, G. S., GODINHO, R. O. 2012. Nitric oxide in skeletal muscle: role on mitochondrial biogenesis and function. *Int J Mol Sci*, 13, 17160-84.
- THOMAS, S. & ROBITAILLE, R. 2001. Differential frequency-dependent regulation of transmitter release by endogenous nitric oxide at the amphibian neuromuscular synapse. *J Neurosci*, 21, 1087-95.
- TITHERADGE, M., HEMMENS, B., MAYER, B. 1998. Enzymology of Nitric Oxide Synthases. *Nitric Oxide Protocols*, 100. Humana Press, 1-32.
- TOMANKOVA, S., ABAFFY, P., SINDELKA, R. 2017. The role of nitric oxide during embryonic epidermis development of *Xenopus laevis*. *Biol Open*, 6, 862-871.
- VAZ, A. R., SILVA, S. L., BARATEIRO, A., FERNANDES, A., FALCÃO, A. S., BRITO, M. A. & BRITES, D. 2011. Pro-inflammatory cytokines intensify the activation of NO/NOS, JNK1/2 and caspase cascades in immature neurons exposed to elevated levels of unconjugated bilirubin. *Exp Neurol*, 229, 381-90.

- VIERRA, D. A. & IRVINE, S. Q. 2012. Optimized conditions for transgenesis of the ascidian *Ciona* using square wave electroporation. *Dev Genes Evol* **222**, 55-61.
- VIZI, E. S., FEKETE, A., KAROLY, R. & MIKE, A. 2010. Non-synaptic receptors and transporters involved in brain functions and targets of drug treatment. *Br J Pharmacol*, 160, 785-809.
- WADA, H., GARCIA-FERNÁNDEZ, J. & HOLLAND, P. W. 1999. Colinear and segmental expression of amphioxus Hox genes. *Dev Biol*, 213, 131-41.
- WANG Y., NEWTON D. C., ROBB G. B., KAU C. L., MILLER T. L., CHEUNG A. H., HALL A. V., VANDAMME S., WILCOX J. N. AND MARSDEN P. A. 1999. RNA diversity has profound effects on the translation of neuronal nitric oxide synthase. *Proc. Natl Acad. Sci.* 96, 12 150–12 155.
- WICHT, H., LACALLI, T. C. 2005. The nervous system of amphioxus: structure, development, and evolutionary significance. *Can J Zool.* 83, 122-150.
- WICKSTEAD, J. H. 1967. Branchiostoma lanceolatum larvae: some experiments on the effect of thiouracil on metamorphosis. *J. Mar. Biol. Assoc. U. K.*, 47, 49–59.
- WINCHELL, C. J., SULLIVAN, J., CAMERON, C. B., SWALLA, B. J. & MALLATT, J. 2002. Evaluating hypotheses of deuterostome phylogeny and chordate evolution with new LSU and SSU ribosomal DNA data. *Mol Biol Evol*, 19, 762-76.
- WINK, D. A., HINES, H. B., CHENG, R. Y., SWITZER, C. H., FLORES-SANTANA, W., VITEK, M. P., RIDNOUR, L. A. & COLTON, C. A. 2011. Nitric oxide and redox mechanisms in the immune response. *J Leukoc Biol*, 89, 873-91.
- WLLLCY, A., 1891. The later larval development of amphioxus. *Q J Microsc Sci.* 32, 183.
- WOOLFE, A., GOODSON M, GOODE DK, SNELL P, MCEWEN GK, VAVOURI T, SMITH SF, NORTH P, CALLAWAY H, KELLY K, WALTER K, ABNIZOVA I, GILKS W, EDWARDS YJ, COOKE JE, ELGAR G. 2005. Highly conserved non-coding sequences are associated with vertebrate development. *PLoS Biol* **3**, e7.
- XU, W., LIU, L. Z., LOIZIDOU, M., AHMED, M. & CHARLES, I. G. 2002. The role of nitric oxide in

- cancer. *Cell Res*, 12, 311-20.
- YAN, J., ZHANG, C., ZHANG, Y., LI, K., XU, L., GUO, L., KONG, Y. & FENG, L. 2013. Characterization and comparative analyses of two amphioxus intelectins involved in the innate immune response. *Fish Shellfish Immunol*, 34, 1139-46.
- YARRELL, W. 1836. A history of British fishes. London: *John Van Voorst*.
- YOON, Y., SONG, J., HONG, S. H. & KIM, J. Q. 2000. Plasma nitric oxide concentrations and nitric oxide synthase gene polymorphisms in coronary artery disease. *Clin Chem*, 46, 1626-30.
- YU, J. K. & HOLLAND, L. Z. 2009. Cephalochordates (amphioxus or lancelets): a model for understanding the evolution of chordate characters. *Cold Spring Harb Protoc*, 2009, pdb.emo130.
- YU, J. K., HOLLAND, L. Z., JAMRICH, M., BLITZ, I. L. & HOLLAN, N. D. 2002. AmphiFoxE4, an amphioxus winged helix/forkhead gene encoding a protein closely related to vertebrate thyroid transcription factor-2: expression during pharyngeal development. *Evol Dev*, 4, 9-15.
- YUE, J. X., YU, J. K., PUTNAM, N. H. & HOLLAND, L. Z. 2014. The transcriptome of an amphioxus, *Asymmetron lucayanum*, from the Bahamas: a window into chordate evolution. *Genome Biol Evol*, 6, 2681-96.
- ZHANG, S. C., HOLLAND, N. D. & HOLLAND, L. Z. 1997. Topographic changes in nascent and early mesoderm in amphioxus embryos studied by DiI labeling and by in situ hybridization for a Brachyury gene. *Dev Genes Evol*, 206, 532-535.
- ZHOU, L., ZHU, D. Y. 2009. Neuronal nitric oxide synthase: structure, subcellular localization, regulation, and clinical implications. *Nitric Oxide*, 20, 223-30.

SCIENTIFIC REPORTS



OPEN

Nitric Oxide regulates mouth development in amphioxus

Giovanni Annona¹, Filomena Caccavale¹, Juan Pascual-Anaya^{1,2}, Shigeru Kuratani², Pasquale De Luca³, Anna Palumbo¹ & Salvatore D'Aniello¹

The development of the mouth in animals has fascinated researchers for decades, and a recent study proposed the modern view of recurrent evolution of protostomy and deuterostomy. Here we expanded our knowledge about conserved traits of mouth formation in chordates, testing the hypothesis that nitric oxide (NO) is a potential regulator of this process. In the present work we show for the first time that NO is an essential cell signaling molecule for cephalochordate mouth formation, as previously shown for vertebrates, indicating its conserved ancestral role in chordates. The experimental decrease of NO during early amphioxus *Branchiostoma lanceolatum* development impaired the formation of the mouth and gill slits, demonstrating that it is a prerequisite in pharyngeal morphogenesis. Our results represent the first step in the understanding of NO physiology in non-vertebrate chordates, opening new evolutionary perspectives into the ancestral importance of NO homeostasis and acquisition of novel biological roles during evolution.

Nitric oxide (NO) is a small and highly diffusible signal molecule that is known to be involved in a wide range of important biological processes. Since its initial discovery as a modulator of vascular activities in mammals, NO has been found to participate in numerous physiological and developmental functions in a wide spectrum of organisms¹. Our understanding of NO signaling has profoundly changed over recent decades. It was originally considered solely as a toxic substance, but nowadays, although harmful at high concentration, NO is believed to be an essential signaling molecule for living organisms. The function of this ambivalent gas depends on the precise balance between its production and consumption. When produced at high levels, for example during inflammation, NO may interact with cellular components, such as DNA, RNA, lipids, and proteins, leading to mutations and altered cell physiology that may lead to carcinogenesis^{2–4}. On the other hand, NO deficiency can cause disorders of endocrine⁵, cardiovascular⁶, musculoskeletal⁷ and immune systems⁸.

The biosynthesis of NO is catalysed by the nitric oxide synthase enzymes (NOS), through two successive mono-oxygenation reactions, from L-Arginine to L-Citrulline with N ω -hydroxy-L-arginine (NOHLA) as an intermediate⁹. Mammalian genomes have three paralogous *Nos* genes with distinct expression patterns and specific functions^{10, 11}: *NosI* or neuronal *Nos* (*nNos*); *NosII* or macrophage inducible *Nos* (*iNos*), and *NosIII* or endothelial *Nos* (*eNos*). All *Nos* genes share a very similar gene structure, with highly conserved intron number, position and phases. At the protein level, they only differ in the presence of the protein-interaction domain (PDZ) in NOSI, which is absent in both NOSII and NOSIII, and in the absence of the inhibitory loop in the region of FMN-binding domain exclusively in NOSII^{12, 13}. Two of these genes, *NosI* and *NosIII*, are typically constitutively expressed, while *NosII* expression levels increase upon microbial infection, generating high and sustained amounts of NO¹⁴. Despite their given names indicating a tissue-specificity, all three *Nos* genes are, in fact, expressed in most tissues and organs. Therefore, we prefer to use the *NosI-II-III* nomenclature. In the central nervous system (CNS) the NO produced by NOSI is implicated in neurogenesis, synaptic plasticity, learning and memory¹⁵, while in the peripheral nervous system it is involved in the control of blood pressure, gut peristalsis and vasodilatation^{14, 16}. NO derived from NOSII, primarily from macrophages, is essential for the control of inflammatory processes induced by intracellular bacteria or parasites¹⁴. Lastly, NO produced by NOSIII, which is the best characterized of the NOS proteins, is a homeostatic regulator of numerous essential cardiovascular functions, such as vasodilatation, inhibition of platelet aggregation and adhesion to the vascular wall, as well as inhibition of vascular inflammation¹⁴.

¹Biology and Evolution of Marine Organisms, Stazione Zoologica Anton Dohrn di Napoli, Villa Comunale 1, 80121, Napoli, Italy. ²Evolutionary Morphology Laboratory, RIKEN, Minatojima-minami 2-2-3, 650-0047, Kobe, Hyogo, Japan. ³RIMAR, Stazione Zoologica Anton Dohrn di Napoli, Villa Comunale 1, 80121, Napoli, Italy. Correspondence and requests for materials should be addressed to S.D. (email: salvatore.daniello@szn.it)

Received: 6 April 2017

Accepted: 6 July 2017

Published online: 16 August 2017

Nos genes are found in all living organisms, including bacteria¹⁷ and plants^{18,19}. During evolution, an ancestral proto-*Nos* gene was duplicated independently in several metazoan lineages, with a remarkable conservation in amino acid sequence and functional domains. Among chordates, the urochordate *Ciona intestinalis* possesses a single *NosI*-like gene containing a PDZ domain, and NO is a critical endogenous regulator of metamorphosis, apoptosis and ERK signaling^{20–22}. As mentioned above, in tetrapod genomes, including mammals, three *Nos* paralogs have been identified^{23–25}, while bony fish possess a variable *Nos* gene repertoire^{23–25}.

Although the role of *Nos* genes is well established in urochordates and vertebrates (so-called olfactores), information available on cephalochordates (sister group of olfactores) is scattered in the literature. Presence of NOS was demonstrated prevalently in adult *Branchiostoma belcheri* tissues, mainly cerebral vesicle, muscle, endostyle and anus²⁶, as well as nerve cord, wheel organ, epithelial cells of gut and midgut diverticulum, gill blood vessels, endostyle and ovary²⁷. Later, NOS involvement in the immune system was demonstrated by Lin *et al.*²⁸. The only attempt to study NOS during amphioxus development showed that the protein is present in the developing intestine (midgut and hindgut) and in the club-shaped gland of *Branchiostoma floridae* larvae²⁹.

The foregoing studies were performed before the identification of the complete set of three *Nos* genes in the *B. floridae* genome: two *NosI*-like (*NosA* and *NosC*) and one *NosII*-like, so-called *NosB*²³. However, phylogenetic analyses showed that they are not one-to-one orthologs of the three vertebrate *Nos* genes, but they derived from an independent duplication in the cephalochordate lineage²³. A comprehensive study aimed at discovering the different biological roles of all *Nos* genes during amphioxus embryogenesis was still missing.

In the present study, we have identified the *Nos* gene repertoire of three cephalochordate species and analysed their evolutionary history in comparison with other chordates. In addition, we have analysed the expression profiles of *Nos* genes in the European amphioxus, *Branchiostoma lanceolatum*. Lastly, we have investigated the nitric oxide localization as well as its biological functions during embryonic development in *B. lanceolatum*. We have found that NO is involved in the formation of the amphioxus mouth, acting in a sharp temporal window at early embryonic stages.

Results

***Nos* genes have independently duplicated in the lancelet lineage.** Previous studies have highlighted the occurrence of several independent lineage-specific *Nos* gene duplications in metazoan evolution, including amphioxus *B. floridae*²³. In order to unravel whether the *Nos* expansion observed in *B. floridae* was present in other amphioxus species and to better define the *Nos* evolutionary history within the cephalochordates, we searched both genomic and transcriptomics databases for *Nos* genes in different cephalochordate species, from two different genera: *Branchiostoma* and *Asymmetron* (see Methods). We found three NOS paralogs in each of the analysed species: *B. belcheri*, *B. lanceolatum* and *Asymmetron lucayanum*. To confirm the orthologous relationships between cephalochordate *Nos* genes, we performed a phylogenetic analysis (Fig. 1). All *B. lanceolatum*, *B. belcheri* and *A. lucayanum* NOS proteins were closely related with high bootstrap values with the previously characterized *B. floridae* NOSA, NOSB and NOC proteins, suggesting that the duplication events that resulted in the three cephalochordate *Nos* genes occurred in the last common ancestor of extant amphioxus (Fig. 1).

Complementary *Nos* gene expression patterns during amphioxus development. To examine whether *Nos* genes have a role in amphioxus development we characterized the temporal and spatial expression pattern of the three *B. lanceolatum* *Nos* genes. Droplet digital PCR (ddPCR) experiments showed a temporal complementary expression between the *B. lanceolatum* *NosB* and *NosC* genes (Fig. 2h–h'). During early developmental stages, strong *NosB* gene expression was detected. Initially *NosB* is expressed at gastrula stage [10 hours post fertilization (hpf)], followed by a decrease in expression levels at neurula stage (24 hpf) (Fig. 2h). At later stages of development *NosB* seems to completely switch off (Fig. 2h). *NosC* expression starts at pre-mouth larval stage (48 hpf) with the highest level of expression occurring at 3 days post-fertilization (dpf) larva (72 hpf) (Fig. 2h'). *NosC* expression levels decrease at 5 dpf larva (120 hpf) (Fig. 2h'). We were not able to detect discernible levels of *NosA* during the embryonic and larval stages analysed, but we observed expression in adult specimens (Fig. 2h'').

Expression patterns in whole-mount *in situ* hybridization preparations, were mostly in agreement with the trend observed in the ddPCR experiments: *NosB* was the first to be detected and its expression was limited to a few developmental stages. *NosB* expression was detected at early- (Fig. 2b) and mid-gastrula stage (Fig. 2c,d) in the endoderm, however it was absent in the area surrounding the blastopore, in the ectoderm and the dorsal mesoderm (Fig. 2b–d). We did not find any specific *NosB* signals at later developmental stages in whole-mount *in situ* hybridization experiments. Afterwards, following *NosB* down-regulation, we detected *NosC* expression from the mid-neurula stage onwards, which was specifically restricted to a few cells in the anterior part of the neural plate, slightly posterior to the neural pore (Fig. 2e). At the pre-mouth larval stage, *NosC* transcripts were detected in the anterior half of the neural tube, from the rostral part to the pigment spot (Fig. 2f). In 3 dpf larvae, the expression in the neural tube disappeared almost completely, remaining only in a few cells located in the most ventral and posterior part of the cerebral vesicle (Fig. 2g). At this stage, we also detected *NosC* expression in the club-shaped gland, which is closely connected to the pharyngeal area (Fig. 2g). The low levels of *NosA* expression revealed by ddPCR experiments were confirmed by the lack of any *in situ* hybridization signal in the developmental stages examined.

Inhibition of the NO signaling prevents the formation of amphioxus mouth and gill slits.

Amphioxus *Nos* genes are expressed in different tissues during development. We assumed therefore that NO signaling could have an important role during embryogenesis of some, if not all, of those tissues. First, we measured endogenous NO levels during *B. lanceolatum* development by monitoring nitrite formation (Griess assay) to finely detect the exact localization of NO, independently of *Nos* transcript expression. From early to late development, we first observed a concentration of 6 nmol nitrite/mg protein at gastrula (10 hpf), followed by a decrease at

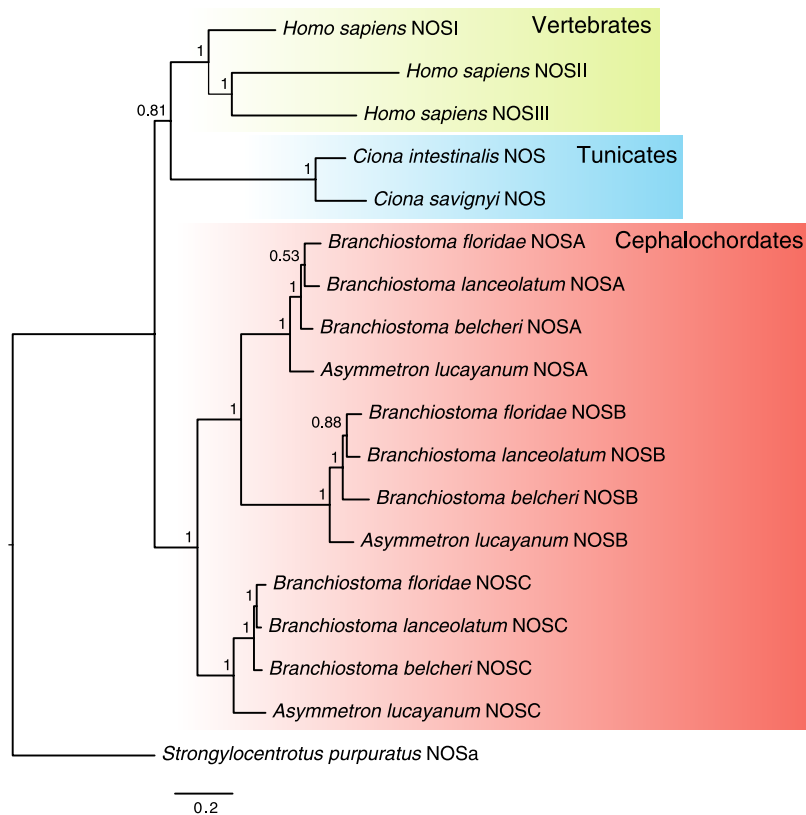


Figure 1. Phylogenetic analyses of NOS proteins in chordates. Bayesian inference-based phylogenetic tree of chordate NOS proteins. Numbers on nodes represent posterior probabilities values. The red box includes cephalochordate proteins, including 3 closely related species of *Branchiostoma* (*B. lanceolatum*, *B. floridae* and *B. belcheri*), plus *Asymmetron lucayanum*. The blue box contains two ascidian species, *Ciona intestinalis* and *Ciona savignyi*. Vertebrate NOS, represented here by *Homo sapiens*, are highlighted by the yellow box. The NOS protein of the sea urchin *Strongylocentrotus purpuratus* (Ambulacraria) was used as an outgroup.

neurula stage (24 hpf) and pre-mouth larvae (48 hpf), with 5 and 4.7 nmol nitrite/mg protein, respectively. At 72 hpf NO levels increased to 23.5 nmol nitrite/mg protein, decreasing again to average levels of 4.6 nmol nitrite/mg protein in adults (Fig. 3a). Next, using DAF-FM-DA, we detected where NO was localized in 48 and 72 hpf larvae. At 48 hpf larva, NO positive cells were abundant along all the neural tube (arrows in Fig. 3b) and in the most caudal extremity of the larvae, probably the future anal region (tandem arrows in Fig. 3b). Additionally, a strong NO fluorescent signal was observed in the corresponding area of the future mouth and gill slits (arrowhead in Fig. 3b). At 72 hpf, we observed a higher density of NO positive cells around the mouth, in the ventral part of the first gill slit and in the club-shaped gland (arrowheads in Fig. 3c). Later a punctate signal is still present in the rostral area as well as caudally in both the hindgut and anus (arrow and tandem arrows, respectively). In order to exclude the previously described endogenous GFP fluorescence in amphioxus^{30,31}, we checked green fluorescence emission in untreated *B. lanceolatum* larvae (negative control), showing a negligible non-specific signal at the same laser intensity as used for DAF-FM-DA experiments (Suppl. Fig. S1).

We next investigated the role of NO during development, and thus the ontogenetic importance of NOS proteins. We experimentally reduced the endogenous NOS-produced NO with treatments using two different NOS inhibitors: N ω -Nitro-L-arginine methyl ester (L-NAME) and 1-(α,α,α -trifluoro-*o*-tolyl)-Imidazole (TRIM) at different temporal windows^{22,32,33} (see Methods; Suppl. Fig. S2 and Fig. 4). Treatments with a concentration of 100 μ M of L-NAME resulted in normal larvae in each of the experimental times assayed, indistinguishable from wild type control treatments (Fig. 4d). Experiments with 1 mM L-NAME added at neurula stage (24 hpf) and maintained to 3 dpf larva stage resulted in larvae in which the mouth and gill slits did not form, without affecting the other morphological features (Fig. 4a). In the experiments performed in other temporal windows, the L-NAME treatment did not induce any body malformations, except when present throughout development from gastrula to larva, giving rise to an abnormal body plan (Suppl. Fig. S2). Increasing the L-NAME concentration to 10 mM produced larvae with an abnormal body plan, presumably due to the toxicity of high drug concentrations rather than a specific effect. As a control for L-NAME treatments we used D-NAME, the inactive D- form enantiomer, at the same experimental conditions. D-NAME did not affect amphioxus development (Fig. 4b).

To understand whether the observed alteration of the buccal area was due to the toxicity of the L-NAME or to a specific inhibition effect on NOS activity, we performed a second independent series of *in vivo* treatments using a different NOS inhibitor (TRIM). Treatments with 50, 75 and 100 μ M TRIM from neurula stage until day 3 of development causes alterations mainly in the mouth and gill slits area of the amphioxus larvae (Fig. 4c, compare

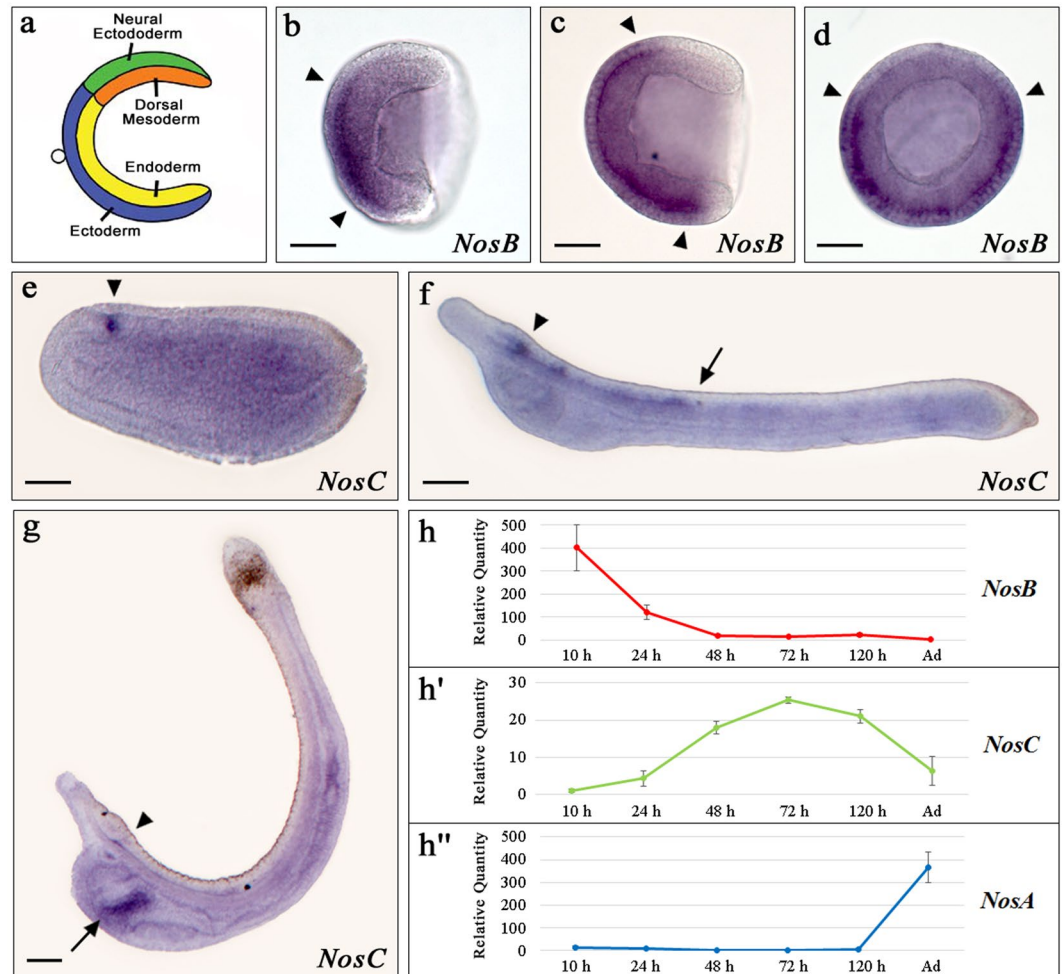


Figure 2. *Nos* genes expression patterns during *Branchiostoma lanceolatum* embryonic development. (a) Scheme of gastrula territory organization; (b) *NosB* expression at early gastrula stage, lateral view, (c) mid-gastrula stage, lateral view and (d) blastopore view [arrowheads indicate the limits of the positive signal]. (e) *NosC* gene expression at mid-neurula stage in neuropore (arrowhead); (f) at pre-mouth larva in brain vesicle (arrowhead) and in neural tube (posterior limit, arrow); (g) at larva 3 dpf in the brain vesicle (arrowhead) and club-shaped gland (arrow). In (h-h'') the ddPCR results of the three *Nos* genes in embryonic development are represented; P-value <0,05. Embryos orientation: anterior to the left (except 2d), dorsal to the top. Scale bars: 50 μ m.

with Fig. 4a). There was a significant increase in the proportion of larvae with severe phenotype (no mouth opening) in a dose dependent manner (50 to 100 μ M) (Fig. 4h). To better characterize the head malformation, we treated larvae with 100 μ M TRIM and then examined by scanning electron microscopy (SEM). While the general animal morphology was unaffected, mouth and gill slits structures were malformed. We classified this phenotype according to its severity, as either mild (reduction of the mouth opening, Fig. 4f) or severe (absence of the mouth opening, Fig. 4g). We further investigated if these morphological alterations positively correlated with a decreased intracellular NOS-produced NO. NO localization detection by DAF-FM-DA in TRIM treated embryos showed that the mouth absence was associated with the disappearance of NO fluorescent signal (arrowheads in Fig. 4k), which in contrast is present in the untreated animals (arrowheads in Fig. 4j).

Discussion

NO has probably played a crucial role in the early history of life on Earth providing protection to primitive microorganisms, neutralizing the aggressive oxidative effect of rising ozone levels in the atmosphere. NO does not require carrier molecules to cross cell membranes, and can easily reach intracellular targets by diffusion even over large body distances. During animal evolution, NO has acquired several novel functions beyond the mere enhancement of survival³⁴. With this in mind, we tried to gain insight into the evolutionary history of *Nos* genes in chordates, particularly studying in detail both the *Nos* genes repertoire and putative functions of NO in the cephalochordate amphioxus *B. lanceolatum*. Although we previously studied amphioxus *Nos* gene relationships with other metazoan *Nos* genes²³, their evolution within the cephalochordate clade was still unclear. We have confirmed the presence of three *Nos* genes, *NosA*, -*B* and -*C*, in other *Branchiostoma* species, *B. lanceolatum* and

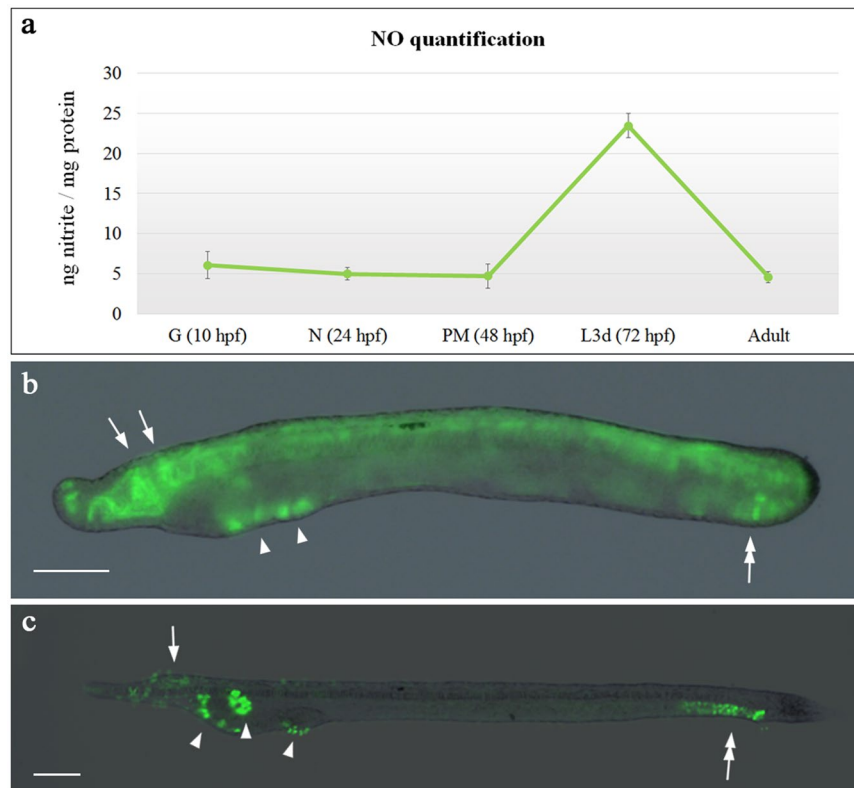


Figure 3. Nitrite quantification and nitric oxide detection in amphioxus embryos. The graph (a) shows the nitrite quantification during embryonic development and in adult obtained by Griess assay, the results are expressed as nmol of nitrite/mg of proteins. Nitric oxide localization by DAF-FM-DA at (b) 48 hpf and (c) 72 hpf. Arrows indicate nervous system; arrowheads show pharyngeal area, mouth and gill slits; tandem arrows indicate hindgut. Embryos orientation: anterior to the left, dorsal to the top. Scale bars: 50 μ m.

B. belcheri, as well as in an *Asymmetron* species, *A. lucayanum*. *Branchiostoma* and *Asymmetron* represent lineages diverged directly from the last common ancestor of extant cephalochordates³⁵, and therefore comparisons between them are informative to determine the condition of the latter (Fig. 1). Our phylogenetic analysis clearly shows that both *Branchiostoma* and *Asymmetron* *Nos* paralogs are one-to-one orthologous *Nos* genes, suggesting that the duplication events that originated cephalochordate *NosA*, *-B* and *-C* paralogous genes, happened in their last common ancestor (Fig. 1).

While we did not detect *NosA* expression, we found a complementary expression of *NosB* and *NosC* (Fig. 2h–h'). *NosB* was highly expressed during gastrulation (Fig. 2b–d). Interestingly, NO is thought to be involved in cell division and cell motility during gastrulation in *Drosophila* and *Xenopus*^{36, 37}. Therefore, it is tempting to hypothesize that also in amphioxus NOSB may exert important roles during gastrulation. NO levels in whole embryos were in general concordant with *Nos* expression levels, suggesting that NOS likely exert their roles by means of NO production and, importantly, in a regulated fashion during amphioxus development. *NosC* expression starts at the neurula stage in a few cells in the most anterior part of the neural plate (Fig. 2e), then expands from this most anterior region to the pigmented spot at pre-mouth larvae (Fig. 2f) and later gets restricted to a few cells of the cerebral vesicle and to the club-shaped gland at 3 dpf larvae (Fig. 2g). Although direct comparison between *Nos* expression patterns in nervous systems between vertebrates and cephalochordates is difficult³⁸, it seems that a similarity exists between zebrafish *NosI* gene (expressed at 24 hpf in differentiating neurons and then in the major areas of the brain) and amphioxus *NosC* gene expression^{39, 40}. Moreover, our NO localization experiments showed that NO partially coincides with the expression patterns of *NosC* gene at pre-mouth larvae, like in the cerebral vesicle and neural tube. Altogether, these results suggest a putative involvement of *NosC* in amphioxus CNS function, although further experiments are needed to find out what this function might be.

Besides the expression in the CNS, we observed a peak of *NosC* transcript levels (Fig. 2h') that was mainly localized, together with significant amounts of NO, in the pharyngeal area in 3-dpf larvae (compare Figs 2g and 3c). This stage represents a pre-metamorphic developmental phase possessing an already formed neural tube, functional muscles and an open mouth on the left side of the body, in addition to other embryonic transitory organs: endostyle, pre-oral pit and club-shaped gland. Interestingly, the presence of an intensively innervated portion of the pharynx in pre- and post-metamorphic larvae has been demonstrated, indicating that the club-shaped gland, the pre-oral pit and the endostyle are probably involved in important morphological processes in amphioxus

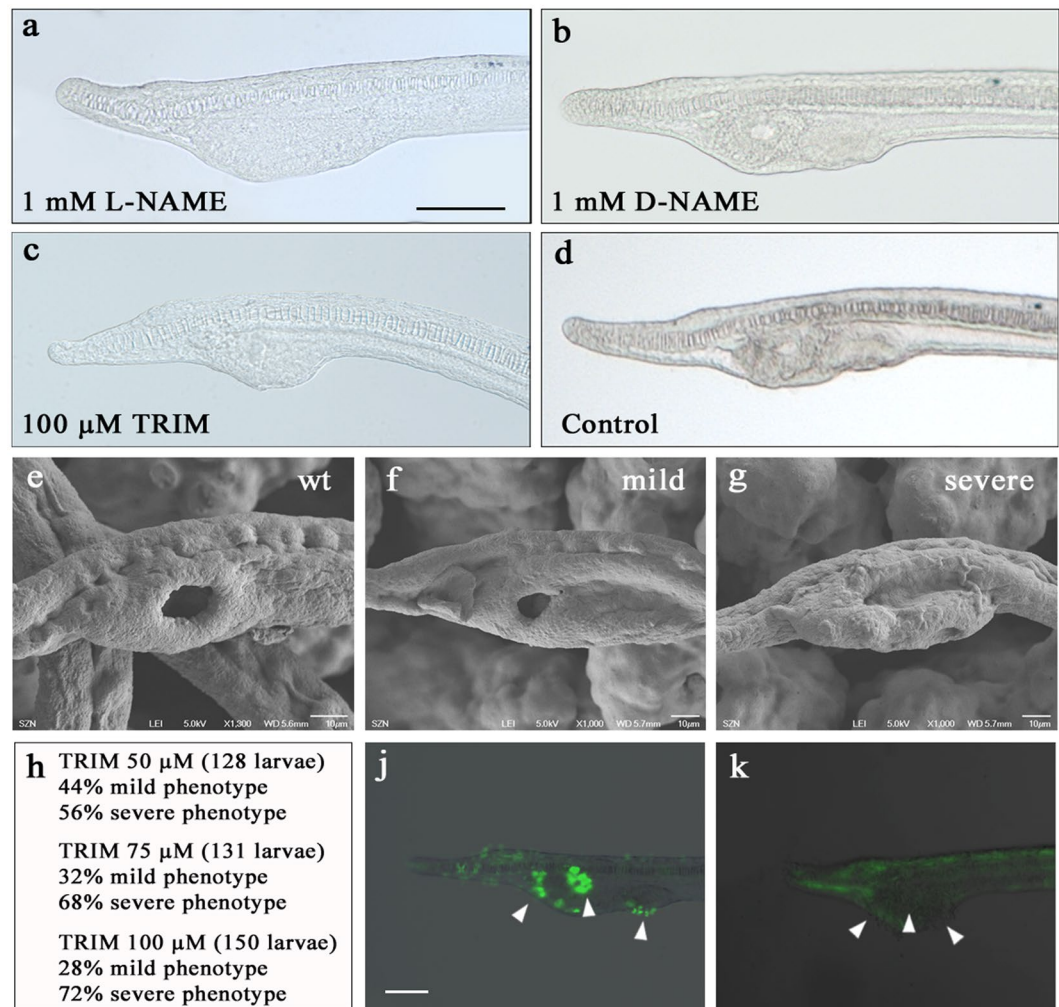


Figure 4. Drug treatments of amphioxus embryos. Amphioxus embryos were treated with L-NAME, D-NAME and TRIM, then the phenotype of 72 hpf larvae was observed. 1 mM L-NAME induces malformations in the mouth and gill slits area (a), not observed in the case of 1 mM of the D- enantiomer (D-NAME) (b). 100 μM TRIM-treated larvae show a phenotype similar to that observed with L-NAME (c). Control untreated larva kept in FSW (d). Next, 100 μM TRIM-treated larvae were observed by SEM. Control larvae in DMSO/FSW (e). TRIM-treated larvae with mild and severe phenotype (f–g). Percentages of larvae with mild and severe phenotypes at increasing drug concentrations, and the respective number of larvae observed (h). NO detection by DAF-FM-DA in untreated larvae mouth and gill slits are shown by arrowheads in (j). The absence of NO in mouth and gill slits of TRIM-treated larvae is indicated by arrowheads (k–j). Scale bars: 50 μm in (a–d) and (k–j).

mouth opening and rostral metamorphosis⁴¹. Here we showed *NosC* expression in the club-shaped gland, therefore we assume a possible involvement of this organ in the morphogenesis of pharyngeal structures.

NO is the final product of the Kinin-Kallikrein pathway, which in adult vertebrates usually participates in inflammation processes, as well as in the regulation of blood pressure. Recently, this pathway has been proposed to be active in the so-called “extreme anterior domain” of *Xenopus* and zebrafish embryos and to be essential for craniofacial development⁴². *Nosl*-morphants and TRIM treated frog embryos at neurula stage developed abnormal cranio-facial structures with a complete absence of the mouth⁴². Addition of a NO donor led to a complete rescue of the facial development, demonstrating that NO is necessary for mouth development in vertebrates⁴². Decreasing endogenous NO levels in amphioxus upon NOS inhibition, similarly to vertebrates, has led to the development of amphioxus larvae with a compromised pharyngeal structure, showing severely reduced or absent mouth and gill slits (Fig. 4). Interestingly, this developmental abnormality was observed only when the NO depletion was carried out during a sharp temporal window. The capability of the embryo to recover the correct morphology after the removal of the drug at 36 hpf (that is after 12 hours of treatment) allowed us to demonstrate the precise time interval in which NO is likely to have a role in mouth and pharynx formation: between 36 and 48 hpf. This suggests that also in amphioxus the embryonic origin of the prospective chordate primary mouth is under direct NO control during the neurula stage. Because of its characteristics, the amphioxus mouth still represents a longstanding enigma with regards to its evolutionary origin, homology relationships and differences with other chordate mouths. Recently, Nodal signaling in amphioxus has been shown to control left-right asymmetric

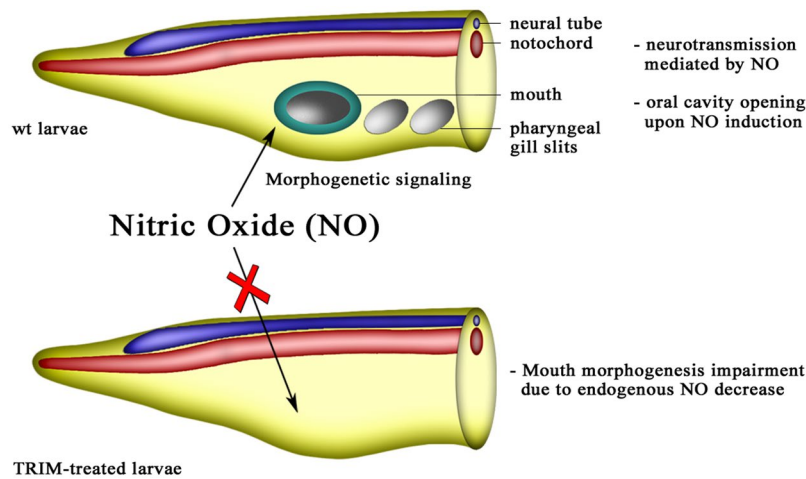


Figure 5. Nitric Oxide role during amphioxus larval development. Schematic representation of the rostral part of amphioxus larvae indicates possible involvement of NO in mouth development. The conspicuous depletion of endogenous NO by NOS inhibition (TRIM-treated larvae) leads to an abnormal phenotype without a mouth.

development, in which the mouth is a prominent feature⁴³. An independent study proposed that a mesodermal vesicle becomes intimately juxtaposed to the nascent mouth at the early larval stage under the control of several genes belonging to the Nodal-Pitx signaling pathway⁴⁴.

In conclusion, the results of the present study showed for the first time the crucial role of NO as an endogenous regulator of mouth formation in amphioxus (Fig. 5). The balance of NO levels in the pharynx-surrounding area is likely to be a prerequisite for the correct morphogenesis of the mouth. Future studies are needed to investigate if there is any relationship between NO and Nodal-Pitx pathway in amphioxus mouth morphogenesis, and to clarify whether the Kinin-Kallikrein signaling, discovered in vertebrates, is conserved in amphioxus.

Methods

Ethics Statement. Adult amphioxus specimens (*B. lanceolatum*) were collected from an endemic population of the Gulf of Naples (Italy), according to the authorization of Marina Mercantile (D. Lgs. 09/01/2012, n.4). All procedures were in compliance with current available regulations for the experimental use of live animals in Italy.

Animal care and embryo collection. Animals were kept in an open circulating system reproducing natural thermal and light conditions, development of the gonads was periodically monitored. Ripe males and females were induced to spawn and the embryos were cultured at 18 °C as described in literature⁴⁵. Embryos used for total RNA extraction were collected and fixed in EUROzol (Euroclone) and stored at –80 °C until used. For *in situ* hybridization experiments embryos were transferred into 4% paraformaldehyde (PFA) in MOPS/EGTA solution (0.1 M MOPS pH 7.5; 2 mM MgSO₄; 1 mM EGTA; 0.5 M NaCl in DEPC-H₂O) and dehydrated in ice-cold 70% EtOH in DEPC water and kept at –20 °C until used.

Identification of lancelet *Nos* genes and phylogenetic analysis. *B. lanceolatum* *Nos* genes were annotated in the genome draft version BL71nemr, kindly provided by the “*Branchiostoma lanceolatum* genome consortium”. *B. lanceolatum* *Nos* gene sequences are available in the Suppl. Fig. S3. *B. belcheri* *Nos* genes were identified from the automated predictions of NCBI (corresponding accession numbers in Suppl. Table S4). To find *A. lucayanum* *Nos* genes we screened a previously published transcriptome assembly^{46, 47} (DDBJ/EMBL/NCBI accession numbers GESY00000000 and GETC00000000). Accession numbers of *A. lucayanum* transcripts corresponding to each *Nos* paralog are available in Suppl. Table S4. Briefly, we performed TBLASTN searches using amino acid sequences of the three NOSA, NOSB and NOSC proteins from *B. floridae*, and candidate scaffolds, contigs or transcripts were further analysed by means of GeneWise2 as implemented in the EBI website^{48, 49} and manual curation. Other NOS proteins included in the phylogenetic analysis were collected from public databases such as Ensembl and NCBI (see Suppl. Table S4 for accession numbers).

For the phylogenetic analysis, NOS amino acid sequences were aligned using the MUSCLE algorithm⁵⁰ as implemented in MEGA v7, release 7161111-i386⁵¹ with default parameters, and saved in FASTA format. The alignment was trimmed by trimAl version 1.2rev59⁵², using the ‘-automated1’ parameter. The trimmed alignment was then formatted into a nexus file using readAl⁵⁰ (bundled with the trimAl package) (Suppl. File S5). A Bayesian inference tree was inferred using MrBayes 3.2.6⁵³, under the assumption of an LG + I + G evolutionary model. Two independent MrBayes runs of 1,000,000 generations, with 4 chains each, were performed. The tree was considered to have reached convergence when the standard deviation was stabilized under a value of <0.01. A burn-in of the 25% of the trees was performed to generate the consensus tree (750,000 post-burn trees).

Cloning and riboprobes preparation. Total RNA, from *B. lanceolatum* adult tissues (for *NosA*) or embryos (for *NosB* and *NosC*), was extracted using EUROzol (EuroClone) reagent and chloroform, and precipitated from

the aqueous phase with isopropyl alcohol. cDNA was synthesized from 0.5–1 µg of total RNA using the SMART PCR cDNA Synthesis Kit (Clontech). Different fragments corresponding to the three *B. lanceolatum* *Nos* genes were amplified using specific primers, designed in order to avoid cross-hybridization among the three paralogous genes (Suppl. Table S6), and cloned into the pGEM-T Easy Vector (Promega). Antisense Digoxigenin-UTP riboprobes were synthesized using the SP6 or T7 RNA polymerases and the (DIG) RNA Labeling Kit (Roche).

Droplet digital polymerase chain reaction (ddPCR). Expression profiles of *B. lanceolatum* *Nos* genes were analysed by Droplet digital PCR (ddPCR) in biological triplicates. Total RNA was extracted from embryos at different developmental stages: gastrula (10 hpf), middle neurula (24 hpf), pre-mouth larva (48 hpf), 3 dpf and 5 dpf larvae. Approximately 500 ng of total RNA extracted from each time point was reverse transcribed to cDNA using Super Script Vilo kit (Invitrogen). cDNA (approx. 3 ng) was mixed with 10 µl of 2X ddPCR Evagreen Supermix, 0.5 pM of each primer and nuclease-free water to a total reaction volume of 20 µl, then loaded into a sample well of a DG8 Cartridge for the QX200/QX100 droplet generator, according to the QX200/QX100 Droplet Generator Instruction Manual. Thermal cycling was then performed on the droplets using the C1000 Touch Thermal Cycler with 96-deep well reaction module according to the following protocol: enzyme activation at 95 °C for 10 min (1 cycle), denaturation at 94 °C for 30 sec followed by annealing/extension at 60 °C for 30 sec (40 cycles), enzyme deactivation at 98 °C for 10 min (1 cycle) followed by hold at 4 °C. All reagents and equipment used for ddPCR were from Bio-Rad Laboratories. The absolute gene expression level per well for the probes and reference genes were quantified using QuantaSoft software. The gene expression values for each sample were normalized to the housekeeping gene *Ribosomal protein L32 (RPL32)*⁵⁴ and reported as relative quantity compared to the lowest expression level of each *Nos* gene, respectively. The results for the three *Nos* genes at each developmental stage were subjected to Student t-test; a *P*-value of less than 0.05 was considered significant.

Whole-mount *in situ* hybridization. For whole-mount *in situ* hybridization, embryos were re-hydrated in 1X PBT, treated with proteinase K (5 µg/ml) to facilitate riboprobe penetration; the reaction was stopped by adding 4 µl of 10% glycine and then washed with 2 mg/ml glycine in a phosphate buffered saline solution containing 0.1% Tween-20 (PBT). The embryos were re-fixed in PBT containing 4% PFA for 1 h at RT, subsequently washed in 0.1 M triethanolamine and then with 0.1 M triethanolamine plus acetic anhydride, to prevent non-specific background staining. Embryos were washed with PBT several times, pre-hybridized at 60 °C for 1 h and finally hybridized by shaking at 65 °C overnight, in DEPC-H₂O hybridization buffer (50% deionized formamide; 100 µg/ml Heparin; 5X SSC; 0.1% Tween-20; 5 mM EDTA; Denhardt's 1 mg/ml; yeast RNA 1 mg/ml). The day after post-hybridization, washes were performed in decreasing concentrations from 5X to 2X of SSC 50% formamide/dH₂O at hybridization temperature and then at room temperature in decreasing concentrations of SSC, from 2X to 0.2X in dH₂O. An RNase step at 37 °C was included. Embryos were incubated overnight in primary antibody (anti-DIG AP, Roche), pre-adsorbed at 1:3000, with rocking at 4 °C. The signal was revealed at room temperature using BM-Purple substrate (Roche). Afterwards embryos were washed several times in PBT, postfixed in 4% PFA for 20 min, mounted in 80% glycerol in PBS, and photographed under Axio Imager 2 (Zeiss).

NO measurement assay (Griess). The endogenous NO concentration was measured indirectly from the nitrite content using the Griess reagent, according to Green and collaborators⁵⁵. Adult specimens and embryos at different developmental stages were homogenized in PBS and centrifuged at 20000 g for 30 min at 4 °C. Total protein concentration was determined by the Bradford assay using a Bio-Rad Protein Assay Reagent (Bio-Rad), bovine serum albumin was used as a standard. The supernatant of each sample was then analysed for nitrite content using a spectrophotometer ($\lambda = 540$) and reported as nmol of nitrite per mg of protein. The experiment was performed on biological triplicates for each sample.

***In vivo* NO modulation assays with L-NAME and TRIM.** We decreased the NO production during amphioxus development using two types of drugs that alter the NOS activity: an analog of arginine, N ω -Nitro-L-arginine methyl ester hydrochloride (L-NAME, Sigma Aldrich, stock solution in filtered sea water, FSW) and 1-(α,α,α -trifluoro-*o*-tolyl)-Imidazole (TRIM, Cayman Chemical, stock solution in DMSO) which interferes with binding of both L-arginine and tetrahydrobiopterin to their respective sites on the NOS enzymes. Untreated control larvae were raised in FSW. Additional controls included: inactive enantiomer N ω -Nitro-D-arginine methyl ester hydrochloride (D-NAME, Sigma Aldrich) for L-NAME, and DMSO for TRIM. The treatments were started and blocked at different developmental stages and the phenotype was always observed at 3 dpf larvae (Suppl. Fig. S2). All the experiments shown in Suppl. Fig. S2 were performed with 100 µM, 1 mM and 10 mM L-NAME at 18 °C as pilot experiments. We repeated the *in vivo* experiments adding the TRIM at the neurula stage, which proved to be the most sensitive stage to drug treatment. Therefore, 24 hpf embryos (neurula stage) were treated with 50, 75 and 100 µM TRIM for the time periods indicated in Suppl. Fig. S2. Larvae at 72 hpf were fixed in 4% PFA, dehydrated and stored in 70% ethanol, and the morphology was initially analysed using a stereoscope and then, for image acquisition, using a Zeiss EVO MA LS Scanning Electron Microscope.

***In vivo* NO localization assay.** NO localization was performed using 4-amino-5-methylamino-2',7'-difluorofluorescein diacetate (DAF-FM-DA), the most sensitive cell permeable and non-fluorescent reagent that combines with NO forming benzotriazole, a fluorescent compound⁵⁶. Embryos at different developmental stages were incubated for 20 min in the dark with 5 µM DAF-FM-DA in FSW. After treatment the animals were washed and incubated in FSW for 30 min and quickly fixed in 4% PFA. The fluorescence was visualised with ZEISS Axio Imager Z1 fluorescence microscope equipped with a $\lambda_{EXC} = 470 \pm 40$, $\lambda_{EM} = 525 \pm 50$ filter.

References

- Moncada, S. & Higgs, E. A. The discovery of nitric oxide and its role in vascular biology. *Br J Pharmacol* **147**(Suppl 1), S193–201, doi:10.1038/sj.bjp.0706458 (2006).
- Dedon, P. C. & Tannenbaum, S. R. Reactive nitrogen species in the chemical biology of inflammation. *Arch Biochem Biophys* **423**, 12–22 (2004).
- Li, C. Q. & Wogan, G. N. Nitric oxide as a modulator of apoptosis. *Cancer Lett* **226**, 1–15, doi:10.1016/j.canlet.2004.10.021 (2005).
- Calabrese, V. *et al.* Nitric oxide in the central nervous system: neuroprotection versus neurotoxicity. *Nat Rev Neurosci* **8**, 766–775, doi:10.1038/nrn2214 (2007).
- Vargas, F., Moreno, J. M., Wangenstein, R., Rodríguez-Gómez, I. & García-Están, J. The endocrine system in chronic nitric oxide deficiency. *Eur J Endocrinol* **156**, 1–12, doi:10.1530/eje.1.02314 (2007).
- Liu, V. W. & Huang, P. L. Cardiovascular roles of nitric oxide: a review of insights from nitric oxide synthase gene disrupted mice. *Cardiovasc Res* **77**, 19–29, doi:10.1016/j.cardiores.2007.06.024 (2008).
- Tidball, J. G. & Wehling-Henricks, M. Nitric oxide synthase deficiency and the pathophysiology of muscular dystrophy. *J Physiol* **592**, 4627–4638, doi:10.1113/jphysiol.2014.274878 (2014).
- Karpuzoglu, E. & Ahmed, S. A. Estrogen regulation of nitric oxide and inducible nitric oxide synthase (iNOS) in immune cells: implications for immunity, autoimmune diseases, and apoptosis. *Nitric Oxide* **15**, 177–186, doi:10.1016/j.niox.2006.03.009 (2006).
- Bryan, N. S., Bian, K. & Murad, F. Discovery of the nitric oxide signaling pathway and targets for drug development. *Front Biosci (Landmark Ed)* **14**, 1–18 (2009).
- Griffith, O. W. & Stuehr, D. J. Nitric oxide synthases: properties and catalytic mechanism. *Annu Rev Physiol* **57**, 707–736, doi:10.1146/annurev.ph.57.030195.003423 (1995).
- Alderton, W. K., Cooper, C. E. & Knowles, R. G. Nitric oxide synthases: structure, function and inhibition. *Biochem J* **357**, 593–615 (2001).
- Salerno, J. C. *et al.* An autoinhibitory control element defines calcium-regulated isoforms of nitric oxide synthase. *J Biol Chem* **272**, 29769–29777 (1997).
- Daff, S., Sagami, I. & Shimizu, T. The 42-amino acid insert in the FMN domain of neuronal nitric-oxide synthase exerts control over Ca(2+)/calmodulin-dependent electron transfer. *J Biol Chem* **274**, 30589–30595 (1999).
- Förstermann, U. & Sessa, W. C. Nitric oxide synthases: regulation and function. *Eur Heart J* **33**, 829–837, 837a–837d, doi:10.1093/eurheartj/ehr304 (2012).
- Zhou, L. & Zhu, D. Y. Neuronal nitric oxide synthase: structure, subcellular localization, regulation, and clinical implications. *Nitric Oxide* **20**, 223–230, doi:10.1016/j.niox.2009.03.001 (2009).
- Förstermann, U. *et al.* Nitric oxide synthase isozymes. Characterization, purification, molecular cloning, and functions. *Hypertension* **23**, 1121–1131 (1994).
- Crane, B. R., Sudhamsu, J. & Patel, B. A. Bacterial nitric oxide synthases. *Annu Rev Biochem* **79**, 445–470, doi:10.1146/annurev-biochem-062608-103436 (2010).
- Crawford, N. M. Mechanisms for nitric oxide synthesis in plants. *J Exp Bot* **57**, 471–478, doi:10.1093/jxb/erj050 (2006).
- Kumar, A., Castellano, I., Patti, F. P., Palumbo, A. & Buia, M. C. Nitric oxide in marine photosynthetic organisms. *Nitric Oxide* **47**, 34–39, doi:10.1016/j.niox.2015.03.001 (2015).
- Comes, S. *et al.* Regulatory roles of nitric oxide during larval development and metamorphosis in *Ciona intestinalis*. *Dev Biol* **306**, 772–784, doi:10.1016/j.ydbio.2007.04.016 (2007).
- Ercolesi, E. *et al.* Protein nitration as footprint of oxidative stress-related nitric oxide signaling pathways in developing *Ciona intestinalis*. *Nitric Oxide* **27**, 18–24, doi:10.1016/j.niox.2012.03.012 (2012).
- Castellano, I., Ercolesi, E. & Palumbo, A. Nitric oxide affects ERK signaling through down-regulation of MAP kinase phosphatase levels during larval development of the ascidian *Ciona intestinalis*. *PLoS One* **9**, e102907, doi:10.1371/journal.pone.0102907 (2014).
- Andreakis, N. *et al.* Evolution of the nitric oxide synthase family in metazoans. *Mol Biol Evol* **28**, 163–179, doi:10.1093/molbev/msq179 (2011).
- González-Domenech, C. M. & Muñoz-Chápuli, R. Molecular evolution of nitric oxide synthases in metazoans. *Comp Biochem Physiol Part D Genomics Proteomics* **5**, 295–301, doi:10.1016/j.cbd.2010.08.004 (2010).
- Martínez-Ruiz, A. & Lamas, S. Two decades of new concepts in nitric oxide signaling: from the discovery of a gas messenger to the mediation of nonenzymatic posttranslational modifications. *IUBMB Life* **61**, 91–98, doi:10.1002/iub.144 (2009).
- Zhang, S. C., Li, L., Li, H. Y. & Guo, H. R. Histochemical localization of constitutive nitric oxide synthases in amphioxus *Branchiostoma belcheri tsingtauense*. *J. Mar Biol Assoc UK* **82**, 1041–1042, doi:10.1017/S0025315402006641 (2002).
- Chen, D., Lin, Y. & Zhang, H. Characterization and expression of two amphioxus DDAH genes originating from an amphioxus-specific gene duplication. *Gene* **410**, 75–81, doi:10.1016/j.gene.2007.11.021 (2008).
- Lin, Y. *et al.* Characterization of the immune defense related tissues, cells, and genes in amphioxus. *Sci China Life Sci* **54**, 999–1004, doi:10.1007/s11427-011-4237-z (2011).
- Godoy, L., González-Duarte, R. & Albalat, R. S-Nitrosogluthathione reductase activity of amphioxus ADH3: insights into the nitric oxide metabolism. *Int J Biol Sci* **2**, 117–124 (2006).
- Deheyn, D. D. *et al.* Endogenous green fluorescent protein (GFP) in amphioxus. *Biol Bull* **213**, 95–100, doi:10.2307/25066625 (2007).
- Yue, J. X., Holland, N. D., Holland, L. Z. & Deheyn, D. D. The evolution of genes encoding for green fluorescent proteins: insights from cephalochordates (amphioxus). *Sci Rep* **6**, 28350, doi:10.1038/srep28350 (2016).
- Bishop, C. D. *et al.* Analysis of nitric oxide-cyclic guanosine monophosphate signaling during metamorphosis of the nudibranch *Phestilla sibogae* Bergh (Gastropoda: Opisthobranchia). *Evol Dev* **10**, 288–299, doi:10.1111/j.1525-142X.2008.00238.x (2008).
- Migliaccio, O., Castellano, I., Romano, G. & Palumbo, A. Stress response to cadmium and manganese in *Paracentrotus lividus* developing embryos is mediated by nitric oxide. *Aquat Toxicol* **156**, 125–134, doi:10.1016/j.aquatox.2014.08.007 (2014).
- Feelisch, M. & Martin, J. F. The early role of nitric oxide in evolution. *Trends Ecol Evol* **10**, 496–499 (1995).
- Kon, T. *et al.* Phylogenetic position of a whale-fall lancelet (Cephalochordata) inferred from whole mitochondrial genome sequences. *BMC Evol Biol* **7**, 127, doi:10.1186/1471-2148-7-127 (2007).
- Kuzin, B., Roberts, I., Peunova, N. & Enikolopov, G. Nitric oxide regulates cell proliferation during *Drosophila* development. *Cell* **87**, 639–649 (1996).
- Peunova, N., Scheinker, V., Ravi, K. & Enikolopov, G. Nitric oxide coordinates cell proliferation and cell movements during early development of *Xenopus*. *Cell Cycle* **6**, 3132–3144, doi:10.4161/cc.6.24.5146 (2007).
- Wicht, H. & Lacalli, T. C. The nervous system of amphioxus: structure, development, and evolutionary significance. *Canadian Journal of Zoology* **83**, 122–150, doi:10.1139/z04-163 (2005).
- Holmqvist, B., Ellingsen, B., Forsell, J., Zhdanova, I. & Alm, P. The early ontogeny of neuronal nitric oxide synthase systems in the zebrafish. *J Exp Biol* **207**, 923–935 (2004).
- Poon, K. L., Richardson, M., Lam, C. S., Khoo, H. E. & Korzh, V. Expression pattern of neuronal nitric oxide synthase in embryonic zebrafish. *Gene Expr Patterns* **3**, 463–466 (2003).
- Kaji, T., Shimizu, K., Artinger, K. B. & Yasui, K. Dynamic modification of oral innervation during metamorphosis in *Branchiostoma belcheri*, the oriental lancelet. *Biol Bull* **217**, 151–160, doi:10.1086/BBLv217n2p151 (2009).

42. Jacox, L. *et al.* The extreme anterior domain is an essential craniofacial organizer acting through Kinin-Kallikrein signaling. *Cell Rep* **8**, 596–609, doi:10.1016/j.celrep.2014.06.026 (2014).
43. Soukup, V. *et al.* The Nodal signaling pathway controls left-right asymmetric development in amphioxus. *Evodevo* **6**, 5, doi:10.1186/2041-9139-6-5 (2015).
44. Kaji, T., Reimer, J. D., Morov, A. R., Kuratani, S. & Yasui, K. Amphioxus mouth after dorso-ventral inversion. *Zoological Lett* **2**, 2, doi:10.1186/s40851-016-0038-3 (2016).
45. Fuentes, M. *et al.* Insights into spawning behavior and development of the European amphioxus (*Branchiostoma lanceolatum*). *J Exp Zool B Mol Dev Evol* **308**, 484–493, doi:10.1002/jez.b.21179 (2007).
46. Yue, J. X., Yu, J. K., Putnam, N. H. & Holland, L. Z. The transcriptome of an amphioxus, *Asymmetron lucayanum*, from the Bahamas: a window into chordate evolution. *Genome Biol Evol* **6**, 2681–2696, doi:10.1093/gbe/evu212 (2014).
47. Yue, J. X. *et al.* Conserved Noncoding Elements in the Most Distant Genera of Cephalochordates: The Goldilocks Principle. *Genome Biol Evol* **8**, 2387–2405, doi:10.1093/gbe/evw158 (2016).
48. Birney, E. & Durbin, R. Using GeneWise in the Drosophila annotation experiment. *Genome Res* **10**, 547–548 (2000).
49. Li, W. *et al.* The EMBL-EBI bioinformatics web and programmatic tools framework. *Nucleic Acids Res* **43**, W580–584, doi:10.1093/nar/gkv279 (2015).
50. Edgar, R. C. MUSCLE: multiple sequence alignment with high accuracy and high throughput. *Nucleic Acids Res* **32**, 1792–1797, doi:10.1093/nar/gkh340 (2004).
51. Kumar, S., Stecher, G. & Tamura, K. MEGA7: Molecular Evolutionary Genetics Analysis Version 7.0 for Bigger Datasets. *Mol Biol Evol* **33**, 1870–1874, doi:10.1093/molbev/msw054 (2016).
52. Capella-Gutiérrez, S., Silla-Martínez, J. M. & Gabaldón, T. trimAl: a tool for automated alignment trimming in large-scale phylogenetic analyses. *Bioinformatics* **25**, 1972–1973, doi:10.1093/bioinformatics/btp348 (2009).
53. Ronquist, F. *et al.* MrBayes 3.2: efficient Bayesian phylogenetic inference and model choice across a large model space. *Syst Biol* **61**, 539–542, doi:10.1093/sysbio/sys029 (2012).
54. Kozmikova, I., Candiani, S., Fabian, P., Gurska, D. & Kozmik, Z. Essential role of Bmp signaling and its positive feedback loop in the early cell fate evolution of chordates. *Dev Biol* **382**, 538–554, doi:10.1016/j.ydbio.2013.07.021 (2013).
55. Green, L. C. *et al.* Analysis of nitrate, nitrite, and [15N] nitrate in biological fluids. *Anal. Biochem.* **126**, 131–138 (1982).
56. Kojima, H. *et al.* Fluorescent Indicators for Imaging Nitric Oxide Production. *Angew Chem Int Ed Engl* **38**, 3209–3212 (1999).

Acknowledgements

This work was supported by the *Branchiostoma lanceolatum* genome consortium that provided access to the *B. lanceolatum* genome sequence. A special acknowledgement to Stéphanie Bertrand and Héctor Escrivá for hosting us at the Observatoire Océanologique de Banyuls sur Mer (France), providing us adult and embryos samples, and for their useful suggestions. We are grateful to Immacolata Castellano for helping us with NO quantification assay, Nicholas D. Holland, Danila Voronov and Demián Burguera for helpful suggestions. We thank Alberto Macina and Davide Caramiello for assistance with the amphioxus culture; Giovanni Gragnaniello and Giampiero Lanzotti for technical help with the SEM. Filomena Caccavale was supported by a SZN PhD fellowship and Giovanni Annona by a post-doctoral fellowship from Regione Campania within the POR Campania FSE 2007/2013-2014/2020 programme. This study was funded by a Marie Curie Career Integration Grant FP7-PEOPLE to Salvatore D'Aniello (grant number PCIG09-GA-2011-293871).

Author Contributions

Giovanni Annona and Filomena Caccavale performed all the experiments with amphioxus embryos; Juan Pascual-Anaya performed the phylogenetic analysis; Pasquale De Luca performed and analysed the Droplet Digital PCR experiments; Shigeru Kuratani discussed the data; Anna Palumbo contributed to the design of experiments regarding NO measurement and *in vivo* interference; Salvatore D'Aniello conceived the project and contributed to all phases of its progression. Giovanni Annona, Filomena Caccavale, Juan Pascual-Anaya and Salvatore D'Aniello wrote the manuscript and all the authors approved it.

Additional Information

Supplementary information accompanies this paper at doi:10.1038/s41598-017-08157-w

Competing Interests: The authors declare that they have no competing interests.

Publisher's note: Springer Nature remains neutral with regard to jurisdictional claims in published maps and institutional affiliations.



Open Access This article is licensed under a Creative Commons Attribution 4.0 International License, which permits use, sharing, adaptation, distribution and reproduction in any medium or format, as long as you give appropriate credit to the original author(s) and the source, provide a link to the Creative Commons license, and indicate if changes were made. The images or other third party material in this article are included in the article's Creative Commons license, unless indicated otherwise in a credit line to the material. If material is not included in the article's Creative Commons license and your intended use is not permitted by statutory regulation or exceeds the permitted use, you will need to obtain permission directly from the copyright holder. To view a copy of this license, visit <http://creativecommons.org/licenses/by/4.0/>.

© The Author(s) 2017